MITOCHONDRIAL TARGETING OF WILD-TYPE AND MUTANT HUMAN PROTOPORPHYRINOGEN OXIDASE (PPOX)

Lester M. Davids, M.Sc (Med) (UCT)

Thesis Presented for the Degree of

Doctor of Philosophy

in the Department of Medicine

University of Cape Town

November 2003

ACKNOWLEDGEMENTS

In a project of this nature, there are so many people who consciously and/or subconsciously contributed through the years to the motivation, discipline and ultimate completion of this dissertation. If I by any chance have omitted anyone, I apologize but here is an attempt to highlight those people who have made a significant impact.

It was a great privilege to have experienced supervision of the quality that I have during the course of this dissertation from Professor Peter Meissner ("my captain") and Dr Anne Corrigall. They have been a constant source of inspiration and encouragement mixed with their own unique blends of discipline, humour and patience. Most of all, I have come to value their friendships immensely. Thank-you.

I would also like to thank :

- Prof. Harry Dailey, Dr Amy Medlock and Tamara Dailey (Department of Microbiology, University of Georgia, Athens, Georgia, USA) for providing us with the pTrcHis-PPOX vector and the initial oligonucleotide sequences for the PPOX17 construct. Also for affording me the opportunity to spend time in their lab for 5 weeks in June 2000 to learn stopped-flow kinetic methodology.

- Prof. Richard Hift for input regarding the clinical aspects of variegate porphyria.

- Prof. Ralph Kirsch and the secretarial staff of the Dept. of Medicine.

- Profs Dave McIntosh and Trevor Sewell for helpful discussions and ideas regarding structural biology.

- Dr Heinrich Hoppe for assistance with the digital overlay of GFP and Mitotracker Red photographs.

- Prof. Sue Kidson for input regarding molecular biology aspects and helpful advice.

- Valerie Hancock for technical assistance, lively discussion and her "the cup is half-full" enthusiasm.

- Leslie Frith and Mr Mick "fit, fit, fit!!" Wells for technical assistance.

- My superb colleagues through the years – Brandon Davidson, Kwanele Siziba, Mbulelo Maneli, Edward Sturrock, Vivienne Woodburne, Helen Botes, Richard Kirsch, Brent Jennings, Xolani William, Heather Epstein and Maglona Paul.

- For keeping everything pretty clean and tidy – Leslie Martin (and his laugh!), Moegamat Samuels, Abdoeragmann Benjamin (Benjy) and Amiena Adams

- My wonderful wife for always being there as my best friend, a constant source of support, understanding, encouragement, love and a shoulder to rest on when things got "hectic". Thank-you so much.

- My parents and the rest of my supportive family.

- To all my friends "back at the ranch" for their encouragement and support.

- The Wellcome Trust for their financial assistance under the international Senior Research Fellowship programme (of which Prof. Peter Meissner is a recipient).

- Lastly, to the Great I AM, for being a very real part of my life.

DEDICATION

I dedicate this thesis to my wife, Virginia, and the rest of our family – Gizmo, Sheena and BB.

"Science is the game we play with God to find out what His rules are"

ABSTRACT

MITOCHONDRIAL TARGETING OF WILD-TYPE AND MUTANT HUMAN PROTOPORPHYRINOGEN OXIDASE (PPOX)

Variegate porphyria (VP) is an autosomal dominant disorder of heme metabolism resulting from a deficiency in protoporphyrinogen oxidase (PPOX), the penultimate enzyme in the heme biosynthetic pathway. The disease is biochemically characterized by a reduced PPOX enzyme activity and an overproduction and increased excretion of porphyrins and porphyrin precursors.

PPOX is an inner mitochondrial (mt) membrane protein with a recently reported N-terminal mt targeting signal. However, this signal remains to be fully characterized. This study, firstly, examined the effect of 3 South African VP mutations (H20P, R59W, R168C) on mt targeting of the enzyme using an *in vitro* system. Wild-type PPOX, and the above mutants, created by site-directed mutagenesis, were cloned into a green fluorescent protein (GFP) expression vector. H20P showed a total lack of mt targeting, in contrast to R59W and R168C where mt targeting was observed, suggesting the presence of a mt targeting sequence at the PPOX N-terminus.

Secondly, amino acids 1-24 were examined to ascertain the minimal sequence required for mt targeting. Eight PPOX-GFP chimeric fusion proteins (PPOX12, PPOX14, PPOX15, PPOX16, PPOX17, PPOX20, PPOX24 and PPOXΔ1-17-GFP) were constructed by PCR-based mutagenesis and cloned into GFP as above. Seventeen was the minimal number of amino acids required for targeting. Unexpectedly, PPOXΔ1-17-GFP targeted, suggesting one or more additional internal mt targeting signals.

As overall charge and α-helicity are characteristics of N-terminal targeting signals, the effect of both of these on targeting was investigated. To examine charge, Arg3 (the only positive charge in the 17-residue targeting sequence) was altered to serine, lysine and glutamic acid residues. Furthermore, the results showed that not only is overall charge important, but that the specific positive residue providing the charge must be considered. Finally, H20S, H20A, H20K, H20E, H20G and H20P all targeted the mitochondrion apart from H20P. This illustrated the dramatic effect a proline (H20P) has on the translocation of PPOX to the mitochondrion, presumably through disruption of its α-helix.

November 2003

ABBREVIATIONS AND SYMBOLS

General

°C	degrees celsius
µg	micrograms
µl	microlitre
µM	micromolar
Å	angstrom
ALDH	aldehyde dehydrogenase
APS	ammonium persulphate
ATG	start codon (methionine)
ATP	adenosine triophosphate
bp	base pairs
C-	carboxy (terminal)
cDNA	complementary deoxyribonucleic acid
CHO	Chinese hamster ovary cells
COS	Monkey kidney cells
Da	daltons
DMEM	Dulbecco's modified eagle medium
DMSO	dimethylsulfoxide
DNA	deoxyribonucleic acid
dNTP	deoxynucleotide triphosphate
DOTAP	[1-(2,3 Dioleoyloxy)propyl]-N,N,N-trimethylammonium methylsulphate
DPMC	dipyrromethane cofactor
dsDNA	double stranded DNA
EDTA	Ethylenediaminetetraacetic acid
EGFP	enhanced green fluorescent protein
ES	enzyme substrate
FAD	flavin adenine dinucleotide
FCS	fetal calf serum
FMN	flavin mononucleotide
GFP/BFP/YFP/CFP	green/blue/yellow/cyan fluorescent protein
g	centrifugal force
GIP	general import pore
h	hour
HD	heteroduplex
HepG2	Human hepatoma cell line
HRM	heme regulatory motif
Hsp	heat-shock protein
IRE	iron-response element
IM	inner membrane (mitochondrial)
IMS	intermembrane space (mitochondrial)

IVS	intervening sequence (intronic)
kb	kilobases
kDa	kilodaltons
L	litre
LB	Luria-Bertani
MCS	multiple cloning site
mg	milligram
min	minutes
ml	millilitre
mM	millimolar
M	Molar (moles/litre)
mRNA	messenger ribonucleic acid
MSF	mitochondrial import stimulation factor
mtHsp	mitochondrial heat-shock protein
N-	amino (terminal)
NAC	nascent-associated polypeptide complex
ng	nanogram
nm	nanometer
nmol	nanomole
OD	optical density
OM	outer mitochondrial membrane
ORF	open reading frame
OTC	ornithine transcarbamoylase
PAGE	polyacrylamide gel electrophoresis
PBS	phosphate-buffered saline
PCR	polymerase chain reaction
pmol	picomole
pTrcHis	6-histidine tagged plasmid
RAC	ribosome-associated complex
RNA	ribonucleic acid
rpm	revolutions per minute
RT-PCR	reverse transcriptase PCR
s	second
SDS	sodium dodecyl sulphate
SDS-PAGE	sodium dodecyl sulphate polyacrylamide gel electrophoresis
SSCP	single stranded conformation polymorphism
SV40T	simian virus large T antigen
TEMED	N,N,N,N-Tetramethylethylenediaamine
TGA	stop codon
TIM	translocase of the inner membrane
TOM	translocase of the outer membrane
Tris	Tris(hydroxymethyl)methylamine
TE	Tris/ EDTA
TBE	Tris/borate/EDTA
UTR	untranslated region

UV	ultraviolet
WT	wild-type

Amino acids

A	alanine	Ala
C	cysteine	Cys
D	aspartic acid	Asp
E	glutamic acid	Glu
F	phenylalanine	Phe
G	glycine	Gly
H	histidine	His
I	isoleucine	Ile
K	lysine	Lys
L	leucine	Leu
M	methionine	Met
N	asparagine	Asn
P	proline	Pro
Q	glutamine	Gln
R	arginine	Arg
S	serine	Ser
T	threonine	Thr
V	valine	Val
W	tryptophan	Trp
Y	tyrosine	Tyr

DNA nucleotide base

A	adenine
T	thymine
C	cytosine
G	guanine

Enzymes of the heme biosynthetic pathway

ALAS	5-aminolevulinic acid synthase
ALAD	5-aminolevulinic acid dehydratase
PBGD	Porphobilinogen deaminase
UROIIIS	Uroporphyrinogen III synthase
UROD	Uroporphyrinogen decarboxylase
CPOX	Coproporphyrinogen oxidase
PPOX	Protoporphyrinogen oxidase
FC	Ferrochelatase

Porphyrias (in order of deficient enzyme as listed on previous page)

ALADP	5-ALA dehydratase porphyria
AIP	acute intermittent porphyria
CEP	congenital erythropoietic porphyria
PCT	porphyria cutanea tarda
HEP	hepatoerythropoietic porphyria
HCP	hereditary coproporphyria
VP	variegate porphyria
HVP	homozygous variegate porphyria
EPP	erythropoietic protoporphyria

Pattern of inheritance

AA	acute attack
AD	autosomal dominant
AR	autosomal recessive
PS	photosensitivity

Symbols

Δ	deletion of
α	alpha
β	beta
δ	delta
μ	micro
U	endonuclease units

TABLE OF CONTENTS

Chapter 7 : Mitochondrial targeting of engineered N-terminal PPOX-GFP fusion constructs

Chapter 8 : Overview, implications and future directions

List of Appendices

List of Figures

List of Tables

CHAPTER 1 : PORPHYRINS AND THE HEME BIOSYNTHETIC PATHWAY

CHAPTER 1 : PORPHYRINS AND THE HEME BIOSYNTHETIC PATHWAY

1.1 Introduction

Tetrapyrroles are indispensable for life, serving as pigments and cofactors in many biological reactions. Found throughout the biological kingdoms, from archaebacteria to plants and animals, they participate in a broad spectrum of essential biological reactions. Heme, an iron-containing tetrapyrrolic complex (ferroprotoporphyrin), is the end-product of a tightly regulated pathway involving a series of chemical reactions catalysed by specific enzymes. Once conjugated to a variety of proteins (hemoproteins), it plays a role, amongst others, in cellular metabolism, cellular respiration and oxygen transport (Beri and Chandra 1993). As this dissertation concerns protoporphyrinogen oxidase (PPOX), the penultimate enzyme in the heme biosynthetic pathway, this chapter includes an overview of porphyrins, heme synthesis and regulation, and the enzymes involved in the heme biosynthetic pathway.

1.2 Description of tetrapyrroles and porphyrin chemistry

Porphyrins, "the pigments of life" (Battersby et al. 1980), are tetrapyrrole macrocycles consisting of four weakly aromatic pyrrole rings linked by methene bridges. The four pyrrole rings are designated A-D and the four methene bridges α, β, γ and δ (Fig. 1.1). The tetrapyrrole macrocycle in its oxidised porphyrin state is a highly aromatic, rigid, planar structure with eight positions where side chains can be attached. They are numbered from 1 to 8 according to the Fischer nomenclature. The type of side chain determines the physical characteristics of the porphyrin (Table 1.1). Note that, varying the arrangement of side chain substituents around the porphyrin ring results in a number of possible different isomeric porphyrin forms. For example, uroporphyrinogen and coproporphyrinogen can occur in four possible isomeric forms. Two of these forms, uroporphyrinogen III and coproporphyrinogen III, occur in nature and are biologically active isomers, whereas uroporphyrinogen

I and coproporphyrinogen I are produced non-enzymatically and are not utilised biologically.

Table 1.1 Names and side-chain substituents of porphyrins. A : $-CH_2COOH$; E : $-CH_2CH_3$; M : $-CH_3$; P : $-CH_2CH_2COOH$; V : $-CH=CH_2$

PORPHYRIN	Substituent on positions 1-8							
	1	**2**	**3**	**4**	**5**	**6**	**7**	**8**
Uroporphyrin-I	A	P	A	P	A	P	A	P
Uroporphyrin-III	A	P	A	P	A	P	P	A
Heptacarboxylic porphyrin	A	P	A	P	A	P	P	M
Heptacarboxylic porphyrin	M	P	A	P	A	P	P	M
Pentacarboxylic porphyrin	M	P	M	P	A	P	P	M
Coproporphyrin-I	M	P	M	P	M	P	M	P
Coproporphyrin-III	M	P	M	P	M	P	P	M
Isocoporphyrin-III	M	E	A	P	M	P	P	M
Harderoporphyrin-IX	M	V	M	P	M	P	P	M
Protoporphyrin-IX	M	V	M	V	M	P	P	M
Deuteroporphyrin-IX	M	H	M	H	M	P	P	M
Mesoporphyrin-IX	M	E	M	E	M	P	P	M

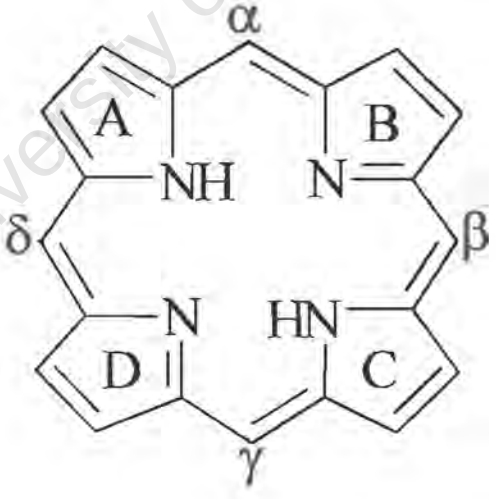

Figure 1.1 The tetrapyrrole structure of porphyrins showing the four pyrrole rings joined by methene bridges (indicated in red).

An important property of the porphyrin macrocycle is the availability of ligand binding sites within. This attribute gives these compounds the ability to bind metals, particularly iron to form heme, magnesium to form chlorophylls, and cobalt bound to corrins (modified porphyrin rings) vital for the formation of vitamin B_{12} (Scott et al. 1972; Battersby and McDonald 1975; Jones 1976; Bissell and Schmid 1987). These metalloporphyrins are widely distributed throughout the plant and animal kingdoms where they are essential for many processes such as photosynthesis, oxygen transport, electron transport and the reduction of molecular oxygen (Bissell 1985).

Porphyrins exhibit red fluorescence when irradiated with UV light of an approximate wavelength of 400nm. The absorption spectra of porphyrins show absorption in the visible (VIS) regions of the electromagnetic spectrum with a major band in the region of 400nm called the Soret band (Soret 1883). Their main absorption bands have very high extinction coefficients (up to 4 x 10^5M) (Smith 1975). It is important to realise that "porphyrin" tetrapyrroles mostly exist *in vivo* as the partially conjugated, less stable hexahydro-reduced, colourless porphyrinogen form (Falk 1964; Marks 1969; Smith 1975).

1.3 The heme biosynthetic pathway

1.3.1 General description

The ability of the porphyrin macrocycle to bind iron results in the formation of heme. Heme itself is only functional when bound to various proteins to form hemoproteins. These hemoproteins play a role in oxygen binding (hemoglobin, myoglobin), respiration and detoxification of reactive oxygen species (various oxidases, peroxidases and catalases), electron transfer (cytochromes), protection mechanisms against xenobiotics (cytochrome P450 enzymes), and nitrogen fixation (nitrogenase). Recently it has been reported P450 cytochromes make up 65% of hemoproteins, the oxidases and catalases 20%, and the final 15% comprises the mitochondrial respiratory

catalases 20%, and the final 15% comprises the mitochondrial respiratory cytochromes (Deybach and Puy, 2003). The importance of hemoproteins in the human genome is illustrated by ~137 000 citations recorded to date (1975-2003 Medline database search on "hemoproteins"; www.ncbi.nih.gov/entrez/).

Heme also functions as a prosthetic group in proteins of signal transduction cascades that generate central regulatory and messenger molecules such as cyclic 3'-5' monophosphate (cGMP) (guanylate cyclase), steroid hormones, or nitric oxide (nitric oxide synthase) (Grimm 2003). In addition, the function of heme extends over transcriptional and translational control to the processing, assembly, and stability of various other erythroid and non-erythroid heme-containing proteins (Ponka 1999; Thunell et al. 2000)

Structurally, heme is an iron-containing complex of the protoporphyrin-IX (PP-IX) molecule with a central iron atom in the centre. PP-IX is a rigid planar molecule consisting of four pyrrole rings linked by 4 methene bridges. Two propionic acid, two vinyl and 4 methyl side chains are attached to the pyrrole rings (Fig. 1.2). Since all the pyrrole rings lie in a common plane, the four ligand bonds from the porphyrin to the iron atom at its centre will have a tendency to lie in the plane of the porphyrin ring.

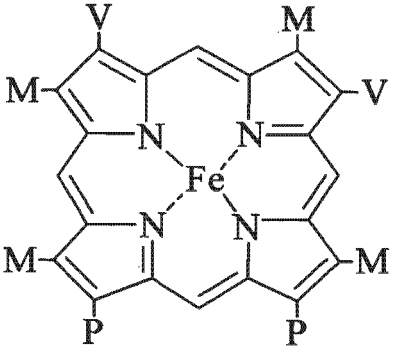

Figure 1.2 The tetrapyrrole structure of the heme molecule showing the ferrous iron (Fe^{2+}) in the centre. M = methyl ($-CH_3$), V = vinyl ($-CH=CH_2$), and P = propionate ($-CH_2\ CH_2COOH$) groups.

1.3.2 Heme synthesis

In mammals, the formation of heme is accomplished by the sequential action of eight distinct enzymes. It is produced by a well-defined metabolic pathway, initiated in the mitochondrial matrix, continuing in the cytosol, and ultimately returning to the highly reducing environment of the mitochondrion (Bloomer and Straka 1988). The pathway starts with the condensation of glycine and succinyl - co-enzyme A (CoA) to form 5-aminolevulinate (5-ALA) under the control of the mitochondrial enzyme ALA synthase (ALAS) (Fig 1.3, 1). Succinic acid and glycine can be viewed as providing the constituent carbon and nitrogen atoms for heme. ALA leaves the mitochondrion and once in the cytosol, ALA dehydratase (ALAD) (Fig 1.3, 2) catalyses the condensation of two molecules of ALA to form the pyrrole subunit of the porphyrin ring, porphobilinogen (PBG). Four molecules of PBG are then assembled by PBG deaminase (PBGD) (Fig 1.3, 3) to form an "unrearranged" bilane, hydroxymethylbilane. In the absence of uroporphyrinogen cosynthetase, hydroxymethylbilane spontaneously undergoes chemical cyclisation to form the type I uroporphyrinogen isomer which is biologically non-functional. Concurrently, uroporphyrinogen cosynthetase (UROIIIS)(Fig 1.3, 4) performs the necessary intramolecular rearrangement and ring closure of the bilane to form uroporphyrinogen III, the first of a series of porphyrinogens. Uroporphyrinogen decarboxylase (UROD) (Fig 1.3, 5) catalyses the stepwise decarboxylation of uroporphyrinogen III, which has eight carboxylated side-chains, through hepta-, hexa- and penta-carboxylic porphyrinogen intermediates to form the tetracarboxylic porphyrinogen, coproporphyrinogen. The process returns to the mitochondrion where coproporphyrinogen oxidase (CPOX) (Fig 1.3, 6) produces the dicarboxylic porphyrinogen, protoporphyrinogen by oxidative decarboxylation of the propionate side-chains in peripheral positions 2 and 4, to vinyl groups. Protoporphyrinogen is enzymatically oxidised by PPOX (Fig 1.3, 7) to give protoporphyrin and the pathway is completed by the formation of heme through the insertion of ferrous ion (Fe^{2+}) into the porphyrin ring by the terminal enzyme, ferrochelatase (FC) (Fig 1.3, 8).

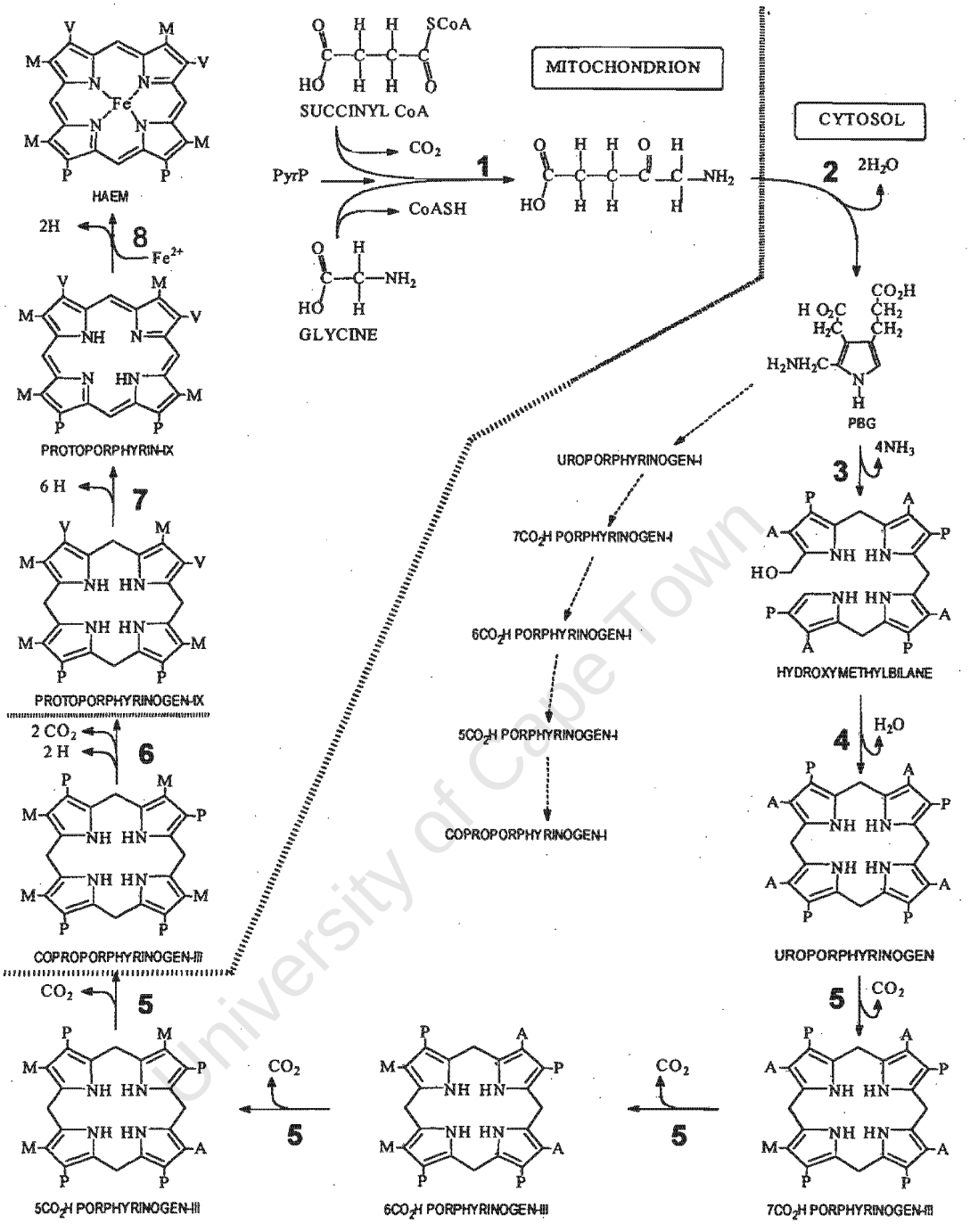

Figure 1.3 Heme biosynthesis involves eight enzyme catalysed "pyrrolic" reactions which are located sequentially, in the mitochondria, cytosol and finally mitochondria. M = methyl ($-CH_3$), V = vinyl ($-CH=CH_2$), P = propionate ($-CH_2CH_2COOH$), and A = acetate ($-CH_2COOH$). 1: ALAS; 2: ALAD; 3: PBGD; 4: UROIIIS; 5: UROD; 6: CPOX; 7: PPOX; 8: FC.

1.3.3 Heme regulation

Heme regulation in mammalian systems has always been a subject of discussion in the scientific community. Although it is now well established that ALAS is the first and rate-limiting step in the pathway, it is becoming clear that all other pathway enzymes appear to be under at least some form of additional transcriptional control. While regulation of the pathway by ALAS will not be the subject of detailed discussion here, it seems pertinent to review the current scientific thinking on the involvement of ALAS and the other pathway enzymes, and their roles in regulating heme synthesis.

Heme occurs in all metabolically active cells and is produced at its highest rate in erythropoietic cells and hepatic cells. Both tissues employ a different regulatory mechanism to control enzyme gene expression and heme synthesis. The difference in regulation is most pronounced in ALAS. Two different genes, ALAS-1 and ALAS-2 encode this enzyme (Bawden et al. 1987; Riddle et al. 1989; Cox et al. 1991). ALAS-1 is ubiquitously expressed, whereas the ALAS-2 gene is specific for erythroid cells (Watanabe et al. 1983, 1984; Bishop 1990; Bishop et al. 1990). The erythroid-specific expression of ALAS-2 has led to it being known as ALAS-E (erythroid), whereas the ALAS-1 gene is referred to as ALAS-H (housekeeping) or ALAS-N (non-erythroid).

The two ALAS isoenzymes are structurally similar but they are encoded by different mRNAs resulting in distinctly different regulatory and untranslated regions (May and Bawden 1981; Andrew et al. 1990). Over the past few years, the regulation of heme by ALAS-1 has been speculated to be at a transcriptional level (May et al. 1986; Srivastava et al. 1988), translational level (Yamamoto et al. 1982), as well as at the level of ALAS-1 enzyme activity (Scholnick et al. 1972). However, current ideas favour the concept of control at the transcriptional level as illustrated by recent studies on the ALAS-1 promoter (Roberts and Elder 2001) and transcription factor binding sites (Giono et al. 2001; Guberman et al. 2003). What is clear is that the regulation of heme at the point of ALAS-1 in the pathway remains complex.

Whereas ALAS-1 is feedback-inhibited by heme, the synthesis of mammalian ALAS-2 is not. Expression and regulation of erythroid heme synthesis are linked to the differentiation events initiated by erythropoietin as well as iron availability and globin chain production (Cotner et al. 1989; May et al. 1995; Weiss et al. 1997). Through the action of erythropoietin, a number of genes necessary for erythroid cell differentiation become expressed, including ALAS-2. Transcription of ALAS-2 is regulated by motifs in its promoter (Surinya et al. 1997, 1998; Sadlon et al. 1999), whereas translation is linked to iron availability through an iron-responsive element binding protein control mechanism (Bhasker et al. 1993; Melefors et al. 1993). A third level of regulation is due to the presence of cytosolic heme. If present, this heme can regulate translation of ALAS-2 (Smith and Cox 1997) as well as the protein's translocation to mitochondria, through the binding of heme regulatory motifs in the signal sequence of the precursor protein (Lathrop and Timko 1993).

Another level of control of heme regulation is at the level of PBGD. Two different isoforms of this enzyme are encoded on one mammalian gene. Furthermore, the gene contains erythroid-specific and house-keeping promoter elements embedded within a single promoter region. The house-keeping promoter is upstream from the erythroid-specific one and even though the two promoters appear to be regulated independently, when RNA polymerase activates transcription of the housekeeping promoter, the entire erythroid promoter is transcribed. The subsequent housekeeping protein is 17 amino acids shorter than the erythroid-specific form at its N-terminus (Grandchamp et al. 1987; Beale and Yeh 1999).

Despite the main regulation of heme synthesis occurring at the level of the early enzymes, it is clear that certain other downstream pathway enzymes may also be involved as they possess genes encoding both housekeeping and erythroid-specific promoter elements and a few exhibit erythroid-specific splice variants and tissue-specific expression patterns (Table 1.2). The *ALAD* gene for example, is identical in erythroid and non-erythroid cells, but its mRNA displays a different tissue-specific posttranscriptional pattern (Chretien et al. 1988; Mignotte et al. 1989; Kaya et al. 1994). The remaining enzymes of

the heme pathway, UROD, CPOX, PPOX and FC, all possess single promoters with none of them exhibiting alternate splicing variants. Table 1.2 represents a summary of currently known regulatory gene factors for the ALAS genes as well as the other enzymes in the heme biosynthetic pathway.

Table 1.2 Gene regulatory regions of the heme biosynthetic enzymes. AP1, transcription factor; ELKF, erythroid-like Kruppel factor; IRE, iron recognition element; NFκβ, nuclear factor kappa beta; NRF-1/2, nuclear-related factor 1 or 2; NF-E2, nuclear factor E2, Sp1, transcription factor

Enzyme/Gene	Tissue specificity	Gene regulatory regions	Reference	C/somal location
ALAS-1 (ALAS-H)	Non-erythroid	Sp1, NFκβ, NRF-1, TATA site	(Roberts and Elder 2001)	3p21
ALAS-2 (ALAS-E)	Erythroid	GATA-1, EKLF, NF-E2, erythroid-specific enhancers, Sp1, IRE	(Surinya et al. 1997, 1998)	Xp11.21
ALAD	Housekeeping and erythroid	Sp1, AP1, CCAAT motif, GATA-1, CACCC motif	(Kaya et al. 1994)	9q34
PBGD	Housekeeping and erythroid	NF-E2, CCAAT, GF-1 binding site, CACCC motif	(Mignotte et al. 1989)	11q23
UROIIIS	Housekeeping and erythroid	NF1, AP1, Oct1, NRF2, GATA-1, NF-E2	(Aizencang et al. 2000)	10q25.2-q26.3
UROD	Housekeeping and erythroid	Putative Sp1, TATA-like motif	(Romana et al. 1987a)	1p34.1
CPOX	Housekeeping	CACCC, multiple GATA and Sp1sites	(Martasek et al. 1994; Taketani et al. 1994)	3q11.2-3q12
PPOX	Housekeeping	Sp1, CCAAT, GATA-1	(Taketani et al. 1995; Dailey and Dailey 1996; Puy et al. 1996)	1q22-23
FC	Erythroid and housekeeping	Sp1, GATA-1, NF-E2	(Tugores et al. 1994; Magness et al. 1998)	18q21.3

Interestingly, there has been recent speculation on the involvement of FC in heme regulation eg. the role of FC and the presence of a [2Fe-2S] cluster in the mammalian enzyme. Although the function of the cluster is presently unknown, its assembly is a prerequisite for functional enzyme activity and a deficiency in cellular iron results in diminished FC activity. It follows therefore that while there is no iron responsive element known to date, the [2Fe-2S] cluster could become the site of iron regulation of heme synthesis (Dailey, personal communication).

1.4 Enzymes of the Heme Biosynthetic Pathway

1.4.1 ALA Synthase (EC 2.3.1.37)

Commencing in the eukaryotic mitochondrion, the pathway starts with ALAS catalysing the reaction of the 2-carbon atom of glycine with the electrophilic carbonyl carbon of succinyl CoA. As with other pyridoxal 5' phosphate-dependent enzymes, this first step involves the formation of a Schiff base between the amino group of glycine and the aldehyde of pyridoxal 5-phosphate. This is followed by the deprotonation of glycine which establishes a stabilised carbanion or equivalent nucleophilic species, that reacts with succinyl CoA, displacing CoA to form 2-amino-3-ketoadipic acid. Finally, the carboxyl carbon of glycine is decarboxylated enzymatically via ALAS to yield ALA (Fig 1.4).

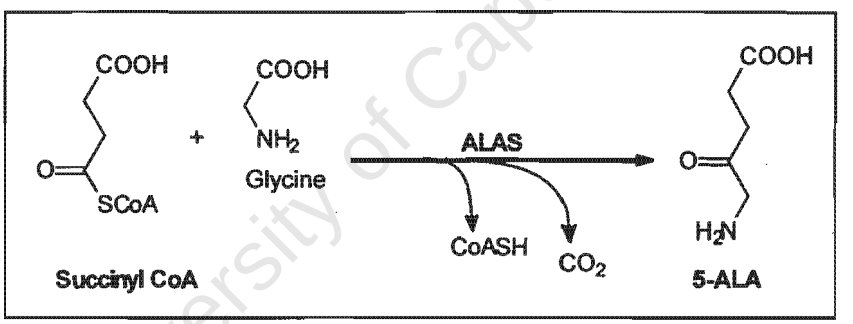

Figure 1.4 Biosynthesis of 5-ALA from glycine and succinyl CoA by ALAS

ALAS-1, a 64kDa protein, is found in all non-erythroid cells (Sutherland et al. 1988; Bishop 1990), whereas ALAS-2 is expressed in erythroid cells and has an associated molecular weight of 59kDa (Bishop et al. 1990; Cox et al. 1990).

In the absence of a crystal structure for ALAS, the identity of catalytic groups at the active site has been investigated by site-directed mutagenesis and by comparison between the amino acid sequences and 3-D structures of a number of pyridoxal 5'-phosphate-dependent proteins (Ploux and Marquet 1996). In the first step of the mechanistic reaction, a lysine forms the Schiff

base with pyridoxal 5'-phosphate. This invariant lysine has been identified as lysine-313 in the mouse ALAS-2 sequence and is clearly involved in catalysis, as site-directed mutagenesis of this amino acid, leads to almost complete loss of enzyme activity (Ferreira et al. 1993). Besides the equivalent lysine (lysine-248), *Rhodobacter sphaeroides* (Toney et al. 1995; Alexeev et al. 1998), showed a number of other conserved amino acids which play a role at the catalytic site. Two histidines at positions 142 and 217 are involved in the enzymatic decarboxylation of glycine. In addition, an invariant arginine (R256), and aspartic acid (aspartate-214) present in several other pyridoxal 5'-phosphate-dependent enzymes, proved to be important for binding the carboxyl group of glycine, and charge stabilisation of the positive pyridine nitrogen, respectively. Site-directed mutagenesis of the equivalent arginine (arginine-439) (Tan et al. 1998) and aspartate (Gong et al. 1998) in mouse ALAS-2, also showed dramatic effects on enzyme activity.

Human ALAS is synthesised in cytosolic ribosomes as a pre-enzyme, which is then imported into and processed within the mitochondrion to yield the mature form of the enzyme (Yamauchi et al. 1980; Srivastava et al. 1983; Volland and Urban-Grimal 1988). Early studies on the subcellular location of ALAS showed that it is loosely bound to the inner mitochondrial membrane but generally available within the mitochondrial matrix (McKay et al. 1969). The idea of the matrix location of ALAS is supported by a study that showed mature ALAS interacting with the ATP-specific beta subunit of succinyl CoA synthase (SCSβA) on the matrix side of the inner mitochondrial membrane (Furuyama and Sassa 2000). The question of how ALAS reaches the mitochondrial matrix was originally studied by Volland and Urban-Grimal (1988) who showed that despite removal of the entire presequence in yeast ALAS, the protein still managed to become fully internalised in the mitochondrion. Thus, the amino-terminal signal, if indispensable as a matrix targeting signal, could be replaced by an internal sequence or a particular folding for recognition by the import machinery (Volland and Urban-Grimal 1988). A recent study using chemically synthesised murine ALAS N-terminal presequence translocating peptides provided evidence in support of the ALAS presequence containing all the characteristics for mitochondrial recognition

and initial import. In addition, the study confirmed that high heme concentrations inhibit the translocation of the ALAS precursor into mitochondria through a heme regulatory motif (HRM) (Lathrop and Timko 1993; Goodfellow et al. 2001).

Comparison of amino acid sequences from various sources with respect to ALAS-2 (Ferreira et al., 1995), has led to the knowledge that this form of the enzyme consists of a C-terminal ancestral core, with a variable N-terminal region that is involved in mitochondrial import and regulatory mechanisms. This N-terminal domain of the newly synthesized protein clearly is not necessary for enzymatic activity and serves as the mitochondrial "presequence", allowing for efficient translocation of the protein from the nucleus to the mitochondrion. This N-terminal region has been reported to be 56 amino acids in length and is cleaved on translocation into and through the mitochondrion.

Molecular biological approaches to ALAS has yielded cDNA clones to chicken (Borthwick et al. 1984; Borthwick et al. 1985) and rat liver *ALAS* (Srivastava et al. 1988) as well as genomic clones to chicken liver *ALAS* (Maguire et al. 1986). The genes for *ALAS-1* and *ALAS-2* have been cloned and mapped to chromosomal locations 3p21 (Sutherland et al. 1988; Bishop et al. 1990) and Xp11.21 (Bishop et al. 1990; Cox et al. 1990), respectively. Despite the lack of literature on the gene structure of human *ALAS-1*, studies on the rat show that the *ALAS-1* gene spans more than 14kb and consists of 11 exons (Yomogida et al. 1993). The promoter region of the gene contains several regulatory elements, including motifs such as a TATA box and NRF-1 binding sequence (Roberts and Elder 2001) (table 1.2)

The human *ALAS-2* gene spans 22kb and comprises 11 exons. Exon 2 encodes the N-terminal signal sequence required for mitochondrial import, exons 3 and 4 encode a variable region of the N-terminal end, and exons 5-11 encode the highly conserved C-terminal portion of the mature protein. The region encoded by exons 5-11 has 73% identity with *ALAS-1* and contains the enzyme's catalytic domain. Exon 1 encompasses the 5'-UTR which contains

the sequence for the IRE associated with the ALAS-2 enzyme (Cotner et al. 1989; Bottomley 2003).

1.4.2 ALA Dehydratase (EC 4.2.1.24) (Porphobilinogen Synthase)

The next step in the pathway occurs in the cytoplasm; and involves the dimerisation of two molecules of ALA to form the monopyrrole, PBG (Jordan 1991; Jaffe 1995). This step is catalysed by the enzyme ALAD, also referred to as PBG synthase (Jordan and Woodcock 1991) (Figure 1.5). The enzyme is best described as a tetramer of dimers ie. an octamer and each dimer has one active site that can bind two molecules of ALA (Jaffe 1995). These two molecules of ALA are bound at distinct positions ie. the A and P-site (Shoolingin-Jordan et al. 1996, 1997; Shoolingin-Jordan 1998). The ALA molecule contributing the acetate group and the amino-methyl group of PBG binds at the A-site. The ALA contributing the propionate side chain and the pyrrolic nitrogen binds at the P-site.

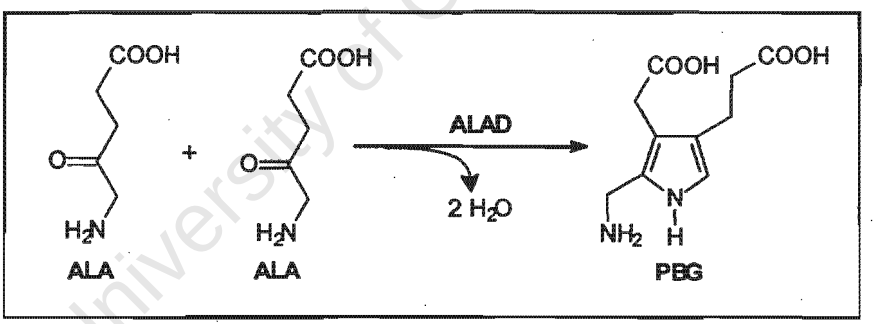

Figure 1.5 Biosynthesis of PBG from ALA by ALAD.

There is an ordered binding in which the keto- group of the ALA contributing the propionate side chain first forms a transient covalent bond with a conserved lysine (human Lys-252) in the P-site. Once there is bound substrate at the P-site with an available 5-amino group, binding of the second ALA molecule onto the enzyme at the A-site occurs. Binding of the second substrate at the A-site is dependent on the presence of a divalent metal ion. Typically, the required metals are Zn^{2+} or Mg^{2+} (Abdulla and Haeger-Aronsen 1971; Haeger-Aronsen et al. 1971; Senior et al. 1996). Removal of these divalent ions prevents binding and results in loss of activity, but has no effect on ALA binding at the P-site (Norton et al, 1998). In mammalian systems up to

a maximum of eight Zn^{2+} ions can bind onto an ALA dehydratase octamer (Wu et al. 1974; Tsukamoto et al. 1980).

Crystallisation and X-ray characterisation of ALAD from *Escherichia coli* (Senior et al. 1997), *Saccharomyces cerevisiae* (Erskine et al. 1997; Erskine et al. 1999a; Erskine et al. 1999b) and *Pseudomonas aeruginosa* (Frankenberg et al. 1999) confirmed that each subunit of the ALAD homo-octamer occupy the corners of a cube and exist as an $(\alpha/\beta)_8$- or TIM-barrel fold with the N-terminus extended away from the barrel in the form of an arm of approximately 40 amino acids (Warren et al. 1998; Erskine et al. 1999b). Furthermore, in *P. aeruginosa,* ALAD structural analysis revealed that in each dimer the monomers differed from one another by having a "closed" and an "open" active site pocket. Whereas no metal ions were found in the active site of both monomers, a single well-defined and highly hydrated Mg^{2+} was identified only in the closed form, about 14Å away from the Schiff base forming nitrogen atom of the active site lysine. Based on this information a structure-based mechanism of action involving Mg^{2+} allosteric binding at the active site and rate enhancement has been proposed (Frankenberg et al. 1999). In contrast, the X-ray structure of yeast 5-ALAD indicates a two-metal centre with scope for binding either two zinc ions, or a zinc ion and a magnesium ion. One zinc ion is coordinated to cysteines-133, 135 and 143, and a water molecule. This metal ion is near the active site lysine residue (Lys263, yeast numbering) and is likely to play a vital catalytic role. In lead poisoning, the zinc is exchanged for lead, leading to inactivation of the enzyme (Erskine et al. 1999b).

The genes encoding *ALAD*s have been sequenced and their cDNAs and protein products characterised from several sources such as human (Wetmur et al. 1986a; Wetmur et al. 1986b); rat (Bishop et al. 1986); *E. coli* (Echelard et al. 1988); *Chlamydomonas reinhardtii* (Matters and Beale 1995); soybean (Kaczor et al. 1994); *Bradyrhizobium japonicum* (Chauhan and O'Brian 1993); pea (*Pisum sativum L.*) (Boese et al. 1991); and *P. aeruginosa* (Frankenberg et al. 1998). A single gene containing separate erythroid and housekeeping promoters undergoes alternative splicing to give rise to two tissue-specific

forms of ALAD (Kaya et al. 1994; Bishop et al. 1996). It has been proposed that this novel expression of erythroid-specific and housekeeping transcripts apparently evolved to ensure that there is enough supply of heme for high-level tissue-specific haemoglobin production (Bishop et al. 1996).

1.4.3 Porphobilinogen Deaminase (EC 4.3.1.8) (Hydroxymethylbilane Synthase)

PBGD, also known as hydroxymethyl-bilane synthase (Jordan 1990), catalyzes the deamination and head-to-tail polymerization of four molecules of PBG. This reaction, initiated in the cytosol, produces the first tetrapyrrole in the pathway, the linear tetrapyrrole hydroxymethylbilane (preuroporphyrinogen) (Fig 1.6).

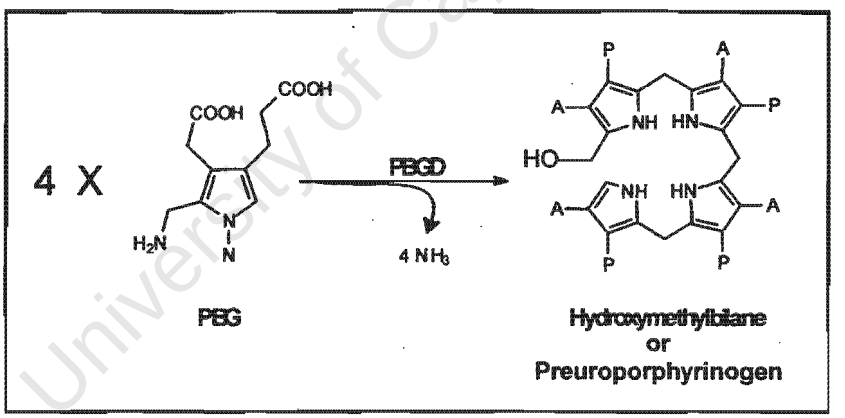

Figure 1.6 Biosynthesis of hydroxymethylbilane from PBG by PBGD. A = acetate, P = propionate

PBGDs have a unique prosthetic group called the dipyrromethane cofactor (DPMC) (Jordan and Warren 1987). This cofactor is attached covalently to a cysteine (Cys242 in *E. coli*) residue through a thioether linkage (Jordan et al. 1988b). The cofactor provides a covalent attachment point for the four substrate molecules that form the product (Jordan and Warren 1987; Hart et al. 1988), acting as a primer that is elongated in a stepwise mechanism (Warren and Jordan 1988). Thus the sequential reaction of four deaminated substrate molecules to the DPMC results in enzyme-substrate (ES)

intermediate complexes ES (with one PBG molecule attached), ES2 (with two PBG molecules attached), ES3 and ES4 (Fig 1.7) resulting in the product, preuroporphyrinogen. This product is finally released by hydrolytic cleavage, leaving the DPMC still linked to the enzyme. Interestingly, the DPMC, once formed, remains permanently and covalently bound to the enzyme during catalysis and is not incorporated into the product (Jordan et al. 1988b).

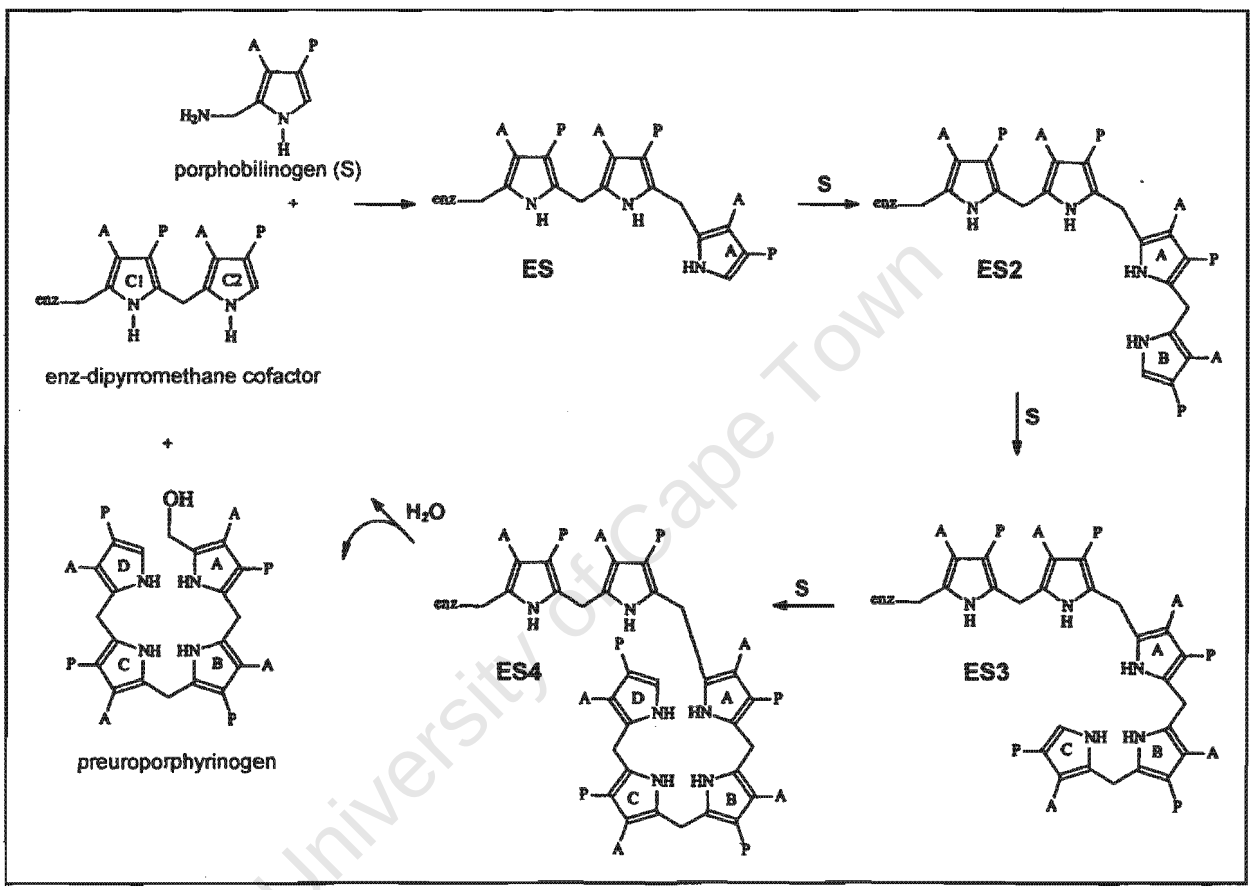

Figure 1.7 The catalytic cycle of PBGD. Porphobilinogen is deaminated and reacts with DPMC to form the ES complex. Successive reactions generate ES_2, ES_3 and ES_4 complexes. A = $-CH_2CO_2H$; P = $-CH_2CH_2CO_2H$

PBGD has been purified from many sources, often as a complex together with the next enzyme in the pathway, UROIIIS (Sancovich et al. 1969; Llambias and Batlle 1970; Frydman and Feinstein 1974) (see next section). Purification is reported from both eukaryotic and prokaryotic sources such as spinach (Higuchi and Bogorad 1975); human erythrocytes (Anderson and Desnick 1980; Corrigall et al. 1991); *R. spheroides* (Davies and Neuberger 1973; Jordan and Shemin 1973); and *E. coli* (Hart and Battersby 1985). The purified

protein exists as a 35 to 44 kDa monomer, with optimal activities at pH 8.0-8.5 (Jordan 1990).

PBGD was the first enzyme of the heme biosynthetic pathway to have its three dimensional (3-D) structure solved (Jordan et al. 1992; Louie et al. 1992). Since then a number of studies have further characterised the enzyme structurally (Lambert et al. 1994; Louie et al. 1996; Shoolingin-Jordan et al. 2003a; Shoolingin-Jordan et al. 2003b). Although the bulk of work has been done on *E. coli*, sequence comparisons between PBGDs from all species suggest they share a similar 3-D structure and mechanism of activity (Louie et al. 1996). The structure of the enzyme in *E. coli* reveals a protein folded into three domains, I (N-terminal), II (central) and III (C-terminal) of approximately 100 amino acids each, linked to one another by flexible strands. Domains I and II despite having a similar topology, make a few direct interactions but form an extensive active site cleft at their interface. Domain III is an open-faced, three-stranded anti-parallel beta sheet, with one face covered by three alpha-helices. The DPMC linked to cysteine 242 (*E. coli* numbering) protrudes from domain III into the mouth of the cleft. The cleft in turn is lined with positively charged, highly conserved arginine residues which form ion pairs with the acidic side chains of the cofactor (Lambert et al. 1994; Louie et al. 1996; Shoolingin-Jordan 1998).

Lambert et al. (1994) showed that flexible segments between domains I and II play a role in a hinge mechanism thereby facilitating conformational changes in the enzyme. In addition, the relatively few hydrophobic contacts between the three domains, suggests that during the stepwise reactions with four porphobilinogen molecules, the enzyme is able to change conformation substantially to accommodate the growing tetrapyrrole chain as the elongation process proceeds (Louie et al. 1996).

In mammals, the *PBGD* gene consists of 15 exons extending over 10kb of DNA (Deybach and Puy 1995). In humans, the gene has been mapped to chromosome 11q23.3 (Chretien et al. 1988). Different isoforms are produced through alternative splicing of exon 1 and 2. Splicing exon 1 to exon 3 results

in the expression of the housekeeping form, *PBGD-H*. The combination of exons 2 and 3 produces an erythroid form, *PBGD-E*. Exon 2 does not contain an AUG translation-initiating codon, and translation of the erythroid-specific mRNA is initiated at an AUG located in exon 3. Exon 1 contains an AUG, which is spliced into the same reading frame as the AUG in exon 3. Thus, translation of *PBGD-H* produces a protein that differs from *PBGD-E* by the absence of 17 amino acids (encoded by exon 1) at its N-terminus (Grandchamp et al. 1987). The thought of only one transcript per tissue-specific form was recently challenged by the discovery of an additional 176bp erythroid-specific transcript (*PBGD-EA*). Interestingly, despite clear demonstration of this transcript (Gubin and Miller 2001) in primary erythroid cell cultures, bone marrow and fetal liver, no expression was present in human erythroleukemia (HEL) cells.

1.4.4 Uroporphyrinogen III Synthase (EC 4.2.1.75) (Uroporphyrinogen III Cosynthase)

The next step in the pathway involves the closure of the tetrapyrrole ring in a reaction catalyzed by the enzyme UROIIIS in which hydroxymethylbilane is converted to uroporphyrinogen III (Jordan 1991).

The reaction involves the elimination of water and the joining of the A and D rings. The cyclization involves the intramolecular inversion of the terminal D ring so that the repeating pattern of acetic acid and propionic acid side chains is interrupted leading to two adjacent acetic acid side chains on the A and D rings (Shoolingin-Jordan 2003) (Fig 1.8). If UROIIIS is absent *in vitro* or not functional *in vivo*, its substrate, hydroxymethylbilane, will cyclize to form uroporphyrinogen I (uro'gen I) (Jordan and Woodcock 1991). Although the cyclization is spontaneous in the absence of enzyme, the conversion of hydroxymethylbilane to uroporphyrinogen III in the presence of UROIIIS, is much faster than the conversion of hydroxymethylbilane to uro'gen I. While uro'gen I can be used as a substrate by the next enzyme in the pathway, it cannot be converted to protoporphyrin and heme. Originally, it was suggested

that UROIIIS was complexed to the previous enzyme in the pathway, but this was later shown not to be the case (Jordan 1990).

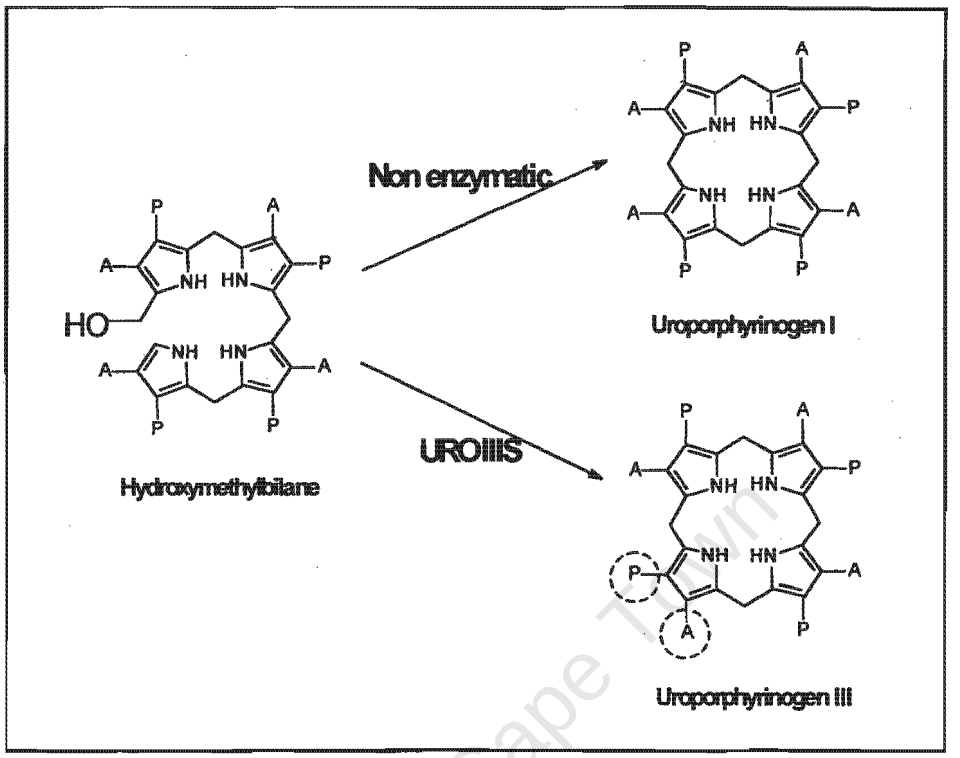

Figure 1.8 Closure of the tetrapyrrole ring by UROIIIS. A = acetate, P = propionate. The interrupted pattern of side chains is indicated by broken circles.

UROIIIS has been isolated and purified to homogeneity from many sources including rat (Kohashi et al. 1984; Smythe and Williams 1988), *Euglena gracilis* (Hart and Battersby 1985), *E. coli* (Alwan et al. 1989) and human erythrocytes (Tsai et al. 1987). There is no evidence for a cofactor and the human enzyme has an isoelectric point of 5.5, and a pH optimum of 7.4 (Tsai et al. 1987; Desnick et al. 1998). All forms appear to exist as monomeric subunits with molecular weights of approximately 30 kDa and are extremely thermolabile (Jordan 1990).

The crystal structure of UROIIIS, resolved at 1.85Å (Mathews et al. 2001), shows some insight into how this comparatively small enzyme (~28kDa) can promote such a complex reaction. The enzyme has a bi-lobed structure reminiscent of a dumb-bell. It is comprised of 2 α/β domains (ie. a combination of α-helices and β-sheets) linked by two anti-parallel β-strands. The N-terminal (domain I) resembles a flavodoxin fold, whereas domain II has

similarities to a DNA glycosylase-like fold. The enzyme's active site has tentatively been identified from the presence of approximately 10 conserved residues, several of which line a cleft between the two α/β domains (Schubert et al. 2002). Three of these residues, Ser63, Tyr168 and Thr228 (human numbering), are thought to be involved in binding catalysis. Interestingly, only the Tyr168 and Thr228 had significant effects on enzyme activity after site-directed mutagenesis experiments showing that Ser63, despite being well conserved, had little effect on catalysis (Mathews et al. 2001; Schubert et al. 2002).

The genes encoding this enzyme have been isolated from several sources including animals and bacteria (Jordan et al. 1988a; Tsai et al. 1988; Amillet and Labbe-Bois 1995; Stamford et al. 1995; Xu et al. 1995). The original isolation of a full-length cDNA for *UROIIIS* revealed 5' and 3' UTRs of 196 and 284bp, respectively. In addition, it showed an ORF of 798bp spanning 10 exons and encoding a protein of 265 amino acids with a molecular mass of 28kDa (Tsai et al. 1988). *UROIIIS* has been mapped to chromosome 10q25-q26.3 (Astrin et al. 1991). Recent information on the genomic organisation of the 34kb human *UROIIIS* gene reveals the presence of 2 promoters that generate housekeeping and erythroid-specific transcripts with unique 5'-untranslated sequences (exon 1-2A) followed by 9 common coding exons (2B-10) (Aizencang et al. 2000; Solis et al. 2001).

The mouse gene, located on chromosome 7 (Bensidhoum et al. 1994), revealed 5' and 3' UTRs of 144 and 623bp, respectively, with an ORF of 798bp encoding a 265 amino acid polypeptide with a molecular mass of 28.5kDa (Xu et al. 1995). The mouse gene shares an 80% nucleotide and 78% amino acid identity with that of the human gene.

1.4.5 Uroporphyrinogen Decarboxylase (EC 4.1.1.37)

UROD, a soluble cytoplasmic protein, catalyses the conversion of uroporphyrinogen III to coproporphyrinogen III. This conversion is accomplished by the successive decarboxylation of the four acetic acid groups to methyl groups and in the process, the production of four molecules of CO_2 (Jordan, 1990) resulting in the formation of 4-carboxylic acid porphyrinogen-III (Jackson et al. 1976).

At physiological substrate concentrations, this reaction occurs in an orderly manner with the carboxyl groups removed in a clockwise direction starting at ring D and proceeding through A, B, and C before the final formation of the coproporphyrinogen-III (Jackson et al. 1976; Luo and Lim 1993) (Fig 1.9). The hepta-, hexa- and penta-carboxylic acid porphyrinogens intermediates formed in this reaction are stable porphyrinogen species which are detectable *in vivo*. Each intermediate acts as the substrate for further decarboxylation until the requisite coproporphyrinogen-III is formed. Although early work on the enzyme speculated there to be more than one enzyme for the decarboxylation reactions (Batlle et al. 1986), it is now known that only one enzyme with broad substrate specificity is involved.

UROD has been purified from human erythrocytes (de Verneuil et al. 1983; Elder et al. 1983; Mukerji and Pimstone 1992; Roberts and Elder 1997); bovine liver (Straka and Kushner 1983); chicken erythrocytes (Kawanishi et al. 1983; Seki et al. 1986); *E. gracilis* (Juknat et al. 1989); *S. cerevisiae* (Felix and Brouillet 1990) and *R. sphaeroides* (Jones and Jordan 1993). Although the UROD proteins were originally suggested to be monomeric (Elder et al. 1983), x-ray crystallography has confirmed the dimeric nature of the protein. Assembly of the dimer aligns the active site clefts opposite one another, suggesting a functionally important interaction between the catalytic centres (Whitby et al. 1998).

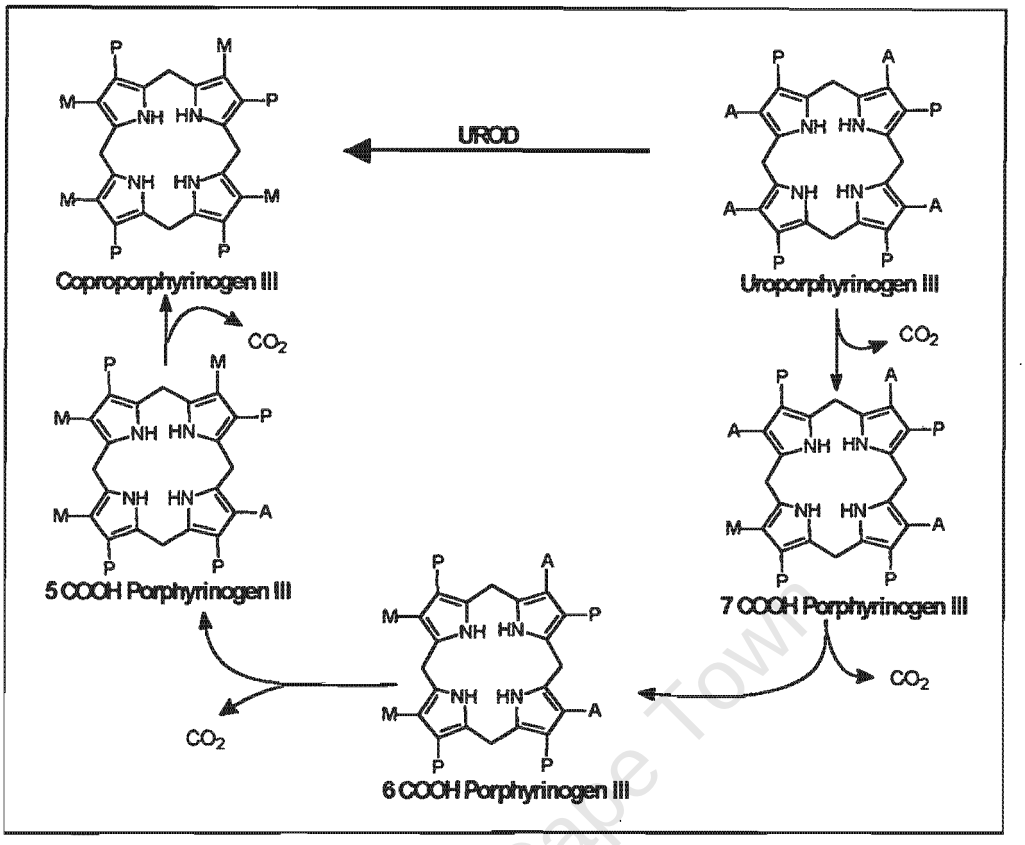

Figure 1.9 Biosynthesis of coproporphyrinogen III from uroporphyrinogen III by UROD. A = acetate, P = propionate, M = methyl.

One active site of a subunit opposite another could be expected to influence the decarboxylation pathway. However, the specificity of UROD for the respective acetic and propionic acid sidechains, make it unlikely that any crucial interactions between the enzyme and the substituents on the rings on either side of the pyrrole occupying the active site, would occur (Shoolingin-Jordan 2003). In addition, it is speculated that the dimeric nature of the enzyme plays a key role in the order of decarboxylation, so that under substrate-limiting conditions intermediates may linger within the confines of the catalytic site and be channelled within the dimeric enzyme structure from one subunit to the other in an ordered process. The conserved residues within the active site, Asp86 and Tyr164 in the human enzyme (Asp82 and Tyr159 in *Nicotiana tabaccum*), have been implicated in the decarboxylation mechanism. The cleft is lined by numerous conserved residues including invariant side chains of Arg37, Arg41 and His339 (human numbering) which are potential candidates for binding the negatively-charged carboxylic acid

side chains (ie. substrate recognition) (Martins et al. 2001a; Martins et al. 2001b).

The genes encoding *UROD* in humans and rat have been cloned, sequenced and characterised (Romeo et al. 1986; Romana et al. 1987b). Sequence homology between the two species show 85% and 90% homology at the DNA and protein levels, respectively (Wu et al. 1996). In humans, *UROD* maps to chromosome 1p34 (de Verneuil et al. 1983; Dubart et al. 1986). The human gene comprises 10 exons with two transcriptional start sites (Romana et al. 1987a), separated by six nucleotides, and the same polyadenylation site. It encodes a 367 amino acid homodimer (Phillips et al. 1997) with a monomeric molecular weight of 40 kDa. Interestingly, the same transcriptional start site is used in all tissues (Romeo et al. 1986).

1.4.6 Coproporphyrinogen oxidase (EC 1.3.3.3)

At this point heme synthesis returns to the mitochondrion where CPOX, the sixth enzyme in the pathway, catalyses the oxidative decarboxylation of coproporphyrinogen III to protoporphyrinogen IX. The 2- and 4- propionate residues of the A and B rings of coproporphyrinogen III are converted to vinyl groups, while the substituents on the C and D rings are untouched (Dailey 1990) (Fig 1.10). Two forms of CPOX exist in nature, an aerobic form found in eukaryotes and an anaerobic form found in some prokaryotes. This chapter focuses on the aerobic form found in eukaryotes.

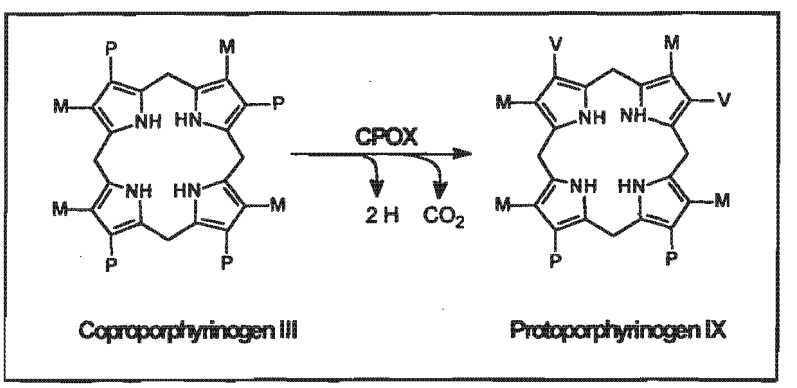

Figure 1.10 Biosynthesis of protoporphyrinogen IX from coproporphyrinogen III by CPOX. P = propionate, M = methyl, V = vinyl.

Aerobic CPOX has been purified from a number of sources including bovine liver (Yoshinaga and Sano 1980), mouse liver (Bogard et al. 1989), and *S. cerevisiae* (Camadro et al. 1986). The gene has been sequenced from a number of sources including barley and tobacco (Kruse et al. 1995), soybean (Madsen et al. 1993), *Salmonella typhimurium* (Xu and Elliott 1993), *E. coli* (Troup et al. 1994), *S. cerevisiae* (Zagorec et al. 1988), mouse (Kohno et al. 1993), and man (Martasek et al. 1994; Taketani et al. 1994). Human CPOX is a globular homodimer with a subunit molecular mass of approximately 50 kDa (Martasek et al. 1997). Expressed in *E. coli* and purified, human CPOX has been found to contain no detectable cofactors or metals (Medlock and Dailey 1996). Although an earlier report suggested that mouse CPOX has a bound copper ion (Kohno et al. 1996), no supporting evidence for such a metal was found for human CPOX (Medlock and Dailey 1996).

Despite being easy to purify, very little information regarding its crystal structure has been published. A recent x-ray report (Colloc'h et al. 2002) comparing urate oxidase and CPOX, concluded that CPOX appears to be divided into two contiguous tunnelling-fold domains ie. the functional CPOX dimer is built around a tunnel with the substrate sitting above it, on the N- and C-terminal side. This model is supported by mutation data and is consistent with the chemical amounts expected for substrate processing by CPOX.

Mammalian CPOX is associated with the inner side of the mitochondrial outer membrane. Being nuclear-encoded, it is initially synthesised in the cytosol as a preprotein before being translocated to the mitochondrion. The newly synthesised CPOX has an N-terminal cleavable presequence. In 1994, Taketani et al. proposed the presequence to be 31 amino acids in length (Taketani et al. 1994). This was in contrast to the 110 amino acid presequence suggested by others at the time (Delfau-Larue et al. 1994; Martasek et al. 1994). Recently, however, mitochondrial targeting studies have shown CPOX to contain the longer leader sequence (Susa et al. 2003). The necessity for this longer leader sequence remains puzzling in light of it being cleaved upon entry to the mitochondrion.

The cDNA sequence of human *CPOX* has been cloned, sequenced and characterized (Delfau-Larue et al. 1994; Martasek et al. 1994; Taketani et al. 1994; Medlock and Dailey 1996). The gene spans approximately 14kb, consists of seven exons and six introns (Delfau-Larue et al. 1994), and is located on chromosome 3q11.2 (Cacheux et al. 1994). It is a single copy gene with multiple transcriptional initiation sites. It contains two polyadenylation signals which play a role in tissue-specific expression of *CPOX* mRNA (Martasek et al. 1997).

1.4.7 Protoporphyrinogen Oxidase (EC 1.3.3.4)

The penultimate step of the pathway is catalyzed by PPOX. As this dissertation focuses on variegate porphyria (VP) and the *PPOX* gene, this enzyme is discussed in detail in the following chapter (Chapter 3).

1.4.8 Ferrochelatase (EC 4.99.1.1) (Protoheme ferrolyase)

The final step in the pathway is the insertion of ferrous iron (Fe^{2+}) into the protoporphyrin IX macrocycle to form heme/ protoheme and is catalyzed by the enzyme FC. The mechanism of this catalysis is relatively conserved among species (Dailey 1996). During catalysis the enzyme transiently binds ferrous iron, protoporphyrin, and heme. For metalation (the insertion of iron), several criteria need to be met namely; porphyrin macrocycle distortion, pyrrole proton loss, outer sphere complexation and iron-ligand dissociation (Lavallee 1988).

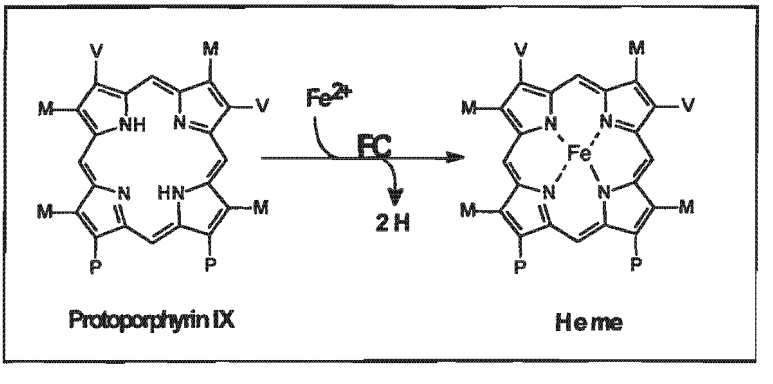

Figure 1.11 Insertion of Iron into protoporphyrin IX molecule by FC. P = propionate, M = methyl, V = vinyl.

FC is thought to follow an ordered sequential "bi-bi" reaction mechanism in which Fe^{2+} binds the enzyme before porphyrin (Dailey and Fleming 1983). Following metal binding to enzyme, the porphyrin undergoes distortion into a non-planar structure that facilitates porphyrin metal-chelation (Lavallee 1988; Blackwood et al. 1997). Raman resonance spectroscopy of yeast FC demonstrated simultaneous tilting, or doming, of all four pyrrole rings on porphyrin distortion (Blackwood et al. 1997; Blackwood et al. 1998). Metal-chelation then occurs with the concomitant removal of the two pyrrolic protons (Fig 1.11).

Since FC binds a planar macrocyclic porphyrin as substrate and releases a planar macrocyclic porphyrin with an iron inserted, the protein must either have a mechanism to distinguish between the two macrocycles, or bind both substrate and product poorly enough that the product will not remain bound to the enzyme following catalysis. The general consensus regarding the insertion of iron into the porphyrin ring is that macrocycle distortion is the most probable and thermodynamically favourable process (Dailey and Dailey 2003).

Eukaryotic FCs were first purified from rat liver (Taketani and Tokunaga 1981) and subsequently from mouse liver (Dailey et al. 1986), bovine liver (Taketani and Tokunaga 1982), human liver (Mathews-Roth et al. 1987) and chicken erythrocytes (Hanson and Dailey 1984) They are nuclear-encoded and synthesised in the cytoplasm as a preprotein with an amino terminal mitochondrial targeting sequence (Karr and Dailey 1988). This sequence targets the precursor protein to the matrix side of the inner mitochondrial membrane. Although this review concentrates on the eukaryotic form of FC, in plants it appears that two FCs are produced, one targeted toward mitochondria and the other toward chloroplasts (Chow et al. 1998). The human ferrochelatase gene encodes a 423 amino acid protein precursor with a molecular weight of 47 kDa. This precursor is modified into a smaller mature protein of 42 kDa through cleavage of a putative leader sequence comprising 54 amino acids at the N-terminus. It is membrane associated with no membrane-spanning domains. Characterisation of human and mouse FCs

demonstrated the presence of a single, labile iron-sulphur [2Fe-2S] cluster at the carboxyl end of the protein (Dailey et al. 1994a; Dailey et al. 1994b).

The determination of the crystal structures of FC from *Bacillus subtilis* (Al-Karadaghi et al. 1997) and man (Wu et al. 2001) have revealed interesting features in the two forms (Table 1.3).

Table 1.3 : Crystallographic data of *B. subtilis* and human FC.

***B.subtilis* (Al-Karadaghi et al. 1997)**	**Human (Wu et al. 2001)**
Crystal structure at 1.9Å, water-soluble monomer	Crystal structure at 2.0Å, m embrane-associated homodimer of 86K
Crystal dimensions = 60 x 39 x 43Å	Crystal dimensions = 65 x 45 x 40Å 48% α-helices; 14% β-sheets
Identifiable cleft containing upper lip of $\alpha 1_l$ and $\alpha 2_l$ and lower lip containing loop between residues 221 and 233	N-terminal loop (residues 95-104) which comprises part of the "lip" of the active site pocket and a C-terminal extension (residues 390-423) involved in co-ordination of the [2Fe-2S] cluster and dimer stabilization
Cleft ~25Å deep; conserved catalytically important residue = H183	12 residue N-terminal α-helical insertion found in the lip region putatively involved in membrane association (Gora et al. 1999; Dailey et al. 2000; Wu et al. 2001)
No [2Fe-2S] cluster	Each active site pocket consists of two hydrophobic lips composed of residues 90-130 and 300-311

A catalytic model (based on modification of previous work (Lavallee 1988)) has been proposed (Dailey and Dailey 2003). In this model, pyrrole proton abstraction occurs from the surface of the porphyrin via a conserved histidine residue (H263, human numbering), with a group of highly conserved carboxylate residues forming a pathway for proton movement away from the active site. The macrocycle is at this point ready to receive a bivalent metal ion. Although FC may catalyse the insertion of other metal ions such as cobalt or zinc, the selection of ferrous iron for chelation is mediated by both enzyme and cell-controlled restriction processes (Dailey 1996). It is suggested that iron entry may be facilitated or regulated via a chain of conserved residues located on the opposite side of the pocket from the His263 residue. Access to

the active site for the two substrates may occur via distinct routes in eukaryotes, with porphyrin entering from the membrane-facing surface and iron approaching from a surface that is separate from the membrane surface proper (Dailey 2002).

Destined to associate with the matrix side of the inner mitochondrial membrane, FC has a 54 N-terminal amino acid presequence which is proteolytically removed upon entry into the mitochondrion. Translocation across the mitochondrial membranes require a transmembrane potential (Karr and Dailey 1988). Studies which involved removal of the targeting sequence (Prasad and Dailey 1995) show FC associated with all cellular membranes but no inner membrane localisation. Interestingly, even with improperly localised enzyme, cells are still able to synthesise sufficient heme for near normal growth.

The *FC* gene was first sequenced from *S. cerevisiae* (Gokhman and Zamir 1990; Labbe-Bois 1990), followed by the murine gene (Taketani et al. 1990; Brenner and Frasier 1991). The human *FC* gene is made up of 11 exons, spans 45 kb (Taketani et al. 1992) and is located on chromosome 18q21.3 (Brenner et al. 1992). The gene is expressed at low levels in all tissue, but is upregulated during erythropoiesis (Lake-Bullock and Dailey 1993). Two mRNAs, transcribed from a single gene, have been isolated differing in their 3' end (Nakahashi et al. 1990; Brenner and Frasier 1991). Predominance of one of these transcripts upon induction of erythropoietic differentiation has suggested that the regulation of transcripts at two different polyadenylation sites may be erythroid and nonerythroid specific (Chan et al. 1993) (see earlier section on Heme regulation).

CHAPTER 2 : THE PORPHYRIAS

CHAPTER 2 : THE PORPHYRIAS

2.1 The Porphyrias

A deficiency of any enzyme (Waldenstrom 1957; Brodie et al. 1977a; Brodie et al. 1977b; Elder and Wyvill 1982; Rimington 1985; Grandchamp and Nordmann 1988; Kappas et al. 1989) detailed in the previous chapter, leads to a specific type of porphyria (Table 2.1). Even though this dissertation focuses on the deficiency of PPOX and the resultant clinical condition, VP (see chapter 3), this chapter briefly summarises the current literature regarding the enzyme deficiency, porphyrin accumulation, genetic mutations and mode of inheritance of the different porphyrias.
The erythroid form of the first enzyme, ALAS-2, is defective in sex-linked sideroblastic anaemia and will not be discussed here.

The clinical sequelae are broadly categorized into two groups, acute neurological attacks and photocutaneous sensitivity. The distinction between the acute and non-acute porphyrias appears to be the potential or non-potential for the precursors (5-ALA and PBG) to accumulate. (Moore 1987). Accumulation of porphyrinogens (or their oxidized forms, porphyrins), appears to be associated with photosensitivity.

The most practical classification for the management of porphyrias, is based on the presence or absence of acute attacks. Thus, the four *acute* porphyrias are ALAD porphyria, AIP, HCP and VP and are associated with neurological symptoms and elevated plasma and urinary concentrations of 5-ALA and PBG. The remaining three porphyrias are never associated with the acute attacks, but may be associated with photcutaneous sensitivity.

Table 2.1 : Summary of the porphyrias.

Disorder	Enzyme	Inheritance	Clinical Effects
ALADP	ALA Dehydratase	AR	AA
AIP	PBG deaminase (Hydroxymethylbilane synthase)	AD	AA
CEP	Uroporphyrinogen III synthase	AR	PS
PCT	Uroporphyrinogen decarboxylase	AD (*however, 80% of cases are the acquired/sporadic form*)	PS
HCP	Coproporphyrinogen oxidase	AD	AA + PS
VP	Protoporphyrinogen oxidase	AD	AA + PS
EPP	Ferrochelatase	AR	PS

ALADP, 5-aminolevulinic acid dehydratase porphyria; AIP, acute intermittent porphyria; CEP, congenital erythropoietic porphyria; PCT, porphyria cutanea tarda; HCP, hereditary coproporphyria; VP, variegate porphyria; EPP, erythropoietic protoporphyria; PBG, porphobilinogen; AR, autosomal recessive; AD, autosomal dominant; AA, acute attacks; PS, photosensitivity.

Worldwide prevalence generally lists PCT, AIP and EPP as the three most common porphyrias. These differ from each other with regard to clinical manifestations, tests that are important for diagnosis, and effective therapies (Anderson 2003). Although the porphyrias have a worldwide distribution, some countries have an exceptionally high frequency (eg. AIP in Scandinavia and variegate porphyria (VP) in South Africa). The high frequency of VP in South Africa has been attributed to a founder effect. PCT is also encountered here (Dean 1971; Meissner et al. 1987; Meissner et al. 1996).

In discussing treatment relating to the porphyrias, one has to bear in mind that although many of the porphyrias are inherited as dominant traits, in most families only a limited proportion of the carriers will express the clinical phenotype of the disease. More will have biochemical abnormalities with few or no symptoms, and mostly an undetermined number may be unaffected in any way other than carrying a specific mutation. Indeed, the lack of phenotype/genotype correlation is a major question currently under

investigation by some workers. It is therefore essential that a holistic approach to therapy be followed. Examinations of patients suspected of having porphyria should include clinical evaluation, biochemical study (which enables one to classify the patient to a specific form of porphyria). If possible, enzymatic assay(s) and genetic studies to confirm an enzyme deficiency, its level, and the causal genetic mutation should follow (Lecha et al. 2003).

Treatment for the porphyrias are generally classified into the same two groups as the presenting symptomology ie. acute attacks and skin disease. Although the underlying biological mechanism of the acute attack is not well known, the marked increase in the production of porphyrin precursors (5-ALA and PBG) during attacks have been well documented (Bonkowsky and Schady 1982; Meyer et al. 1998). Over the last decade, therapeutic approaches to the acute attacks have included those that are specific (glucose and heme administration), supportive (rapid hospitalization) and preventative (investigation and removal of the precipitating cause of the attack).

Although these treatment modalities can be applied in the case of the acute attack (Manning and Gray 1991; Hift et al. 1997), the same cannot be said for the treatment of associated skin disease. For example, treatment approaches using repeated phlebotomy or low-dose chloroquine or hydroxychloroquine may be highly effective in treating patients with PCT. However, VP, HCP, CEP and even mild cases of EPP are unresponsive to these treatment measures (Cramers and Jepsen 1980). Although specific treatment regimes for the porphyrias mentioned here will not be discussed in this chapter, treatment related to VP is discussed in chapter 3.

2.2 Specific Syndromes of Porphyria

2.2.1 Aminolevulinic Acid Dehydratase-Deficient (ALAD) Porphyria

ALAD porphyria is caused by a deficiency in the ALAD enzyme. Although it is customary to abbreviate this porphyria as ALAD porphyria, it was originally termed "Doss porphyria" after the investigator who described the first two cases (Doss et al. 1979). Patients with ALAD genetic defects showed markedly elevated urinary aminolevulinic acid (ALA), but variation of the clinical disease ranged from asymptomatic to a severe porphyric syndrome (Sassa 1998).

ALAD porphyria is inherited as an autosomal recessive trait (Doss et al. 1979; Fujita et al. 1987; Thunell et al. 1987; Kappas et al. 1989, 1995) and is extremely rare with only 7 unrelated cases having been reported since 1979. These were of European, Hispanic or Japanese origin (Doss et al. 1980; Thunell et al. 1987; Hassoun et al. 1989; Wolff et al. 1991; Muraoka et al. 1995). Three cases have been shown to be compound heterozygotes bearing a single base substitution, unique to each patient, on each ALAD allele (Sassa 1998).

2.2.2 Acute Intermittent Porphyria (AIP)

A deficiency in the PBGD enzyme results in AIP. AIP is recognized by a marked overproduction and excretion of porphyrin precursors and porphyrins with increased activity of hepatic 5-ALAS. The condition may remain clinically latent throughout life in many of those who inherit the trait (Deybach and Puy 2003). Symptoms appear any time after puberty, but often not until the third or fourth decade of life, and more commonly in women than men. The disease rarely manifests in childhood (Elder et al. 1997; Grandchamp 1998). The major clinical manisfestations are abdominal pain and other neurovisceral and circulatory disturbances (Bonkowsky and Schady 1982).

AIP is inherited as an autosomal dominant disorder and is generally thought to be the most common type of acute porphyria in most countries. Up to 200

different mutations in the PBGD gene have been identified. These include missense, nonsense, splicing mutations as well as insertions and deletions (Lee and Anvret 1987; Scobie et al. 1990; Gu et al. 1991; Picat et al. 1991; Daimon et al. 1993a; Daimon et al. 1993b; Whatley et al. 1995; Lundin and Anvret 1997; Robreau-Fraolini et al. 2000).

2.2.3 Congenital Erythropoeitic Porphyria (CEP)

CEP or Gunther's disease, was the first recognized porphyria (Gunther 1911). It results from a deficiency in UROS (Romeo and Levin 1969; Deybach et al. 1981). Although the activity of UROS is sufficient for heme formation, lack of activity leads to an accumulation of uroporphyrin I and coproporphyrin I in bone marrow, erythrocytes and plasma. These are excreted in urine and faeces. The marked porphyrin accumulation accounts for the disease manifestations (Anderson 2003). CEP is clinically characterized by a severe cutaneous sensitivity and hemolytic anaemia (de Verneuil et al. 2003). In addition to the cutaneous photosensitivity, there may be photomutilation with contraction of digits, loss of nose, lips and ears (Murphy et al. 1995). These changes usually begin in early life, rather than post-pubertally as is the case with the more typical autosomal dominant disorders. Neuropathic features are not found in this disease, and there is no apparent sensitivity to drugs, hormones, and diet (Kramer et al. 1977; Deybach et al. 1981).

Inherited as an autosomal recessive trait, CEP is genetically heterogenous (Fontanellas et al. 1996; Xu et al. 1996; Desnick et al. 1998) including missense, nonsense, frameshift, splicing defects and promoter mutations. Recently, 4 mutations were found in the gene's erythroid-specific promoter and were shown to impair erythroid-specific transcription to various levels. Significantly these mutations helped identify functionally important GATA1 and CP2 transcriptional binding elements involved in erythroid-specific heme biosynthesis (Solis et al. 2001).

2.2.4 Porphyria Cutanea Tarda (PCT)

PCT, the most common form of porphyria encountered worldwide, results from a deficiency in the UROD enzyme. Decreased UROD activity leads to overproduction, accumulation, and increased excretion of porphyrins formed by oxidation of the substrates and intermediates of this reaction. Based on erythrocyte enzyme activity, PCT can be divided into two types : sporadic (type I) and familial (type II) (de Verneuil et al. 1978). A small number of PCT cases (<5% of reported cases) which are clinically and biochemically indistinguishable from the sporadic form are clustered in families with affected individuals and have been labeled as a type III PCT form (Roberts et al. 1988; D'Alessandro Gandolfo et al. 1989; Held et al. 1989; Bulaj et al. 2000b; Barbieri et al. 2003). However, it is not clear whether this can be classified as a distinctive group as an inheritance pattern has not been established (Bulaj et al. 2000b; Elder 2003).

In sporadic PCT, UROD deficiency occurs in the hepatic tissues with erythrocyte UROD remaining active whereas in the familial form UROD deficiency occurs in all tissues including hepatic and erythroid (Elder and Tovey 1977; Elder et al. 1978). No mutations of the gene for the UROD enzyme or its upstream promoter have been found in sporadic PCT (Brady et al. 2000), although it remains possible that there may be mutations in uncharacterized promoter regions or at other loci (Garey et al. 1993). Clinically, sporadic PCT is clearly associated with a number of related factors which include hepatic iron overload (Edwards et al. 1989), alcohol consumption (Elder 2003), oestrogen therapy (Becker 1965; Roenigk and Gottlob 1970; Bulaj et al. 2000a; Bulaj et al. 2000b) and hepatotropic viruses (Fargion et al. 1992).

Elder and others report that familial PCT accounts for approximately 20% of all their PCT patients (Elder et al. 1989; Held et al. 1989; Koszo et al. 1992) (Adjarov and Elder, 1988; Elder, 2003), and is inherited as an autosomal dominant trait but with low clinical penetrance (de Verneuil et al. 1978), with probably less than 10% of those affected ever developing disease. A variety

of UROD mutations have been found in this form of the disease (Garey et al. 1989; McManus et al. 1996; Moran-Jimenez et al. 1996; Brady et al. 2000; Cappellini et al. 2001), with a few identified in more than one family (Garey et al. 1990; Roberts et al. 1995; Mendez et al. 1998).

Where patients are homoallelic for a UROD mutation, or are heteroallelic for two such mutations, a severe phenotype known as hepatoerythropoietic porphyria (HEP) may result. HEP is rare (only some 30 cases reported to date) (Elder 2003), and is expressed clinically as severe photosensitivity and photomutilation, with onset in childhood (Hift et al. 1993; Meguro et al. 1994; Elder and Roberts 1995; Roberts et al. 1995; Moran-Jimenez et al. 1996).

2.2.5 Hereditary Coproporphyria (HCP)

HCP results from a partial deficiency of CPOX (Elder et al. 1976; Grandchamp and Nordmann 1977; Grandchamp et al. 1977; Nordmann et al. 1977). The most prominent biochemical feature of HCP is accumulation of coproporphyrinogen III. When the disease is active there is a marked increase in coproporphyrinogen III excretion in the urine and faeces. Urinary 5-ALA porphobilinogen and uroporphyrin are also increased during acute attacks. Although the acute attacks in HCP appear to be less frequent and less severe than those experienced in AIP, severe motor neuropathy and death from respiratory paralysis can occur and has been previously reported (Barohn et al. 1994). The presence of skin lesions are rare, with most cases being reported from Britain, Europe and North America (Brodie et al. 1977b; Anderson 2003).

The enzyme deficiency is inherited as an autosomal dominant trait and although a variety of mutations in the *CPOX* gene have been described in HCP, most occur in only one affected family (Martasek 1998; Lamoril et al. 2001), and some involve highly conserved amino acids (Rosipal et al. 1999).

2.2.6 Variegate Porphyria (VP)

VP results from a partial deficiency of protoporphyrinogen oxidase (PPOX, EC 1.3.3.4) that is inherited as an autosomal dominant trait. As the understanding of PPOX deficiency and VP is directly relevant to this dissertation, a detailed review of VP and PPOX follows in chapter 3.

2.2.7 Erythropoietic Porphyria (EPP)

EPP, caused due to the partial deficiency of FC, was reported on in 1961 (Magnus et al. 1961). The disease is described mostly in Caucasians, but occurs in other races as well, including Blacks (Poh-Fitzpatrick 1977). In EPP, excess protoporphyrin-IX accumulates primarily in bone marrow reticulocytes, is increased in circulating erythrocytes and plasma, and excreted in bile and faeces. Urinary porphyrin and porphyrin precursor concentrations are therefore normal in this porphyria (Anderson 2003). Interestingly, the concentrations of protoporphyrin in erythrocytes, plasma and faeces remain relatively stable for many years with liver function and liver protoporphyrin content usually remaining normal (Sarkany et al. 1994).

The major clinical feature associated with EPP is cutaneous photosensitivity. In contrast to PCT, VP, HCP and CEP, which is marked by a vesiculo-erosive pattern of skin injury, EPP's photosensitivity is an immediate hypersensitivity. Characteristically, increased sun exposure leads to problems of burning, stinging and painful erythema and edema in sun-exposed areas. Although not common, hepatic complications may develop and are sometimes the major presenting feature of this disease (Singer et al. 1978). When this occurs, protoporphyrin content of the liver increases markedly leading to its deposition in hepatocytes and bile canaliculi with resultant liver damage (Avner et al. 1981; Bloomer 1988; Berenson et al. 1992). Left untreated, EPP could necessitate liver transplantation (Anderson 2003).

Analyses of the *FC* gene have revealed a number of mutations including missense mutations (Lamoril et al. 1991; Brenner et al. 1992; Imoto et al.

1996), splicing abnormalities (Nakahashi et al. 1992; Sarkany et al. 1994; Wang et al. 1994), intragenic deletions (Todd et al. 1993; Schneider-Yin et al. 1995; Henriksson et al. 1996), and nonsense mutations (Schneider-Yin et al. 1994) associated with functional deficiency of FC. Reports by Bloomer and Rufenacht on patients with protoporphyric liver failure (a severe phenotype) revealed splice site, insertions, deletions or nonsense mutations (Bloomer et al. 1998; Rufenacht et al. 1998). These results establish genetic heterogeneity in the most severe phenotype of protoporphyria. The gene mutations result in a major structural alteration in the ferrochelatase protein (Bloomer et al. 1998). Earlier enzymatic studies performed in some affected families showed EPP to have a complex pattern of inheritance (Bloomer et al. 1976; Norris et al. 1990) suggestive of autosomal dominance (Lamoril et al. 1991; Gouya et al. 2002). However, a study by Gouya et al. (2002) showed that clinical expression of EPP appears to require inheritance of a low expression *FC* allele (IVS3-48T/C) trans to a severe *FC* mutation resulting in an autosomal recessive (AR) pattern of inheritance. A recent UK study confirmed the association between the IVS3-48T/C allele and overt EPP and provided evidence for a minimum prevalence of 3% for AR EPP among the patients (111) studied (Mason et al. 2003).

CHAPTER 3 : PROTOPORPHYRINOGEN OXIDASE AND VARIEGATE PORPHYRIA

CHAPTER 3 : PROTOPORPHYRINOGEN OXIDASE AND VARIEGATE PORPHYRIA

3.1 Introduction

This chapter focuses on PPOX, the penultimate enzyme of the heme biosynthetic pathway, and the disease associated with its deficiency, VP. PPOX is reviewed with respect to its enzymatic mechanism in converting protoporphyrinogen-IX to protoporphyrin-IX, flavin adenine dinucleotide (FAD) binding site and subcellular location. Although PPOX has been isolated, purified and characterized from a number of different eukaryotic and prokaryotic organisms, this chapter will primarily focus on the eukaryotic form. The discovery, isolation and eventual sequencing of the *PPOX* gene are also reviewed. The prevalence of VP, its associated clinical features, and the mutations in the *PPOX* gene leading to the disease, concludes the chapter.

Reaction mechanism : Eukaryotic PPOX (EC 1.3.3.4) catalyzes the conversion of protoporphyrinogen-IX (proto'gen-IX) to the fully conjugated, planar protoporphyrin IX molecule via a six electron oxidation during which the methylene bridges in proto'gen-IX are converted to methene bridges (Fig 3.1).

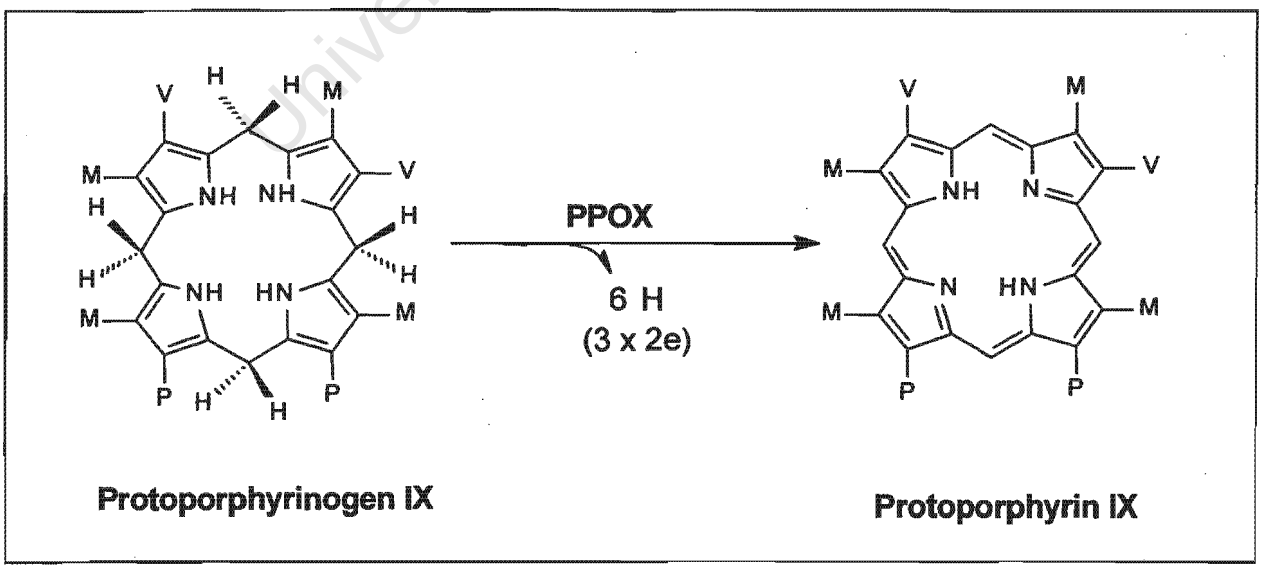

Fig. 3.1 Six electron oxidation of protoporphyrinogen-IX to protoporphyrin-IX by PPOX. M = methyl; P = propionate; V = vinyl.

Proto'gen-IX also undergoes rapid non-enzymatic auto-oxidation in the presence of oxygen and light at neutral and acidic pH (Dailey 1990). To date, in the absence of a crystal structure, there has been very little direct evidence to suggest a catalytic mechanism for eukaryotic PPOX. However, in prokaryotes clearly more than one mechanism exists since these can survive under both aerobic and anaerobic conditions (Klemm and Barton 1987; Camadro and Labbe 1996; de Marco et al. 2000).

Since eukaryotic PPOX contains no redox-active metals, it was postulated that the reaction mechanism involved three two-electron oxidation reactions. Dailey and Dailey (1997) suggested that two possible mechanisms may exist. In the first, PPOX would bind the porphyrinogen substrate and carry out the complete reaction without release of the macrocycles until completion. Alternatively, PPOX may catalyze three independent oxidation reactions with the release of tetrahydro and dihydro- intermediates; a model similar to that of the decarboxylations catalysed stepwise by UROD (Dailey and Dailey 1997). Indeed, preliminary work using stopped flow kinetics support this suggestion (unpublished data, personal communication with Dr Dailey). Recently, the latter suggestion has been supported by a proposed mechanism using stereochemical principles ie. one of the positions on the macrocycle is the site for the oxidation reaction (loss of "hydride") while the other is the site for the tautomerisation process (loss of H+). These processes occur using hydrogen atoms from opposite faces of the macrocycle resulting in the overall transformation being viewed as a three step-wise desaturation process consuming three molecules of oxygen and generating three molecules of hydrogen peroxide (Akhtar 2003).

PPOX protein : Since the initial partial purification of mammalian PPOX from rat liver mitochondria, purification and characterization of the enzyme has been reported from numerous sources including mouse (Dailey and Karr 1987; Ferreira and Dailey 1988; Proulx and Dailey 1992), cattle (Siepker et al. 1987), yeast (Camadro et al. 1994), *R. sphaeroides* (Jacobs and Jacobs 1981), *Aquifex aeolicus* (Wang et al. 2001), barley and soybean (Jacobs and Jacobs 1987; Jacobs et al. 1989); *Desulfovibrio gigas* (Klemm and Barton

1985); spinach (Matringe et al. 1992; Watanabe et al. 2000); *Arabidopsis thaliana* (Narita et al. 1996), tobacco (Lermontova et al. 1997), potato plant (Johnston et al. 1998) and maize (de Marco et al. 2000). The molecular weights for the oxygen-dependent PPOXs lie within the range 51-57kDa and it appears that most of these exist either as monomers as in *B. subtilis* (Dailey et al. 1994), *S. cerevisiae* (Camadro et al. 1994), and bovine enzymes (Siepker et al. 1987), or homodimers as in mouse (Dailey et al. 1995), *Myxococcus xanthus* (Dailey and Dailey 1996a) and human PPOX (Nishimura et al. 1995b; Dailey and Dailey 1996b). All PPOXs are relatively specific for their natural substrate proto'gen-IX though most will oxidise the non-physiological dicarboxylic mesoporphyrinogen IX to a limited extent. *B. subtilis* PPOX can additionally utilise coproporphyrinogen III as a substrate (Dailey et al. 1994).

Siepker et al. (1987) were the first to draw attention to the presence of a tightly bound flavin adenine dinucleotide in the bovine liver enzyme. This claim was subsequently supported for the mouse liver enzyme by Proulx and Dailey (1992) who characterized the flavin in the enzyme as flavin mononucleotide (FMN). The aerobic bacterium *M. xanthus* was reported to be a flavoprotein non-covalently associated with FAD (Dailey and Dailey 1996b). The identification of the flavin cofactor in association with PPOX was an important discovery since it shed light on the ability of the protein to transfer six electrons during the oxidation of protoporphyrinogen-IX. The cloned human enzyme was found to contain 0.5 FAD per PPOX monomer and since the enzyme was shown to be a dimer, the enzymatically functional protein contains one FAD molecule. Gene/protein homology sequence analysis show that PPOXs are members of a protein superfamily which contain the human (Nishimura et al. 1995b), mouse (Taketani et al. 1995b), plant (Narita et al. 1996), yeast (Camadro and Labbe 1996), and bacterial (Dailey and Dailey 1996b) forms of PPOX, animal phytoene desaturases and monoamine oxidases (Dailey and Dailey 1998). These proteins share significant sequence homology in a 60 N-terminally-located amino acid region that includes the βαβ-ADP binding fold forming part of the dinucleotide cofactor binding motif (GXGXXG) presumably involved in flavin binding in PPOX (Fig. 3.2) (Dailey et al. 1994; Camadro and Labbe 1996; Hansson et al. 1997).

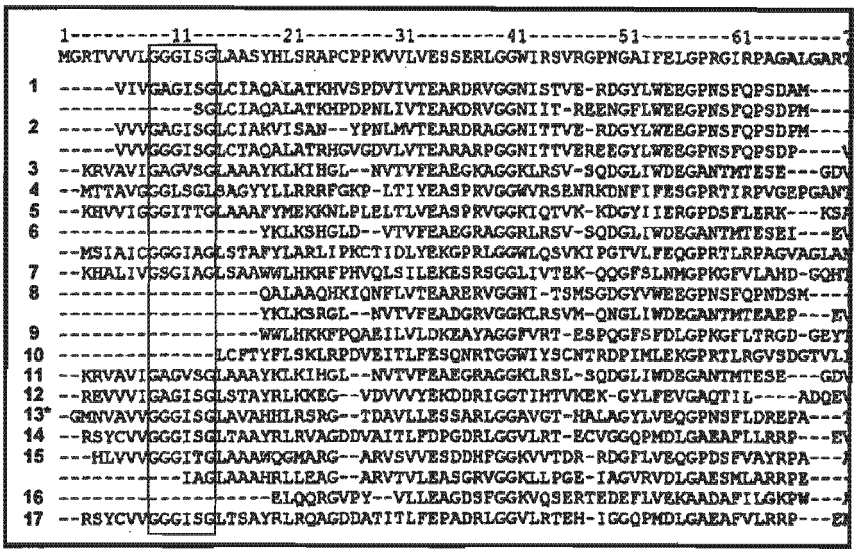

Fig. 3.2 Sequence alignment of the first 70 amino acid residues of PPOX from 18 different organisms using the Jpred multiple sequence alignment program (www.expasy.ch). *Top,* human PPOX (*H. sapiens*). Seventeen PPOX sequences are numbered on the left. 1, *Cichorium intybus (chicory)*; 2, *Solanum tuberosum*; 3, *Nicotiana tabacum*; 4, *Drosophila melanogaster*; 5, *Bacillus subtilis*; 6, *Glycine max (soybean)*; 7, *Chlamydia trachomatis*; 8, *Chlamydomonas reinhardtii*; 9, *Chlamydomonas pneumoniae*; 10, *Saccharomyces cerevisiae*; 11, *Solanum tuberosum*; 12, *Aquifex aeolicus;* 13, *Myxococcus xanthus*; 14, *Mycobacterium leprae;* 15, *Propionibacterium freudenreichii*; 16, *Dynococcus radioduran*; 17, *Mycobacterium tuberculosis*. *Red boxed area,* highly conserved dinucleotide-binding motif (GXGXXG).

PPOX structure : The PPOX crystal structure remains unsolved. However, improved molecular techniques such as site-directed mutagenesis, and the application of structural biological principles in combination with predictive software technology, have allowed some insight into the overall structure of PPOX. Indeed, reports by Fraunberg et al. (2003) and Morgan et al. (personal communication) in addition to results from this study, sheds some more light on PPOX structure (summarized in chapter 7, table 7.1).

Subcellular localization : Although PPOX was originally reported to be solubilized and isolated from a rat mitochondrial membrane fraction, the precise submitochondrial location was only established in 1985 (Deybach et al. 1985). Using a mitochondrial sub-fractionation method involving digitonin,

these researchers showed that the enzyme was embedded within the inner membrane of rat liver mitochondria. The existence of PPOX embedded in the lipid inner mitochondrial membrane in isolation was questioned by Ferreira et al. (1988). They suggested that the substrates of both PPOX and FC would not be expected to be freely present in the hydrophobic milieu of the phospholipid bilayer. Alternatively, they proposed that the terminal three enzymes of the biosynthetic pathway: CPOX, PPOX and FC are arranged in a complex where the product of one enzyme could be directly channeled to the next without being diluted in the phospholipid matrix. In addition, the close association of PPOX and FC may help explain the accumulation of both copro- and protoporphyrins in the excretions of VP patients (Ferreira et al. 1988). However, later studies using radiolabeled substrates and quantification of substrate utilization and product formation, demonstrated that substrate channeling between the terminal three enzymes is not obligatory (Proulx et al. 1993).

The majority of mitochondrial-destined proteins are nuclear-encoded and possess specific characteristics within the first 20-60 amino acid residues (presequences) which confer mitochondrial targeting specificity (see chapter 4). Although the presequences/mitochondrial targeting sequences do not show amino acid homology, they do share similar physico-chemical properties such as having a net positive charge and the ability to form amphiphilic α-helices (von Heijne 1985; Roise and Schatz 1988). It was previously reported that the *PPOX* gene did not encode typical mitochondrial targeting and import sequences or contain membrane-spanning regions (Puy et al. 1996; Kirsch et al. 1998). A recent report to the contrary (Von Und Zu Fraunberg et al. 2003), remains the only information published thus far regarding translocation of human PPOX from the nucleus, targeting to the outer mitochondrial membrane, binding with outer membrane machinery and import into the mitochondrion.

Although a number of previous studies involving other PPOX species (Arnould et al. 1999; Che et al. 2000; Watanabe et al. 2000; Watanabe et al. 2001) highlight certain features indicative of mitochondrial targeting, lack of

sequence homology make it hard to correlate these to human PPOX. For example, work with yeast PPOX suggested that the protein is synthesized as a precursor that is rapidly converted to the active form but that this maturation does not involve the removal of an N-terminal mitochondrial targeting sequence (Camadro et al. 1994; Camadro and Labbe 1996). Furthermore, later work showed that yeast PPOX is anchored to the inner mitochondrial membrane by amphipathic helical domains through the process of acylation (Arnould et al. 1999). Neither of these features have been reported for human PPOX. Interestingly, the yeast PPOX sequence contains several hydrophobic domains, none longer than 15 residues, and is therefore unlikely to form membrane-spanning segments (Arnould et al. 1999). Although human PPOX has no reported transmembrane-spanning domains, a recent study by von und zu Fraunberg et al. (2003) highlights the necessity of an N-terminal hydrophobic motif (LXXXIXXL, residues 8-15) for efficient mitochondrial targeting.

An important feature of PPOX mitochondrial targeting highlighted by the von Fraunberg group concerns additional downstream (ie. internal) mitochondrial targeting sequences of the "primary" N-terminal sequence. By using PPOX-GFP fusion constructs, these workers show that the human PPOX sequence with the first 24 residues removed, still targets the mitochondrion suggesting the possibility of additional downstream/internal mitochondrial targeting signals. Although not common, examples of such proteins include the cytochrome heme lyases (Folsch et al. 1996; Arnold et al. 1998; Diekert et al. 1999). von und zu Fraunberg et al. (2003) suggest that an additional downstream targeting signal may act as a "secondary" backup signal in patients who have a mutation in the "primary" N-terminal signal as in the case of their homozygous patient with an I12T mutation. Interestingly, recent work in which fused human PPOXs containing N and C-terminal deletions or missense mutations show that all the information required for efficient mitochondrial import is contained within the first 250 amino acids of PPOX with a "major" import signal located between residues 151 and 175 thus suggesting that the more proximal N-terminal signal is required as an additional targeting signal for fully efficient import (Morgan et al., personal communication).

PPOX gene : Cloning and expression of the *B. subtilis hemY* gene in *E.coli* (Hansson and Hederstedt 1992; Dailey et al. 1994) paved the way toward the the eventual sequencing and expression of prokaryotic *PPOXs* from *B.subtilis* (Hansson and Hederstedt 1992), *E.coli* (Sasarman et al. 1993) and *M. xanthus* (Dailey and Dailey 1996a). *PPOX* genes have also been identified and sequenced in mouse (Dailey et al. 1995), yeast (Camadro and Labbe 1996), spinach (Che et al. 2000); *Arabidopsis thaliana* (Narita et al. 1996), *Nicotiana tabacum* (tobacco plant) (Lermontova et al. 1997) and potato (Johnston et al. 1998). There are currently 17 *PPOX* sequences listed in Genbank (Fig 3.2).

The human *PPOX* gene (*HPPOX*) encodes a 477 amino acid protein with an associated molecular weight of 50.8kDa (Nishimura et al. 1995a). The coding sequence is 1431 nucleotide base pairs (bp), comprising 13 exons spanning a region of approximately 5.5kb (Roberts et al. 1995). This 5.5kb region includes a promoter and enhancer sequence 660bp upstream from the initiation site (Puy et al. 1996). The promoter region contains a Sp1 factor, CCAAT and GATA-1 motifs involved in gene regulation (Taketani et al. 1995a; Dailey and Dailey 1996b; Puy et al. 1996). Exon 1, 9bp of exon 2 (5' region) and the last 300bp of exon 13 (3' region) represent the untranslated regions. *HPPOX* has a single mRNA transcript of 1.8kb. Other regulatory regions found in the gene include start and termination codons, a 5'-UTR stem-loop structure (Dailey et al. 1995) and a consensus polyadenylation signal and polyadenylation site downstream from the termination site (Taketani et al. 1995a; Dailey and Dailey 1996b; Puy et al. 1996).

Although originally assigned to chromosome 14q32 (Bissbort et al. 1988), using fluorescent *in situ* hybridization, *HPPOX* is now known to be located on chromosome 1q22-23 (Roberts et al. 1995; Taketani et al. 1995a).

3.2 Variegate Porphyria (VP, MIM 176200)

VP is a low penetrance, autosomal dominant disorder, associated with both acute attacks and photosensitivity, and results from a deficiency in the PPOX enzyme.

Prevalence : The prevalence of VP in South Africa has never been accurately determined as the disease is frequently both clinically and biochemically non-expressed. Currently it is suggested that as many as 30 000 South Africans may carry the gene defect (Meissner et al. 2003). The R59W mutation in exon 3 was the first SA mutation to be reported (Meissner et al. 1996a) and is prevalent in approximately 95% of all SA VP cases. The R59W defect in SA originated in the Netherlands as mutational analysis and microsatellite marker linkage have confirmed a direct relationship between South African and Dutch VP patients (de Rooij et al. 1997a). The identification of a VP-causing mutation in the *PPOX* gene in a black South African has also shown VP to exist, although rare, in the indigenous peoples of Africa (Corrigall et al. 2001). Besides VP being common in SA due to a founder effect, it has a worldwide distribution with cases having been reported from the USA and Europe and the UK (Corey et al. 1980; Mustajoki 1980; Deybach et al. 1981; Martasek et al. 1983; Tidman et al. 1989; Herrick et al. 1991; Aquaron et al. 1992; Whatley et al. 1999). In the UK, VP has been estimated to occur with a prevalence roughly one-third that of AIP, or approximately 0.5 per 100 000 (Elder 1997), whereas in Finland, the prevalence has been estimated at 1.3 per 100 000 (Mustajoki 1980). Other early reports of VP include cases from India (Handa et al. 1975); Taiwan (Tu, JB, Metabolism, 1971); Japan (Kodama et al. 1979); Israel (Krakowski et al. 1979), Australia (Coakley et al. 1990) and Central Africa (Durosinmi et al. 1991).

3.2.1 Clinical features

VP presents with two principal clinical features: acute neurovisceral crises (attacks) and photocutaneous sensitivity (skin disease). Clinical symptoms only manifest post-pubertally. Early reports describe the absence of clinical symptoms in 10% of patients (Eales et al. 1980). Currently in South Africa ~61% of patients are asymptomatic (Hift et al. 1997).

Acute attack : Currently acute attacks are relatively uncommon, and most patients with any of the acute porphyrias will never experience an attack at all. Indeed, the incidence of acute symptoms has been estimated to be 10-20% for AIP (Kappas et al. 1995); 30% for HCP (Martasek 1998) and 4% for VP (Meissner et al. 2001).

Clinically, the acute attack presents as episodic and may or may not be associated with an obvious precipitating event (such as the administration of porphyrinogenic medication or menstruation). The attack is characterized by a typical constellation of symptoms; notably severe abdominal pain, vomiting, ileus and constipation (Kirsch et al. 1998) accompanied by few clinical signs and by an absence of peritonism and features of autonomic neuropathy (Yeung Laiwah et al. 1987; Blom et al. 1996). If untreated, these may proceed to a motor neuropathy resembling the Guillain-Barre syndrome (McEneaney et al. 1993; Bont et al. 1996). This neuronal injury is characterised by severe axonal necrosis (Winderbank and Bonkovsky 1992) and once established, it is slowly reversible and typically months to years are required before full function is regained (Meyer et al. 1998).

The pathogenetic mechanisms whereby the acute attack is established are poorly understood. The most likely hypotheses include ALA neurotoxicity and haem deficiency, acting either directly within the neuron or via a deficiency of one or more essential haemoproteins (Meyer et al. 1998).

Skin disease : A cardinal feature of this aspect is the increased fragility of the skin of the sun-exposed surfaces of the face and dorsal surfaces of the

hands. In addition, minor traumas can lead to detachment of the epidermis from the dermis with a resulting blister or raw area oozing serum. These lesions generally heal rapidly with minimal scarring in the absence of infection but secondarily affected lesions could lead to disfiguring pigmented scars or areas of depigmentation. An associated facial feature includes hypertrichosis (Hift 2000). The presence of an immediate photosensitivity in patients with VP, more typical of EPP, has been reported in other studies (Rimington and Belcher 1967; Mustajoki and Koskelo 1976; Mustajoki 1978).

3.2.2 Biochemical profile

VP was described clinically and biochemically in 1937 (Van den Bergh and Grotepass 1937) and it was realised that, unlike AIP and CEP, the biochemical hallmark of this disease was the over-excretion of porphyrins in the stool (Barnes 1945, 1958). Today we know that abnormal porphyrin excretion is usually only apparent after puberty and thus, appropriate tests must be chosen according to the circumstances and the index of suspicion. In addition, diagnoses have been further enhanced with the elucidation of the DNA sequence for PPOX in 1995 which has now allowed a diagnosis based not only on biochemical characteristics, but also on a molecular approach.

3.2.3 Diagnosis of VP

Stool and Urine

For many years the standard method for diagnosis of VP was urine and stool porphyrin analysis. In overt VP large amounts of coproporphyrin and protoporphyrin are present in the stool in both the acute and non-acute phase (Hift 2000). In the acute attacks the excretion of urinary PBG and porphyrins is greatly increased and is accompanied by an increase in faecal uroporphyrin and, to a lesser extent, hepta- (C7), hexa- (C6) and pentacarboxylic (C5) porphyrin in addition to the already raised later-occurring porphyrin intermediates (Hift 2000).

Plasma

A newer, better technique is plasma porphyrin fluorescence scanning (Poh-Fitzpatrick 1980). Plasma is scanned for porphyrin fluorescence at an excitation wavelength of 405nm between 580 and 650nm (emission). An emission maximum of 625-626nm is reported to be a specific test for VP and will distinguish it from PCT (emission maximum of 619nm) (Corey et al. 1980; Long et al. 1993; Gregor et al. 1994; Da Silva et al. 1995). Interestingly, a recent study by Hift et al. (2003) illustrates that the traditional stool porphyrin analysis is poorly sensitive in detecting gene carriers. In contrast, plasma fluoroscanning is considerably more sensitive in detecting carriers. However, neither test is useful in children and mutational detection analysis (see below) remain the most appropriate test (Hift et al., 2003).

PPOX activity

Although PPOX activity has been demonstrated in cultured skin fibroblasts, peripheral leukocytes and lymphocytes, cultured lymphoblasts and hepatocytes (Brenner and Bloomer 1980; Deybach et al. 1981; Viljoen et al. 1983; Meissner et al. 1986; Li et al. 1989), the low levels of expressed activity, coupled with difficulties of the assay make this a much less useful modality in the diagnosis of VP. Interestingly, with the sequence of PPOX known and the availability of improved molecular techniques, one could postulate a technique based on analyses of patient blood. This would involve the transcription of PPOX from mRNA using RT-PCR methodology, cloning of the defective gene cDNA into expression vectors and expression of the protein via an *in vitro* bacterial system. One would therefore be obtaining an "in vivo" picture using "*in vitro*" methodology. Although feasible, the time and expense used to perfect this assay render it impractical as a routine diagnostic test. However, this could theoretically be used under certain circumstances to characterise a VP-causing mutant PPOX.

DNA mutational analysis/genetic screening

DNA mutational analysis for the diagnosis of VP has to be tempered with the knowledge that VP is a heterogenous genetic condition. In the 8 years following the first descriptions of mutations in the *PPOX* gene sequence accounting for VP (Deybach et al. 1996; Kauppinen et al. 1996; Meissner et al. 1996b; Roberts et al. 1996; Warnich et al. 1996), more than 115 mutations have been identified in families with VP from around the world (Table 3.1). In addition to the R59W defect in SA (Meissner et al. 1996b) 9 other mutations have been reported (Meissner et al. 2003), further highlighting the heterogeneity of this condition. However, the contribution of these 9 to the pool of the disease is small, and thus in South Africa alone, screening for the R59W defect is highly sensitive and specific for the diagnosis of VP.

PPOX mutations responsible for VP

The rapid accumulation of mutation data is undoubtedly due to the availability of automated sequencing available to molecular geneticists. The mutations in *PPOX* comprise small insertions or deletions introducing a frame shift and a premature stop codon (32.2%), in-frame insertions or deletions (2.5%), missense mutations, including whole codon deletions and some that alter the initiation codon (42.3%), changes in invariant nucleotide splice sites (16.1%), or, in one (IVS7-9T>G), the creation of an additional splice acceptor site used in preference to the normal site and nonsense mutations (6.8%). These figures are based on an analysis of the mutations listed in table 3.1. Although allelic heterogeneity extends to a number of other countries (Table 3.1), founder effects have been reported in Finland where a single point mutation (R152C) accounts for 60% of all VP families (Kauppinen et al. 1997), and Chile where a frameshift mutation in exon 11 (1194-1198delTACAC) is found in 4 unrelated families (Frank et al. 2001a).

Table 3.1 Reported sequence variations in the PPOX gene. Mutations are numbered from the A of the initiating methionine codon of the PPOX cDNA sequence reported by Nishimura et al. (1995) (Genbank Accession no. D38537). Certain mutations have been redesignated in accordance with this convention but the original reported notation used by the reporting authors is stated in the comments.

Exon/Intron and Mutations	Effect	Country	No. of families	References and Comments
EXON 2				
1A>G	M1V	France	1	(Whatley et al. 1999)
1A>C	M1L	France	1	(Whatley et al. 1999)
1A>T	M1L	Lebanon	1	(Frank et al. 1999)
2T>C	M1T	Ireland / Poland	1	(Frank et al. 1999)
3G>C	M1I	France	1	(Whatley et al. 1999)
3G>A	M1I	Sweden	1	(Wiman et al. 2003)
31G>A	G11S	USA	1	(Frank et al. 2001b)
35T>C	I12T	Finland	2	(Kauppinen et al. 1997); (von und zu Fraunberg and Kauppinen 2000), (reported as 35C>T, presumed misprint); (Kauppinen et al. 2001), Compound heterozygote with P256R.
45G>C	L15F	UK	7	(Whatley et al. 1999)
		SA	1	(Corrigall et al. 2001)
59A>C	H20P	SA	1	(Warnich et al. 1998); (Hift et al. 1997)
78insC	Frameshift, premature stop codon	Finland	1	(von und zu Fraunberg and Kauppinen 2000); (von und zu Fraunberg et al. 2001)
INTRON 2				
IVS2-2A>C	Splicing defect, premature stop codon in exon 3	Finland	1	(von und zu Fraunberg and Kauppinen 2000); (von und zu Fraunberg et al. 2001)
EXON 3				
113G>C	R38P	France	1	(Whatley et al. 1999)
119G>A	G40E	France	1	(Whatley et al. 1999)
157-160delATCT	Frameshift, premature stop codon	UK	1	(Whatley et al. 1999); (Donnelly et al. 2002)
165insAG	Frameshift, premature stop codon	Germany	1	(Lam et al. 1997)
175C>T	R59W	SA	Common, founder mutation	(Meissner et al. 1996b); (Warnich et al. 1996)
		Holland	5	(de Rooij et al. 1997b)
199-200insT	Frameshift, premature stop codon	France	1	(Whatley et al. 1999)
202G>A	G68R	Italy	1	(D'Amato et al. 2003)
218T>C	L73P	UK, Italy	1	(Whatley et al. 1999), (Di Pierro et al. 2003)
INTRON 3				
IVS3-1G>C	Splicing defect, deletion of exon 4	France	1	(Whatley et al. 1999)
EXON 4				
251T>G	V84G	UK	1	(Whatley et al. 1999)
254T>C	L85P	France	2	(Whatley et al. 1999)
306insC	Frameshift;premature stop codon	Italy	1	(Patti et al. 2003)
317A>C	H106P	Argentina	1	(De Siervi et al. 2000)
338G>C	Splicing defect, deletion of exon 4, premature stop codon in exon 5	Finland	2	(von und zu Fraunberg et al. 2001)

INTRON 4				
IVS4+1G>A	Splicing defect	USA	1	(Frank et al. 2001b), reported as 337+1G>A in text and 333+1G>A in table 1.
EXON 5				
363-364insC	Frameshift, premature stop codon	UK	2	(Whatley et al. 1999)
376-377delCT	Frameshift, premature stop codon	UK	1	(Whatley et al. 1999)
384G>A	W129U (stop codon)	Italy	1	(D'Amato et al. 2003)
396G>T	E133X (nonsense mutation)	Germany	1	(Frank et al. 1998b)
413G>C	R138P	SA	1	(Corrigall et al. 2000b), compound heterozygote with R59W
418_419delAA	Frameshift, premature stop codon	Italy	1	(D'Amato et al. 2003)
428A>T	D143V	France	1	(Whatley et al. 1999)
454C>T	R152C	France, Sweden	1	(Whatley et al. 1999); (Wiman et al. 2003)
		Finland	2	(Kauppinen et al. 1997);133;136
460del23	Frameshift, premature stop codon	UK	1	(Whatley et al. 1999)
461T>C	L154P	France	1	(Whatley et al. 1999)
470A>C	Deletion of exon 5 and 20bp retention of intron 5	Finland	1	(von und zu Fraunberg et al. 2001)
INTRON 5				
None reported to date				
EXON 6				
472G>A	V158M	France	1	(Whatley et al. 1999)
472G>C	V158L	Sweden	1	(Wiman et al. 2003)
502C>T	R168C	SA	1	(Meissner et al. 1996b); (Warnich et al. 1996), compound heterozygote with R59W
503G>A	R168H	France/UK	2	(Whatley et al. 1999)
		Holland	1	(de Rooij et al. 1997b)
		USA / Germany	No detail	(Frank et al. 1997)
		Chili	3	(Frank et al. 2001a)
G505G>A	G169E	UK	1	(Roberts et al. 1998);(Frank et al. 1998d), compound heterozygote with G358R
515C>T	A172V	France	1	(Whatley et al. 1999)
528-529insT	Frameshift, premature stop codon	France	1	(Whatley et al. 1999)
532C>G	L178V	Argentina	1	(De Siervi et al. 2000)
538-539delAT	Frameshift, premature stop codon	SA	1	(Corrigall et al. 1998), reported as 537delAT
		UK	2	(Whatley et al. 1999)
542-556del15	Frameshift, premature stop codon	France	1	(Whatley et al. 1999)
565delC	Frameshift, premature stop codon	UK	1	(Whatley et al. 1999)
565C>T	Q189X (nonsense mutation)	UK	4	(Whatley et al. 1999), reported as E189X
		US/Holland	1	(Frank et al. 2001b)
571G>T	E191X (nonsense mutation)	US / Germany	1	(Frank et al. 2001b)
593T>G	L198X (nonsense mutation)	France	1	(Whatley et al. 1999)
604delC	Frameshift, premature stop codon	Sweden	1	(Wiman et al. 2003)
614C>T	A205V	Sweden	1	(Wiman et al. 2003)
INTRON 6				
IVS6+1G>T	Deletion of exon 6	France	1	(Whatley et al. 1999)
IVS6-1G>T	Deletion of exon 7	France	1	(Whatley et al. 1999)
IVS6+7G>A	Not determined (but relatively close to intron/exon boundary)	Denmark	1	(Christiansen et al. 2001)

EXON 7				
657ins12	A219KANA	UK	1	(Roberts et al. 1998), compound heterozygote with IVS11-11T>G
657-658ins12	A219KASA	UK	1	(Palmer et al. 2001), Compound heterozygotes with IVS11-1G>A
672G>A	W224X (nonsense mutation)	France	2	(Whatley et al. 1999)
694G>C	G232R	France, Italy	2,1	(Deybach et al. 1996);(Whatley et al. 1999);(D'Amato et al. 2003)
695G>C	G232R	France	1	(Whatley et al. 1999)
745-746insC	Frameshift, premature stop codon	France	1	(Deybach et al. 1996); (Whatley et al. 1999)
745-746insG	Frameshift, premature stop codon	France	1	(Deybach et al. 1996); (Whatley et al. 1999)
745delG	Frameshift, premature stop codon	France and UK	2	(Whatley et al. 1999)
759delA	Frameshift, premature stop codon	Italy	1	(D'Amato et al. 2003)
759-760delAG	Frameshift, premature stop codon	Japan	1	(Maeda et al. 2000), reported as 759delAG
769delG;770T>A	Frameshift, premature stop sodon	SA	1	(Corrigall et al. 2001)
803G>A	W268X (nonsense mutation)	UK	2	(Whatley et al. 1999)
INTRON 7				
IVS7+2T>C	Deletion of exon 7	UK	1	(Whatley et al. 1999)
IVS7+1del18	Splicing defect, exon 7 deleted	UK	1	(Roberts et al. 1998), compound heterozygote with G358R
IVS7-9T>G	Creation of an additional splice acceptor site results in 8bp added to 5' end of exon 6	UK	1	(Whatley et al. 1999)
EXON 8				
841-843delCAC	H281del	France	3	(Whatley et al. 1999)
848T>A	I283N	Italy	1	(D'Amato et al. 2003)
849insT	Frameshift, premature stop codon	Holland	1	(de Rooij et al. 1997b), reported as 1126+T
845T>A	V282D	UK	2	(Whatley et al. 1999)
851G>T	S284I	Italy	1	(Patti et al. 2003)
856delA	Frameshift, premature stop codon	France	1	(Whatley et al. 1999)
868G>A	V290M	SA	1	(Corrigall et al. 2001)
868G>C	V290L	UK	1	(Whatley et al. 1999)
915-916delTG	Frameshift, premature stop codon	US/Italy	1	(Frank et al. 2001b)
INTRON 8				
None reported to date				
EXON 9				
872T>C	L291P	Holland	5	(de Rooij et al. 1997b)
884T>C	L295P	UK	6	(Whatley et al. 1999)
916-917delCT	Frameshift, premature stop codon	Sweden	1	(Wiman et al. 2003)
INTRON 9				
IVS9-1G>C	Deletion of exon 10	UK	1	(Whatley et al. 1999)
EXON 10				
988G>C	G330R	Sweden	1	(Wiman et al. 2003)
998A>T	H333L	Holland	1	(de Rooij et al. 1997b), reported as within exon 9
1004T>G	V335G	France	1	(Whatley et al. 1999)
1013C>G	S338X (nonsense mutation)	Italy	1	(D'Amato et al. 2003)
1043A>G	Y348C	SA	1	(Corrigall et al. 2000a), compound heterozygote with R59W
1046A>C	D349A	UK	1	(Roberts et al. 1998), homozygote
1048T>C	S350P	UK	1	(Whatley et al. 1999)

1061C>T	P354L	Italy	1	(Bonuglia et al. 2003), compound heterozygote with 397G>A
1072G>A	G358R	UK	2	(Roberts et al. 1998), compound heterozygotes with G169E and IVS7+1del18 (Frank et al. 1998d)
1043-1044insT	Frameshift, premature stop codon	Argentina	2	(De Siervi et al. 2000), reported as 1320insT
1053-1054insT	Frameshift, premature stop codon	UK	1	(Whatley et al. 1999)
1081-1082insG	Frameshift, premature stop codon	UK	1	(Whatley et al. 1999)
1082-1083insC	Frameshift, premature stop codon	France	6	(Whatley et al. 1999)
1083delT	Frameshift, premature stop codon	France	1	(Whatley et al. 1999)
		USA	1	(Frank et al. 2001b)
1083-1084insG	Frameshift, premature stop codon	France	1	(Whatley et al. 1999)
1090-1091delAG	Frameshift, premature stop codon	UK	1	(Whatley et al. 1999)
1091insA	Frameshift, premature stop codon	USA	1	(Frank et al. 2001b)
1093G>A	V365M	No details	No details	(Frank et al. 1997)
INTRON 10				
IVS10-1G>T	Deletion of exon 11	France	1	(Whatley et al. 1999)
IVS10+1G>A	Aberrant splicing, premature stop codon	China	1	(Lam et al. 2001)
IVS10+2T>G	Splicing defect	Italy	1	(D'Amato et al. 2003)
EXON 11				
1106T>C	L369P, predicted to be disease related considering introduction of non-flexible proline	Denmark	1	(Christiansen et al. 2001), reported as 1383T>C
1119G>A	W373X	France	1	(Whatley et al. 1999)
1123C>T	Q375X (nonsense mutation)	Canada	1	(Corrigall et al. 2001)
1136C>Ains13	Frameshift, premature stop codon	Holland	1	(de Rooij et al. 1997b), reported as 1413C>A+13bp
1144-1145delGT	Frameshift, premature stop codon	American / Indian	1	(Frank et al. 2001b)
1147-1148delGT	Frameshift, premature stop codon	France	1	(Whatley et al. 1999)
1194-1198delTACAC	Frameshift, premature stop codon	Chile	4	(Frank et al. 2001a), reported as 1239delTACAC
1203A>C	L401F	Finland	1	(von und zu Fraunberg et al. 2001)
INTRON 11				
IVS11-1T>G	Normal mRNA <90%	UK	1	(Roberts et al. 1998), compound heterozygote with A219KANA
IVS11-1G>A	Probable deletion of exon 11 and frameshift	UK	1	(Palmer et al. 2001), compound heterozygote with A219KASA
EXON 12				
1274-1275delGT	Frameshift, premature stop codon	UK	1	(Whatley et al. 1999)
1281G>A	W427X (nonsense mutation)	UK	1	(Whatley et al. 1999)
1287delA	Frameshift, premature stop codon	France	2	(Whatley et al. 1999)
1289insT	Frameshift, premature stop codon	Holland	1	(de Rooij et al. 1997b), reported as 1566+T
INTRON 12				
IVS12+1delG	Deletion of exon 12	France	2	(Whatley et al. 1999)
IVS12+1G>C	Splicing defect	USA, Italy	1	(Frank et al. 2001b), reported as 1290+1G>C
IVS12+2T>G	Splicing defect	Sweden	1	(Wiman et al. 2003)
IVS12+2-3insT	Splicing defect	Sweden	1	(Wiman et al. 2003)
IVS12-2A>G	Deletion of exon 13	UK	1	(Whatley et al. 1999)
		Turkey	1	(Frank et al. 2001b), reported as 1292-2A>G in text and 1291-2A>G in table 1. Could be same patient as reported by Whatley et al. (1999).

EXON 13				
1292-1293delAG	Frameshift, premature stop codon	UK	2	(Whatley et al. 1999)
1297G>C	A433P	UK	1	(Roberts et al. 1998), homozygote
1299delT	Frameshift, premature stop codon	Japan	1	(Maeda et al. 2000)
1303C>T	Q435X	UK	5	(Whatley et al. 1999)
		USA	1	(Frank et al. 2001b)
1320insT	Frameshift, premature stop codon	Argentina	2	(De Siervi et al. 2000)
1330delT	Frameshift, premature stop codon	Chile	1	(Frank et al. 2001a)
1330-31delCT	Frameshift, premature stop codon	Sweden	1	(Wiman et al. 2003)
1331T>C	L444P	UK	1	(Whatley et al. 1999)
1342G>A	G448R	Japan	2	(Maeda et al. 2000)
1348T>C	S450P	UK / European	1	(Frank et al. 1997); (Frank et al. 1998c)
1357G>A	G453R	UK	1	(Whatley et al. 1999)
1358G>T	G453V	UK	1	(Whatley et al. 1999)
1384-1385delAG	Frameshift, premature stop codon	France	1	(Whatley et al. 1999)
INTRON 13				
None reported to date				

Two mutations were found in both France and Britain in unrelated families (Whatley et al. 1999). Both occur at potentially hypermutable sites: a CpG dinucleotide on the antisense strand (R168H), and a polyG tract (745delG). The R168H mutation has also been described in three other populations (de Rooij et al. 1997b; Frank et al. 1997; Frank et al. 2001a) although it is unclear whether these are, indeed, unrelated individuals. The R168C mutation was described in South Africa (Meissner et al. 1996b; Warnich et al. 1996). A few other mutations (M1L, L15F, R152C, 538-539delAT, Q189X, 1083delT, Q435X) occur in more than one country but it is unknown whether or not the patients are related. There is always a possibility that DNA samples from a single patient might be sent for investigation to laboratories in more than one country and reported in different studies. Recently a number of novel PPOX mutations have been reported in individual Italian (D'Amato et al. 2003; Patti et al. 2003) and Swedish (Wiman et al. 2003) families.

Genotype/phenotype correlation

To date no significant correlation has been demonstrated between the type of mutation - missense, nonsense, splice site or frameshift - and a specific clinical presentation, such as photosensitivity or the acute attack.

Furthermore, the frequencies of each type of presentation appear to be similar in France, the UK (Whatley et al., 1999), Finland (von und zu Fraunberg et al. 2001) and South Africa (Hift 2000) (and probably in the rest of the world). This suggests that allelic heterogeneity does not substantially alter the pattern of clinical expression of the disease, and that VP in any one geographical region is clinically representative of the disease elsewhere. The PPOX genotype does not appear to be a significant determinant of clinical severity (Hift 2000; Meissner et al. 2003).

Therapy

Therapeutic approaches to VP relate to the acute attacks and cutaneous photosensitivity. Chief forms of therapy of the acute attacks include administration of carbohydrates (glucose) (Doss and Verspohl 1981; Doss et al. 1985), heme (in the form of heme arginate) (Mustajoki and Nordmann 1993; Mustajoki et al. 1994; Elder 1997; Hift et al. 1997; Kirsch et al. 1998) or heme oxygenase inhibitors together with heme (Drummond 1987; Galbraith and Kappas 1989). Other forms of therapy include administration of propanolol in an attempt to control the adrenergic overactivity of the porphyric crisis (Hift 2000).

The prevention of cutaneous symptoms is difficult and treatments such as repeated venesections, hemodialysis, administration of chloroquine and β-carotene have been shown to have little to no effect (Kirsch et al. 1998; Meissner et al. 2003). Preventative measures such as protection from sunlight using proper clothing still remains the most effective way to avoid cutaneous symptoms.

3.3 Homozygous variegate porphyria

So-called "homozygous variegate porphyria" (HVP) results from the same mutations on both alleles (homoallelic) or different mutations on 2 alleles (heteroallelic) of the *PPOX* gene. The first cases of HVP were described by Kordac et al. (1984) and since then, a number of cases have been reported

worldwide (Kordac et al. 1985; Murphy et al. 1986; Mustajoki et al. 1987; Coakley et al. 1990; Norris et al. 1990; D'Alessandro Gandolfo et al. 1991; Hift et al. 1993; Roberts et al. 1998; Corrigall et al. 2000a). Of these, six were reported to be heteroallelic (Meissner et al. 1996b; Frank et al. 1998a; Roberts et al. 1998; Palmer et al. 2001) and two patients reported to be homoallelic for missense mutations preserved some residual PPOX activity *in vitro* (~9-25% of wild-type) (Roberts et al. 1998).

HVP generally presents within days to months of birth and occasionally at mid to late adolescence. The condition is characterized by severe photosensitivity, delayed neurological development, seizures and nystagmus. Structural abnormalities of the hands and growth retardation lead to severe deformity and short stature, respectively. In addition, patients have markedly reduced PPOX activity in their lymphocytes or cultured fibroblasts (0-20% of normal) (Mustajoki et al. 1987; Norris et al. 1990).

Molecular biology : Mutations reported in the "homozygous" state are indicated in table 3.1. Despite a severe decrease in PPOX activity in HVP patients (Hift et al. 1993; Roberts et al. 1998), there is evidence to suggest that some residual PPOX activity is always present in the surviving homozygote or compound heterozygote. For example, the R59W mutation in exon 3 exhibits <1% catalytic activity (Meissner et al. 1996b) whereas the R168C mutation in exon 6 is associated with some residual activity (17%) (Maneli et al., 2003). Thus, mutations that abolish activity are lethal in the homozygous state and are found only in heterozygous VP, while the milder mutations, such as R168C, are not clinically apparent in heterozygotes but may be present in HVP (Whatley et al. 1999). This suggestion was supported by a other studies (Kauppinen et al. 1997; Roberts et al. 1998; Corrigall et al. 2000a). Of interest was that in all the reported conditions the substantial loss of activity could be tolerated albeit at the cost of disease of variable severity.

CHAPTER 4 : MITOCHONDRIAL TARGETING

CHAPTER 4 : MITOCHONDRIAL TARGETING

4.1 Introduction

As mitochondrial targeting of PPOX forms the central emphasis of this dissertation, it is pertinent to discuss and review the current literature thereof. Hence, this chapter reviews the route of nuclear-encoded mitochondrial-destined proteins from the point of their translation to their eventual location in either the outer mitochondrial membrane, intermembrane space, inner membrane or mitochondrial matrix. The outer and inner mitochondrial machinery which allow translocation are discussed, and the full import pathway summarised. However, in accordance with the objectives of this thesis, it focuses on the mitochondrial targeting sequence of proteins and its inherent characteristics which allow efficient mitochondrial recognition. Finally, as fusion proteins of PPOX and green fluorescent protein (GFP) form the bulk of the experimental work, GFPs and their use as fluorescent markers of proteins, are included.

Many cellular proteins reside and function in locations remote from their nuclear encoding and cytoplasmic sites of synthesis. The system of compartmentalization which targets and translocates these proteins to their particular destinations during, or following synthesis, has always been intriguing. It has long been known that the specificity of these systems reside in both the targeted proteins themselves, and in cellular elements that recognise and compartmentalise them (Horwich et al. 1985a). Furthermore, amino acid sequences which confer such specificity have been identified in synthesised polypeptides targeted to the endoplasmic reticulum (Walter et al. 1984), the nucleus (Hall et al. 1984; Kalderon et al. 1984) and the mitochondria (Hay et al. 1984).

Although mitochondrial DNA encodes a few proteins for the organelle itself, the vast majority of mitochondrial proteins are encoded by nuclear genes and synthesised on cytosolic ribosomes. Most often, these proteins contain a transient amino-terminal sequence (presequences) which is cleaved after

mitochondrial localization to release the mature protein (Glick and Schatz 1991). These mature proteins are then imported into one of four mitochondrial compartments: the outer membrane (OM), intermembrane space (IMS), inner membrane (IM) or matrix. Despite presequences being proteolytically cleaved by specific proteases in the matrix and on the outer face of the inner membrane, research over the past decade has shown a few exceptions. Certain mitochondrial proteins have no N-terminal presequence, but contain a targeting sequence located in the mature part of the protein ie. an internal targeting sequence (Folsch et al. 1996; Diekert et al. 1999). Others have shown that proteins destined for the inner mitochondrial membrane may contain 2 distinct signals - one at the N-terminus driving it to the OM and one required for further internal mitochondrial compartmentalization (Arnold et al. 1998). Interestingly, a mitochondrial matrix-bound protein which is not proteolytically processed (Hammen et al. 1994) and another mitochondrial protein which is catalytically active before import, have been described (Hammen et al. 1994; Williams et al. 2000).

Although presequences contain all the necessary information for targeting the majority of proteins to their correct intramitochondrial locations (Hurt et al. 1986), no significant sequence homology has been detected among those whose primary structure is known. Characteristically, however, these sequences lack acidic amino acids, are rich in basic, hydrophobic and hydroxylated amino acids; and can potentially fold into amphiphilic α-helices (Roise et al. 1986) (see 4.4.1).

For a presequence to target a nuclear-encoded mitochondrial protein efficiently, it is necessary for it to interact with a number of cytosolic and mitochondrial membrane-bound receptor-type proteins. It has become evident that transport into the mitochondria is complex since many precursor proteins have to translocate across both the outer and inner mitochondrial membranes (Pfanner and Neupert 1990; Glick and Schatz 1991; Segui-Real et al. 1992). Protein components destined for the mitochondrial matrix and inner membrane are found to pass these two membranes simultaneously at

translocation contact sites (Schleyer and Neupert 1985). These sites are in close proximity as polypeptide segments as short as 50 amino acid residues are sufficient to span both membranes at these sites (Rassow et al. 1990). However, despite their proximity, each translocation system operates independently of each other (Hwang et al. 1989; Hwang and Schatz 1989). Furthermore, under certain conditions, translocation intermediates *en route* from the outer to the inner membrane expose major segments of their sequence in the intermembrane space (Hwang et al. 1991; Rassow and Pfanner 1991; Jascur et al. 1992), suggesting that the mitochondrial membranes contain separate translocation machineries which cooperate in a dynamic fashion during protein transfer into the matrix (Glick and Schatz 1991; Pfanner et al. 1992; Segui-Real et al. 1993).

As the movement of mitochondrial-destined proteins from the nucleus to their correct location within the mitochondrion is a complex process involving numerous factors, the main points are summarized in the following paragraphs.

4.2 Summary of Protein Import

Most mitochondrial proteins are synthesized as preproteins (ie. mature protein + presequence) on cytosolic polysomes and are subsequently imported into the mitochondrion. After their synthesis in the cytosol, proteins have to be maintained in a translocation-competent form. This competent conformation is mediated predominantly by the cytosolic heat-shock proteins (Hsps) of the Hsp70 class in addition to a number of other cytosolic proteins.

Hsps stabilize and protect bound polypeptides by preventing irregular interactions leading to denaturation and aggregation (Bukau and Horwich 1998). This is important as ribosomal translation or intracellular protein transport are prone to expose either unfolded protein segments to the environment, or require posttranslational folding and/or unfolding events (Netzer and Hartl 1998). In general, five classes of Hsps have been distinguished viz. Hsp70, Hsp60, Hsp90, Hsp100 (the numerical value

designates the molecular weight of the protein) and small Hsp (Jakob and Buchner 1994; Hartl 1996). Of this group, only Hsp70, Hsp60 and Hsp100 have been identified as interacting with mitochondria. Hsp70 functions in the cytosol as opposed to Hsp60 and Hsp100, which function in the mitochondrial matrix.

Other cystosolic proteins implicated in maintaining precursor proteins in a competent import state include - targeting factor, a 28 kDa protein, affinity purified using a signal peptide (Ono and Tuboi 1986, 1988; Ono 2002); mitochondrial import stimulation factor (MSF), a heterodimer of 66kDa, isolated from rat liver (Hachiya et al. 1993), which acts on aggregated precursors to restore solubility and import competence into mitochondria (Hachiya et al. 1994; Komiya et al. 1997); nascent-associated polypeptide complex (NAC), a heterodimeric protein that when purified, stimulates effective import of a nascent-chain of malate dehydrogenase into isolated yeast mitochondria (Funfschilling and Rospert 1999) and ribosome-associated complex (RAC), another heterodimeric nascent protein-binding factor which assists precursors to maintain a conformation compatible with the translocase of the outer mitochondrial membrane (TOM) complex on the mitochondrial surface (Gautschi et al. 2001).

Preproteins, maintained in a translocation competent state by cytosolic chaperones, bind import receptors of the outer membrane ie. the TOMs. The main import receptor in humans is a heterodimer of Tom20 and Tom22 (the numerical value refers to the size of the protein in daltons (Fig. 4.1, 1). The membrane anchor of Tom20 is located at the immediate amino terminus and the remainder of the protein forms a domain on the cytosolic side of the membrane (Schneider et al. 1991). Similarly, Tom22, which contains a single internal membrane anchor, has an amino-terminal domain exposed to the cytosol (Kiebler et al. 1993; Saeki et al. 2000). The purified cytosolic domain of each subunit of the Tom20-Tom22 receptor specifically binds presequences of cleavable mitochondrial preproteins, indicating that each receptor subunit can function independently. Presequences interact with Tom22 in an electrostatic manner, in contrast to Tom20, where the interaction

is hydrophobic (Brix et al. 1997). In addition, Pfanner and co-workers showed that the negatively charged Tom22 recognises the positively-charged face of an amphipathic presequence whereas, Tom20 binds to the hydrophobic (back) side of a presequence (Pfanner et al. 1997). Tom22 functions as the central import receptor as it is essential for cell viability under all growth conditions in contrast to Tom20 which is not (Lithgow et al. 1994; Honlinger et al. 1995).

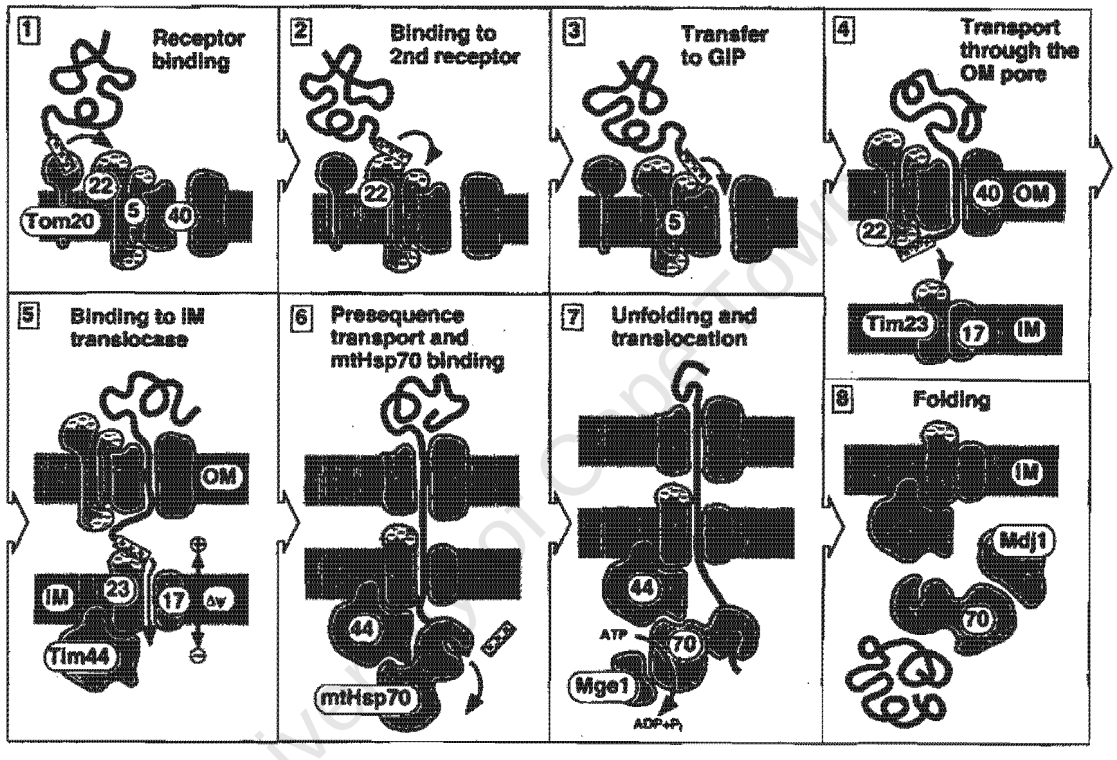

Figure 4.1 Summary of import of mitochondrially-destined preproteins from the cytosol to the mitochondrial matrix. (*from (Pfanner and Geissler 2001)*. For detail, see text.

The protein is then gradually guided across the outer membrane by further binding to the small protein Tom5 (Fig. 4.1, 2) and completes its translocation of the outer membrane by moving through the Tom40 complex, known as the general import pore (GIP) (Fig. 4.1, 3). Carrier preproteins with internal targeting information preferentially use the heterodimeric receptors Tom70-Tom37 (not shown in figure) but are directed to the same Tom 40 import channel. The pore size of reconstituted Tom40 was determined to be

approximately 20-22Å (Hill et al. 1998) in agreement with electron micrographic analyses (Kunkele et al. 1998). A typical preprotein with an amino terminal presequence is translocated across the mitochondrial membrane as a linear chain (Rassow et al. 1990) and whether it is in an extended or α-helical conformation, a pore with a diameter of 20-22Å, could easily accommodate it (Pfanner and Chacinska 2002).

After passage across the outer membrane, certain preproteins first bind to mature proteins in the IMS, whereas others immediately insert into import sites of the inner membrane called translocases of the inner membrame (TIMs) (Fig. 4.1, 4). Interestingly, the TIMs are not stably connected to the TOMs as they function independently of each other.

The central building block of the TIMs is the TIM23 complex. The TIM23 complex consists of a peripherally attached motor system viz. mtHsp70, its membrane anchor Tim44 and a number of co-chaperones (Fig. 4.1, 5). Tim23 and Tim17 are stably associated in a 90kDa core complex and are responsible for the formation of the import channel/s across the inner membrane (Kubrich et al. 1994; Dekker et al. 1997; Ryan et al. 1998; Moro et al. 1999). A change in membrane potential ($\Delta\psi$) is required for translocation of a preprotein across the inner mitochondrial membrane channel (Bauer et al. 2000). Tim23 contains a hydrophilic N-terminal domain on the intermembrane side with a net negative charge and appears to be translocation-specific to precursors with a positively-charged N-terminal mitochondrial matrix targeting signal (Sirrenberg et al. 1996; Bauer et al. 2000; Pfanner 2000) and hydrophobic stop-transfer signals (Hoogenraad et al. 2002). Both Tim23 and Tim17 are in close contact with a preprotein in transit but cannot substitute for one another, even though they are of similar sequence, as each protein is essential for cell viability (Hoogenraad et al. 2002).

Mitochondrial Hsp70, is an essential component of the mitochondrial import machinery (Kang et al. 1990; Scherer et al. 1990). After the initial membrane potential (ψ)-driven translocation of the N-terminal presequence, mtHsp70 is

required for translocation of the remainder of the precursor polypeptide across the inner membrane in an ATP-dependent manner (Gambill et al. 1993) (Fig. 4.1, 6). As in the case of Hsp70 in the cytosol, mtHsp70 supports the unfolding of precursor polypeptides (Voos et al. 1993). Under physiological conditions, mtHsp70 binds to Tim44 in an ATP-bound state afterwhich the ATP is rapidly hydrolysed. The stable complex of mtHsp70 with Tim44 contains only ADP, while free mtHsp70 additionally contains considerable amounts of ATP (von Ahsen et al. 1995). Tim44 is not the only partner protein of mtHsp70 engaged in protein import. The co-chaperone Mge1 interacts with mtHsp70 bound to a precursor peptide (Fig. 4.1, 7), promoting the reaction cycle of mtHsp70 (Westermann et al. 1996; Dekker and Pfanner 1997; Westermann and Neupert 1997). MtHsp70 also interacts with Mdjl. Together, these two proteins keep presequences in an unfolded state and prevent misfolding and aggregation (Pfanner et al. 1997). Release of mtHsp70 from the protein is stimulated by the action of Mgel and the subsequent binding of ATP.

Most presequences are then cleaved by a mitochondrial processing peptidase (MPP) (Mori et al. 1980; Ou et al. 1989) directly or alternatively, acted upon by peptidyl prolyl cis/trans isomerases allowing the protein to fold into its final conformation (Fig. 4.1, 8).

4.3 Mitochondrial targeting sequence (often referred to as the "presequence")

The N-terminal presequence contains the majority of information necessary for successful mitochondrial import and subsequent proteolytic processing (Hartl et al. 1989; Horwich et al. 1991). Interestingly, not all signal sequences are removed after import by proteases eg. mammalian rhodanese, 3-oxoacyl-CoA thiolase (Hammen et al. 1994).

Gene fusion experiments have established that a mitochondrial presequence attached to virtually any mature protein can direct the targeting and import of chimeric precursor proteins into the mitochondria (Hurt et al. 1985b; Pilgrim

and Young 1987). The presequence for a protein destined to be imported into the mitochondria must first bind to the mitochondrial outer membrane - an association made possible by hydrophobic interactions of the membrane with an amphiphilic α-helix. Interestingly, deleting as much as one-half or even two-thirds of the residues in the presequence often has little effect on targeting and import (Hurt et al. 1985b). However, although the C-terminal portion of the N-terminal presequence can be deleted without impairing import, import is completely abolished upon deletion of the N-terminal portion in a number of proteins, including yeast cytochrome c oxidase subunit IV (Hurt et al. 1985a), pig aspartate aminotransferase (Nishi et al. 1989) and yeast alcohol dehydrogenase III (Pilgrim and Young 1987). To confirm the importance of the N-terminal domain, a deletion study using δ-aminolevulinate synthetase (ALAS), showed that the presence of its 9 N-terminal amino acids were sufficient to achieve 60% mitochondrial import whereas a fusion protein with the presequence lacking the N-terminal domain, was poorly imported (Haldi and Guarente 1989). This, and a number of further studies has generally established that common conformational features, such as α-helical amphiphilicity, the presence of N-terminally located hydrophobic motifs, as well as an overall net positive charge are the physical basis for mitochondrial presequences to perform their targeting and import functions. These characteristics are detailed below.

4.3.1 α-Helical amphiphilicity

The ability of mitochondrial presequences to form amphiphilic α-helices ie. a helical region where charged amino acids are found facing an opposing region of neutral polar amino acids, has been documented (Roise et al. 1986; von Heijne 1989). Whether α-helical amphiphilicity is essential for mitochondrial targeting and import of a presequence remains controversial – a point addressed in this thesis. The importance of amphiphilicity was questioned when an artificially designed "apparently" non-amphiphilic presequence proved effective as a mitochondrial import signal (Roise et al. 1986). It was later shown experimentally that this non-amphiphilic protein was

indeed highly amphiphilic as measured by its ability to insert into phospholipid monolayers, highlighting amphiphilicity as a necessary requirement for mitochondrial presequence function (Roise et al. 1988). Studies by Hammen and colleagues (1996) utilising NMR, circular dichroism and fluorescence spectroscopy to investigate mitochondrial presequence characteristics in the presence of structure-inducing model membrane systems, provided supportive evidence. Using three different peptides located at the N-terminus, they showed that targeting precursor proteins formed a continuous α-helical structure when in contact with dodecyl phosphocholine micelles ie. a simulated membrane model. They thus concluded that the amphiphilicity of the peptides is the major factor determining the affinity of interaction with model membrane systems. Significantly, the three peptides used in the study each contained different lengths of helical segments, ranging between three and five turns. This is important as the first turn in α-helices (approx. 4 amino acid residues) create a hydrogen bond that stabilises the start of the helix. Every additional residue added thereafter, adds another hydrogen bond thus stabilising the helix even further (Creighton, 1993). In addition, the study showed that the peptides display very different distributions of hydrophobic and hydrophilic side chains about the helical axis. These patterns suggest that different amphiphilic characteristics of targeting presequences could lead to corresponding differences in their abilities to interact with membranes (Hammen et al. 1996a).

In contrast, a study using deletion mutants in soybean, indicated that the α-helix alone was not sufficient to support competent mitochondrial import but a combination of correctly positioned positive amino acids at the N-terminus and an α-helix was required (Tanudji et al. 1999). Thus, a combination appears necessary in plants, whereas an α-helical amphiphilic element alone, can possibly support efficient import into rat liver mitochondria, highlighting possible different intracellular requirements between plant and animal species with respect to mitochondrial targeting and import (Tanudji et al. 1999). The requirement of both the α-helix and another characteristic to effect efficient targeting and import, was further demonstrated by a recent study using deletion mutants of the tobacco plant (*N. plumbaginifolia)* linked to GFP (Duby

et al. 2001). They illustrated that efficient import depends additionally on the presence of hydrophobic residues (see 4.3.3). All presequences studied thus far, show a tendency to form helices when placed in an environment that favours the adoption of secondary structure. It is possible that membrane binding induces helix formation, so that if the helix is the bioactive conformation of the presequence, it would be allowed to interact correctly with import receptors. Interestingly, when the presequence adopts a helical structure it can bind to an apolar groove in Tom20 via hydrophobic, rather than ionic interaction. In other words, Tom20 recognises the potential of the presequence to form an amphiphilic α-helical structure, but not its positive charges (Abe et al. 2000).

4.3.2 Positively charged residues

Although α-helicity appears important for targeting, the requirement of a net positive charge has also been documented as necessary for correct functioning of a presequence. The critical role of positively charged amino acid residues within mitochondrial presequences was primarily demonstrated using human ornithine transcarbamoylase (OTC) (Horwich et al. 1985a; Horwich et al. 1985b; Horwich et al. 1986). Within the OTC presequence, four arginine residues (positions 6, 15, 23 and 26) individually substituted with glycines had variable effects on mitochondrial import. Importantly, overall positivity in addition to positive charges at defined positions of the presequence were necessary for effective import. Substitution of the arginine at position 23 of the OTC precursor with glycine resulted in a complete loss of targeting function (Horwich et al. 1986). However, when this arginine (Arg23) was substituted with an amino acid residue supporting the formation of an α-helical structure, the modified precursor was imported into mitochondria. These findings indicate that not only is the presence of an arginine at a particular position important for normal import function, but that local regions in the midportion of the presequence exhibit a defined secondary structure (most likely α-helical) that appears essential for function (Hartl et al. 1989).

This necessity of a defined secondary structure for mitochondrial import competence is further illustrated by a study in which synthetic oligonucleotides were used to construct artificial presequences. These presequences contained arginines, serines and leucines and when these three amino acid residues were adjusted to match the ratios of basic, hydroxylated and hydrophobic residues in natural mitochondrial presequences, correct mitochondrial targeting was effected. However, when they were merely added as a sequence, mitochondrial targeting was abolished. Interestingly, this raises the possibility that the function of these peptides does not require a specific primary amino acid sequence, but merely a particular overall balance between positively charged, hydrophobic and hydroxylated residues arranged so as to allow formation of a particular secondary structure (Allison and Schatz 1986).

The role of positively charged arginine residues within the presequences was further examined by the introduction of a series of mutations in rat heart mitochondrial malate dehydrogenase cDNA (Chu et al. 1987a, b). Arg14 was chosen as a target for mutagenesis due to its presence in the pentapeptide Ala-Ala-Leu-Arg-Arg – a motif conserved in other rat transit peptides (Grant et al. 1986). Import into the mitochondrion was related to a specific order of amino acids ie. Arg = Lys > Ala≥ Asn = His = Gln > Glu. Substitution of a single amino acid residue could influence import in a manner that depended upon the charge of that residue. Although arginine is remarkably abundant in translocating peptides, and may be required for import, substitution with lysine results in no loss of import function. Thus net positive charge, rather than the identity or location of the amino acid side chain bearing the charge, appears to be the important feature contributing to functional import.

A later study by Hammen et al. (1996) created a positive charge at different positions in the presequence of mitochondrial aldehyde dehydrogenase (ALDH) and showed that the replacement of Arg by Gln at the N-terminal, had no significant effect on import. However, replacement of both N-terminal Arg residues at positions 3 and 10, produced a precursor that was poorly imported. Importantly, provided an overall net positive charge was maintained

in the N-terminal segment of a presequence, even negative charges could be tolerated without having a significant effect on import competence (Hammen et al. 1996b; Hammen and Weiner 1998).

The possibility that leader peptides interact electrostatically may explain how net positive charge plays a role in import of the precursor. As the potential gradient across the mitochondrial inner membrane is orientated with a relatively negative charge at the inside, it is conceivable that the positively charged presequence can be "electrophoresed" across the membrane (Horwich et al. 1987). Furthermore, Schleyer and colleagues showed that the electrochemical gradient was only required for translocation of leader peptides and not adjoining mature sequences (Schleyer and Neupert 1985). Another possibility is that the positively charged peptide interacts with a negatively charged protein such as an outer membrane receptor molecule, or a protein that comprises a channel. A recent report on the mitochondrial protein import receptor Tom20 showed that the positive charges of the presequence are not required for the interaction with the mitochondrial outer membrane receptors, but that they function in other steps during import (Abe et al. 2000). This includes recognition by other components of the TIM/TOM complexes, including Tom22, Tom5 and Tim23. Additionally, since mitochondrial membranes possess a negative surface charge, it can be argued that the extent of binding of the presequences to these membranes is governed by electrostatic, and subsequently stabilised by hydrophobic interactions (Schatz 1997).

4.3.3 Hydrophobicity

The necessity of a hydrophobic domain within the presequence for efficient import into mitochondria was shown in a study by Allison and Schatz (1986) who used three artificial presequences differing in length and amino acid composition. They showed that specific sequence motifs such as positive charges and/or amphiphilic helices may not be necessary for targeting function and that the mitochondrial import machinery may have to recognise more general features of amino acid presequences such as a minimum

hydrophobic domain. Von Heijne (1985) had earlier reported that in contrast to mitochondrial presequences, presequences of secreted proteins share at least two distinct domains : an N-terminal charged region and a subsequent hydrophobic region.

Gruehler and colleagues (1997) reported that a hydrophobic domain, when in proximity to a matrix-targeting sequence, can effect translocation across the outer membrane as well as maintain a translocating polypeptide in the TIM channel. These authors suggest that the common denominator for maintaining a preprotein in the TIM channel is therefore a suitably positioned hydrophobic core rather than a sorting signal specific for one mitochondrial subcompartment over another (Gruhler et al. 1997).

The idea of mitochondrial presequences interacting with various presequence binding proteins during import into the mitochondria proposes that the presequence contains multiple recognition elements, and that such elements are not necessarily identical. A recent study on the N-terminal presequence of the $F_1\beta$ precursor of *N. plubaginifolia* showed that when hydrophobic residues were replaced by hydrophilic residues, a drastic reduction in import resulted, suggesting that hydrophobic residues are essential for import competence of the precursor (Duby et al. 2001). Consistent with these studies, von und zu Fraunberg and colleagues (2003) recently reported that in the N-terminal recognition sequence (residues 1-28) of human PPOX, replacing a single hydrophobic leucine or isoleucine with a hydrophilic residue of the same size, prevented mitochondrial import.

Concluding comment

Although the targeting of proteins destined for the mitochondrion is complex and consists of a number of processes and intracellular factors, targeting sequences found predominantly at the N-terminus (or C-terminus in some cases), cause efficient mitochondrial targeting, outer membrane binding and subsequent import. As discussed above, these targeting sequences contain

definite characteristics (alpha-helicity, charge, hydrophobicity) but whether any one of these specifically, or in combination are needed to effect efficient targeting, remains undecided.

4.4 Green Fluorescent Protein

The GFPs are a unique class of proteins involved in bioluminescence of many Cnidaria. An initial report on the GFP chromophore structure (Shimomura and Shimomura 1982) resulted in the eventual cloning of a cDNA (*gfp10*) for the jellyfish, *Aequorea victoria* (Prasher et al. 1992). *Aequorea* GFP consists of 238 amino acids existing as a monomer with a molecular weight of 27kDa (Shimomura and Shimomura 1982). Purified GFP absorbs blue light (maximally at 395nm with a minor peak at 470nm) and emits green light (peak emission at 509nm with a shoulder at 540nm) (Morin and Hastings 1971b, a). The protein requires the presence of oxygen to emit this light (Heim et al. 1994) and its fluorescence is independent of cell type or location. In addition, it is resistant to photobleaching and remains stable under a wide variety of conditions – characteristics which make it ideal to serve as a reporter or marker in gene expression studies (Inouye and Tsuji 1994). GFP also represents an ideal fluorescent probe which can be expressed in living cells (Venerando et al. 1996; Tarasova et al. 1997; Kim et al. 2002) and has been used to demarcate subcellular compartments such as the nucleus (Ellenberg and Lippincott-Schwartz 1999; Ellenberg et al. 1999), endoplasmic reticulum (Kaether and Gerdes 1995), and the mitochondrion (Rizzuto et al. 1995). Consequently, the size and shape of GFP and the differing pHs and redox potentials of these organelles do not appear to constitute any serious barriers (Llopis et al. 1998; Greenbaum et al. 2002). Nevertheless, one should always bear these possibilities in mind.

Although the wild-type *Aequorea* GFP is used as a reporter molecule, its excitation at 395nm results in increased background autofluorescence and photoisomerization (Billinton and Knight 2001). Thus, knowledge of the primary structure of GFP was used to create mutants with improved spectral characteristics. It was found that mutations in the 20 amino acids around and

including the chromophore (residues 55-74) alter the spectral characteristics as a result of changes in the chromophore structure, expression and folding (Heim et al. 1995; Siemering et al. 1996; Yang et al. 1996; Davis and Vierstra 1998; Haseloff 1999; Haseloff et al. 1999). Pioneering work in altering spectral properties was conducted by Heim and colleagues (1994) using random mutagenesis in bacterial colonies. One mutant which has a tyrosine to histidine substitution at position 66 (Y66H), resulted in a significantly blue-shifted GFP derivative described as blue fluorescent protein (BFP). This protein is maximally excited at 382nm with a peak emission at 448nm. Unfortunately, its fluorescent intensity was only 57% relative to wild-type GFP (Heim et al. 1994). A second mutation tyrosine to tryptophan at position 66 (Y66W) results in another blue-shifted derivative, with a maximal excitation at 458nm and emission at 480nm, called cyan fluorescent protein (CFP).

Due to GFP emitting within the same spectral sphere as autofluorescence, a new way was sought to distinguish between the two. By using fluorescence intensity-enhancing mutations, Heim et al. (1995) created point mutations within the chromophore. They showed that mutating a serine to a threonine at postion 65 (S65T) resulted in a single excitation peak between 470 and 490nm with the subsequent loss of an unstable 395nm excitation peak. This mutant is preferred over previously made mutants in that it exhibits the longest wavelength of excitation and emission (489 and 511, respectively) which closely matches standard microscopic fluorescein filter sets. Its peak amplitude of excitation is also 6-fold greater than wild-type GFP (Heim et al. 1995).

Following these studies, a synthetic mutant was engineered. This "enhanced" GFP gene (EGFP) incorporates 190 silent base mutations resulting in an open reading frame (ORF) composed entirely of preferred human codons (Chiu et al. 1996; Zolotukhin et al. 1996). EGFP exhibits 17-fold brighter fluorescence than the S65T derivative in human embryonic kidney cells (Yang et al. 1996). Currently, human codon-optimized versions of blue, cyan and yellow fluorescent proteins (EBFP, ECFP and EYFP, respectively) are commercially available. In this study, we have used expression vectors

containing the enhanced version of the green fluorescent protein allowing cloning of our gene to create amino (pEGFP-N1) or carboxy terminal (pEGFP-C1) fusion proteins.

Notwithstanding the possibility of even further future developments in the field of fluorescent markers and fluorescent microscopy, EGFP has become an attractive fluorescent tag to monitor subcellular activities such as gene expression, protein-protein interaction, trafficking and localization *in vivo* in real time (Leffel et al. 1997).

CHAPTER 5 : THESIS DEVELOPMENT AND SUMMARY

CHAPTER 5 : THESIS DEVELOPMENT AND SUMMARY

5.1 Introduction

As detailed in chapters 2 and 3, mutations in the *PPOX* gene lead to a defective enzyme with reduced activity resulting in the clinical condition, VP. The high incidence of VP in South Africa, due to a founder gene effect (R59W) (Meissner et al. 1996), has resulted in this disease and *PPOX* being the focus of studies performed in the Lennox Eales Porphyria Laboratories. Since the discovery of the R59W mutation in 1996, 9 other mutations in South African VP individuals have been described (Meissner et al. 1996; Warnich et al. 1996; Corrigall et al. 1998; Corrigall et al. 2000, 2001).

Human *PPOX*, a nuclear-encoded gene, is translated in the cytoplasm whereupon it becomes translocated to the mitochondrion. It is situated on the cytoplasmic side of the inner mitochondrial membrane (Deybach et al. 1985). In the majority of mitochondrial-targeted proteins, a targeting signal is required to reach their destination. This dissertation focuses primarily on mitochondrial targeting of PPOX.

Some data exists on targeting of the human mitochondrial-located heme biosynthetic enzymes specifically ALAS, PPOX, CPOX and FC. It is known that ALAS (Yamauchi et al. 1980; Srivastava et al. 1983; Volland and Urban-Grimal 1988), CPOX (Delfau-Larue et al. 1994; Martasek et al. 1994; Taketani et al. 1994; Susa et al. 2003) and FC (Dailey et al. 1994) all have presequences which direct these enzymes to their specific locations within the mitochondrion. Furthermore, recent reports on CPOX (Susa et al. 2003) and PPOX (Von Und Zu Fraunberg et al. 2003) have reported some detail on their mitochondrial targeting features. However, at the beginning of this PhD project the mitochondrial targeting of PPOX remained to be fully elucidated. With the advent of improved site-directed mutagenic and transfection methods we considered it valid to investigate this topic, using clinically relevant mutations as an initial context in which to examine this.

5.2 This study

This study begins with the examination of three clinically relevant South African VP mutations - H20P, R59W and R168C (Chapter 6). In order to understand the significance and effect on mitochondrial targeting of these PPOX mutations, site-directed mutagenesis was used to re-create them *in vitro* and chimeric PPOX-GFP fusion proteins engineered. Liposomal-mediated transient transfections allowed the fusion proteins to be visualized by fluorescent microscopic analysis. The failure of H20P to target the mitochondrion stimulated our interest and led us to examine the N-terminal region of PPOX in more detail.

Thus, in Chapter 7 the question of whether PPOX has an N-terminally located mitochondrial presequence is addressed, and if so, what the minimum number of required amino acids are for efficient targeting. A series of different-sized PPOX N-terminal fragments were engineered as GFP chimeras and analysed for mitochondrial localization. The results showed that the 17 N-terminal amino acids are sufficient to target the mitochondrion.

The possibility existed that PPOX had one or more additional downstream/internal targeting sequences, as had been alluded to in an earlier publication by Taketani et al. (1995). Hence a fusion protein lacking the proposed N-terminal presequence was engineered.

Net positive charge, α-helicity and hydrophobicity are all characteristics of mitochondrial presequences (Roise 1988; Roise and Schatz 1988; Roise and Maduke 1994). The effect of charge on our proposed PPOX presequence was examined by replacing the only positively charged arginine residue (R3) in that sequence with conservative and non-conservative replacements. The resultant mutant constructs (R3E and R3K) did not target in contrast to R3S that did.

In addition, predictive secondary structure software was utilized to delineate N-terminal α-helices in the PPOX sequence and examine the relevance of α-helicity within the presequence. A series of mutations (H20S, H20A, H20K, H20E, H20G and H20P) at the H20 position were engineered and showed that only the H20P abolished mitochondrial targeting.

Deleting the 17-residue N-terminal targeting sequence allowed us to demonstrate the presence of downstream/internal targeting signals. Based on these findings, and those already published, structural biological principles were used to formulate a possible scenario of PPOX mitochondrial translocation. Towards the end of this study a publication by von Fraunberg et al. (2003) centering on hydrophobicity of the N-terminal presequence was published. In particular they examined the effects of mutating certain residues (Leu-8, Ile-12 and Leu-15) within a putative hydrophobic motif (LXXXIXXL) at the PPOX N-terminus and the effect these had on mitochondrial targeting. In addition, von Fraunberg and others (Morgan et al., personal communication) alluded to the presence and importance of downstream targeting signals. In this study we concur with these reports, but present additional data which allows further conclusions to be drawn.

CHAPTER 6 : MITOCHONDRIAL TARGETING OF ENGINEERED HUMAN WILD TYPE AND VP-CAUSING PPOX-GFP MUTANTS

CHAPTER 6 : MITOCHONDRIAL TARGETING OF ENGINEERED HUMAN WILD TYPE AND VP-CAUSING PPOX-GFP MUTANTS

6.1 Introduction

Prior to 1996 the diagnosis of VP was based solely on biochemical (urine and stool porphyrin analysis) and clinical features. However, the discovery and sequencing of the *PPOX* gene in 1995 (Dailey et al. 1994; Hansson and Hederstedt 1994; Taketani et al. 1995) paved the way for the subsequent identification of the gene defect (R59W) responsible for approximately 95% of VP cases in South Africa (Meissner et al. 1996b; Warnich et al. 1996). Kinetic data has illustrated that this mutation reduces the activity of PPOX enzyme by approximately 50% with less than 1% residual activity expressed in recombinant R59W PPOX (Meissner et al. 1996b; Dailey and Dailey 1997; Maneli et al. 2003).

Two other VP-causing mutations (R168C and H20P) were also identified at that time (Meissner et al. 1996a; Warnich et al. 1996). The R168C mutation was found in a young South African female compound heterozygous individual ie. in addition to the R168C mutation she carries the common R59W mutation. Interestingly, she was the first individual in whom the R59W mutation was identified. A recent publication in our laboratory revealed that R168C is associated with some residual activity (~17%) (Maneli et al. 2003). This is in agreement with the suggestion of Roberts et al. (1998) that in a compound heterozygote a severe mutation is always accompanied by a lesser mutation with some residual activity. H20P was found in two members of a South African VP family who tested R59W negative (Warnich et al. 1996; Hift et al. 1997). The H20P, like the R59W, is a severe mutation resulting in a drastic reduction in PPOX enzyme activity. To date, the above two mutations have not been identified in any other SA VP families. In our laboratory a partial kinetic characterization of the above three mutations has recently been performed (Maneli et al. 2003).

The effects of missense mutations in the translated region of *PPOX* may vary. Theoretically, binding, substrate specificity, catalysis, ability to bind the cofactor or to translocate to the mitochondrion or the correct compartment within, could be affected. When this study commenced our lab had a standing interest in the R59W, H20P and R168C mutations. The R59W mutation in exon 3 is found in approximately 95% of all South African VP patients. H20P in exon 2 is located within the enzyme's putative co-factor binding domain, and R168C in exon 6 is of interest to us as it was first identified in an individual who also had the common R59W mutation ie. a compound heterozygous condition. It was therefore deemed pertinent to assess whether the mutations adversely affect mitochondrial targeting of the PPOX product. It is conceivable that if targeting is affected, this could represent an alternative or additional mechanism of PPOX enzyme deficiency.

6.2 Objectives

- To create the VP-causing mutations of interest (H20P, R59W and R168C) *in vitro* using site-directed mutagenesis
- To engineer PPOX-GFP (wild-type) and mutant PPOX-GFP fusion proteins and express them in human cells in an *in vitro* culture system
- To microscopically analyse the ability of the PPOX-GFP and mutant PPOX-GFP to translocate to the mitochondrion (be targeted to the mitochondrion)

6.3 Methods

6.3.1 Site-directed mutagenesis

Wild type human PPOX cDNA, previously cloned into the pTrcHis-B expression vector, was kindly donated by Professor HA Dailey, University of Georgia, Athens, Georgia, USA. The PPOX cDNA is flanked by unique N-terminal Bgl II, and C-terminal Hind III restriction endonuclease sites.

Principle

The Promega GeneEditor Site-directed mutagenesis system was used to create all three clinical mutants. This system uses antibiotic selection to obtain a high frequency of mutants. The selection oligonucleotides provided encode mutations that alter the ampicillin resistance gene, thus creating a new, additional resistance to the GeneEditor antibiotic selection mix. The selection oligonucleotide is annealed to the double-stranded DNA template at the same time as the mutagenic oligonucleotide. Synthesis and ligation of the mutant strand links the two oligonucleotides. The resistance to the antibiotic selection mix encoded by this mutant DNA strand facilitates selection of the desired mutation. The efficiency of mutagenesis is improved by an initial transformation into competent *mut*S cells. This relatively unstable repair minus strain of *E. coli* (it lacks the DNA mismatch repair mechanism), is used to avoid selection against the desired mutation. Due to its instablility, a second transformation is performed in JM109 cells to ensure segregation of mutant and wild type plasmids, resulting in a high proportion of mutants.

Procedure

In order to allow in-frame ligation of the clinical mutants into a GFP expression vector, the stop codon (TGA) at the end of the wild-type *PPOX* cDNA was first modified into a Hind III site by site-directed mutagenesis. This cDNA was then used as a template for creating the three mutants. The mutants were engineered using the GeneEditor kit as follows: A 6ml overnight culture of human PPOX was prepared, the cells harvested by centrifugation, and a plasmid miniprep performed (appendix 3). The extracted DNA was quantified on a GeneQuant spectrophotometer.

Four sets of oligonucleotides were designed to cover the entire *PPOX* cDNA sequence enabling polymerase chain reaction (PCR) to be performed on the cDNA, generating 4 fragments (appendix 1.6.2). In addition, mutagenic oligonucleotides were designed for creation of the desired mutants. All mutagenic oligonucleotides were 5'-phosphorylated as this significantly increases the number of mutant clones. The mutagenic and selection

oligonucleotide used were complimentary to the same strand of DNA to achieve coupling of the antibiotic selection to the desired mutation. The appropriate hybridisation (annealing) temperature for each mutant oligonucleotide, was determined by performing gradient PCR on the relevant cDNA fragment, using either the fragment forward or reverse oligonucleotide, together with the appropriate mutagenic oligonucleotide (appendix 1.3). Extracted DNA from wild type PPOX was used as template. The hybridisation temperatures utilised are shown in table 6.1.

The hybridisation reactions were prepared by mixing appropriate amounts of DNA template, phosphorylated selection and mutant oligonucleotides, hybridisation buffer and deionised water. After heating at the appropriate hybridisation temperature, the reaction was cooled to 37°C. Mutant strand synthesis and ligation was performed using T4 DNA polymerase and T4 DNA ligase in a 10x synthesis buffer (see appendix 1.3).

Table 6.1: Optimum hybridisation temperatures as determined by gradient PCR

Mutants	Hybridisation temperatures (°C)
H20P	53
R59W	57
R168C	40

Transformation of BMH 71-18 mutS competent cells

After thawing, 100μl *mut*S competent cells were placed in chilled culture tubes and 1.5μl of mutagenesis reaction added. After standing on ice for 10min, cells were heat-shocked for 50s at exactly 42°C without shaking, then placed on ice for 2min. Nine hundred μl of LB medium at room temperature (without antibiotic) was added to the reaction. Incubation for 1h at 37°C with shaking, followed, to allow expression of the resistance gene. A 5ml LB culture containing GeneEditor Antibiotic Selection Mix was then prepared from the above, and incubated overnight at 37°C with shaking (appendix 1.4).

Plasmid DNA Purification

The plasmid DNA was purified from the above overnight culture using the Wizard Plus SV miniprep DNA purification procedure (appendix 3) and quantified on a GeneQuant spectrophotometer.

Transformation into JM109

This transformation is detailed in Appendix 1.5. Briefly, two transformations were performed (approximately 2.5ng and 5ng of plasmid DNA used). Thawed supercompetent (>10^8 cfu/μg) JM109 cells were transferred into pre-chilled tubes. Cells were heat-shocked and room temperature SOC medium added to each transformation reaction. Reactions were incubated for 1h at 37°C with shaking and the cells plated on ampicillin/ antibiotic selection mix plates and incubated at 37°C for 12 – 14h. A selection of single colonies were inoculated into 10ml LB medium containing 100μg/ml ampicillin in each case, and grown overnight, with shaking at 37°C. Glycerol stocks were prepared for each culture growth and stored at -70°C. Plasmid minipreps were performed on the remains of the culture growth and the DNAs quantified on a GeneQuant spectrophotometer.

6.3.2 Mutational analysis

The appropriate cDNA fragment (which included the mutation) was amplified by PCR utilising DNA (approximately 250ng) extracted from each of the cultures (see appendix 3 for details). The PCR products were analysed on a 6% polyacrylamide gel to check for successful amplification of pure product. Where possible, appropriate restriction analysis was utilised to screen colonies as outlined in appendix 1.6.3. If not, simultaneous single stranded conformation polymorphism and heteroduplex analysis (SSCP/HD) (appendix 6) was applied. Thereafter, direct sequencing was performed on DNA extracted from a positive colony. Once a mutation had been confirmed, the entire cDNA sequence was sequenced to ensure the absence of any erroneous mutations due to PCR error.

6.3.3 Ligation into GFP expression vector

Principle

The pEGFP-N1 expression vector encodes a red-shifted variant of wild-type GFP optimized for brighter fluorescence and higher expression in mammalian cells. The multiple cloning site (MCS) in this vector is located between the immediate early constitutive cytomegaly virus promoter ($P_{CMV\ IE}$) and the EGFP coding sequence. This allows genes cloned into the MCS to be expressed as fusions to the N-terminus of EGFP, if they are in the same reading frame and there are no intervening stop codons. To ensure replication in mammalian cells containing the SV40 large T antigen, the vector contains an SV40 origin of replication. In addition, the presence of a neomycin/kanamycin resistance gene cassette allows transiently transfected eukaryotic cells to be selected using any one of these antibiotics. Finally, the vector provides a pUC origin of replication for propagation in *E. coli.*

Procedure

This procedure is detailed in appendix 2.2. Briefly, the pEGFP-N1 plasmid, wild-type PPOX and the mutants H20P, R59W and R168C, were digested with Bgl II/Hind III. Ligation reactions were prepared by adding 3µl of the digested pEGFP-N1 plasmid to 5µl of each of PPOX wild-type and mutants. One µl each of 10x ligase buffer and T4 DNA ligase enzyme completed a 10µl volume per reaction. The reaction mixtures were incubated overnight at 4°C followed by transformation into supercompetent JM109 cells (appendix 1.5) overnight. Screening for positive colonies was done using both a rapid screening method (appendix 1.6.1), and a PCR-based method using oligonucleotides that flank the PPOX-GFP interface (the interface is defined as the point where the PPOX and GFP sequences meet) (appendix 1.7). Glycerol stocks were made of potential positive colonies and plasmid DNA extracted (appendix 3). The extracted DNA was quantified and PCR performed using PPOX-GFP interface oligonucleotides. The PCR products were purified and directly sequenced (appendix 1.6.4) to confirm in-frame PPOX-GFP ligation.

6.3.4 Rapid screening of bacterial colonies

Principle

One of the essential prerequisites for gene cloning is an efficient method to select bacteria that have been transformed with recombinant plasmids. The selection becomes more difficult when the cloning vector contains only one selectable marker, or the ligation is particularly difficult. As the *PPOX* cDNA (1.4kb) was subcloned from a 4.4kb pTrcHis expression vector into a 4.7kb GFP vector, rapid screening on the basis of size provided an efficient method of selecting potential positive colonies.

Procedure

The method used was a modification of that of Sekar (1987) and is detailed in appendix 1.6.1.

6.3.5 PCR-based confirmation of bacterial colonies

Procedure

This method is detailed in appendix 1.7. Briefly, a specific set of oligonucleotides were designed to produce a PCR product that included the PPOX construct and PPOX-GFP interface. Once the PCR was optimised the oligonucleotide set (appendix 1.7) was used to identify positive PPOX-GFP fusion constructs.

6.3.6 Transfection into HepG2s

Principle

A number of methods have been developed to transfer DNA into eukaryotic cells for the study of gene regulation and expression. These methods include the use of calcium phosphate or other divalent cations, polycations, retroviruses, microinjection and electroporation. However, all of these methods suffer from one or more problems related to cellular toxicity, poor reproducibility, inconvenience or inefficiency of DNA delivery. To avoid these problems, a cationic liposome-mediated transfection method was used. In principle, the transfection reagent, N-[1-(2,3 Dioleoyloxy)propyl]-N,N,N-trimethylammonium methylsulphate (DOTAP), is mixed with the DNA resulting in spontaneously formed complexes which can be added directly to the tissue culture medium. This method of DNA transfer to the eukaryotic cells is very "gentle", avoiding the cytotoxic effects encountered with other transfection methods.

Procedure

This procedure is detailed in appendices 7 and 8. Briefly, HepG2 cells were cultured in a 10cm petri-dish containing 10ml DMEM enriched with 10% FCS. Cells were lifted using a 10% trypsin solution and re-plated onto 35mm^2 coverslips in 6-well tissue-culture dishes. After overnight adherence, the cells were washed twice with room temperature 1 x phosphate-buffered saline (PBS) and transfected with the appropriate plasmid DNA for 18h as detailed in appendix 8. After a brief rinse with PBS, unfixed cells were mounted onto microscopic coverslips and viewed by fluorescent microscopy (appendix 9). Every transfection was performed in duplicate and a positive (pOTC-GFP) and negative (GFP only) transfection control included in every experiment. In certain experiments a red mitochondrial-specific dye (Mitotracker) was added to the cells 30 min before the end of the experiment. This dye served to show co-localisation of the PPOX-GFP fusion proteins and mitochondria by a resultant orange/yellow fluorescence ie. red overlaid by green.

6.3.7 Microscopic analysis

Principle

Using GFP as an intracellular fluorescent tag has revolutionized protein and molecular biology. The increased use of GFP expression vectors to visualize fusion proteins of interest has meant that new, and updated, fluorescence imaging and microscopic methods are constantly being sought. In this dissertation a combination of basic fluorescent microscopy and computer-based visualization programmes, allowed the GFP fusion proteins to be analysed and discriminated against cellular autofluorescence.

Procedure

The coverslip-mounted cells were viewed at overall magnifications of 200x, 400x and 1000x. All photographs presented are at a total magnification of 1000x. The fusion proteins were visualized using a long pass filter set with an excitation range of 450-490nm and an emission wavelength of 520nm. The images were captured using a digital camera and processed via Zeiss

Axiovision software. Overlay images were created using Adobe Photoshop, v5.

6.4 Results and Discussion

6.4.1 Engineering of VP-causing mutations

In wild-type human PPOX DNA an additional HindIII restriction endonuclease cutting site was successfully engineered upstream of the stop codon and confirmed by direct sequencing as shown in Fig 6.1. (Prior to this engineering, the Hind III downstream of the stop codon of Fig 6.1 was a unique site.)

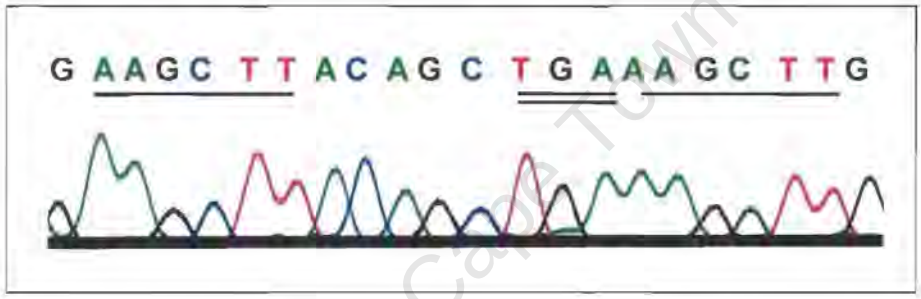

Fig 6.1 Partial sequence using a forward oligonucleotide of the *PPOX* carboxy terminal end indicating the incorporated Hind III restriction endonuclease sites to enable removal of the stop codon (TGA). Hind III sites are single underlined and the stop codon is doubly underlined.

After removal of the stop codon, three VP-causing mutants H20P, R59W and R168C were successfully engineered using site-directed mutagenesis and confirmed by direct sequencing (Figs 6.2 and 6.3).

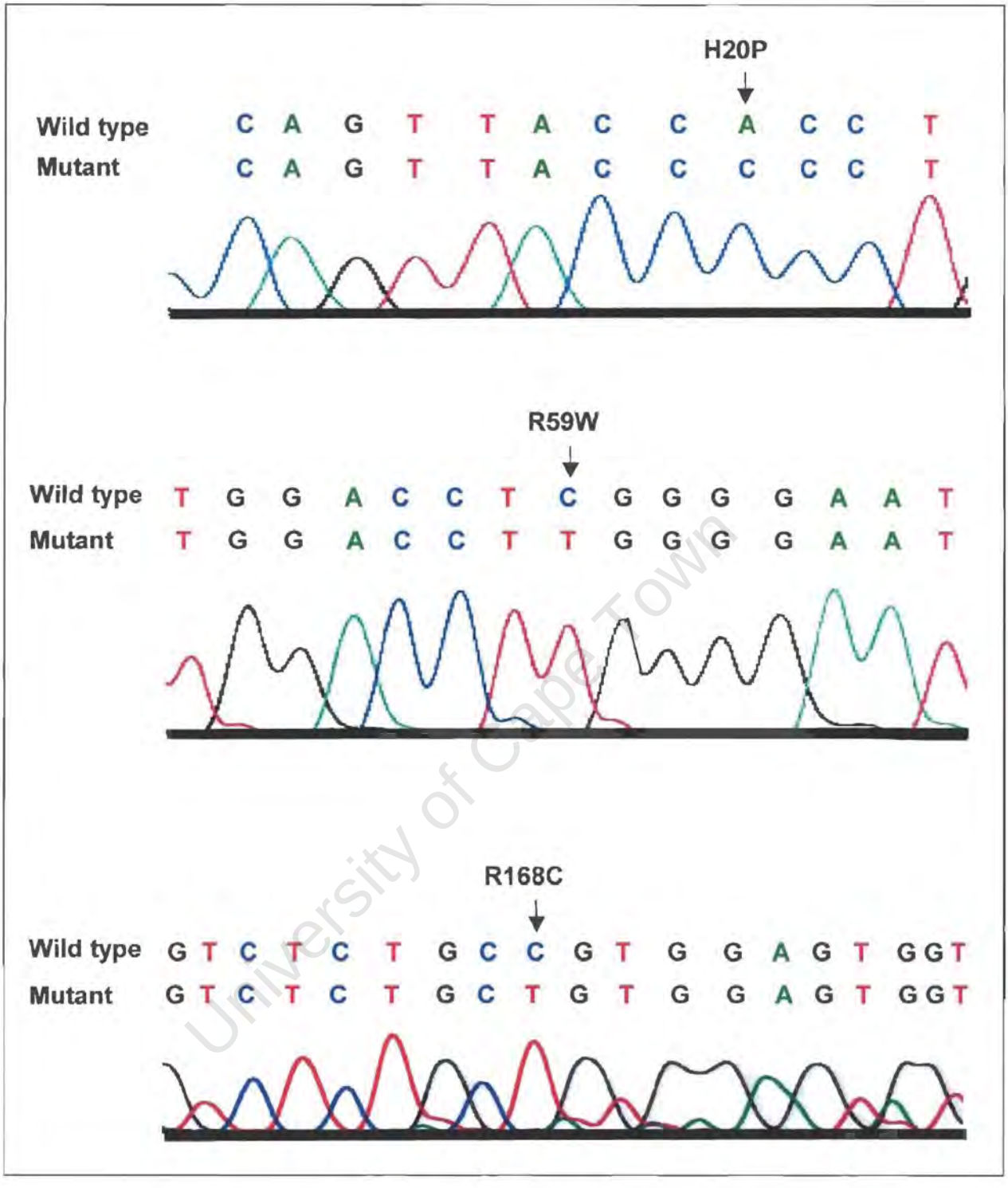

Fig 6.2 Direct sequencing using forward oligonucleotide of respective fragments of engineered *PPOX* cDNA. In each case, the wild-type sequence is indicated above.

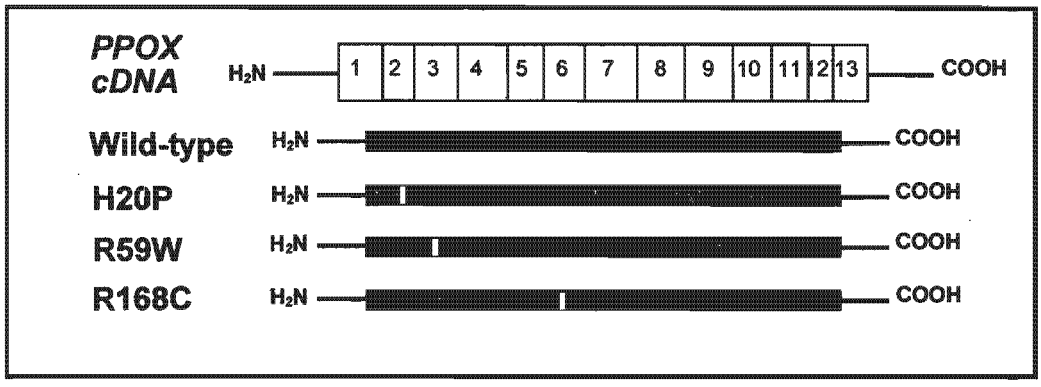

Fig 6.3 Schematic diagram of wild-type and the three VP-causing mutants engineered. *Top*, exon structure of human PPOX cDNA. *Bottom*, Exonic positions of mutations created by site-directed mutagenesis (white bars).

In the transformation of *mutS* competent cells the recommended volume of antibiotic selection mix added to the overnight culture was reduced by 50% as repeated attempts using the amount referred to in the manufacturer's protocol proved unsuccessful. Although co-transfection of cells with both wild type and mutant plasmids was occasionally problematic during transformation into JM109 cells, a reduction in the amount of DNA used in the transformation reaction eliminated this problem.

Figure 6.4 shows combined SSCP/HD analysis used to identify H20P positive clones. In this instance no heteroduplexes were visible as the single strands were allowed to run far into the gel to ensure good resolution.

Figure 6.5 shows Ava I restriction analysis on a 6% polyacrylamide gel used to identify the R59W positive clones.

BsaJ1 restriction analysis was used to identify positive R168C clones (Fig 6.6).

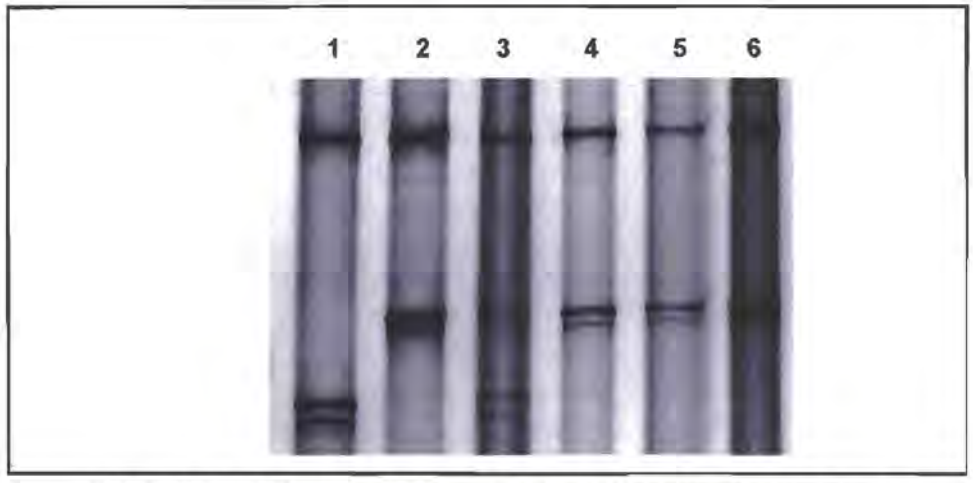

Fig 6.4 SSCP of the PCR product of fragment 1 to identify the H20P mutant. *Lane 1*, H20P +ve colony, *lanes 2 & 4-6*, H20P –ve colonies, *lane 3*, R59W (positive control).

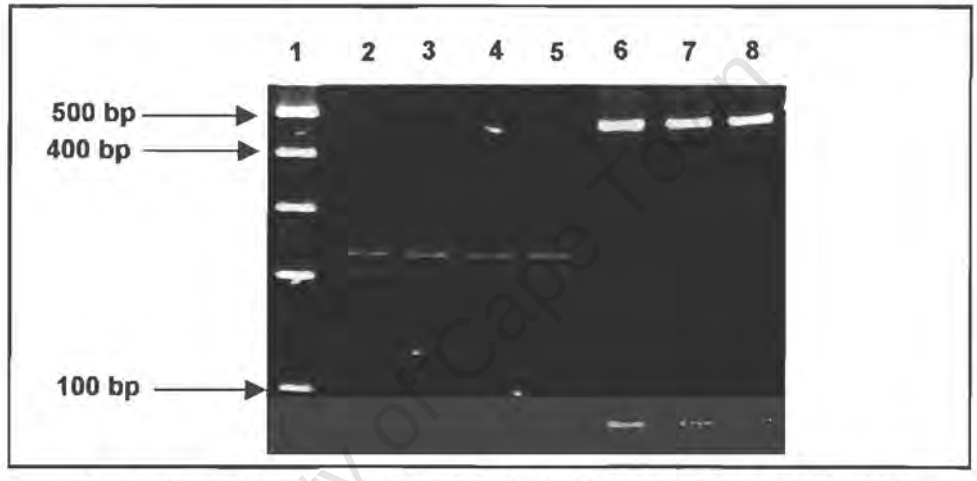

Fig 6.5 Ava I restriction analysis of the PCR product of fragment 1 to identify the R59W mutant. *Lane 1*, bp markers, *lanes 2-5*, wild-type (post-digestion), and *lanes 6-8* are positive R59W clones (post-digestion).

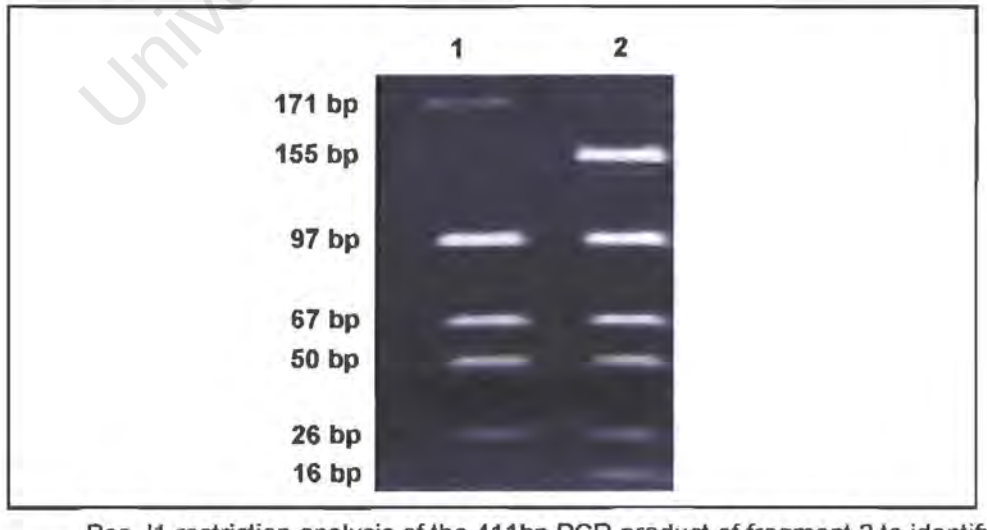

Fig 6.6 Bsa J1 restriction analysis of the 411bp PCR product of fragment 2 to identify the R168C mutant. *Lane 1*, digested R168C positive clone, *lane 2,* Wild-type PPOX fragment 2. The sizes indicated on the left are based on a 25bp marker omitted from this figure due to it being adjacent to a number of irrelevant lanes.

6.4.2 Engineering of PPOX-GFP fusion proteins

Direct sequencing was performed in both wild-type PPOX and all 3 VP-causing mutants to confirm in-frame ligation into the GFP expression vector as seen in figure 6.7.

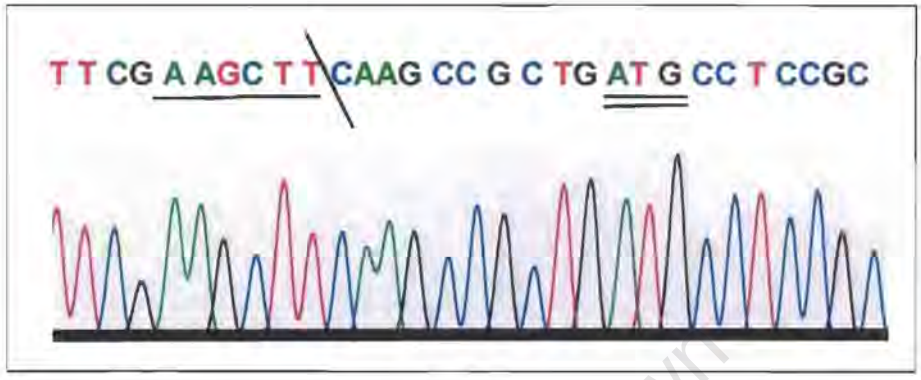

Fig 6.7 Partial direct sequence using the forward oligonucleotide of the R59W-GFP fusion protein. The HindIII site is underlined and the start site of the GFP vector is doubly underlined. The "\" indicates the PPOX-GFP ligation interface.

6.4.3 Mitochondrial targeting of fusion proteins

Wild-type PPOX-GFP : Predictably, the wild-type PPOX-GFP fusion protein targeted to the mitochondrion (Fig 6.8A1). For orientation and visualization, the cells are outlined in white with their nuclei encircled in red (Fig 6.8A1-3). Mitochondrial-specific targeting was confirmed by the co-localization of MitoTracker Red, a dye that accumulates and fluoresces red in the reduced environment of active mitochondria (Fig 6.8A1-3). Intracellularly, the mitochondrial localization was very clear, presenting as punctate, fluorescent oval or cigar-shaped tubes (depending on the orientation of the mitochondrion) characteristic of the specific localization in the OTC presequence positive control (Fig 6.8F). This was in contrast to the diffuse, cytosolic pattern exhibited by the EGFP vector (negative control) (Fig 6.8E).

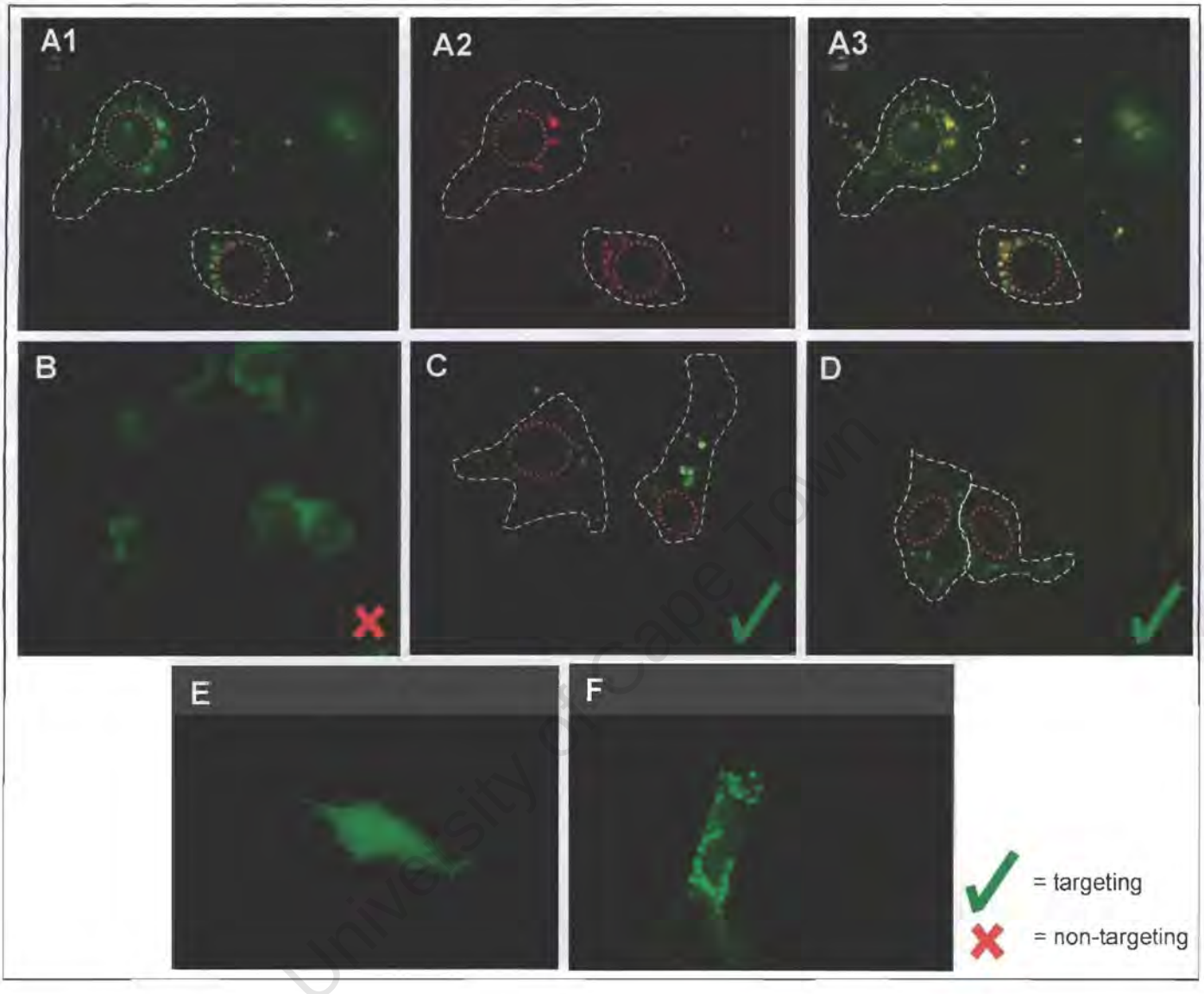

Fig 6.8 PPOX-GFP fusion proteins transfected into HepG2 cells visualized by fluorescent microscopy. *A1*, Wild-type PPOX-GFP demonstrating intracellular mitochondrial localization. *A2*, MitoTracker red fluorescence. *A3*, Merged (green overlaid with red) image. Cells are outlined by dotted lines and the nuclei are circled in red. *B*, H20P-GFP fusion protein showing a diffuse cytosolic pattern of fluorescence. *C*, R59W-GFP fusion protein with the cells outlined by white dotted lines. *D*, R168C-GFP fusion protein. *E*, EGFP vector transfected alone acting as a negative control. *F*, OTC-GFP fusion protein used as a positive control of intracellular mitochondrial localization. All photographs were captured at 1000X magnification under oil and processed using Zeiss Axiovision software. Merged images were processed using Adobe Photoshop software.

Very little autofluorescence was visible. Autofluorescence may be problematic as it fluoresces at similar wavelengths and masks the true GFP signal. This problem was overcome as follows :
Mounting medium containing an "anti-fade" agent was utilized, the cells were not fixed with any standard fixative such as paraformaldehyde (known to increase autofluorescence) and the slides mounted and viewed.

The other aspect that may become problematic is photobleaching. All fluorescent dyes bleach over time due to the formation of oxygen radicals as a side product of the photochemistry of fluorescence. These then react with the dyes and destroy them (Lippincott-Schwartz et al. 2003; Lippincott-Schwartz and Patterson 2003; Zimmermann et al. 2003). Photobleaching is especially problematic with fluorescence microscopy due to the high intensity of the illumination. This problem was overcome in this study by the use of the mounting medium (Permafluor, which contains radical scavengers) and EGFP, the enhanced version of the GFP expression vector series, which showed low levels of photobleaching.

H20P-GFP : H20P-GFP did not localize in the mitochondrion and exhibited a cytoplasmic distribution (Fig 6.8B) comparable to the negative control (Fig 6.8E). His20, despite not being highly conserved through PPOX species (Fig 6.8), is located close to the putative GXGXXG dinucleotide binding motif which may account for the loss in enzymatic activity displayed biochemically (Maneli et al. 2003). Thus, it would be difficult to conclude that H20P VP is actually due to lack of mitochondrial targeting alone, as the H20P clinically results in a severe reduction in enzyme activity and typical cutaneous VP most probably due to the influence of the mutation on FAD binding.

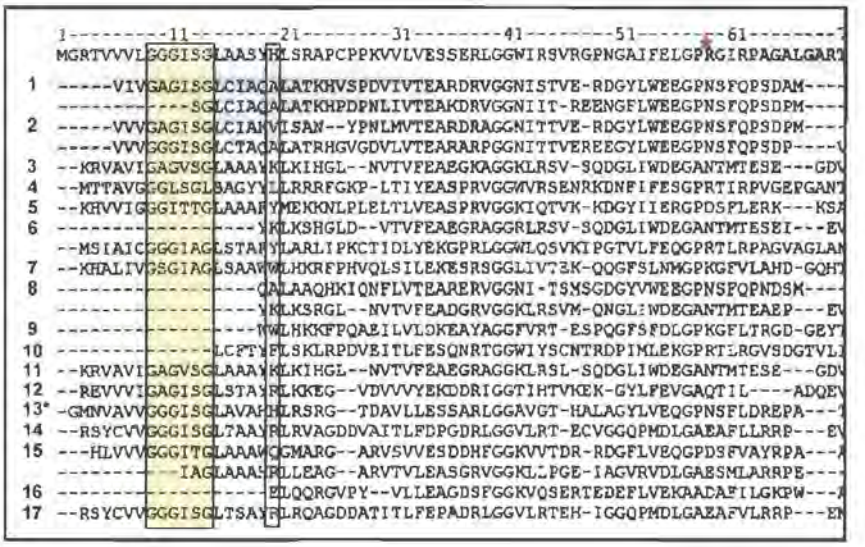

Fig. 6.9 Sequence alignment of the first 70 amino acid residues of PPOX from 18 different organisms using the Jpred multiple sequence alignment program (www.expasy.ch). *Top*, human PPOX (*H. sapiens*). Seventeen PPOX sequences are numbered on the left. 1, *Cichorium intybus (chicory)*; 2, *Solanum tuberosum*; 3, *Nicotiana tabacum*; 4, *Drosophila melanogaster*; 5, *Bacillus subtilis*; 6, *Glycine max (soybean)*; 7, *Chlamydia trachomatis*; 8, *Chlamydomonas reinhardtii*; 9, *Chlamydomonas pneumoniae*; 10, *Saccharomyces cerevisiae*; 11, *Solanum tuberosum*; 12, *Aquifex aeolicus*; 13, *Myxococcus xanthus*; 14, *Mycobacterium leprae*; 15, *Propionibacterium freudenreichii*; 16, *Dynococcus radioduran*; 17, *Mycobacterium tuberculosis*. *Yellow boxed area*, highly conserved dinucleotide-binding motif. *Grey boxed area*, His20 residue. The Arg59 residue is marked by a red asterisk. *M. xanthus* (13*) is the only other organism in which His20 is conserved.

Interestingly, an unusually high frequency of mutations in the *PPOX* gene associated with the replacement of wild-type amino acids by proline has been reported in UK VP patients (Whatley et al. 1999b). Thirty five percent of their missense mutations represent a substitution by proline. The majority are leucine to proline substitutions. Other mutations reported include a serine to proline mutation at codon 450 (S450P) (Frank et al. 1998) and an arginine to proline at codon 138 (R138P) (Corrigall et al. 2000). Proline is known to decrease protein flexibility (Tian et al. 1998) as it is bonded covalently to the nitrogen atom of the peptide backbone and thus has no amide hydrogen for use as a donor in hydrogen bonding or resonance stabilization of the peptide bond of which it is part. Moreover, the cyclic five-membered proline ring

imposes rigid constraints on rotation about the nitrogen-carbon bond of the peptide backbone (Creighton 1993).

H20P is located in a region predicted to be a putative N-terminal α-helical domain involved in mitochondrial targeting (residues 11-24) (Von Und Zu Fraunberg et al. 2003). These authors report a computer-predicted helix starting with a glycine residue at position 11. However, basic structural biological principles would suggest that the helix starts at position 12 with the isoleucine residue (see chapter 7). The H20 residue of PPOX falls in approximately the middle of the α-helix. Although proline residues may be tolerated at the start of α-helices and may be accommodated in long α-helices, the substitution of the histidine with a proline could well be expected to have a considerable impact on helix formation with a subsequent loss of secondary conformation. To date, the existence of a proline residue in the middle of a helix is described in only one protein namely, mellitin (a protein found in Bee venom) (Kreil 1975). It is probable that PPOX requires the α-helix for interaction with outer mitochondrial machinery and subsequent localization possibly explaining the resultant lack of targeting in the H20P-GFP mutant.

Interestingly, 7 missense mutations in the PPOX gene which resulted in the replacement of a residue with a proline (R38P, L73P, L85P, L154P, L295P and L444P) had no effect on translocation of PPOX-YFP (yellow fluorescent protein) to mitochondria Morgan, R., personal communication). It would appear that in the case of the H20P it is its "position" in the center of a critical α-helix that is sufficient to disrupt the helix and therefore targeting. This positional aspect causing a disruption at the secondary structural level is further highlighted by two points. Firstly, none of the 8 naturally occurring mutations reported by von Fraunberg et al. (2003) abolished mitochondrial targeting. However, the I12T mutation, in a shortened N-terminal 28 amino acid construct, did abolish targeting. Secondly, of the 22 mutations studied by Morgan et al. (2002), only V335G disrupted mitochondrial import and it appears that this mutation abolishes targeting due to a direct effect on protein

folding rather than an alteration of sequence required for targeting (Morgan, R., personal communication).

R59W-GFP : The R59W mutation had no effect on mitochondrial targeting of the fusion PPOX protein as evidenced by specific intracellular mitochondrial localization (Fig 6.8C). The R59W mutation occurs in a CpG trinucleotide, known to confer a high probability of mutation, particularly with a C to T transversion (Cooper and Krawczak 1990). Furthermore, it falls within the 60 bp flanking region of the putative FAD dinucleotide-binding motif of PPOX (Nishimura et al. 1995; Dailey and Dailey 1996). Recent work in our laboratory has shown that the R59W mutation is associated with greatly reduced enzyme activity and FAD binding was altered (Maneli et al. 2003). Study of the R59 residue using various mutants (R59W, R59S, R59I and R59K) created by site-directed mutagenesis has revealed that the positive charge at R59 is directly involved in catalysis and not in FAD binding. The fact that R59W does not bind FAD is more likely the result of its aromatic bulky nature.

R168C-GFP : The replacement of a basic arginine residue with a neutral, sulphur-containing amino acid cysteine at codon 168 did not affect mitochondrial localization (Fig 6.8D). The R168C mutation occurs at a evolutionary conserved site reported to be located within a putative membrane-anchoring domain (residues 150-205 in yeast PPOX) (Arnould et al. 1999). More recent predictive studies suggest the membrane-anchoring domain to be located at residues 142-192 (Morgan et al., personal communication) with two predictive helices at residues 158-167 and 177-191 (Von Und Zu Fraunberg et al. 2003) flanking a fold (residues 168-176). Although this places the R168C mutation within the protein fold (Morgan et al., personal communication) with the possibility of altering enzyme conformation, it seems to have no adverse effect on mitochondrial targeting (Fig 6.7D). This despite the site being a hypermutable CpG site as evidenced by the presence of a R168H mutation having been reported thrice, although it is unclear whether these are, indeed, unrelated individuals (de Rooij et al. 1997; Frank et al. 1998; Whatley et al. 1999a). The lack of effect of the R168C mutation on secondary structure was surprising as an additional cysteine residue could

cross-react to form alternative disulphide linkages thus changing the three dimensional shape of the protein. The mitochondrial targeting of two previously reported mutants (R152C-GFP and R168H-GFP) gave a similar result in COS-1 cells (Morgan et al. 2002; Von Und Zu Fraunberg et al. 2003) as our R168C-GFP mutant.

6.5 Conclusions

- The 3 mutations of interest (H20P, R59W and R168C) were successfully engineered into an EGFP expression vector.
- The H20P mutation in the PPOX protein completely abolishes mitochondrial targeting most likely due to a severe effect on secondary structure at the level of α-helix formation.
- The R59W and R168C VP-causing mutations have no adverse effect on intracellular mitochondrial targeting.
- Even though the R168C mutation creates an additional cysteine with the possibility of disulphide bridge formation, its mitochondrial location suggests that no adverse conformational effect is caused at a secondary structural level.
- Based on the fact that the H20P mutant does not target, whereas R59W and R168C do, the N-terminal region of PPOX appears to contain important structural motifs/consensus sequences for efficient translocation of PPOX from the nucleus to the mitochondrion.

Because of the apparent involvement of the N-terminus, we investigated this region of PPOX in more detail (Chapter 7).

CHAPTER 7 : MITOCHONDRIAL TARGETING OF ENGINEERED N-TERMINAL PPOX-GFP FUSION CONSTRUCTS

CHAPTER 7 : MITOCHONDRIAL TARGETING OF ENGINEERED N-TERMINAL PPOX-GFP FUSION CONSTRUCTS

7.1 Introduction

As detailed in chapter 4, the vast majority of mitochondrial proteins are encoded by nuclear genes and synthesised on cytosolic ribosomes, usually as precursors with transient amino-terminal presequences. These precursors are then translocated through the intracellular cytoplasm towards the mitochondrion where they are finally localized in one of the four mitochondrial compartments. In most cases, upon import, the presequences are proteolytically cleaved by specific proteases in the matrix and on the outer face of the inner membrane (Glick and Schatz 1991). Although presequences contain all the necessary information for targeting the majority of attached proteins to their correct intramitochondrial locations (Hurt et al. 1986), no significant sequence homology exists among those whose primary structure is known. Characteristically, however, these sequences lack acidic amino acids, are rich in basic, hydrophobic and hydroxylated amino acids; and can potentially fold into amphiphilic α-helices (Roise et al. 1986). The bulk of proteins imported into the mitochondrion contain signal sequences at the amino terminal end (Pfanner 2000). However, some have signal sequences at the carboxyl terminus allowing import in a carboxy-to-amino terminal direction (Lee et al. 1999).

Of the mitochondrial PPOXs studied to date only *A. thaliana* (Narita et al. 1996) and spinach (Watanabe et al. 2000) have cleavable presequences that direct mitochondrial import. In the yeast PPOX the first 13 residues at the N-terminus may function as a non-cleavable targeting sequence (Camadro and Labbe 1996). An earlier study on the characterization of HPPOX reported the lack of a classical mitochondrial targeting N-terminal presequence or a membrane spanning domain (Dailey and Dailey 1996). However, the N-terminal 28 residues of HPPOX (residues 1-28) have some features characteristic of a presequence and it does not form an amphipathic helix

(Nishimura et al. 1995). These 28 amino acid residues have recently been shown to contain an independently functioning mitochondrial targeting signal (Von Fraunberg, 2003). However, at the commencement of this work there remained the necessity to examine the possibility that the PPOX N-terminus plays a role in mitochondrial targeting.

This chapter therefore examines the PPOX N-terminus as a potential mitochondrial targeting sequence, the characteristics therein that affect targeting and localization, and the effect specific mutations potentially have on the secondary structure of the sequence and their subsequent effect on targeting.

7.2 Objectives

- To identify whether the PPOX N-terminus contains a functional mitochondrial targeting sequence.
- Assuming the N-terminus possesses some targeting functionality, to establish the minimal length required to effect such targeting.
- Establish whether overall positive charge has any effect on the targeting efficiency of the potential PPOX N-terminal mitochondrial targeting sequence.
- Examine whether changes at the H20 position may have any significant effect on mitochondrial targeting.
- Identify whether PPOX possesses additional mitochondrial targeting signals downstream of the N-terminal located sequence.

7.3 Methods

7.3.1 Prediction of secondary structure

Principle

PredictProtein is a secondary structure predictor for an input amino acid sequence. It compares the input sequence with a large database (PROSITE) and the results are shown as predictions of multiple sequence alignments (PSI-BLAST and MAXHOM) and secondary protein structural information such as alpha helices and beta sheet content (Rost 1996).

Procedure

Secondary structure prediction of the human PPOX (accession number, X99450) using the PredictProtein computer programme was performed (Appendix 10.2). The predicted secondary structures relevant to this study are displayed in Fig 7.1.

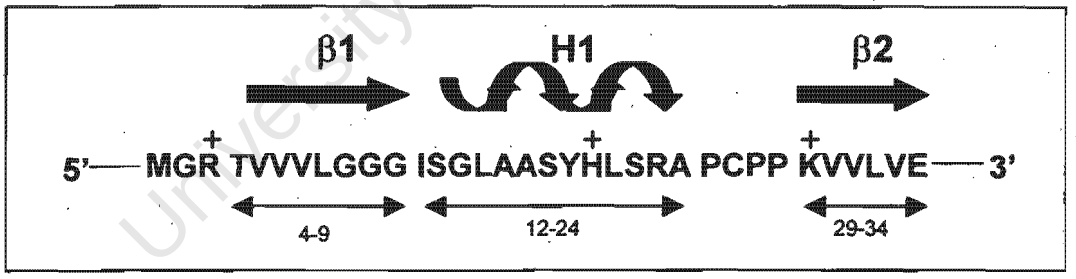

Fig 7.1 Secondary structure prediction of the first 34 amino acid residues of the human PPOX N-terminus analysed by the PredictProtein software programme (http://cubic.bioc.columbia.edu/pp res/). β, beta-sheets (residues 4-9 and 29-34), H, alpha-helix (residues 12-24). Positively-charged residues are indicated with a "+".

Based on the prediction, a series of PPOX-GFP constructs were designed and successfully engineered (Fig 7.2). Thus, to investigate –

i) the minimum number of N-terminal residues required for mitochondrial targeting, we created the PPOX12-, 14-, 15-, 16-, 17-, 20- and 24 residue-GFP constructs (Fig 7.2A);

ii) the effect of charge on the potential N-terminal 17-residue targeting signal, we replaced the only charged residue (positive Arg3) with a glutamic acid (ie. a negative overall charge), lysine (conservative replacement) and serine residue (neutralizing overall charge) (Fig 7.2B);

iii) the effect, if any, that a disruption within the first PPOX α-helix (residues 12-24) may have on mitochondrial targeting, we replaced His20 with a serine (H20S), alanine (H20A), lysine (H20K), glutamic acid (H20E), glycine (H20G) and proline (H20P) residue (Fig 7.2C);

iv) the possibility of additional targeting signals located internally in the PPOX sequence, we engineered a construct (PPOXΔ1-17) lacking the N-terminal 17-residue targeting signal (Fig 7.2D).

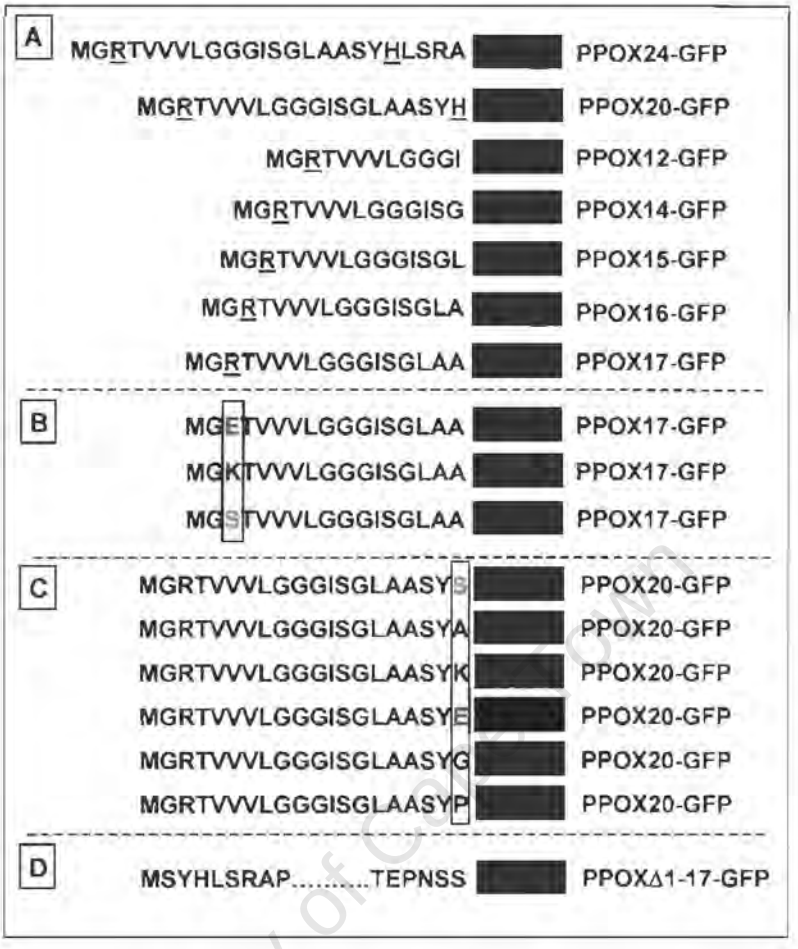

Fig 7.2 Schematic presentation of PPOX-GFP constructs engineered. A, The constructs were tested in the sequence as listed (see text). Positively-charged residues are underlined. B, 17-residue N-terminal mitochondrial targeting sequence constructs. Arg3 (wild-type) was altered to the residues as indicated in colour. C, 20-residue constructs with His20 (wild-type) altered to the residues indicated in colour. *D*, PPOX-GFP construct with a deletion (Δ) of residues 1-17 to identify potential downstream/internal targeting signals. Colour code for sections B and C : Red, negatively charged residue; blue, positively charged residues; brown, neutral residues; black, hydrophobic residues.

7.3.2 PCR-based mutagenesis

Principle

Oligonucleotides were designed to enable amplification by PCR of the desired fragments. The fragments were flanked by unique Bgl II and HindIII restriction enzyme sites.

Procedure

The method is detailed in appendix 2.1. Briefly, a range of oligonucleotides were designed (see table 6, appendix 2.1) and the appropriate PCR programmes optimised (table 7, appendix 2.1) to produce specific-sized products.

Restriction digestion and ligation into GFP vector

PCR products and the GFP vector were digested with Bgl II/Hind III restriction enzymes and ligation performed overnight at 4°C (vector : PCR product :: 1 : 7) as detailed in appendix 2.2.

Transformation into JM109s

This transformation is detailed in Appendix 1.5. Briefly, supercompetent (>10^8 cfu/μg) JM109 cells (100μl) were transformed with cDNA. Cells were heat-shocked and after adding SOC medium (900μl) at room temperature, incubated for 1h at 37°C with shaking. Cells were plated and incubated at 37°C overnight. A selection of single colonies were inoculated into 10ml LB medium and grown overnight. Glycerol stocks were prepared for each culture growth and stored.

7.3.3 Identification of PPOX-GFP fusion constructs

Principle

Three methods were used to identify and confirm correctly engineered PPOX-GFP fusion constructs.

Procedure

Rapid screening of bacterial colonies

The method used was a modification of that of Sekar (1987) and is detailed in appendix 1.6.1. Briefly, randomly selected colonies are transferred to a reference master plate which is then incubated overnight. While transferring to the master plate, a small amount (~10% of the bacterial colony) of the colonies is resuspended in 5μl of protoplasting buffer (see Appendix 13) and incubated at room temperature. Samples are loaded under 2μl lysis buffer (in each gel well) and electrophoresed through a 0.8% agarose gel (Appendix 13). The gel is then viewed and photographed under UV illumination.

Identification by PCR

See appendix 2.3.1. Briefly, a specific set of oligonucleotides were designed to produce a PCR product (table 8, appendix 2.3.1) that included the PPOX construct and the PPOX-GFP interface. Once the PCR conditions were optimised (table 9, appendix 2.3.1), PCR was performed to identify positive PPOX-GFP fusion constructs.

Identification by restriction analysis

By using the same restriction enzymes used to clone the PPOX construct into GFP (ie. Bgl II/Hind III), restriction enzyme analysis was used to identify positive PPOX-GFP fusion constructs. The method is detailed in appendix 2.3.2.

Confirmation by direct sequencing

After identification of potential positive PPOX-GFP constructs the PCR fragments were sent for direct sequencing as detailed in appendix 2.3.3.

7.3.4 Plasmid DNA Purification

The plasmid DNA from a confirmed positive clone was purified from the above overnight culture using the Wizard Plus SV miniprep DNA purification procedure (appendix 3) and quantified.

7.3.5 Transfection into HepG2s

As described in chapter 6.

7.3.6 Microscopic analysis

As described in chapter 6.

7.4 Results and Discussion

A. Identification of a PPOX N-terminal targeting signal

Engineering of PPOX-GFP fusion constructs

Direct sequences of all the constructs shown in Fig 7.2A, were obtained. PPOX20-, and PPOX15-GFP are shown as examples (Fig 7.3A & B) of in-frame GFP ligations. In addition, all constructs were also confirmed by restriction analysis (Fig 7.3C).

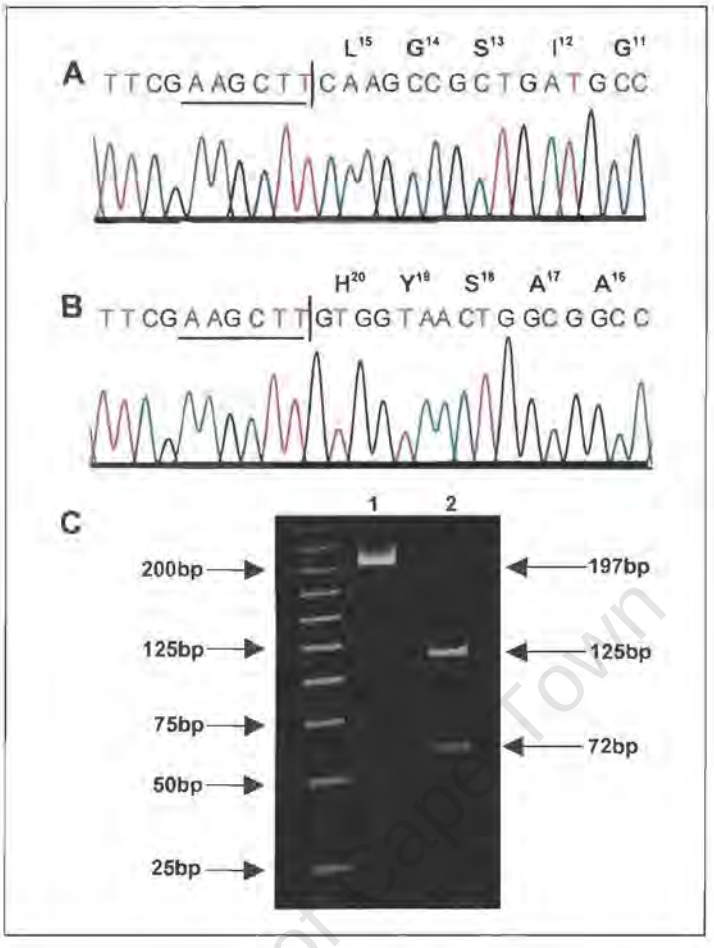

Fig 7.3 Partial reverse direct sequencing of PPOX15-GFP (*A*) and PPOX20-GFP (*B*) and restriction enzyme analysis on a 6% acrylamide gel (*C*) to confirm in-frame ligation. Amino acid residues are indicated above the sequence according to their genetic codes. The code is located above the central nucleotide of the codon and its numbered position in the PPOX sequence is superscripted. The Hind III site is underlined. *C*, PPOX24-GFP PCR fragment (197bp) using oligonucleotides flanking the PPOX-GFP interface, followed by digestion with Bgl II/Hind III. The 25bp marker is shown on the left. *Lane 1*, undigested PCR fragment, *lane 2*, digested fragment (respective sizes are shown on the right).

Problems such as low ligation efficiency and incorrectly-sized ligated products were initially encountered when gel-purified GFP expression vector and PPOX PCR fragments were ligated. These may have resulted from remaining salts and solvents within the agarose gels. The problem was solved by adopting a "shotgun" ligation approach in which unpurified PPOX fragments and GFP vector were digested and immediately ligated in a ratio of PPOX fragment : GFP :: 7 : 1.

PPOX24- and PPOX20-GFP both targeted the mitochondrion (Fig 7.4A and B). The construct size was then reduced to 12 residues (PPOX12-GFP) resulting in a lack of targeting (Fig 7.4C). Residues were then progressively added until targeting was re-established. PPOX14, 15 and 16 (Fig 7.4D-F) did not target the mitochondrion. In these cases they demonstrated a fluorescent distribution pattern comparable to the negative control (Fig 7.4I). However, PPOX17-GFP targeted efficiently exhibiting a specific mitochondrial localization pattern of fluorescence (Fig 7.4G) comparable to the positive control (Fig 7.4H). These data suggest that the first 17 N-terminal amino acid residues of the PPOX protein contain a functional signal for mitochondrial targeting and supports the finding of von Fraunberg et al. (2003) of a mitochondrial targeting signal for PPOX within the first 28 N-terminal amino acids. Although the PPOX N-terminus is not considered to have the ability to form an amphiphillic helix (Nishimura et al. 1995), analysis of the first 17 residues using predictive helical software (http://www.site.uottawa.ca/~turcotte/resources/HelixWheel) (appendix 10) indicate the ability of the 17 residues to form an amphipathic α-helix ie. charged residue/s situated opposite hydrophobic residues (Fig 7.5). Amphipathic helices have been shown to be important for recognition by the translocation machinery in mitochondria in particular the Tom20 import receptor (von Heijne 1986). A recently constructed α-helical computer model of the PPOX N-terminus (residues 6-23) shows that it could interact with a hydrophobic groove on the surface of Tom20 which suggests a possibly mechanism for mitochondrial import (Von Und Zu Fraunberg et al. 2003).

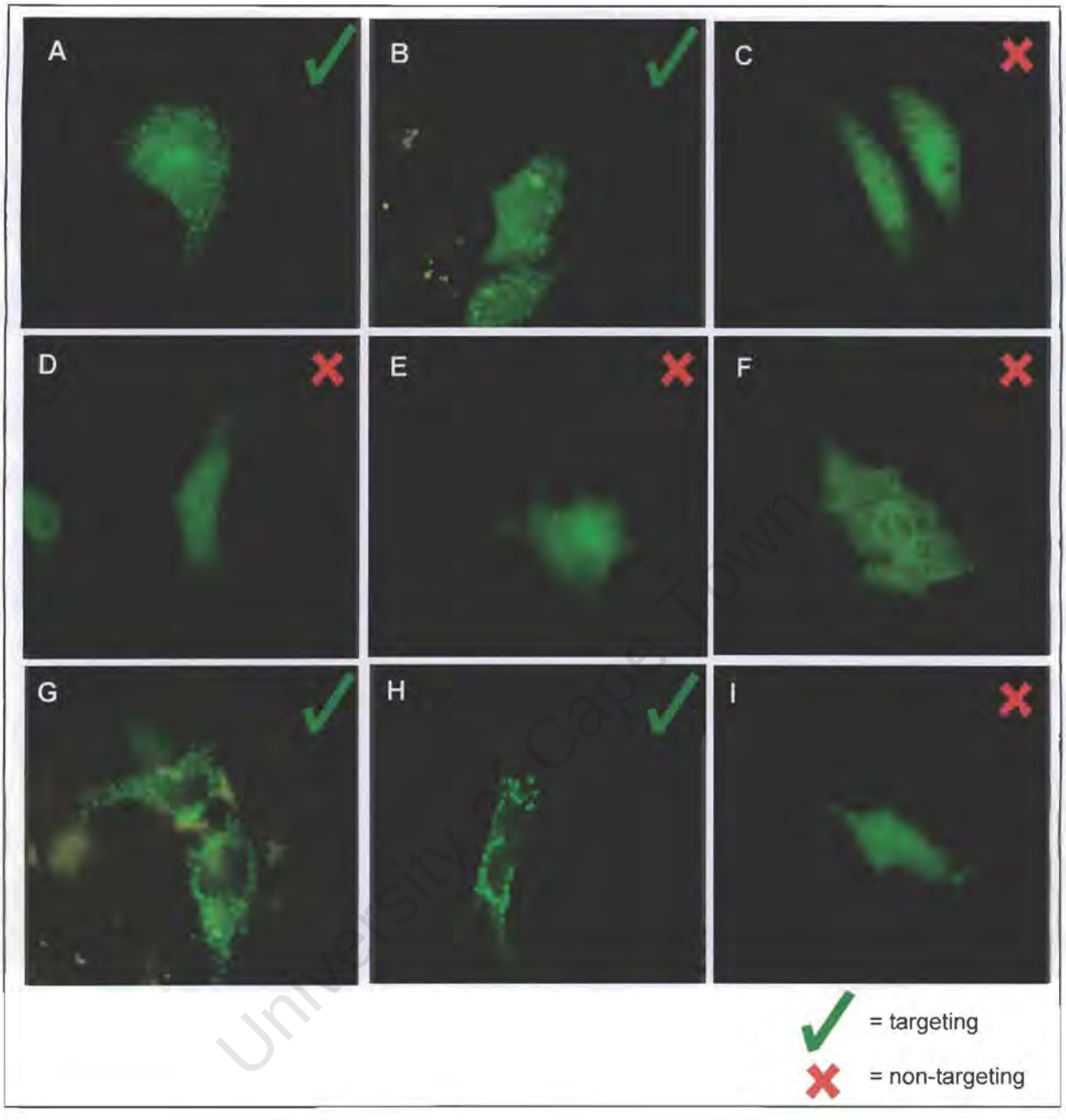

Fig 7.4 Series of PPOX-GFP constructs and controls transfected into HepG2 cells. *A*, PPOX24-GFP; *B*, PPOX20-GFP; *C*, PPOX12-GFP; *D*, PPOX14-GFP; *E*, PPOX15-GFP; *F*, PPOX16-GFP; *G*, PPOX17-GFP, *H*, OTC-GFP fusion protein (positive control of intracellular mitochondrial localization); *I*, EGFP vector transfected alone (negative control). All photographs were captured at 1000X magnification under oil and processed using Zeiss Axiovision software.

Based on the experiments presented thus far, we cannot conclude that the N-terminus is functional in targeting PPOX to the mitochondrion *in vivo*. However, it clearly is capable of targeting a protein to the mitochondrion and therefore deserved further investigation and discussion. *Why would PPOX17-GFP target, but not PPOX16-GFP ?*

In the absence of PPOX crystal structure information our discussion on this point remains speculative. Earlier secondary structure analysis of the PPOX protein (Nishimura et al. 1995) revealed an α-helix flanked by two beta sheets. It has been predicted that the α-helix commences at residue 11 (Gly11) (Von Und Zu Fraunberg et al. 2003). However, the secondary structure prediction performed in our study and structural principles suggest that due to the flexibility of the glycine residue and its potent helix breaker potential (Chou and Fasman 1974), that the helix starts at Ile-12. Due to a helix consisting of 3.6 residues per turn, the first turn will be completed by residue Ala-16 with the establishment of one stabilizing hydrogen bond. With the addition of every residue thereafter, another hydrogen bond will be formed. The helix, a potential requirement for targeting, would therefore be more stabilized with 17 amino acid residues (2 H-bonds) than with 16 (1 H-bond). The weaker the helix the less likely it would be to engender the correct structural properties required for targeting recognition.

N-terminal mitochondrial signal sequences placed at the carboxy terminus have been shown to mediate import in a carboxyl-to amino-terminal direction (Pfanner et al. 1987; Lee et al. 1999). To investigate the (in)ability of the 17 N-terminal amino acid residues to target PPOX when located at the C-terminus, a GFP-PPOX17 construct was engineered ie. the 17 amino acid targeting sequence was placed at the carboxy terminus of GFP (Fig 7.6A). The carboxy terminal-located targeting sequence did not result in localization of PPOX to the mitochondrion. Instead, a diffuse cytoplasmic distribution of fluorescence was evident (Fig 7.6B).

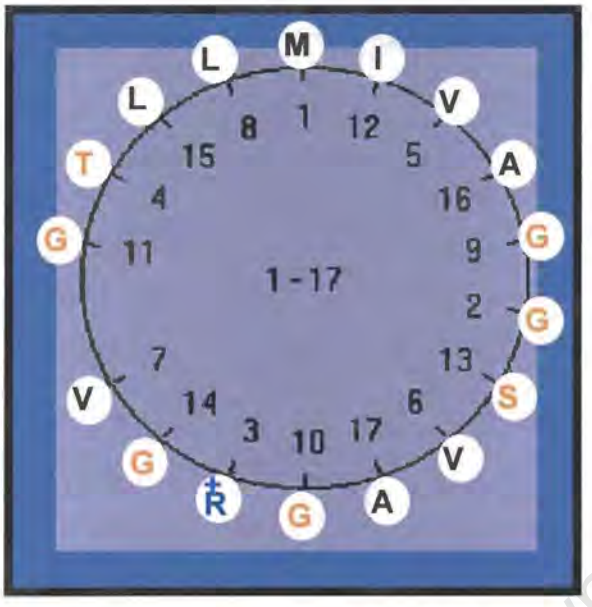

Fig 7.5 Predicted α-helical wheel diagram of residues 1-17 of human PPOX. Hydrophobic, neutral and positively charged residues are indicated in black, brown and blue, respectively. Predictive software used was shareware found at : (http://www.site.uottawa.ca/~turcotte/resources/HelixWheel)

Fig 7.6 GFP-PPOX17 construct transfected into HepG2 cells illustrating that attachment of PPOX17 to the carboxy terminus of GFP did not facilitate mitochondrial targeting.

B. Effect of net positive charge on the N-terminal targeting signal

Engineering of GFP constructs

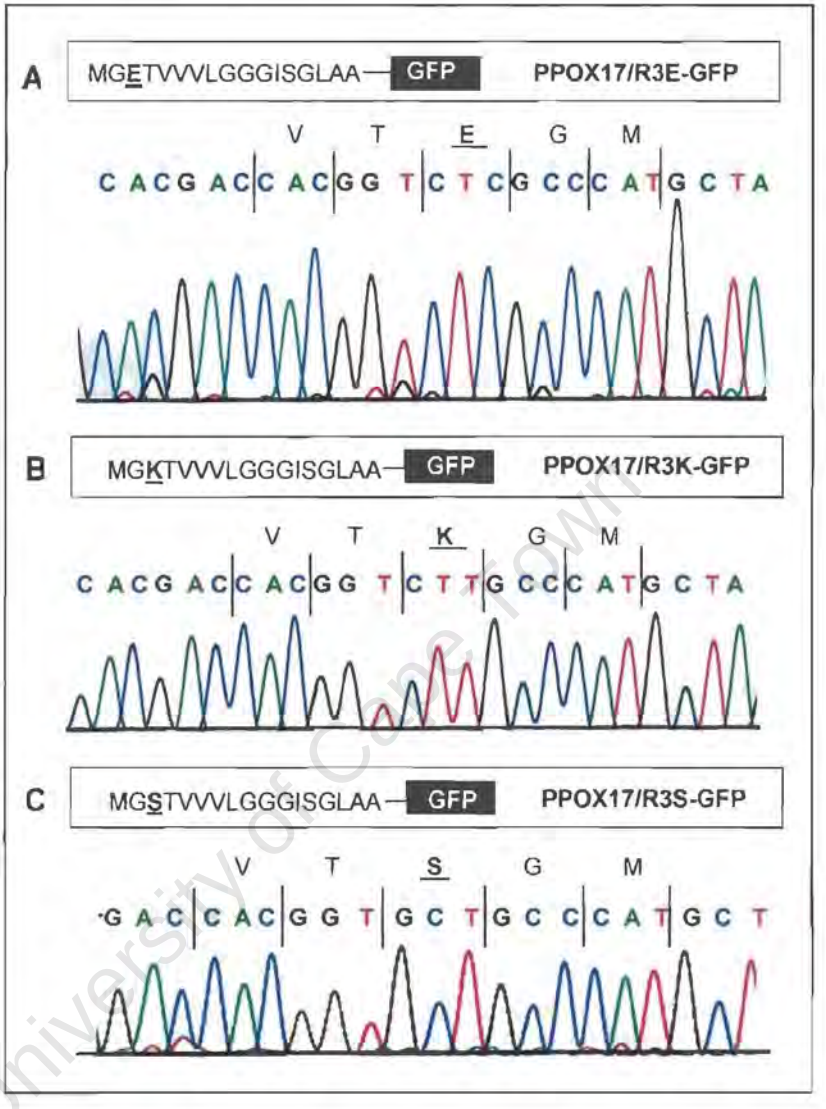

Fig 7.7 Schematic diagram showing constructs and partial direct reverse sequences of PPOX17-GFP. Arg3 was successfully altered to : *A*, glutamic acid (R3E); *B*, lysine (R3K); and *C*, serine (R3S). Altered residues are in bold and underlined. Amino acid residues are indicated above the direct sequence.

Arg3, the only positively charged residue within the 17 N-terminal amino acid targeting sequence was successfully altered to a glutamic acid (R3E) – negative replacement, lysine (R3K) – conservative replacement and serine (R3S) – neutral replacement (Fig 7.7).

Microscopic analysis of mitochondrial targeting

R3E : Changing Arg3 to a negatively-charged glutamic acid, which rendered a negative net charge for the PPOX17 construct, abolished mitochondrial targeting (Fig 7.8A). This lack of targeting could be expected as overall positivity is one of the characteristic features reported for N-terminal mitochondrial targeting sequences (Grant et al. 1986; Chu et al. 1987). Although the PPOX17 construct only contains one positive residue (which is fewer positive residues than most targeting sequences (Tzschoppe et al. 2000)), the Arg3 could still effect targeting as overall positivity is postulated to be involved in ionic interactions between the sequence and the outer mitochondrial machinery (Tom22) (Brix et al. 1997; Brix et al. 1999). A recent report on targeting of the BCS1 inner mitochondrial protein confirms positivity of the N-terminal targeting sequence as the characteristic required for high affinity binding to the Tom20 receptor while a stretch of lysine-rich residues show preference for the Tom22 receptor (Stan et al. 2003). Interestingly, a negative charge within the presequence can sometimes be tolerated as long as the overall charge remains positive (Hammen and Weiner 1998). As mitochondrial membranes possess a negative surface charge, it is thought that the positive charge/s in the presequence could function by directing the precursor proteins into the organelle. An alternative mode of action of the positive charges is that they assist in induction of helical structure (Hammen et al. 1996).

R3K : R3K did not target to the mitochondria. This lack of targeting in the conservative replacement (R3K) was somewhat surprising (Fig 7.8B). However, the possibility that the identity or location of the amino acid side-chain bearing the charge is vital for targeting, cannot be excluded. Structurally, arginine has three non-polar methylene groups and the strong

basic δ-guanido group (appendix 11). With a pK_a value of ±12, the guanido group is ionized over the entire pH range in which proteins exist naturally. The guanido group is planar and the positive charge is effectively distributed over the entire group. In contrast, the lysine side-chains consist of a hydrophobic chain of four methylene groups capped by an amino group. Although it is also ionized under most physiological conditions, a fraction of its amino groups remain non-ionized and readily undergo a variety of acylation, alkylation, arylation and amidination reactions. Moreover, lysine residues could also reversibly form Schiff bases with aldehydes and cofactors such as pyridoxal phosphate. The reactivity of the lysine side-chains make it possible to convert them to a variety of analogues that have positive, negative or no charge under physiological conditions (Creighton 1993). Thus we can speculate that in the case of the PPOX mitochondrial targeting sequence, replacing Arg3 with a lysine could lead to some unknown intracellular reaction with the lysine side-chains, effectively preventing mitochondrial targeting.

R3S : Replacement of Arg3 by an aliphatic, neutral serine residue resulted in mitochondrial targeting (Fig 7.8C). This result suggests that when the overall charge of the 17 amino acid N-terminal targeting sequence is neutralized, some other defined secondary structural characteristic (such as α-helicity) may be sufficient to effect correct targeting. Hammen reports that if the positive charges are removed in rat liver aldehyde dehydrogenase import competence can be retained, providing a more stable helix is formed (Hammen et al. 1996; Hammen and Weiner 1998). Consequently, one could speculate that replacing Arg3 with a small and unreactive serine residue may create an environment which stabilizes the helix more than the arginine does.

Fig 7.8 Series of PPOX-GFP constructs to examine the effect of changing the net charge of the mitochondrial targeting sequence. *A*, PPOX17/R3E-GFP; *B*, PPOX17/R3K-GFP; *C*, PPOX17/R3S-GFP.

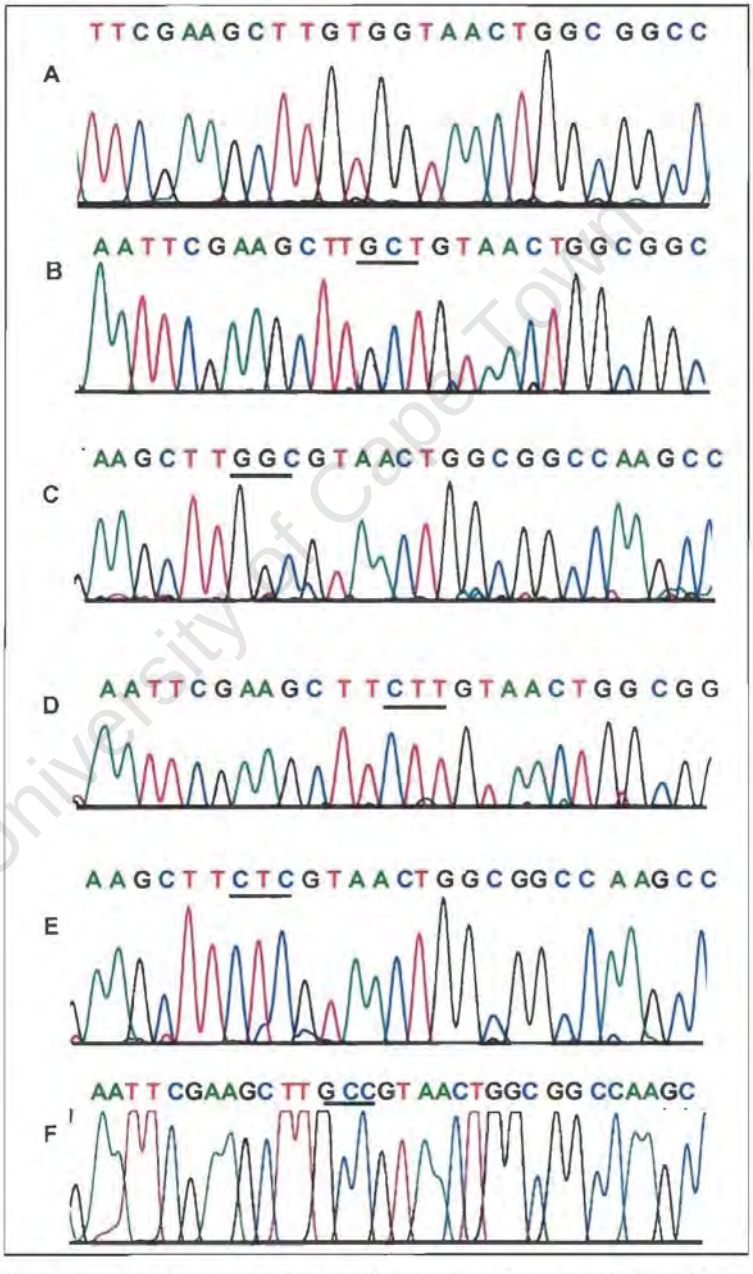

Fig 7.9 Partial direct reverse sequencing of engineered H20 constructs *A*, PPOX20-GFP (wild-type); *B*, PPOX20/H20S-GFP; *C*, PPOX20/H20A-GFP; *D*, PPOX20/H20K-GFP; *E*, PPOX20/H20E; *F*, PPOX20/H20G. In all cases the changed residues are underlined.

C. Effect of disruption at the His20 position within the PPOX α-helix (residues 12-24)

The PPOX20-GFP construct (PPOX N-terminal residues 1-20) encompasses two-thirds of the predicted α-helix and resulted in mitochondrial targeting (Fig. 7.4B). However, since the VP-causing mutation H20P abolished mitochondrial targeting (Fig 6.7B) the effect of mutations at this position were examined for their predicted effect on helical formation and subsequent mitochondrial targeting.

Engineering of GFP constructs

His20 in the N-terminal PPOX sequence was successfully changed to a serine (H20S), alanine (H20A), lysine (H20K), glutamic acid (H20E), glycine (H20G) and proline (H20P) using PCR-based mutagenesis and confirmed by direct sequencing (Fig 7.9).

Microscopic analysis of mitochondrial targeting

Alteration of His20 to H20S, H20A, H20K, H20E or H20G-GFP resulted in mitochondrial targeting (Fig 7.10A-E) with the same specific pattern of localization as the OTC-GFP positive control (Fig 7.10G). In contrast, however, targeting was abolished in H20P (Fig 7.10F).

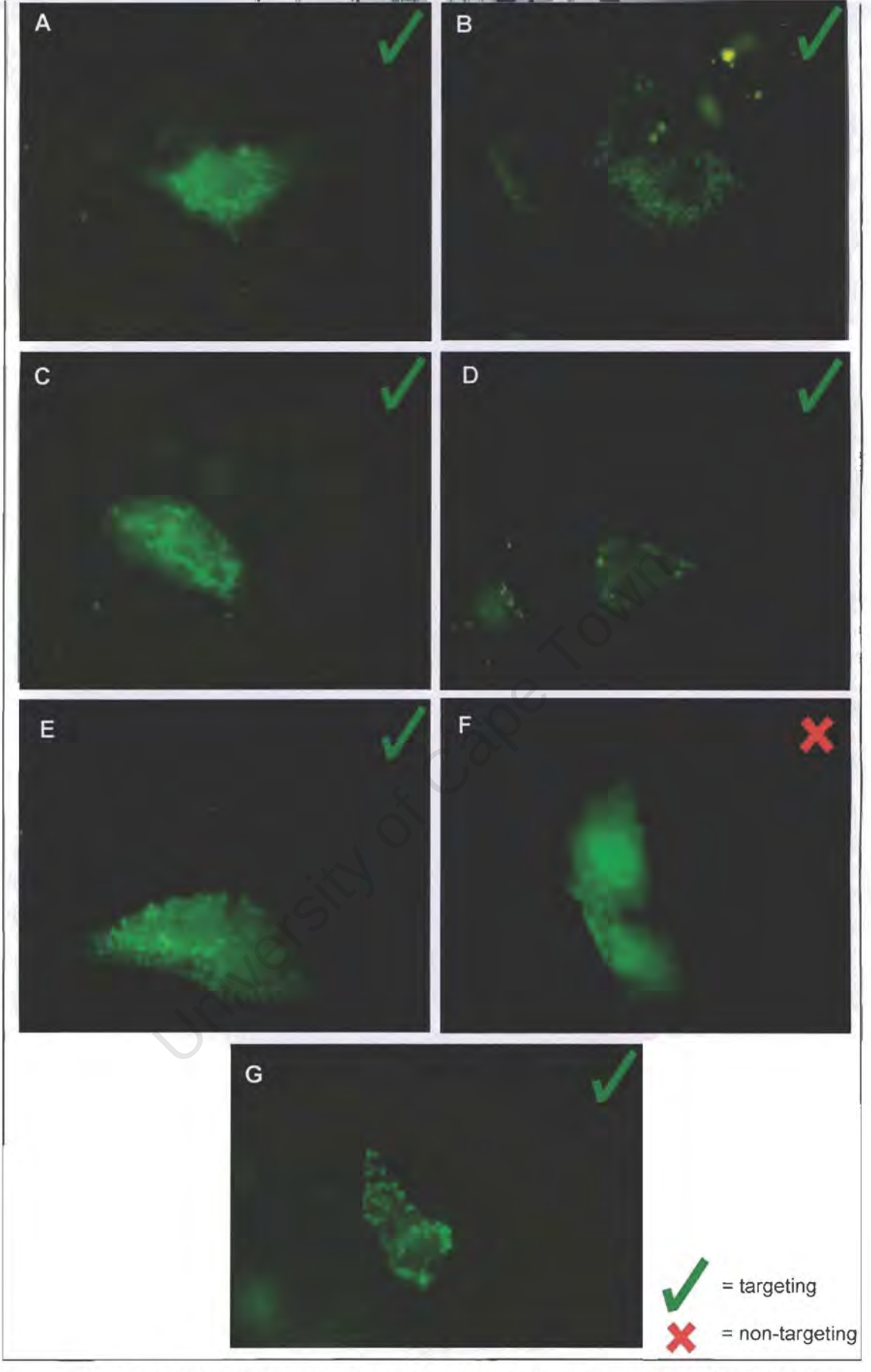

Fig 7.10 Series of PPOX-GFP constructs mutated at the H20 position. *A*, PPOX20/H20S-GFP; *B*, PPOX20/H20A-GFP; *C*, PPOX20/H20K-GFP; *D*, PPOX20/H20E-GFP; *E*, PPOX20/H20G-GFP; *F*, PPOX20/H20P-GFP; *G*, OTC-GFP fusion protein (positive control).

Both proline and glycine are strong α-helix breakers in contrast to glutamic acid and alanine which are strong helix formers (Chou and Fasman 1974). Histidine is an α-helix former, thus alteration of the H20 residue could affect mitochondrial targeting due to conformational change. The ability of the H20G-GFP construct to target was unexpected (Fig 7.10E). Although glycine is considered to have a high potential as a helix breaker, its lack of a large side-chain gives the polypeptide backbone at the glycine residue much greater conformational flexibility. In addition, the position of the glycine residue within the helix ie. start, end or centre, contributes to helical formation. In this instance, glycine is found at the end of the helix (position 20) and hence may not exert a significant conformational change in contrast to if positioned in the centre of the helix.

Although various amino acids are thought to have different tendencies to form α-helices, it has been extremely difficult to quantify these tendencies as naturally occurring polypeptides are generally either insoluble or preferentially form other conformations. The best recent values of the relative intrinsic helix-forming tendencies were measured using short peptides of defined sequences. This study suggests that helix-forming tendencies vary more than was previously thought and that it probably depends on the sequence/environment in which the amino acid occurs (O'Neil and DeGrado 1990). Nevertheless, it was clear that one factor limiting the helix-forming tendencies of residues with branched side-chains is that only certain conformations of the side-chain are compatible with helical formation. Despite both histidine and proline having polar side-chains, the five-membered ring of proline imposes rigid constraints on the conformation of the polypeptide backbone which resulted in an abolition of mitochondrial targeting. It is known that this cyclic nature of proline, irrespective of its position within the helix, adversely affects helix formation (Creighton 1993).

D. Identification of additional targeting signals within the PPOX sequence

Engineering of GFP constructs

It was important to ascertain whether the targeting signal was located solely at the N-terminal end of PPOX or whether an additional signal(s) exist. A construct in which the first 17 amino acid residues were removed (PPOXΔ1-17-GFP) was successfully engineered and confirmed through rapid screening (Fig 7.11A) and direct sequencing (Fig 7.11B).

Microscopic analysis of mitochondrial targeting

Transfection of the PPOXΔ1-17-GFP construct demonstrated mitochondrial targeting (Fig 7.12) indicating the presence of an additional mitochondrial targeting signal(s). This result concurs with the recent findings of von Fraunberg et al. (2003a,b) of the presence of additional mitochondrial targeting signals downstream of the first 28 N-terminal PPOX amino acids ie. an internal targeting sequence (Von Und Zu Fraunberg and Kauppinen 2003; Von Und Zu Fraunberg et al. 2003). They have identified 3 helical leucine-rich segments downstream of the N-terminus which can direct PPOX to the mitochondrion when replacing the N-terminal targeting signal, and thus appears to contribute to internal mitochondrial targeting signaling of PPOX (Von Und Zu Fraunberg and Kauppinen 2003). These authors suggest (as in the case of an I12T homozygous patient) the internal signal(s) acts as a backup system directing the presequence into mitochondria if the N-terminal primary signal fails. However, this may result in less specific and efficient targeting (Zara et al. 1992) and result in sub-optimal intramitochondrial compartmentalization.

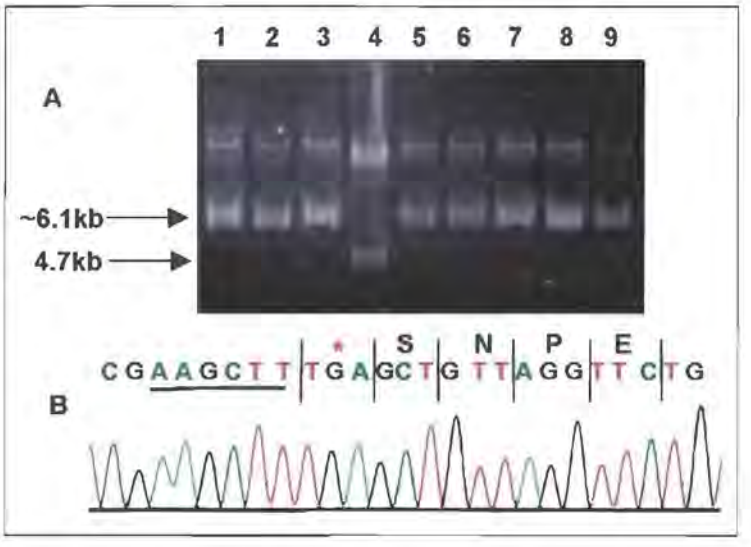

Fig 7.11 Confirmation of positive PPOXΔ1-17-GFP colonies. *A,* Rapid screening technique on a 0.8% agarose gel. *Lanes 1-3 and 5-9*, positive colonies, lane 4, GFP vector. *B,* partial direct sequencing using a reverse oligonucleotide. The HindIII site is underlined. The asterisk (*) indicates the stop codon (TGA) converted to serine (TCA) via PCR-based mutagenesis to allow in-frame translation. The amino acid residues are shown above the codons.

Fig 7.12 Transfection of the PPOXΔ1-17-GFP construct exhibiting punctate fluorescent ovals indicative of intracellular mitochondrial localization.

It has also been suggested that, as neither deletion of the first 28 N-terminal PPOX residues nor the I12T mutation abolish mitochondrial targeting, the N-terminal region may act as an "artificial" signal (Morgan et al., personal communication) as has been described for the uncoupling protein (UCP1) of the inner mitochondrial membrane (Schleiff and McBride 2000). In the UCP1 study three units/loops (N-terminal, central and downstream) spanning the inner mitochondrial membrane were analyzed for the ability to import the protein into the mitochondrion. As only deletion of the second unit of UCP1 abolished mitochondrial import, the N-terminal unit was considered an "artificial" N-terminal targeting signal for outer membrane insertion. It was postulated therefore that the first (N-terminal) and third units do not function in outer, but rather intramitochondrial compartmentalization.

Morgan et al. (personal communication) take the view that N-terminal and downstream signals are required for fully efficient targeting. They propose that whereas all targeting information is found in the first 250 amino acid residues of PPOX, residues 151-175 contain whole or part of a signal acting as an internal signal to effect efficient mitochondrial targeting. Our work does not exclude this possibility, but rather focuses on and emphasizes the potential ability of the 17 residue N-terminal targeting signal to direct a protein (GFP) at the least, to the mitochondrion.

PPOX appears to fall into both known categories of mitochondrial proteins : those with both N-terminal and internal targeting sequences, and those with non-cleavable presequences. The first group, although not common, include cytochrome c1 which exists as a mitochondrial inner membrane-destined protein containing two distinct targeting signals - an N-terminal and internal targeting sequence (Arnold et al. 1998). In this instance, the N-terminal signal is used for translocation from the nucleus to the mitochondrial outer membrane machinery to effect initial entry into the organelle. Upon entry, the N-terminal sequence is cleaved and the internal signal allows the protein to reach its final destination in the internal membrane. PPOX, however, does not contain a reported cleavable presequence although a computer-predicted cleavage site is present at Gly40. Indeed, cleavage of the presequence would

remove the highly conserved FAD-binding domain (residues 9-14), and render PPOX biologically functionless. Studies by Hammen et al. (1994) suggest that mitochondrial signal sequences with an N-terminal α-helix longer than 11 residues, or three turns, may not have the necessary flexibility present to adopt the conformation recognized by the cleaving protease. In addition, longer helices have a greater affinity for the inner membrane, making it impossible for the protease to cleave the presequence (Hammen et al. 1994).

As mentioned above, human PPOX can also be included in the group of mitochondrial proteins which lack a cleavable presequence (Hoogenraad et al. 2002). This group of proteins generally contain an internal targeting signal preceded by a hydrophobic transmembrane sequence or multiple targeting and membrane insertion signals distributed either throughout the whole protein or the C-terminal portion (Folsch et al. 1996; Folsch et al. 1998; Schleiff and McBride 2000). Although the mammalian PPOX targeting mechanisms seem to follow the route of these proteins, it does not share many of the structural characteristics (it has no membrane spanning domains) (Puy et al. 1996; Kirsch et al. 1998).

E. Structural overview of those areas of PPOX that may be relevant to targeting

Through the course of this dissertation, a number of secondary structural characteristics of the PPOX protein have been predicted by ourselves and others using computer software. Speculation regarding how these characteristics affect functionality, mitochondrial targeting and eventual intramitochondrial location were drawn from the results obtained here and in other studies. The following table summarizes relevant structural and functional information regarding human PPOX gleaned from this and other studies.

Note : It must be borne in mind that using predictive software to characterize an active protein may not be entirely accurate but nevertheless allows speculative conclusions to be drawn. In addition, caution should be taken when drawing conclusions from predicted internal targeting signals fused to GFP as these signals could be viewed as being "out of context" with respect to the overall structure of the protein. Finally, it must also be taken into account that using PPOX-GFP chimeras result in a much larger translated protein than *in vivo,* which may have some deleterious effect on targeting efficiency.

Table 7.1 A summary of relevant structural and functional information on human PPOX. Information obtained from this study is indicated in blue.

Residues	Secondary structure/Function and comments	References
Predicted		
4-10; 29-35	β-sheet - only β-sheets relevant to this study are listed	(Von Und Zu Fraunberg et al. 2003)
8-15	α-helical hydrophobic motif (LXXXIXXL) – the isoleucine (I12) and leucine (L15) residues are highly conserved across species	(Von Und Zu Fraunberg et al. 2003)
10-13; 25-28	Tetrapeptide helical breakers – known to exist at the start and end of helices	This study (see text)
40	Predicted cleavage site – although this could not exist in human PPOX as the FAD binding motif would be lost with subsequent loss of functionality. Only *A. thaliana* (Narita et al. 1996) and spinach PPOX (Watanabe et al. 2001) contain cleavable N-terminal targeting signals.	This study (see text)
11-24 12-24 158-167;177-191	α-helix - based on structural biology principles, this would start at I12 rather than G11 (see text)	(Von Und Zu Fraunberg et al. 2003) This study (see text) Morgan et al., personal communication
168-176	Inter-helical fold	Morgan et al., personal communication
1-17 1-24	N-terminal mitochondrial targeting signal	This study (see text) (Von Und Zu Fraunberg et al. 2003)
18-477 25-477 150-175; 304-319	Region containing putative internal mitochondrial targeting signal(s)	This study (see text) (Von Und Zu Fraunberg et al. 2003) Morgan et al., personal communication
108-117; 198-207; 229-235; 302-311	Hydrophobic domains	(Von Und Zu Fraunberg et al. 2003)
Reported		
142-192	Putative membrane-anchoring domain	(Arnould and Camadro 1998; Arnould et al. 1999)
9-14	FAD-binding domain (GXGXXG) – highly conserved among a large number of FAD binding proteins	(Dailey and Dailey 1998)

7.5 Conclusions

- The presence of an N-terminal human PPOX sequence capable of mitochondrial targeting has been demonstrated.

- The minimal number of residues the N-terminal targeting signal requires to effect efficient mitochondrial targeting is the first 17 residues.

- The placement of the 17-residue targeting signal at the PPOX carboxy terminus does not localize to the mitochondrion.

- Changing the only positively charged residue within the 17-residue targeting signal (Arg3) to a negatively charged glutamic acid, abolished mitochondrial targeting presumably due to the resultant net negative charge.

- The abolition of mitochondrial targeting when replacing the Arg3 with a conservative lysine although surprising, may be due to the presence of some unknown intracellular reaction with the reactive lysine side-chains.

- Neutralizing the charge of the 17-residue targeting signal by replacing Arg3 with a serine does not abolish mitochondrial targeting. The unreactive nature of the serine residue compared to arginine, may lead to increased stability of the α-helix with a higher propensity to effect mitochondrial targeting.

- Altering residues at the H20 position (contained within the predicted α-helix) of PPOX to serine, alanine, lysine and glutamic acid resulted in efficient targeting presumably by virtue of the "helix-forming" properties of these residues.

- Mimicking the VP-causing H20P mutation *in vitro* by altering the H20 residue to proline (H20P) resulted in abolition of mitochondrial targeting probably due to the predicted effect proline residues have on secondary α-helical structure.

- H20G targeted even though glycine is considered a "helix-breaker". This could be due the increased conformational flexibility associated with the glycine residue.

- Mitochondrial targeting of the PPOX protein lacking the 17-residue N-terminal targeting signal ie. PPOXΔ1-17-GFP confirms the presence of additional targeting signals downstream of the N-terminus.

CHAPTER 8 : OVERVIEW, IMPLICATIONS AND FUTURE DIRECTIONS

CHAPTER 8 : OVERVIEW, IMPLICATIONS AND FUTURE DIRECTIONS

8.1 Overview and Implications

This study focused on the mitochondrial targeting mechanism of naturally-occurring ("clinical") and self-engineered human PPOX mutant proteins. The naturally occurring mutants included South African VP-causing mutations of interest to our laboratories. Mitochondrial targeting regions within the protein were characterized using *in vitro* transfection and fluorescent microscopic methodologies.

The study showed that two VP-causing mutations (R59W and R168C) did not affect mitochondrial targeting whereas a mutation at the N-terminal region (H20P) abolished targeting. This implies that the PPOX N-terminal region contains a mitochondrial targeting signal and that the replacement of a histidine with a proline at position 20 (H20P) probably results in a major secondary structural conformational change at the post-transcriptional level. This is the first study describing the effects of naturally occurring South African *PPOX* mutations on mitochondrial targeting.

The results highlighted the potential importance of the PPOX N-terminus as a mitochondrial target signal. Through progressive N-terminal residue deletions (PPOX24, 20, 12, 14, 15 and 16) the first 17 residues (PPOX17-GFP) were shown to contain a signal sufficient to effect targeting of PPOX to the mitochondrion. Secondary structural analysis predicted that these 17 residues contained two stabilizing hydrogen bonds in its helical structure (as opposed to one in the PPOX16 construct) which were sufficient to produce an effective mitochondrial signal. The results of this study lend weight to these predictions.

Placement of the 17-residue fragment at the C-terminus, abolished targeting suggesting the effectiveness of this targeting signal only when positioned at the N-terminus.

Removal of the 17 residue N-terminal targeting signal ie. engineering PPOXΔ1-17-GFP, still allowed mitochondrial targeting. This indicated the

existence of other downstream internal targeting signals operating independently, to effect targeting. This is in agreement with the recent findings of two other groups (Von Und Zu Fraunberg et al. 2003); Morgan et al., personal communication).

Only one positively charged residue (Arg3) exists within the 17 residue N-terminal targeting sequence. Replacing this residue with a negatively charged glutamic acid resulted in the expected abolition of mitochondrial targeting. This demonstrated the importance of positivity within this targeting sequence. The importance of a specific residue (such as arginine) within the targeting sequence was highlighted by a lack of targeting when the arginine was replaced by lysine (conservative replacement). Lack of targeting may be related to the reactivity of the lysine side-chains at the secondary conformational level. However, the possibility of the mitochondrial outer membrane receptors recognizing features other than positive charge such as α-helicity, was demonstrated when replacement of the arginine by serine (neutral replacement) showed no adverse effect on mitochondrial targeting.

The secondary structure prediction of PPOX places the H20P mutation two-thirds into the 12-24 residue α-helix. As α-helicity is considered an important feature for mitochondrial targeting, it was intriguing to investigate how alterations of residues at position 20 would affect overall targeting.

Replacement of His20 by serine, alanine, lysine, glutamic acid or glycine did not affect targeting. These findings suggest either that none of these residues have significant effect on the formation of the α-helix, or that the outer mitochondrial machinery recognizes some other secondary structural motif within the 20-residue sequence. All the residues listed with the exception of glycine predictably should not disrupt α-helical formation. The fact that H20G did target may imply that in the case of the glycine residue, a specific hydrophobic motif within the targeting region facilitates efficient targeting. Alternatively, the possibility also exists that in the case of PPOX the potential flexibility of glycine could be masked by the surrounding secondary

conformation thus allowing targeting. Clearly, replacing His20 with a proline residue had, as in the case of the naturally occurring H20P mutation, a major effect on conformation and hence on targeting to the mitochondrion.

8.2 Proposed mechanism of PPOX targeting

This study's data supports the hypothesis that a signal sequence at the N-terminus together with other more distal elements, effect efficient import of human PPOX to the mitochondrion. On the basis of knowledge learnt through the course of this dissertation, we propose the following transport mechanism for human PPOX to reach the inner mitochondrial membrane :

On translation PPOX is a cytoplasmically–located protein which needs to translocate via the TOMs and TIMs to the inner mitochondrial membrane in order to perform its function (Fig 8.1A). The protein remains in an unfolded state through binding of a chaperone molecule such as Hsc70 – the constitutively expressed mammalian cytosolic isoform of Hsp70 (Fig 8.1B). Interestingly, Hsp70s have been shown to bind to unfolded, hydrophobic segments of proteins maintaining them in an import competent state (Sheffield et al. 1990). Thus, specific hydrophobic regions in the PPOX sequence may have the potential to bind these chaperone molecules. Indeed, hydrophobic "motifs" have already been identified and shown to be potentially important for PPOX targeting (Von Und Zu Fraunberg et al. 2003).

On the other hand, due to secondary structure predictions the possibility of transmembrane spanning domains in PPOX cannot be dismissed and, as in the case of the uncoupling protein (UCP1), translocation to the mitochondrion could be effected by a series of loop structures. PPOX could then interact with the TOM machinery in one of two ways. It could use an internal targeting signal as its primary signal to interact with the dimeric receptor Tom70-Tom34 (which specifically interacts with internal signals) (Schlossmann et al. 1994; Brix et al. 1997) and be guided to and through the general import pore (GIP) into the mitochondrion (Fig 8.1C).

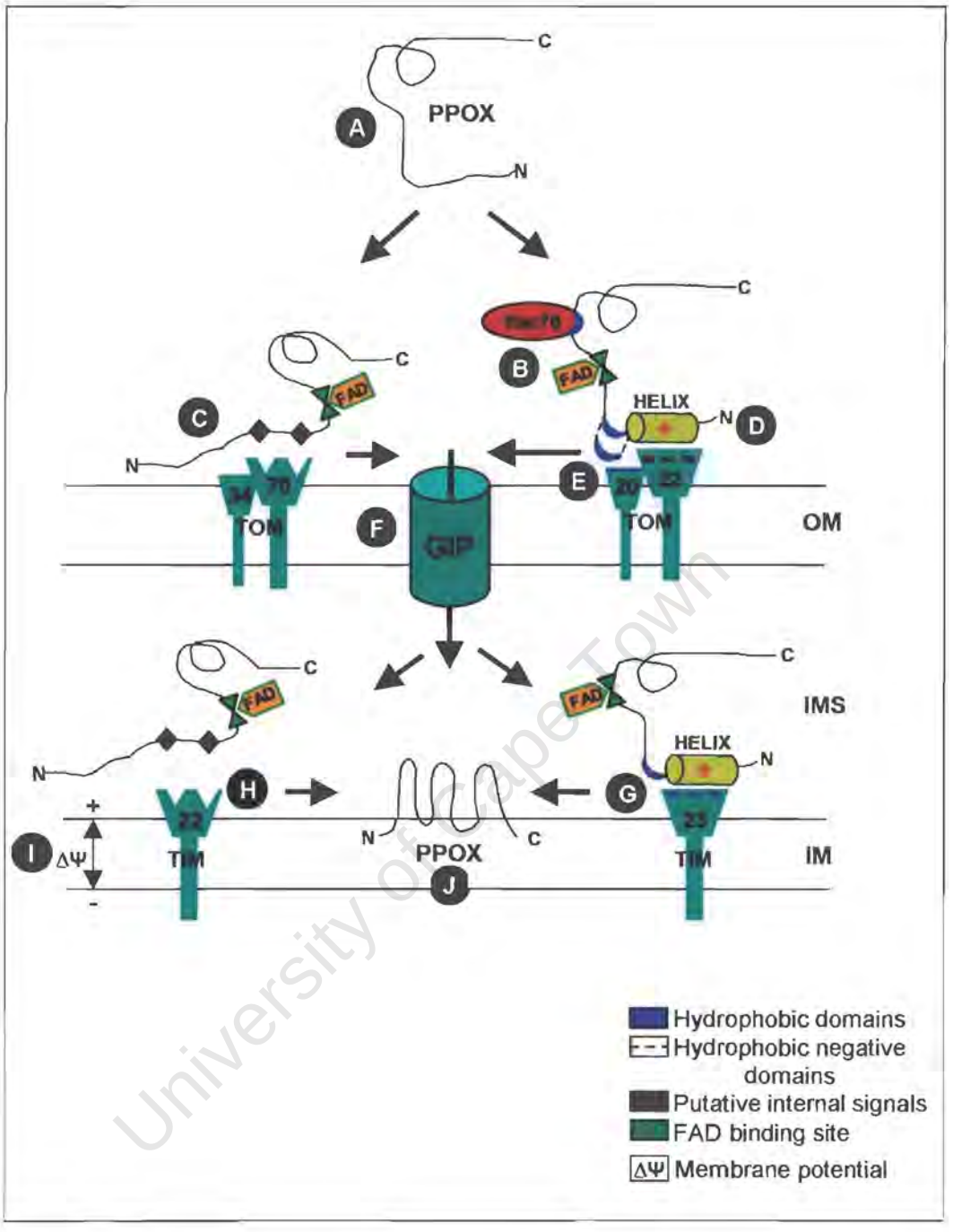

Fig 8.1 Proposed mechanism of PPOX targeting, *A-J*, see text.

Alternatively, PPOX could use its N-terminal targeting signal (residues 1-17) as its primary signal to interact with the heterodimeric Tom20-Tom22 complex prior to movement through the GIP (Fig 8.1D). Although this receptor has been shown to specifically bind cleavable N-terminal targeting sequences, cleavage only occurs at a post-import level. The PPOX protein could therefore theoretically bind to this complex in spite of no apparent cleavage. Significantly, the dimeric Tom20-Tom22 complex can further "refine" its interaction with the PPOX protein as N-terminal targeting signals interact with Tom22 in an electrostatic manner, while the Tom20 interaction is hydrophobic (Fig 8.1E) (Brix et al. 1997). This would imply that either the positive charge (Arg3) or the suggested hydrophobic motif (residues 8-15) in the 1-17 residue PPOX targeting signal, or both, could direct the protein into the GIP (Fig 8.1F).

Once inside the mitochondrion, the PPOX protein would rely on the TIM machinery to localize to its final destination in the inner mitochondrial membrane. At this stage the "bipartite" nature of PPOX (ie. containing N-terminal and internal targeting signals) allows it to use either the TIM23 or TIM22 complex. Tim23 contains a hydrophilic N-terminal domain on the intermembrane side with a net negative charge and appears to be translocation-specific to precursors with a positively-charged N-terminal mitochondrial matrix targeting signal (Fig 8.1G) (Sirrenberg et al. 1996; Bauer et al. 2000; Pfanner 2000). Tim22 on the other hand, binds proteins via internal targeting signals (Fig 8.1H).

A change in membrane potential ($\Delta\psi$) is an additional requirement for translocation of a (pre)protein across the inner mitochondrial membrane channel (Fig 8.1I) (Bauer et al. 2000). However, the position of PPOX facing the cytoplasmic side of the inner membrane, would not need to use the inner membrane potential to effect translocation. Finally, PPOX could then insert into the inner mitochondrial membrane using its putative membrane anchoring domain (residues 142-192) (Fig 8.1J) (Arnould et al. 1999).

The question of *when* PPOX binds the FAD cofactor remains unanswered. Reports on FAD binding to yeast mitochondrial matrix protein, succinate dehydrogenase, provide clues (Robinson and Lemire 1996a,b). These studies show that the protein folds in the presence of a bound Hsp60 chaperone, before FAD attachment occurs and the chaperone does not inhibit FAD attachment nor have any deleterious affect on enzyme activity. Thus, in the case of PPOX we could propose that whether the protein remains in a folded or unfolded state (ie. bound to Hsc70), FAD attachment is an early event without disruption of the protein's integrity.

8.3 Future work

Further characterization of the PPOX enzyme biochemically, molecularly and clinically remains relevant, especially with the crystal structure of human PPOX still unresolved.

Although this study and the recent findings of others have shed light on the *movement* of PPOX from the nucleus to the mitochondrion, the final location of mutant PPOXs remains enigmatic. *In vitro* mitochondrial import assays (Brix et al. 1997; Brix et al. 2000) could help elucidate the mitochondrial import mechanism, or lack thereof, of targeted PPOX mutants. The import mechanism could be refined by isolation of different fractions, followed by fluorescent-activated cell sorter (FACS) analysis.

As R138P and Y348C are known SA VP-causing mutations, investigation into their mitochondrial targeting (in)ability may shed light on the possible active site and the secondary conformational structure. These mutant clones are already available in our laboratory. The R138P mutation lies close to the putative membrane anchoring domain (residues 142-192) (Arnould and Camadro 1998; Arnould et al. 1999). As the Y348C mutation lies in the same vicinity as the V335G mutation (Whatley et al. 1999) which disrupts mitochondrial targeting (Morgan et al., personal communication), investigation of its targeting ability could prove interesting. Furthermore, in light of the fact that the tyrosine is changed to a cysteine, which could result in an altered

conformation due to disulphide bonding, a study of this mutant could be significant.

The interaction of the PPOX targeting signals with outer mitochondrial machinery (TOMs) has been alluded to through computer modeling (Von Und Zu Fraunberg et al. 2003) and could be tested using specific antibodies to the TOMs, PPOX and/or GFP. As discussed in chapter 4, proteins with N-terminal targeting signals use the Tom20-Tom22 outer membrane receptors (compared to those with internal signals which use Tom70-Tom34). It is therefore feasible that by using specific blocking antibodies to the different TOMs through a transient assay it may be possible to identify whether specific PPOX mutants are targeting through using their N-terminal or internal targeting signal(s) or both. Co-localization using fluorescently-labelled antibodies could also identify the interaction of PPOX with the outer machinery. The transient nature of this interaction does however increase the difficulty of this method (Nikolas Pfanner, personal communication).

Undoubtedly, much remains unknown regarding the PPOX structure, its translocation from the nucleus to the mitochondrion, import through the organelle, mechanism of insertion into the inner mitochondrial membrane, interaction with other heme biosynthetic enzymes, cofactor binding and resultant functionality. However, we believe that studies such as those presented in this dissertation are valuable as they all provide some insight into furthering our understanding of the PPOX enzyme and its intracellular organelle-specific targeting mechanism.

Thus, rather like a jigsaw puzzle nearing completion we believe the picture may soon be clear enough to fill in the missing pieces with more precise prediction than has been possible to date. We also believe that what we have learnt and may yet learn by studying PPOX, could be applicable to other proteins as well and expand our understanding of the fundamental principles of mitochondrial targeting.

BIBLIOGRAPHY

BIBLIOGRAPHY

Abdulla, M. and B. Haeger-Aronsen (1971). "ALA-dehydratase activation by zinc." Enzyme **12**(6): 708-10.

Abe, Y., T. Shodai, et al. (2000). "Structural basis of presequence recognition by the mitochondrial protein import receptor Tom20." Cell **100**(5): 551-60.

Aizencang, G. I., D. F. Bishop, et al. (2000). "Uroporphyrinogen III synthase. An alternative promoter controls erythroid-specific expression in the murine gene." J Biol Chem **275**(4): 2295-304.

Akhtar, M. (2003). Coproporphyrinogen III and Protoporphyrinogen IX oxidase. The Iron and Cobalt Pigments : Biosynthesis, Structure and Degradation. K. M. Kadish, K. M. Smith and R. Guilard. California, U.S.A., Academic Press. **12:** 75-92.

Alexeev, D., M. Alexeeva, et al. (1998). "The crystal structure of 8-amino-7-oxononanoate synthase: a bacterial PLP-dependent, acyl-CoA-condensing enzyme." J Mol Biol **284**(2): 401-19.

Al-Karadaghi, S., M. Hansson, et al. (1997). "Crystal structure of ferrochelatase: the terminal enzyme in heme biosynthesis." Structure **5**(11): 1501-10.

Allison, D. S. and G. Schatz (1986). "Artificial mitochondrial presequences." Proc Natl Acad Sci U S A **83**(23): 9011-5.

Alwan, A. F., B. I. Mgbeje, et al. (1989). "Purification and properties of uroporphyrinogen III synthase (co-synthase) from an overproducing recombinant strain of Escherichia coli K-12." Biochem J **264**(2): 397-402.

Amillet, J. M. and R. Labbe-Bois (1995). "Isolation of the gene HEM4 encoding uroporphyrinogen III synthase in Saccharomyces cerevisiae." Yeast **11**(5): 419-24.

Anderson, K. E. (2003). Approaches to Treatment and Prevention of Human Porphyrias. The Porphyrin Handbook : Medical Aspects of Porphyrias. K. M.

Kadish, K. M. Smith and R. Guilard. California, USA, Academic Press. **14:** 247-284.

Anderson, P. M. and R. J. Desnick (1980). "Purification and properties of uroporphyrinogen I synthase from human erythrocytes. Identification of stable enzyme-substrate intermediates." J Biol Chem **255**(5): 1993-9.

Andrew, T. L., P. G. Riley, et al. (1990). Biosynthesis of Heme and Chlorophylls. H. A. Dailey. New York, McGraw-Hill: 163.

Aquaron, R., D. Lacombe, et al. (1992). "Neurological, dermatological and biological manifestations of porphyria variegata. A study of 3 families of Italian origin in Marseilles area." Rev Neurol (Paris) **148**(8-9): 532-40.

Arnold, I., H. Folsch, et al. (1998). "Two distinct and independent mitochondrial targeting signals function in the sorting of an inner membrane protein, cytochrome c1." J Biol Chem **273**(3): 1469-76.

Arnould, S. and J. M. Camadro (1998). "The domain structure of protoporphyrinogen oxidase, the molecular target of diphenyl ether-type herbicides." Proc Natl Acad Sci U S A **95**(18): 10553-8.

Arnould, S., M. Takahashi, et al. (1999). "Acylation stabilizes a protease-resistant conformation of protoporphyrinogen oxidase, the molecular target of diphenyl ether-type herbicides." Proc Natl Acad Sci U S A **96**(26): 14825-30.

Astrin, K. H., C. A. Warner, et al. (1991). "Regional assignment of the human uroporphyrinogen III synthase (UROS) gene to chromosome 10q25.2----q26.3." Hum Genet **87**(1): 18-22.

Avner, D. L., R. G. Lee, et al. (1981). "Protoporphyrin-induced cholestasis in the isolated in situ perfused rat liver." J Clin Invest **67**(2): 385-94.

Barbieri, L., D. Griso, et al. (2003). Acquired porphyria cutanea tarda probably related to antineoplastic therapy in a patient affected by chronic myeloid leukaemia. Porphyrins and Porphyrias 2003, Prague, Czech Republic.

Barnes, H. D. (1945). "A note on porphyrinuria with a resume of eleven South African cases." Clin Proc **4**: 269-275.

Barnes, H. D. (1958). "Porphyria in South Africa : the faecal excretion of porphyria." S Afr Med J **32**: 680-3.

Barohn, R. J., J. A. Sanchez, et al. (1994). "Acute peripheral neuropathy due to hereditary coproporphyria." Muscle Nerve **17**(7): 793-9.

Batlle, A. M., R. E. de Salamanca, et al. (1986). "Photodynamic inactivation of red cell uroporphyrinogen decarboxylase by porphyrins." Int J Biochem **18**(2): 143-7.

Battersby, A. R., C. J. Fookes, et al. (1980). "Biosynthesis of the pigments of life: formation of the macrocycle." Nature **285**(5759): 17-21.

Battersby, A. R. and E. McDonald (1975). Biosynthesis of Porphyrins, Chlorins and Corrins. Porphyrins and Metalloporphyrins. K. M. Smith. Amsterdam, Elsevier: 61-122.

Bauer, M. F., S. Hofmann, et al. (2000). "Protein translocation into mitochondria: the role of TIM complexes." Trends Cell Biol **10**(1): 25-31.

Bawden, M. J., I. A. Borthwick, et al. (1987). "Sequence of human 5-aminolevulinate synthase cDNA." Nucleic Acids Res **15**(20): 8563.

Beale, S. I. and J. I. Yeh (1999). "Deconstructing heme." Nat Struct Biol **6**(10): 903-5.

Becker, F. T. (1965). "Porphyria cutanea tarda induced by estrogens." Arch Dermatol **92**(3): 252-5; discussion 255-6.

Bensidhoum, M., C. M. Ged, et al. (1994). "The cDNA sequence of mouse uroporphyrinogen III synthase and assignment to mouse chromosome 7." Mamm Genome **5**(11): 728-30.

Berenson, M. M., R. Kimura, et al. (1992). "Protoporphyrin overload in unrestrained rats: biochemical and histopathologic characterization of a new model of protoporphyric hepatopathy." Int J Exp Pathol **73**(5): 665-73.

Beri, R. and R. Chandra (1993). "Chemistry and biology of heme. Effect of metal salts, organometals, and metalloporphyrins on heme synthesis and catabolism, with special reference to clinical implications and interactions with cytochrome P-450." Drug Metab Rev **25**(1-2): 49-152.

Bhasker, C. R., G. Burgiel, et al. (1993). "The putative iron-responsive element in the human erythroid 5-aminolevulinate synthase mRNA mediates translational control." J Biol Chem **268**(17): 12699-705.

Billinton, N. and A. W. Knight (2001). "Seeing the wood through the trees: a review of techniques for distinguishing green fluorescent protein from endogenous autofluorescence." Anal Biochem **291**(2): 175-97.

Bishop, D. F. (1990). "Two different genes encode delta-aminolevulinate synthase in humans: nucleotide sequences of cDNAs for the housekeeping and erythroid genes." Nucleic Acids Res **18**(23): 7187-8.

Bishop, D. F., A. S. Henderson, et al. (1990). "Human delta-aminolevulinate synthase: assignment of the housekeeping gene to 3p21 and the erythroid-specific gene to the X chromosome." Genomics **7**(2): 207-14.

Bishop, T. R., P. J. Cohen, et al. (1986). "Isolation of a rat liver delta-aminolevulinate dehydrase (ALAD) cDNA clone: evidence for unequal ALAD gene dosage among inbred mouse strains." Proc Natl Acad Sci U S A **83**(15): 5568-72.

Bishop, T. R., M. W. Miller, et al. (1996). "Genetic regulation of delta-aminolevulinate dehydratase during erythropoiesis." Nucleic Acids Res **24**(13): 2511-8.

Bissbort, S., H. W. Hitzeroth, et al. (1988). "Linkage between the variegate porphyria (VP) and the alpha-1-antitrypsin (PI) genes on human chromosome 14." Hum Genet **79**(3): 289-90.

Bissell, D. M. (1985). "Peculiar purine nucleotides and liver regeneration." Gastroenterology **89**(4): 914-6.

Bissell, D. M. and R. Schmid (1987). Hepatic Porphyrias. Diseases of the Liver. L. Schiff and E. R. Schiff. Philadelphia, JB Lippincott: 1075-1092.

Blackwood, M. E., Jr., T. S. Rush, 3rd, et al. (1997). J. Am. Chem. Soc **119**: 12170-12174.

Blackwood, M. E., Jr., T. S. Rush, 3rd, et al. (1998). "Alternative modes of substrate distortion in enzyme and antibody catalyzed ferrochelation reactions." Biochemistry **37**(3): 779-82.

Blom, H., C. Andersson, et al. (1996). "Assessment of autonomic nerve function in acute intermittent porphyria; a study based on spectral analysis of heart rate variability." J Intern Med **240**(2): 73-9.

Bloomer, J., C. Bruzzone, et al. (1998). "Molecular defects in ferrochelatase in patients with protoporphyria requiring liver transplantation." J Clin Invest **102**(1): 107-14.

Bloomer, J. R. (1988). "The liver in protoporphyria." Hepatology **8**(2): 402-7.

Bloomer, J. R., H. L. Bonkowsky, et al. (1976). "Inheritance in protoporphyria. Comparison of haem synthetase activity in skin fibroblasts with clinical features." Lancet **2**(7979): 226-8.

Bloomer, J. R. and J. G. Straka (1988). Porphyrin Metabolism. The Liver : Biology and Pathobiology. I. M. Arias, W. B. Jakoby, H. Popper, D. Schachter and D. A. Shafritz. New York, Raven Press: 451-466.

Boese, Q. F., A. J. Spano, et al. (1991). "Aminolevulinic acid dehydratase in pea (Pisum sativum L.). Identification of an unusual metal-binding domain in the plant enzyme." J Biol Chem **266**(26): 17060-6.

Bogard, M., J. M. Camadro, et al. (1989). "Purification and properties of mouse liver coproporphyrinogen oxidase." Eur J Biochem **181**(2): 417-21.

Bonkowsky, H. L. and W. Schady (1982). Seminars in Liver Disease. Neurologic manifestations of acute porphyria. R. Schmid. New York, Thieme-Stratton: 108-124.

Bont, A., A. J. Steck, et al. (1996). "[Acute hepatic porphyria and its neurological syndrome]." Schweiz Med Wochenschr **126**(1-2): 6-14.

Bonuglia, M., M. D'Amato, et al. (2003). Homozygous variegate porphyria. First Italian case - long term follow up - identification of novel mutation in PPOX gene. Porphyrins and Porphyrias 2003, Prague, Czech Republic.

Borthwick, I. A., G. Srivastava, et al. (1985). "Complete nucleotide sequence of hepatic 5-aminolaevulinate synthase precursor." Eur J Biochem **150**(3): 481-4.

Borthwick, I. A., G. Srivastava, et al. (1984). "Molecular cloning of hepatic 5-aminolevulinate synthase." Eur J Biochem **144**(1): 95-9.

Bottomley, S. S. (2003). Erythropoeitic Disorders involving Heme Biosynthesis. Medical Aspects of Porphyrins. K. M. Kadish, K. M. Smith and R. Guilard. California, U.S.A., Academic Press. **14:** 1-22.

Brady, J. J., H. A. Jackson, et al. (2000). "Co-inheritance of mutations in the uroporphyrinogen decarboxylase and hemochromatosis genes accelerates the onset of porphyria cutanea tarda." J Invest Dermatol **115**(5): 868-74.

Brenner, D. A. and J. R. Bloomer (1980). "A fluorometric assay for measurement of protoporphyrinogen oxidase activity in mammalian tissue." Clin Chim Acta **100**(3): 259-66.

Brenner, D. A., J. M. Didier, et al. (1992). "A molecular defect in human protoporphyria." Am J Hum Genet **50**(6): 1203-10.

Brenner, D. A. and F. Frasier (1991). "Cloning of murine ferrochelatase." Proc Natl Acad Sci U S A **88**(3): 849-53.

Brix, J., K. Dietmeier, et al. (1997). "Differential recognition of preproteins by the purified cytosolic domains of the mitochondrial import receptors Tom20, Tom22, and Tom70." J Biol Chem **272**(33): 20730-5.

Brix, J., S. Rudiger, et al. (1999). "Distribution of binding sequences for the mitochondrial import receptors Tom20, Tom22, and Tom70 in a presequence-carrying preprotein and a non-cleavable preprotein." J Biol Chem **274**(23): 16522-30.

Brix, J., G. A. Ziegler, et al. (2000). "The mitochondrial import receptor Tom70: identification of a 25 kDa core domain with a specific binding site for preproteins." J Mol Biol **303**(4): 479-88.

Brodie, M. J., M. R. Moore, et al. (1977a). "Haem biosynthesis in peripheral blood in erythropoietic protoporphyria." Clin Exp Dermatol **2**(4): 381-8.

Brodie, M. J., G. G. Thompson, et al. (1977b). "Hereditary coproporphyria. Demonstration of the abnormalities in haem biosynthesis in peripheral blood." Q J Med **46**(182): 229-41.

Bukau, B. and A. L. Horwich (1998). "The Hsp70 and Hsp60 chaperone machines." Cell **92**(3): 351-66.

Bulaj, Z. J., M. R. Franklin, et al. (2000a). "Transdermal estrogen replacement therapy in postmenopausal women previously treated for porphyria cutanea tarda." J Lab Clin Med **136**(6): 482-8.

Bulaj, Z. J., J. D. Phillips, et al. (2000b). "Hemochromatosis genes and other factors contributing to the pathogenesis of porphyria cutanea tarda." Blood **95**(5): 1565-71.

Cacheux, V., P. Martasek, et al. (1994). "Localization of the human coproporphyrinogen oxidase gene to chromosome band 3q12." Hum Genet **94**(5): 557-9.

Camadro, J. M., H. Chambon, et al. (1986). "Purification and properties of coproporphyrinogen oxidase from the yeast Saccharomyces cerevisiae." Eur J Biochem **156**(3): 579-87.

Camadro, J. M. and P. Labbe (1996). "Cloning and characterization of the yeast HEM14 gene coding for protoporphyrinogen oxidase, the molecular target of diphenyl ether-type herbicides." J Biol Chem **271**(15): 9120-8.

Camadro, J. M., F. Thome, et al. (1994). "Purification and properties of protoporphyrinogen oxidase from the yeast Saccharomyces cerevisiae.

Mitochondrial location and evidence for a precursor form of the protein." J Biol Chem **269**(51): 32085-91.

Cappellini, M. D., F. Martinez di Montemuros, et al. (2001). "Seven novel point mutations in the uroporphyrinogen decarboxylase (UROD) gene in patients with familial porphyria cutanea tarda (f-PCT)." Hum Mutat **17**(4): 350.

Chan, R. Y., H. M. Schulman, et al. (1993). "Expression of ferrochelatase mRNA in erythroid and non-erythroid cells." Biochem J **292**(Pt 2): 343-9.

Chauhan, S. and M. R. O'Brian (1993). "Bradyrhizobium japonicum delta-aminolevulinic acid dehydratase is essential for symbiosis with soybean and contains a novel metal-binding domain." J Bacteriol **175**(22): 7222-7.

Che, F. S., N. Watanabe, et al. (2000). "Molecular characterization and subcellular localization of protoporphyrinogen oxidase in spinach chloroplasts." Plant Physiol **124**(1): 59-70.

Chiu, W., Y. Niwa, et al. (1996). "Engineered GFP as a vital reporter in plants." Curr Biol **6**(3): 325-30.

Chou, P. Y. and G. D. Fasman (1974). "Prediction of protein conformation." Biochemistry **13**(2): 222-45.

Chow, K. S., D. P. Singh, et al. (1998). "Two different genes encode ferrochelatase in Arabidopsis: mapping, expression and subcellular targeting of the precursor proteins." Plant J **15**(4): 531-41.

Chretien, S., A. Dubart, et al. (1988). "Alternative transcription and splicing of the human porphobilinogen deaminase gene result either in tissue-specific or in housekeeping expression." Proc Natl Acad Sci U S A **85**(1): 6-10.

Christiansen, L., A. Bygum, et al. (2001). "Mutation screening of the entire coding region of the protoporphyrinogen oxidase gene using denaturing gradient gel electrophoresis and denaturing hplc." Clin Chem **47**(6): 1115-7.

Chu, T. W., P. M. Grant, et al. (1987a). "Mutation of a neutral amino acid in the transit peptide of rat mitochondrial malate dehydrogenase abolishes binding and import." J Biol Chem **262**(32): 15759-64.

Chu, T. W., P. M. Grant, et al. (1987b). "The role of arginine residues in the rat mitochondrial malate dehydrogenase transit peptide." J Biol Chem **262**(26): 12806-11.

Coakley, J., R. Hawkins, et al. (1990). "An unusual case of variegate porphyria with possible homozygous inheritance." Aust N Z J Med **20**(4): 587-9.

Colloc'h, N., J. P. Mornon, et al. (2002). "Towards a new T-fold protein?: the coproporphyrinogen III oxidase sequence matches many structural features from urate oxidase." FEBS Lett **526**(1-3): 5-10.

Cooper, D. N. and M. Krawczak (1990). "The mutational spectrum of single base-pair substitutions causing human genetic disease: patterns and predictions." Hum Genet **85**(1): 55-74.

Corey, T. J., V. A. DeLeo, et al. (1980). "Variegate porphyria. Clinical and laboratory features." J Am Acad Dermatol **2**(1): 36-43.

Corrigall, A. V., R. J. Hift, et al. (2000a). "Homozygous variegate porphyria in South Africa: genotypic analysis in two cases." Mol Genet Metab **69**(4): 323-30.

Corrigall, A. V., R. J. Hift, et al. (2000b). "Homozygous variegate porphyria in South Africa: genotypic analysis in two cases [In Process Citation]." Mol Genet Metab **69**(4): 323-30.

Corrigall, A. V., R. J. Hift, et al. (2001). "Identification of the first variegate porphyria mutation in an indigenous black South African and further evidence for heterogeneity in variegate porphyria." Mol Genet Metab **73**(1): 91-6.

Corrigall, A. V., R. J. Hift, et al. (1998). "Identification and characterisation of a deletion (537delAT) in the protoporphyrinogen oxidase gene in a South African variegate porphyria family." Hum Mutat **12**(6): 403-7.

Corrigall, A. V., P. N. Meissner, et al. (1991). "Purification of human erythrocyte porphobilinogen deaminase." S Afr Med J **80**(6): 294-6.

Cotner, T., A. D. Gupta, et al. (1989). "Characterization of a novel form of transferrin receptor preferentially expressed on normal erythroid progenitors and precursors." Blood **73**(1): 214-21.

Cox, T. C., M. J. Bawden, et al. (1990). "Erythroid 5-aminolevulinate synthase is located on the X chromosome." Am J Hum Genet **46**(1): 107-11.

Cox, T. C., M. J. Bawden, et al. (1991). "Human erythroid 5-aminolevulinate synthase: promoter analysis and identification of an iron-responsive element in the mRNA." Embo J **10**(7): 1891-902.

Cox, T. M. (2003). Protoporphyria. The Porphyrin Handbook : Medical Aspects of Porphyrins. K. M. Kadish, A. G. Smith and R. Guilard. California, U.S.A., Academic Press. **14:** 121-150.

Cramers, M. and L. V. Jepsen (1980). "Porphyria variegata: failure of chloroquin treatment." Acta Derm Venereol **60**(1): 89-91.

Creighton, T. E. (1993). Proteins : Structures and Molecular Properties. New York, W.H. Freeman and Company.

Da Silva, V., S. Simonin, et al. (1995). "Variegate porphyria: diagnostic value of fluorometric scanning of plasma porphyrins." Clin Chim Acta **238**(2): 163-8.

Dailey, H. A. (1990). Conversion of Coproporphyrinogen to Protoheme in Higher Eukaryotes and Bacteria: Terminal Three Enzymes. Biosynthesis of Heme and Chlorophylls. H. A. Dailey. New York, McGraw-Hill Publishing Company**:** 123-163.

Dailey, H. A. (1996). Mechanisms of Metallocenter Assembly. R. P. Hausinger, G. L. Eichorn and L. G. Marzilli. New York, VCH Publishers Inc.**:** 77-98.

Dailey, H. A. (2002). "Terminal steps of haem biosynthesis." Biochem Soc Trans **30**(4): 590-5.

Dailey, H. A. and T. A. Dailey (1996a). "Protoporphyrinogen oxidase of Myxococcus xanthus. Expression, purification, and characterization of the cloned enzyme." J Biol Chem **271**(15): 8714-8.

Dailey, H. A. and T. A. Dailey (1997). "Expression and purification of mammalian 5-aminolevulinate synthase." Methods Enzymol **281**: 336-40.

Dailey, H. A. and T. A. Dailey (2003). Ferrochelatase. The Iron and Cobalt Pigments : Biosynthesis, Structure, and Degradation. K. M. Kadish, K. M. Smith and R. Guilard. California, U.S.A., Academic Press. **12:** 93-121.

Dailey, H. A., T. A. Dailey, et al. (2000). "Ferrochelatase at the millennium: structures, mechanisms and [2Fe-2S] clusters." Cell Mol Life Sci **57**(13-14): 1909-26.

Dailey, H. A., M. G. Finnegan, et al. (1994a). "Human ferrochelatase is an iron-sulfur protein." Biochemistry **33**(2): 403-7.

Dailey, H. A. and J. E. Fleming (1983). "Bovine ferrochelatase. Kinetic analysis of inhibition by N-methylprotoporphyrin, manganese, and heme." J Biol Chem **258**(19): 11453-9.

Dailey, H. A., J. E. Fleming, et al. (1986). "Purification and characterization of mammalian and chicken ferrochelatase." Methods Enzymol **123**: 401-8.

Dailey, H. A. and S. W. Karr (1987). "Purification and characterization of murine protoporphyrinogen oxidase." Biochemistry **26**(10): 2697-701.

Dailey, H. A., V. M. Sellers, et al. (1994b). "Mammalian ferrochelatase. Expression and characterization of normal and two human protoporphyric ferrochelatases." J Biol Chem **269**(1): 390-5.

Dailey, T. A. and H. A. Dailey (1996b). "Human protoporphyrinogen oxidase: expression, purification, and characterization of the cloned enzyme." Protein Sci **5**(1): 98-105.

Dailey, T. A. and H. A. Dailey (1998). "Identification of an FAD superfamily containing protoporphyrinogen oxidases, monoamine oxidases, and phytoene

desaturase. Expression and characterization of phytoene desaturase of Myxococcus xanthus." J Biol Chem **273**(22): 13658-62.

Dailey, T. A., H. A. Dailey, et al. (1995). "Cloning, sequence, and expression of mouse protoporphyrinogen oxidase." Arch Biochem Biophys **324**(2): 379-84.

Dailey, T. A., P. Meissner, et al. (1994c). "Expression of a cloned protoporphyrinogen oxidase." J Biol Chem **269**(2): 813-5.

Daimon, M., Y. Morita, et al. (1993a). "Two new polymorphisms in introns 2 and 3 of the human porphobilinogen deaminase gene." Hum Genet **92**(2): 115-6.

Daimon, M., K. Yamatani, et al. (1993b). "Acute intermittent porphyria caused by a G to C mutation in exon 12 of the porphobilinogen deaminase gene that results in exon skipping." Hum Genet **92**(6): 549-53.

D'Alessandro Gandolfo, L., D. Griso, et al. (1989). "Familial porphyria cutanea tarda with normal erythrocytic urodecarboxylase: an exception to the rule?" Dermatologica **178**(4): 206-8.

D'Alessandro Gandolfo, L., A. Macri, et al. (1991). "Homozygous variegate porphyria: revision of a diagnostic error." Br J Dermatol **124**(2): 211.

D'Amato, M., M. Bonuglia, et al. (2003). Genetic analysis of variegate porphyria in Italy : identification of eight novel mutations in the protoporphyrinogen oxidase gene. Porphyrins and Porphyrias 2003, Prague, Czech Republic.

Davies, R. C. and A. Neuberger (1973). "Polypyrroles formed from porphobilinogen and amines by uroporphyrinogen synthetase of Rhodopseudomonas spheroides." Biochem J **133**(3): 471-92.

Davis, S. J. and R. D. Vierstra (1998). "Soluble, highly fluorescent variants of green fluorescent protein (GFP) for use in higher plants." Plant Mol Biol **36**(4): 521-8.

de Marco, A., S. Volrath, et al. (2000). "Recombinant maize protoporphyrinogen IX oxidase expressed in Escherichia coli forms complexes with GroEL and DnaK chaperones." Protein Expr Purif **20**(1): 81-6.

de Rooij, F. W. M., G. Minderman, et al. (1997a). "Six new protoporphyrinogen oxidase mutations in Dutch variegate porphyria patients and the R59W mutation in historical perspective." Molecular Biology of Hematopoiesis, Hamburg, Germany, Karger.

De Siervi, A., V. E. Parera, et al. (2000). "Two new mutations (H106P and L178V) in the protoporphyrinogen oxidase gene in Argentinean patients with variegate porphyria." Hum Mutat **16**(6): 532.

de Verneuil, H., G. Aitken, et al. (1978). "Familial and sporadic porphyria cutanea: two different diseases." Hum Genet **44**(2): 145-51.

de Verneuil, H., C. Ged, et al. (2003). Congenital Erythropoietic Porphyria. The Porphyrin Handbook : Medical Aspects of Porphyrins. K. M. Kadish, A. G. Smith and R. Guilard. California, USA., Academic Press. **14:** 43-65.

de Verneuil, H., S. Sassa, et al. (1983). "Purification and properties of uroporphyrinogen decarboxylase from human erythrocytes. A single enzyme catalyzing the four sequential decarboxylations of uroporphyrinogens I and III." J Biol Chem **258**(4): 2454-60.

Dean, G. (1971). "Screening tests for porphyria." Lancet **1**(7689): 86-7.

Dekker, P. J., F. Martin, et al. (1997). "The Tim core complex defines the number of mitochondrial translocation contact sites and can hold arrested preproteins in the absence of matrix Hsp70-Tim44." Embo J **16**(17): 5408-19.

Dekker, P. J. and N. Pfanner (1997). "Role of mitochondrial GrpE and phosphate in the ATPase cycle of matrix Hsp70." J Mol Biol **270**(3): 321-7.

Delfau-Larue, M. H., P. Martasek, et al. (1994). "Coproporphyrinogen oxidase: gene organization and description of a mutation leading to exon 6 skipping." Hum Mol Genet **3**(8): 1325-30.

Desnick, R. J., I. A. Glass, et al. (1998). "Molecular genetics of congenital erythropoietic porphyria." Semin Liver Dis **18**(1): 77-84.

Deybach, J. C., V. da Silva, et al. (1985). "The mitochondrial location of protoporphyrinogen oxidase." Eur J Biochem **149**(2): 431-5.

Deybach, J. C., H. de Verneuil, et al. (1981a). "The inherited enzymatic defect in porphyria variegata." Hum Genet **58**(4): 425-8.

Deybach, J. C., H. de Verneuil, et al. (1981b). "Congenital erythropoietic porphyria (Gunther's disease): enzymatic studies on two cases of late onset." J Lab Clin Med **97**(4): 551-8.

Deybach, J. C. and H. Puy (1995). "Porphobilinogen deaminase gene structure and molecular defects." J Bioenerg Biomembr **27**(2): 197-205.

Deybach, J. C. and H. Puy (2003). Acute Intermittent Porphyria : From Clinical to Molecular Aspects. The Porphyrin Handbook : Medical Aspects of Porphyrins. K. M. Kadish, A. G. Smith and R. Guilard. California, USA, Academic Press. **14:** 23-42.

Deybach, J. C., H. Puy, et al. (1996). "Mutations in the protoporphyrinogen oxidase gene in patients with variegate porphyria." Hum Mol Genet **5**(3): 407-10.

Di Pierro, E., E. Rosselli, et al. (2003). Coinheritance of a mutation in PPOX gene and an intronic mutation in the HMBS gene causes a severe porphyria's phenotype. Porphyrins and Porphyrias 2003, Prague, Czech Republic.

Diekert, K., G. Kispal, et al. (1999). "An internal targeting signal directing proteins into the mitochondrial intermembrane space." Proc Natl Acad Sci U S A **96**(21): 11752-7.

Donnelly, J. G., S. Detombe, et al. (2002). "Single-strand conformational polymorphism and denaturing gradient gel electrophoresis in screening for variegate porphyria: identification of two new mutations." Ann Clin Lab Sci **32**(2): 107-13.

Doss, M., F. Sixel-Dietrich, et al. (1985). ""Glucose effect" and rate limiting function of uroporphyrinogen synthase on porphyrin metabolism in hepatocyte culture:

relationship with human acute hepatic porphyrias." J Clin Chem Clin Biochem **23**(9): 505-13.

Doss, M. and F. Verspohl (1981). "The "glucose effect" in acute hepatic porphyrias and in experimental porphyria." Klin Wochenschr **59**(13): 727-35.

Doss, M., R. von Tiepermann, et al. (1980). "Acute hepatic porphyria syndrome with porphobilinogen synthase defect." Int J Biochem **12**(5-6): 823-6.

Doss, M., R. von Tiepermann, et al. (1979). "New type of hepatic porphyria with porphobilinogen synthase defect and intermittent acute clinical manifestation." Klin Wochenschr **57**(20): 1123-7.

Drummond, G. S. (1987). "Control of heme metabolism by synthetic metalloporphyrins." Ann N Y Acad Sci **514**: 87-95.

Dubart, A., M. G. Mattei, et al. (1986). "Assignment of human uroporphyrinogen decarboxylase (URO-D) to the p34 band of chromosome 1." Hum Genet **73**(3): 277-9.

Duby, G., M. Oufattole, et al. (2001). "Hydrophobic residues within the predicted N-terminal amphiphilic alpha-helix of a plant mitochondrial targeting presequence play a major role in in vivo import." Plant J **27**(6): 539-49.

Durosinmi, M. A., O. Adejuyigbe, et al. (1991). "Variegate (mixed) porphyria in a Nigerian girl." Ann Trop Paediatr **11**(1): 95-8.

Eales, L., R. S. Day, et al. (1980). "The clinical and biochemical features of variegate porphyria: an analysis of 300 cases studied at Groote Schuur Hospital, Cape Town." Int J Biochem **12**(5-6): 837-53.

Echelard, Y., J. Dymetryszyn, et al. (1988). "Nucleotide sequence of the hemB gene of Escherichia coli K12." Mol Gen Genet **214**(3): 503-8.

Edwards, C. Q., L. M. Griffen, et al. (1989). "HLA-linked hemochromatosis alleles in sporadic porphyria cutanea tarda." Gastroenterology **97**(4): 972-81.

Elder, G. H. (1997). "Hepatic porphyrias in children." J Inherit Metab Dis **20**(2): 237-46.

Elder, G. H. (2003). Porphyria Cutanea Tarda and Related Disorders. The Porphyrin Handbook : Medical Aspects of Porphyrins. K. M. Kadish, A. G. Smith and R. Guilard. California, USA, Academic Press. **14:** 67-92.

Elder, G. H., J. O. Evans, et al. (1976). "The primary enzyme defect in hereditary coproporphyria." Lancet **2**(7997): 1217-9.

Elder, G. H., R. J. Hift, et al. (1997). "The acute porphyrias." Lancet **349**(9065): 1613-7.

Elder, G. H., G. B. Lee, et al. (1978). "Decreased activity of hepatic uroporphyrinogen decarboxylase in sporadic porphyria cutanea tarda." N Engl J Med **299**(6): 274-8.

Elder, G. H. and A. G. Roberts (1995). "Uroporphyrinogen decarboxylase." J Bioenerg Biomembr **27**(2): 207-14.

Elder, G. H., A. G. Roberts, et al. (1989). "Genetics and pathogenesis of human uroporphyrinogen decarboxylase defects." Clin Biochem **22**(3): 163-8.

Elder, G. H. and J. A. Tovey (1977). "Uroporphyrinogen decarboxylase activity of human tissues [proceedings]." Biochem Soc Trans **5**(5): 1470-2.

Elder, G. H., J. A. Tovey, et al. (1983). "Purification of uroporphyrinogen decarboxylase from human erythrocytes. Immunochemical evidence for a single protein with decarboxylase activity in human erythrocytes and liver." Biochem J **215**(1): 45-55.

Elder, G. H. and P. C. Wyvill (1982). "Measurement of uroporphyrinogen decarboxylase using porphyrinogens prepared by chemical reduction." Enzyme **28**(2-3): 186-95.

Ellenberg, J. and J. Lippincott-Schwartz (1999). "Dynamics and mobility of nuclear envelope proteins in interphase and mitotic cells revealed by green fluorescent protein chimeras." Methods **19**(3): 362-72.

Ellenberg, J., J. Lippincott-Schwartz, et al. (1999). "Dual-colour imaging with GFP variants." Trends Cell Biol **9**(2): 52-6.

Erskine, P. T., R. Newbold, et al. (1999a). "The Schiff base complex of yeast 5-aminolaevulinic acid dehydratase with laevulinic acid." Protein Sci **8**(6): 1250-6.

Erskine, P. T., E. Norton, et al. (1999b). "X-ray structure of 5-aminolevulinic acid dehydratase from Escherichia coli complexed with the inhibitor levulinic acid at 2.0 A resolution." Biochemistry **38**(14): 4266-76.

Erskine, P. T., N. Senior, et al. (1997). "X-ray structure of 5-aminolaevulinate dehydratase, a hybrid aldolase." Nat Struct Biol **4**(12): 1025-31.

Falk, J. E. (1964). Porphyrins and Metalloporphyrins. Amsterdam, Elsevier.

Fargion, S., A. Piperno, et al. (1992). "Hepatitis C virus and porphyria cutanea tarda: evidence of a strong association." Hepatology **16**(6): 1322-6.

Felix, F. and N. Brouillet (1990). "Purification and properties of uroporphyrinogen decarboxylase from Saccharomyces cerevisiae. Yeast uroporphyrinogen decarboxylase." Eur J Biochem **188**(2): 393-403.

Ferreira, G. C., T. L. Andrew, et al. (1988). "Organization of the terminal two enzymes of the heme biosynthetic pathway. Orientation of protoporphyrinogen oxidase and evidence for a membrane complex." J Biol Chem **263**(8): 3835-9.

Ferreira, G. C. and H. A. Dailey (1988). "Mouse protoporphyrinogen oxidase. Kinetic parameters and demonstration of inhibition by bilirubin." Biochem J **250**(2): 597-603.

Ferreira, G. C., P. J. Neame, et al. (1993). "Heme biosynthesis in mammalian systems: evidence of a Schiff base linkage between the pyridoxal 5'-phosphate cofactor and a lysine residue in 5-aminolevulinate synthase." Protein Sci **2**(11): 1959-65.

Folsch, H., B. Gaume, et al. (1998). "C- to N-terminal translocation of preproteins into mitochondria." Embo J **17**(22): 6508-15.

Folsch, H., B. Guiard, et al. (1996). "Internal targeting signal of the BCS1 protein: a novel mechanism of import into mitochondria." Embo J **15**(3): 479-87.

Fontanellas, A., M. Bensidhoum, et al. (1996). "A systematic analysis of the mutations of the uroporphyrinogen III synthase gene in congenital erythropoietic porphyria." Eur J Hum Genet **4**(5): 274-82.

Frank, J., V. M. Aita, et al. (2001a). "Identification of a founder mutation in the protoporphyrinogen oxidase gene in variegate porphyria patients from chile." Hum Hered **51**(3): 160-8.

Frank, J., F. K. Jugert, et al. (1998a). "Recurrent missense mutation in the protoporphyrinogen oxidase gene underlies variegate porphyria." Am J Med Genet **79**(1): 22-6.

Frank, J., F. K. Jugert, et al. (1998b). "Variegate porphyria: identification of a nonsense mutation in the protoporphyrinogen oxidase gene." J Invest Dermatol **110**(4): 449-51.

Frank, J., F. K. Jugert, et al. (2001b). "A spectrum of novel mutations in the protoporphyrinogen oxidase gene in 13 families with variegate porphyria." J Invest Dermatol **116**(5): 821-3.

Frank, J., H. Lam, et al. (1998c). "Molecular basis of variegate porphyria: a missense mutation in the protoporphyrinogen oxidase gene." J Med Genet **35**(3): 244-7.

Frank, J., J. McGrath, et al. (1998d). "Homozygous variegate porphyria: identification of mutations on both alleles of the protoporphyrinogen oxidase gene in a severely affected proband." J Invest Dermatol **110**(4): 452-5.

Frank, J., J. A. McGrath, et al. (1999). "Mutations in the translation initiation codon of the protoporphyrinogen oxidase gene underlie variegate porphyria." Clin Exp Dermatol **24**(4): 296-301.

Frank, J., E. Zaider, et al. (1997). "Variegate Porphyria : Identification of three novel missense mutations in the protoporphyrinogen oxidase gene." Acta Haematol **98 (Suppl 1)**: 377.

Frankenberg, N., T. Kittel, et al. (1998). "Cloning, mapping and functional characterization of the hemB gene of Pseudomonas aeruginosa, which encodes a magnesium-dependent 5-aminolevulinic acid dehydratase." Mol Gen Genet **257**(4): 485-9.

Frydman, R. B. and G. Feinstein (1974). "Studies on porphobilinogen deaminase and uroporphyrinogen 3 cosynthase from human erythrocytes." Biochim Biophys Acta **350**(2): 358-73.

Fujita, H., A. Koizumi, et al. (1987). "Decreased erythrocyte delta-aminolevulinate dehydratase activity after styrene exposure." Biochem Pharmacol **36**(5): 711-6.

Funfschilling, U. and S. Rospert (1999). "Nascent polypeptide-associated complex stimulates protein import into yeast mitochondria." Mol Biol Cell **10**(10): 3289-99.

Furuyama, K. and S. Sassa (2000). "Interaction between succinyl CoA synthetase and the heme-biosynthetic enzyme ALAS-E is disrupted in sideroblastic anemia." J Clin Invest **105**(6): 757-64.

Galbraith, R. A. and A. Kappas (1989). "Pharmacokinetics of tin-mesoporphyrin in man and the effects of tin-chelated porphyrins on hyperexcretion of heme pathway precursors in patients with acute inducible porphyria." Hepatology **9**(6): 882-8.

Gambill, B. D., W. Voos, et al. (1993). "A dual role for mitochondrial heat shock protein 70 in membrane translocation of preproteins." J Cell Biol **123**(1): 109-17.

Garey, J. R., K. F. Franklin, et al. (1993). "Analysis of uroporphyrinogen decarboxylase complementary DNAs in sporadic porphyria cutanea tarda." Gastroenterology **105**(1): 165-9.

Garey, J. R., J. L. Hansen, et al. (1989). "A point mutation in the coding region of uroporphyrinogen decarboxylase associated with familial porphyria cutanea tarda." Blood **73**(4): 892-5.

Garey, J. R., L. M. Harrison, et al. (1990). "Uroporphyrinogen decarboxylase: a splice site mutation causes the deletion of exon 6 in multiple families with porphyria cutanea tarda." J Clin Invest **86**(5): 1416-22.

Gautschi, M., H. Lilie, et al. (2001). "RAC, a stable ribosome-associated complex in yeast formed by the DnaK-DnaJ homologs Ssz1p and zuotin." Proc Natl Acad Sci U S A **98**(7): 3762-7.

Giono, L. E., C. L. Varone, et al. (2001). "5-Aminolaevulinate synthase gene promoter contains two cAMP-response element (CRE)-like sites that confer positive and negative responsiveness to CRE-binding protein (CREB)." Biochem J **353**(Pt 2): 307-16.

Glick, B. and G. Schatz (1991). "Import of proteins into mitochondria." Annu Rev Genet **25**: 21-44.

Gokhman, I. and A. Zamir (1990). "The nucleotide sequence of the ferrochelatase and tRNA(val) gene region from Saccharomyces cerevisiae." Nucleic Acids Res **18**(20): 6130.

Gong, J., G. A. Hunter, et al. (1998). "Aspartate-279 in aminolevulinate synthase affects enzyme catalysis through enhancing the function of the pyridoxal 5'-phosphate cofactor." Biochemistry **37**(10): 3509-17.

Goodfellow, B. J., J. S. Dias, et al. (2001). "The solution structure and heme binding of the presequence of murine 5-aminolevulinate synthase." FEBS Lett **505**(2): 325-31.

Gora, M., J. Rytka, et al. (1999). "Activity and cellular location in Saccharomyces cerevisiae of chimeric mouse/yeast and Bacillus subtilis/yeast ferrochelatases." Arch Biochem Biophys **361**(2): 231-40.

Gouya, L., J. C. Deybach, et al. (1996). "Modulation of the phenotype in dominant erythropoietic protoporphyria by a low expression of the normal ferrochelatase allele." Am J Hum Genet **58**(2): 292-9.

Gouya, L., H. Puy, et al. (1999). "Inheritance in erythropoietic protoporphyria: a common wild-type ferrochelatase allelic variant with low expression accounts for clinical manifestation." Blood **93**(6): 2105-10.

Gouya, L., H. Puy, et al. (2002). "The penetrance of dominant erythropoietic protoporphyria is modulated by expression of wildtype FECH." Nat Genet **30**(1): 27-8.

Grandchamp, B. (1998). "Acute intermittent porphyria." Semin Liver Dis **18**(1): 17-24.

Grandchamp, B., H. De Verneuil, et al. (1987). "Tissue-specific expression of porphobilinogen deaminase. Two isoenzymes from a single gene." Eur J Biochem **162**(1): 105-10.

Grandchamp, B. and Y. Nordmann (1977). "Decreased lymphocyte coproporphyrinogen III oxidase activity in hereditary coproporphyria." Biochem Biophys Res Commun **74**(3): 1089-95.

Grandchamp, B. and Y. Nordmann (1988). "Enzymes of the heme biosynthesis pathway: recent advances in molecular genetics." Semin Hematol **25**(4): 303-11.

Grandchamp, B., N. Phung, et al. (1977). "Homozygous case of hereditary coproporphyria." Lancet **2**(8052-8053): 1348-9.

Grant, P. M., J. Tellam, et al. (1986). "Isolation and nucleotide sequence of a cDNA clone encoding rat mitochondrial malate dehydrogenase." Nucleic Acids Res **14**(15): 6053-66.

Greenbaum, L., D. Schwartz, et al. (2002). "Spectrally resolved microscopy of GFP trafficking." J Histochem Cytochem **50**(9): 1205-12.

Gregor, A., E. Kostrzewska, et al. (1994). "Porphyrin fluorescence in plasma of various types of porphyria." Pol Tyg Lek **49**(12-13): 284-6.

Grimm, B. (2003). Regulatory mechanisms of eukaryotic tetrapyrrole biosynthesis. The Iron and Cobalt Pigments : Biosynthesis, Structure, and Degradation. K. M. Kadish, K. M. Smith and R. Guilard. California, U.S.A., Elsevier Science. **12:** 1-32.

Gruhler, A., I. Arnold, et al. (1997). "N-terminal hydrophobic sorting signals of preproteins confer mitochondrial hsp70 independence for import into mitochondria." J Biol Chem **272**(28): 17410-5.

Gu, X. F., J. S. Lee, et al. (1991). "PCR detection of a G/T polymorphism at exon 10 of the porphobilinogen deaminase gene (PBG-D)." Nucleic Acids Res **19**(8): 1966.

Guberman, A. S., M. E. Scassa, et al. (2003). "Inhibitory effect of AP-1 complex on 5-aminolevulinate synthase gene expression through sequestration of cAMP-response element protein (CRE)-binding protein (CBP) coactivator." J Biol Chem **278**(4): 2317-26.

Gubin, A. N. and J. L. Miller (2001). "Human erythroid porphobilinogen deaminase exists in 2 splice variants." Blood **97**(3): 815-7.

Gunther, H. (1911). "Die haematoporphyrie." Deutsche Arch. Klin.Med. **105**: 89-146.

Hachiya, N., R. Alam, et al. (1993). "A mitochondrial import factor purified from rat liver cytosol is an ATP-dependent conformational modulator for precursor proteins." Embo J **12**(4): 1579-86.

Hachiya, N., T. Komiya, et al. (1994). "MSF, a novel cytoplasmic chaperone which functions in precursor targeting to mitochondria." Embo J **13**(21): 5146-54.

Haeger-Aronsen, B., M. Abdulla, et al. (1971). "Effect of lead on δ-aminolevulinic acid dehydrase activity in red blood cells." Arch Environ Health **23**(6): 440-5.

Haldi, M. and L. Guarente (1989). "N-terminal deletions of a mitochondrial signal sequence in yeast. Targeting information of delta-aminolevulinate synthase is encoded in non-overlapping regions." J Biol Chem **264**(29): 17107-12.

Hall, M. N., L. Hereford, et al. (1984). "Targeting of E. coli beta-galactosidase to the nucleus in yeast." Cell **36**(4): 1057-65.

Hammen, P. K., D. G. Gorenstein, et al. (1994). "Structure of the signal sequences for two mitochondrial matrix proteins that are not proteolytically processed upon import." Biochemistry **33**(28): 8610-7.

Hammen, P. K., D. G. Gorenstein, et al. (1996a). "Amphiphilicity determines binding properties of three mitochondrial presequences to lipid surfaces." Biochemistry **35**(12): 3772-81.

Hammen, P. K., M. Waltner, et al. (1996b). "The role of positive charges and structural segments in the presequence of rat liver aldehyde dehydrogenase in import into mitochondria." J Biol Chem **271**(35): 21041-8.

Hammen, P. K. and H. Weiner (1998). "Mitochondrial leader sequences: structural similarities and sequence differences." J Exp Zool **282**(1-2): 280-3.

Handa, F., K. Kumar, et al. (1975). "A case of variegate porphyria in an Indian." Br J Dermatol **92**(3): 347-50.

Hanson, J. W. and H. A. Dailey (1984). "Purification and characterization of chicken erythrocyte ferrochelatase." Biochem J **222**(3): 695-700.

Hansson, M., M. C. Gustafsson, et al. (1997). "Isolated Bacillus subtilis HemY has coproporphyrinogen III to coproporphyrin III oxidase activity." Biochim Biophys Acta **1340**(1): 97-104.

Hansson, M. and L. Hederstedt (1992). "Cloning and characterization of the Bacillus subtilis hemEHY gene cluster, which encodes protoheme IX biosynthetic enzymes." J Bacteriol **174**(24): 8081-93.

Hansson, M. and L. Hederstedt (1994). "Bacillus subtilis HemY is a peripheral membrane protein essential for protoheme IX synthesis which can oxidize coproporphyrinogen III and protoporphyrinogen IX." J Bacteriol **176**(19): 5962-70.

Hart, G. J. and A. R. Battersby (1985). "Purification and properties of uroporphyrinogen III synthase (co-synthetase) from Euglena gracilis." Biochem J **232**(1): 151-60.

Hart, G. J., A. D. Miller, et al. (1988). "Evidence that the pyrromethane cofactor of hydroxymethylbilane synthase (porphobilinogen deaminase) is bound through the sulphur atom of a cysteine residue." Biochem J **252**(3): 909-12.

Hartl, F. U. (1996). "Molecular chaperones in cellular protein folding." Nature **381**(6583): 571-9.

Hartl, F. U., N. Pfanner, et al. (1989). "Mitochondrial protein import." Biochim Biophys Acta **988**(1): 1-45.

Haseloff, J. (1999). "GFP variants for multispectral imaging of living cells." Methods Cell Biol **58**: 139-51.

Haseloff, J., E. L. Dormand, et al. (1999). "Live imaging with green fluorescent protein." Methods Mol Biol **122**: 241-59.

Hassoun, A., L. Verstraeten, et al. (1989). "Biochemical diagnosis of an hereditary aminolaevulinate dehydratase deficiency in a 63-year-old man." J Clin Chem Clin Biochem **27**(10): 781-6.

Hay, R., P. Bohni, et al. (1984). "How mitochondria import proteins." Biochim Biophys Acta **779**(1): 65-87.

Heim, R., A. B. Cubitt, et al. (1995). "Improved green fluorescence." Nature **373**(6516): 663-4.

Heim, R., D. C. Prasher, et al. (1994). "Wavelength mutations and posttranslational autoxidation of green fluorescent protein." Proc Natl Acad Sci U S A **91**(26): 12501-4.

Held, J. L., S. Sassa, et al. (1989). "Erythrocyte uroporphyrinogen decarboxylase activity in porphyria cutanea tarda: a study of 40 consecutive patients." J Invest Dermatol **93**(3): 332-4.

Henriksson, M., K. Timonen, et al. (1996). "Four novel mutations in the ferrochelatase gene among erythropoietic protoporphyria patients." J Invest Dermatol **106**(2): 346-50.

Herrick, A. L., M. R. Moore, et al. (1991). "Cholelithiasis in patients with variegate porphyria." J Hepatol **12**(1): 50-3.

Hift, R. J. (2000). Variegate Porphyria. PhD Thesis, Dept. of Medicine. Cape Town, University of Cape Town: 307.

Hift, R. J., P. N. Meissner, et al. (1997a). "Variegate porphyria in South Africa, 1688-1996--new developments in an old disease." S Afr Med J **87**(6): 722-31.

Hift, R. J., P. N. Meissner, et al. (1997b). "The clinical diagnosis, prevention and management of the hepatic porphyrias." Trop Gastroenterol **18**(2): 41-4.

Hift, R. J., P. N. Meissner, et al. (1993a). "Hepatoerythropoietic porphyria precipitated by viral hepatitis." Gut **34**(11): 1632-4.

Hift, R. J., P. N. Meissner, et al. (1993b). "Homozygous variegate porphyria: an evolving clinical syndrome." Postgrad Med J **69**(816): 781-6.

Higuchi, M. and L. Bogorad (1975). "The purification and properties of uroporphyrinogen I synthases and uroporphyrinogen III cosynthase. Interactions between the enzymes." Ann N Y Acad Sci **244**: 401-18.

Hill, K., K. Model, et al. (1998). "Tom40 forms the hydrophilic channel of the mitochondrial import pore for preproteins [see comment]." Nature **395**(6701): 516-21.

Honlinger, A., M. Kubrich, et al. (1995). "The mitochondrial receptor complex: Mom22 is essential for cell viability and directly interacts with preproteins." Mol Cell Biol **15**(6): 3382-9.

Hoogenraad, N. J., L. A. Ward, et al. (2002). "Import and assembly of proteins into mitochondria of mammalian cells." Biochim Biophys Acta **1592**(1): 97-105.

Horwich, A. L., M. Cheng, et al. (1991). "Mitochondrial protein import." Curr Top Microbiol Immunol **170**: 1-42.

Horwich, A. L., F. Kalousek, et al. (1987). "The ornithine transcarbamylase leader peptide directs mitochondrial import through both its midportion structure and net positive charge." J Cell Biol **105**(2): 669-77.

Horwich, A. L., F. Kalousek, et al. (1986). "Targeting of pre-ornithine transcarbamylase to mitochondria: definition of critical regions and residues in the leader peptide." Cell **44**(3): 451-9.

Horwich, A. L., F. Kalousek, et al. (1985a). "A leader peptide is sufficient to direct mitochondrial import of a chimeric protein." Embo J **4**(5): 1129-35.

Horwich, A. L., F. Kalousek, et al. (1985b). "Arginine in the leader peptide is required for both import and proteolytic cleavage of a mitochondrial precursor." Proc Natl Acad Sci U S A **82**(15): 4930-3.

Hurt, E. C., M. Goldschmidt-Clermont, et al. (1986). "A mitochondrial presequence can transport a chloroplast-encoded protein into yeast mitochondria." J Biol Chem **261**(25): 11440-3.

Hurt, E. C., U. Muller, et al. (1985a). "The first twelve amino acids of a yeast mitochondrial outer membrane protein can direct a nuclear-coded cytochrome oxidase subunit to the mitochondrial inner membrane." Embo J **4**(13A): 3509-18.

Hurt, E. C., B. Pesold-Hurt, et al. (1985b). "The first twelve amino acids (less than half of the pre-sequence) of an imported mitochondrial protein can direct mouse cytosolic dihydrofolate reductase into the yeast mitochondrial matrix." Embo J **4**(8): 2061-8.

Hwang, S., T. Jascur, et al. (1989). "Disrupted yeast mitochondria can import precursor proteins directly through their inner membrane." J Cell Biol **109**(2): 487-93.

Hwang, S. T. and G. Schatz (1989). "Translocation of proteins across the mitochondrial inner membrane, but not into the outer membrane, requires

nucleoside triphosphates in the matrix." Proc Natl Acad Sci U S A **86**(21): 8432-6.

Hwang, S. T., C. Wachter, et al. (1991). "Protein import into the yeast mitochondrial matrix. A new translocation intermediate between the two mitochondrial membranes." J Biol Chem **266**(31): 21083-9.

Imoto, S., Y. Tanizawa, et al. (1996). "A novel mutation in the ferrochelatase gene associated with erythropoietic protoporphyria." Br J Haematol **94**(1): 191-7.

Inouye, S. and F. I. Tsuji (1994). "Aequorea green fluorescent protein. Expression of the gene and fluorescence characteristics of the recombinant protein." FEBS Lett **341**(2-3): 277-80.

Jackson, A. H., H. A. Sancovich, et al. (1976). "Macrocyclic intermediates in the biosynthesis of porphyrins." Philos Trans R Soc Lond B Biol Sci **273**(924): 191-206.

Jacobs, J. M. and N. J. Jacobs (1987). "Oxidation of protoporphyrinogen to protoporphyrin, a step in chlorophyll and haem biosynthesis. Purification and partial characterization of the enzyme from barley organelles." Biochem J **244**(1): 219-24.

Jacobs, N. J., S. E. Borotz, et al. (1989). "Characteristics of purified protoporphyrinogen oxidase from barley." Biochem Biophys Res Commun **161**(2): 790-6.

Jacobs, N. J. and J. M. Jacobs (1981). "Protoporphyrinogen oxidation in Rhodopseudomonas spheroides, a step in heme and bacteriochlorophyll synthesis." Arch Biochem Biophys **211**(1): 305-11.

Jaffe, E. K. (1995). "Porphobilinogen synthase, the first source of heme's asymmetry." J Bioenerg Biomembr **27**(2): 169-79.

Jakob, U. and J. Buchner (1994). "Assisting spontaneity: the role of Hsp90 and small Hsps as molecular chaperones." Trends Biochem Sci **19**(5): 205-11.

Jascur, T., D. P. Goldenberg, et al. (1992). "Sequential translocation of an artificial precursor protein across the two mitochondrial membranes." J Biol Chem **267**(19): 13636-41.

Johnston, D. J., E. Droz, et al. (1998). "Cloning and characterization of potato cDNAs involved in tetrapyrrole biosynthesis." Plant Physiology **118**: 330.

Jones, O. T. (1976). "Chlorophyll biosynthesis." Phil Trans R Soc Lond (Biol) **273**: 207-225.

Jones, R. M. and P. M. Jordan (1993). "Purification and properties of the uroporphyrinogen decarboxylase from Rhodobacter sphaeroides." Biochem J **293**(Pt 3): 703-12.

Jordan, P. M. (1990). The biosynthesis of 5-aminolevulinic acid and its transformation into coproporphyrinogen in animals and bacteria. Biosynthesis of Heme and Chlorophylls. H. A. Dailey. New York, McGraw-Hill: 55-122.

Jordan, P. M. (1991). Biosynthesis of Tetrapyrroles. New Comprehensive Biochemistry. Amsterdam, Elsevier. **19:** 1-66.

Jordan, P. M., B. I. Mgbeje, et al. (1988a). "Nucleotide sequence for the hemD gene of Escherichia coli encoding uroporphyrinogen III synthase and initial evidence for a hem operon." Biochem J **249**(2): 613-6.

Jordan, P. M. and D. Shemin (1973). "Purification and properties of uroporphyrinogen I synthetase from Rhodopseudomonas spheroides." J Biol Chem **248**(3): 1019-24.

Jordan, P. M. and M. J. Warren (1987). "Evidence for a dipyrromethane cofactor at the catalytic site of E. coli porphobilinogen deaminase." FEBS Lett **225**(1-2): 87-92.

Jordan, P. M., M. J. Warren, et al. (1992). "Crystallization and preliminary X-ray investigation of Escherichia coli porphobilinogen deaminase." J Mol Biol **224**(1): 269-71.

Jordan, P. M., M. J. Warren, et al. (1988b). "Identification of a cysteine residue as the binding site for the dipyrromethane cofactor at the active site of Escherichia coli porphobilinogen deaminase." FEBS Lett **235**(1-2): 189-93.

Jordan, P. M. and S. C. Woodcock (1991). "Mutagenesis of arginine residues in the catalytic cleft of Escherichia coli porphobilinogen deaminase that affects dipyrromethane cofactor assembly and tetrapyrrole chain initiation and elongation." Biochem J **280**(Pt 2): 445-9.

Juknat, A. A., A. Seubert, et al. (1989). "Studies on uroporphyrinogen decarboxylase of etiolated Euglena gracilis Z." Eur J Biochem **179**(2): 423-8.

Kaczor, C. M., M. W. Smith, et al. (1994). "Plant delta-aminolevulinic acid dehydratase. Expression in soybean root nodules and evidence for a bacterial lineage of the Alad gene." Plant Physiol **104**(4): 1411-7.

Kaether, C. and H. H. Gerdes (1995). "Visualization of protein transport along the secretory pathway using green fluorescent protein." FEBS Lett **369**(2-3): 267-71.

Kalderon, D., B. L. Roberts, et al. (1984). "A short amino acid sequence able to specify nuclear location." Cell **39**(3 Pt 2): 499-509.

Kang, P. J., J. Ostermann, et al. (1990). "Requirement for hsp70 in the mitochondrial matrix for translocation and folding of precursor proteins." Nature **348**(6297): 137-43.

Kappas, A., S. Sassa, et al. (1989). The metabolic basis of inherited disease. The Porphyrias. C. R. Wyngaarden and D. S. Frederickson. New York, McGraw-Hill: 1305.

Kappas, A., S. Sassa, et al. (1995). The Porphyrias. The metabolic basis of inherited diseases. C. R. Scriver, A. L. Beaudet, W. S. Sly and D. Valle. New York, McGraw-Hill. **2:** 2103-2159.

Karr, S. R. and H. A. Dailey (1988). "The synthesis of murine ferrochelatase in vitro and in vivo." Biochem J **254**(3): 799-803.

Kauppinen, R., K. Timonen, et al. (1997). "Molecular genetics and clinical characteristics of variegate porphyria." Acta Haematol **98**(Suppl 1): 96.

Kauppinen, R., K. Timonen, et al. (1996). Hepatology. 23,I.

Kauppinen, R., K. Timonen, et al. (2001). "Homozygous variegate porphyria: 20 y follow-up and characterization of molecular defect." J Invest Dermatol **116**(4): 610-3.

Kawanishi, S., Y. Seki, et al. (1983). "Uroporphyrinogen decarboxylase. Purification, properties, and inhibition by polychlorinated biphenyl isomers." J Biol Chem **258**(7): 4285-92.

Kaya, A. H., M. Plewinska, et al. (1994). "Human delta-aminolevulinate dehydratase (ALAD) gene: structure and alternative splicing of the erythroid and housekeeping mRNAs." Genomics **19**(2): 242-8.

Kiebler, M., K. Becker, et al. (1993). "Mitochondrial protein import: specific recognition and membrane translocation of preproteins." J Membr Biol **135**(3): 191-207.

Kim, C. K., H. Haider Kh, et al. (2002). "Nonviral vector for efficient gene transfer to human ovarian adenocarcinoma cells." Gynecol Oncol **84**(1): 85-93.

Kirsch, R. E., P. N. Meissner, et al. (1998). "Variegate porphyria." Semin Liver Dis **18**(1): 33-41.

Klemm, D. J. and L. L. Barton (1985). "Oxidation of protoporphyrinogen in the obligate anaerobe Desulfovibrio gigas." J Bacteriol **164**(1): 316-20.

Klemm, D. J. and L. L. Barton (1987). "Purification and properties of protoporphyrinogen oxidase from an anaerobic bacterium, Desulfovibrio gigas." J Bacteriol **169**(11): 5209-15.

Kodama, T., M. Takagi, et al. (1979). "[A case of variegate porphyria and her hepatic delta-aminolevulinic acid synthetic activity (author's transl)]." Nippon Naika Gakkai Zasshi **68**(10): 1293-300.

Kohashi, M., R. P. Clement, et al. (1984). "Rat hepatic uroporphyrinogen III co-synthase. Purification and evidence for a bound folate coenzyme participating in the biosynthesis of uroporphyrinogen III." Biochem J **220**(3): 755-65.

Kohno, H., T. Furukawa, et al. (1996). "Mouse coproporphyrinogen oxidase is a copper-containing enzyme: expression in Escherichia coli and site-directed mutagenesis." Biochim Biophys Acta **1292**(1): 156-62.

Kohno, H., T. Furukawa, et al. (1993). "Coproporphyrinogen oxidase. Purification, molecular cloning, and induction of mRNA during erythroid differentiation." J Biol Chem **268**(28): 21359-63.

Komiya, T., S. Rospert, et al. (1997). "Binding of mitochondrial precursor proteins to the cytoplasmic domains of the import receptors Tom70 and Tom20 is determined by cytoplasmic chaperones." Embo J **16**(14): 4267-75.

Kordac, V., P. Martasek, et al. (1985). "Increased erythrocyte protoporphyrin in homozygous variegate porphyria." Photodermatol **2**(4): 257-9.

Koszo, F., M. Morvay, et al. (1992). "Erythrocyte uroporphyrinogen decarboxylase activity in 80 unrelated patients with porphyria cutanea tarda." Br J Dermatol **126**(5): 446-9.

Krakowski, A., S. Brenner, et al. (1979). "[Variegate porphyria]." Harefuah **96**(9): 528-32.

Kramer, S., D. M. Becker, et al. (1977). "Enzyme deficiencies in the porphyrias." Br J Haematol **37**(4): 439-45.

Kreil, G. (1975). "The structure of Apis dorsata melittin: phylogenetic relationships between honeybees as deduced from sequence data." FEBS Lett **54**(1): 100-2.

Kruse, E., H. P. Mock, et al. (1995). "Coproporphyrinogen III oxidase from barley and tobacco--sequence analysis and initial expression studies." Planta **196**(4): 796-803.

Kubrich, M., P. Keil, et al. (1994). "The polytopic mitochondrial inner membrane proteins MIM17 and MIM23 operate at the same preprotein import site." FEBS Lett **349**(2): 222-8.

Kunkele, K. P., P. Juin, et al. (1998). "The isolated complex of the translocase of the outer membrane of mitochondria. Characterization of the cation-selective and voltage-gated preprotein-conducting pore." J Biol Chem **273**(47): 31032-9.

Labbe-Bois, R. (1990). "The ferrochelatase from Saccharomyces cerevisiae. Sequence, disruption, and expression of its structural gene HEM15." J Biol Chem **265**(13): 7278-83.

Lake-Bullock, H. and H. A. Dailey (1993). "Biphasic ordered induction of heme synthesis in differentiating murine erythroleukemia cells: role of erythroid 5-aminolevulinate synthase." Mol Cell Biol **13**(11): 7122-32.

Lam, C. W., K. N. Hui, et al. (2001). "Novel splicing mutation of the PPOX gene (IVS10 + 1G-->A) detected by denaturing high-performance liquid chromatography." Clin Chim Acta **305**(1-2): 197-200.

Lam, H., L. Dragan, et al. (1997). "Molecular basis of variegate porphyria: a de novo insertion mutation in the protoporphyrinogen oxidase gene." Hum Genet **99**(1): 126-9.

Lambert, R., P. D. Brownlie, et al. (1994). "Structural studies on porphobilinogen deaminase." Ciba Found Symp **180**: 97-104.

Lamoril, J., S. Boulechfar, et al. (1991). "Human erythropoietic protoporphyria: two point mutations in the ferrochelatase gene." Biochem Biophys Res Commun **181**(2): 594-9.

Lamoril, J., H. Puy, et al. (2001). "Characterization of mutations in the CPO gene in British patients demonstrates absence of genotype-phenotype correlation and identifies relationship between hereditary coproporphyria and harderoporphyria." Am J Hum Genet **68**(5): 1130-8.

Lathrop, J. T. and M. P. Timko (1993). "Regulation by heme of mitochondrial protein transport through a conserved amino acid motif." Science **259**(5094): 522-5.

Lavallee, D. K. (1988). Mechanistic Principles of Enzyme Activity. J. F. Liebman and A. Greenberg. New York, VCH Publishers Inc.: 279-314.

Lecha, M., C. Herrero, et al. (2003). "Diagnosis and treatment of the hepatic porphyrias." Dermatol Ther **16**(1): 65-72.

Lee, C. M., J. Sedman, et al. (1999). "The DNA helicase, Hmi1p, is transported into mitochondria by a C-terminal cleavable targeting signal." J Biol Chem **274**(30): 20937-42.

Lee, J. S. and M. Anvret (1987). "A PstI polymorphism for the human porphobilinogen deaminase gene (PBG)." Nucleic Acids Res **15**(15): 6307.

Leffel, S. M., S. A. Mabon, et al. (1997). "Applications of green fluorescent protein in plants." Biotechniques **23**(5): 912-8.

Lermontova, I., E. Kruse, et al. (1997). "Cloning and characterization of a plastidal and a mitochondrial isoform of tobacco protoporphyrinogen IX oxidase." Proc Natl Acad Sci U S A **94**(16): 8895-900.

Li, F., C. K. Lim, et al. (1989). "Coproporphyrinogen oxidase, protoporphyrinogen oxidase and ferrochelatase activities in human liver biopsies with special reference to alcoholic liver disease." J Hepatol **8**(1): 86-93.

Lippincott-Schwartz, J., N. Altan-Bonnet, et al. (2003). "Photobleaching and photoactivation: following protein dynamics in living cells." Nat Cell Biol **Suppl**: S7-14.

Lippincott-Schwartz, J. and G. H. Patterson (2003). "Development and use of fluorescent protein markers in living cells." Science **300**(5616): 87-91.

Lithgow, T., T. Junne, et al. (1994). "The mitochondrial outer membrane protein Mas22p is essential for protein import and viability of yeast." Proc Natl Acad Sci U S A **91**(25): 11973-7.

Llambias, E. B. and A. M. d. Batlle (1970). "Porphyrin biosynthesis in soybean callus. V. The porphobilinogen deaminase-uroporphyrinogen cosynthetase system. Kinetic studies." Biochim Biophys Acta **220**(3): 552-9.

Llopis, J., J. M. McCaffery, et al. (1998). "Measurement of cytosolic, mitochondrial, and Golgi pH in single living cells with green fluorescent proteins." Proc Natl Acad Sci U S A **95**(12): 6803-8.

Long, C., S. J. Smyth, et al. (1993). "Detection of latent variegate porphyria by fluorescence emission spectroscopy of plasma." Br J Dermatol **129**(1): 9-13.

Louie, G. V., P. D. Brownlie, et al. (1996). "The three-dimensional structure of Escherichia coli porphobilinogen deaminase at 1.76-A resolution." Proteins **25**(1): 48-78.

Louie, G. V., P. D. Brownlie, et al. (1992). "Structure of porphobilinogen deaminase reveals a flexible multidomain polymerase with a single catalytic site." Nature **359**(6390): 33-9.

Lundin, G. and M. Anvret (1997). "Characterization and regulation of the nonerythroid porphobilinogen deaminase promoter." Biochem Biophys Res Commun **231**(2): 409-11.

Luo, J. and C. K. Lim (1993). "Order of uroporphyrinogen III decarboxylation on incubation of porphobilinogen and uroporphyrinogen III with erythrocyte uroporphyrinogen decarboxylase." Biochem J **289**(Pt 2): 529-32.

Madsen, O., L. Sandal, et al. (1993). "A soybean coproporphyrinogen oxidase gene is highly expressed in root nodules." Plant Mol Biol **23**(1): 35-43.

Maeda, N., Y. Horie, et al. (2000). "Three novel mutations in the protoporphyrinogen oxidase gene in Japanese patients with variegate porphyria." Clin Biochem **33**(6): 495-500.

Magnus, I., A. Jarrett, et al. (1961). "Erythropoietic protoporphyria: a new porphyria syndrome with solar urticaria due to protoporphyrinaemia." Lancet **2**: 448-451.

Magness, S. T., A. Tugores, et al. (1998). "Analysis of the human ferrochelatase promoter in transgenic mice." Blood **92**(1): 320-8.

Maguire, D. J., A. R. Day, et al. (1986). "Nucleotide sequence of the chicken 5-aminolevulinate synthase gene." Nucleic Acids Res **14**(3): 1379-91.

Maneli, M. H., A. V. Corrigall, et al. (2003). "Kinetic and physical characterisation of recombinant wild-type and mutant human protoporphyrinogen oxidases." Biochim Biophys Acta **1650**(1-2): 10-21.

Manning, D. J. and T. A. Gray (1991). "Haem arginate in acute hereditary coproporphyria." Arch Dis Child **66**(6): 730-1.

Marks, G. S. (1969). Heme and chlorophyll : Chemical, Biochemical and Medical Aspects. Princeton, New Jersey, Van Nostrand-Rheinhold.

Martasek, P. (1998). "Hereditary coproporphyria." Semin Liver Dis **18**(1): 25-32.

Martasek, P., J. M. Camadro, et al. (1994). "Molecular cloning, sequencing, and functional expression of a cDNA encoding human coproporphyrinogen oxidase." Proc Natl Acad Sci U S A **91**(8): 3024-8.

Martasek, P., J. M. Camadro, et al. (1997). "Human coproporphyrinogen oxidase. Biochemical characterization of recombinant normal and R231W mutated enzymes expressed in E. coli as soluble, catalytically active homodimers." Cell Mol Biol (Noisy-le-grand) **43**(1): 47-58.

Martasek, P., V. Kordac, et al. (1983). "Variegate porphyria and porphyria cutanea tarda." Arch Dermatol **119**(7): 537-8.

Martins, B. M., B. Grimm, et al. (2001a). "Crystal structure and substrate binding modeling of the uroporphyrinogen-III decarboxylase from Nicotiana tabacum. Implications for the catalytic mechanism." J Biol Chem **276**(47): 44108-16.

Martins, B. M., B. Grimm, et al. (2001b). "Tobacco uroporphyrinogen-III decarboxylase: characterization, crystallization and preliminary X-ray analysis." Acta Crystallogr D Biol Crystallogr **57**(Pt 11): 1709-11.

Mathews, M. A., H. L. Schubert, et al. (2001). "Crystal structure of human uroporphyrinogen III synthase." Embo J **20**(21): 5832-9.

Mathews-Roth, M. M., G. L. Drouin, et al. (1987). "Isolation of human ferrochelatase [letter]." Arch Dermatol **123**(4): 429-30.

Matringe, M., J. M. Camadro, et al. (1992). "Localization within chloroplasts of protoporphyrinogen oxidase, the target enzyme for diphenylether-like herbicides." J Biol Chem **267**(7): 4646-51.

Matters, G. L. and S. I. Beale (1995). "Structure and expression of the Chlamydomonas reinhardtii alad gene encoding the chlorophyll biosynthetic enzyme, delta-aminolevulinic acid dehydratase (porphobilinogen synthase)." Plant Mol Biol **27**(3): 607-17.

May, B. K. and M. J. Bawden (1989). "Control of heme biosynthesis in animals. Seminars in Hematology **26**: 150-6.

May, B. K., I. A. Borthwick, et al. (1986). "Control of 5-aminolevulinate synthase in animals." Curr Top Cell Regul **28**: 233-62.

May, B. K., S. C. Dogra, et al. (1995). "Molecular regulation of heme biosynthesis in higher vertebrates." Prog Nucleic Acid Res Mol Biol **51**: 1-51.

McEneaney, D., S. Hawkins, et al. (1993). "Porphyric neuropathy--a rare and often neglected differential diagnosis of Guillain-Barre syndrome." J Neurol Sci **114**(2): 231-2.

McKay, R., R. Druyan, et al. (1969). "Intramitochondrial localization of delta-aminolaevulate synthetase and ferrochelatase in rat liver." Biochem J **114**(3): 455-61.

McManus, J. F., C. G. Begley, et al. (1996). "Five new mutations in the uroporphyrinogen decarboxylase gene identified in families with cutaneous porphyria." Blood **88**(9): 3589-600.

Medlock, A. E. and H. A. Dailey (1996). "Human coproporphyrinogen oxidase is not a metalloprotein." J Biol Chem **271**(51): 32507-10.

Meguro, K., H. Fujita, et al. (1994). "Molecular defects of uroporphyrinogen decarboxylase in a patient with mild hepatoerythropoietic porphyria." J Invest Dermatol **102**(5): 681-5.

Meissner, P. N., T. A. Dailey, et al. (1996a). "A R59W mutation in human protoporphyrinogen oxidase results in decreased enzyme activity and is prevalent in South Africans with variegate porphyria." Nat Genet **13**(1): 95-7.

Meissner, P. N., T. A. Dailey, et al. (1996b). "A R59W mutation in human protoporphyrinogen oxidase results in decreased enzyme activity and is prevalent in South Africans with variegate porphyria [see comments]." Nat Genet **13**(1): 95-7.

Meissner, P. N., R. S. Day, et al. (1986). "Protoporphyrinogen oxidase and porphobilinogen deaminase in variegate porphyria." Eur J Clin Invest **16**(3): 257-61.

Meissner, P. N., R. J. Hift, et al. (2003). Variegate Porphyria. Medical Aspects of Porphyrins. K. M. Kadish, K. M. Smith and R. Guilard. California, U.S.A., Academic Press. **14:** 93-120.

Meissner, P. N., R. J. Hift, et al. (2001). The Porphyrias. The Liver : Biology and Pathobiology. I. M. Arias. Philadelphia, U.S.A., Lippincott Williams and Wilkins: 311-330.

Meissner, P. N., D. M. Meissner, et al. (1987). "Porphyria--the UCT experience." S Afr Med J **72**(11): 755-61.

Melefors, O., B. Goossen, et al. (1993). "Translational control of 5-aminolevulinate synthase mRNA by iron-responsive elements in erythroid cells." J Biol Chem **268**(8): 5974-8.

Mendez, M., L. Sorkin, et al. (1998). "Familial porphyria cutanea tarda: characterization of seven novel uroporphyrinogen decarboxylase mutations and frequency of common hemochromatosis alleles." Am J Hum Genet **63**(5): 1363-75.

Meyer, U. A., M. M. Schuurmans, et al. (1998). "Acute porphyrias: pathogenesis of neurological manifestations." Semin Liver Dis **18**(1): 43-52.

Mignotte, V., L. Wall, et al. (1989). "Two tissue-specific factors bind the erythroid promoter of the human porphobilinogen deaminase gene." Nucleic Acids Res **17**(1): 37-54.

Moore, M. R. (1987). Porphyrins and Products of Haem Biosynthetic Pathway. Disorders of Porphyrin Metabolism. New York, Plenum Publishing Corporation: 21-72.

Moran-Jimenez, M. J., C. Ged, et al. (1996). "Uroporphyrinogen decarboxylase: complete human gene sequence and molecular study of three families with hepatoerythropoietic porphyria." Am J Hum Genet **58**(4): 712-21.

Morgan, R. R., S. V. da, et al. (2002). "Functional studies of mutations in the human protoporphyrinogen oxidase gene in variegate porphyria." Cell Mol Biol (Noisy-le-grand) **48**(1): 79-82.

Mori, M., S. Miura, et al. (1980). "Characterization of a protease apparently involved in processing of pre-ornithine transcarbamylase of rat liver." Proc Natl Acad Sci U S A **77**(12): 7044-8.

Morin, J. G. and J. W. Hastings (1971a). "Biochemistry of the bioluminescence of colonial hydroids and other coelenterates." J Cell Physiol **77**(3): 305-12.

Morin, J. G. and J. W. Hastings (1971b). "Energy transfer in a bioluminescent system." J Cell Physiol **77**(3): 313-8.

Moro, F., C. Sirrenberg, et al. (1999). "The TIM17.23 preprotein translocase of mitochondria: composition and function in protein transport into the matrix." Embo J **18**(13): 3667-75.

Mukerji, S. K. and N. R. Pimstone (1992). "Uroporphyrinogen decarboxylases from human erythrocytes: purification, complete separation and partial characterization of two isoenzymes." Int J Biochem **24**(1): 105-19.

Muraoka, A., I. Suehiro, et al. (1995). "delta-Aminolevulinic acid dehydratase deficiency porphyria (ADP) with syndrome of inappropriate secretion of antidiuretic hormone (SIADH) in a 69-year-old woman." Kobe J Med Sci **41**(1-2): 23-31.

Murphy, A., G. Gibson, et al. (1995). "Adult-onset congenital erythropoietic porphyria (Gunther's disease) presenting with thrombocytopenia." J R Soc Med **88**(6): 357P-358P.

Murphy, G. M., J. L. Hawk, et al. (1986). "Homozygous variegate porphyria: two similar cases in unrelated families." J R Soc Med **79**(6): 361-3.

Mustajoki, P. (1978). "Variegate porphyria." Ann Intern Med **89**(2): 238-44.

Mustajoki, P. (1980). "Variegate porphyria. Twelve years' experience in Finland." Q J Med **49**(194): 191-203.

Mustajoki, P. and P. Koskelo (1976). "Hereditary hepatic porphyrias in Finland." Acta Med Scand **200**(3): 171-8.

Mustajoki, P., S. Mustajoki, et al. (1994). "Effects of heme arginate on cytochrome P450-mediated metabolism of drugs in patients with variegate porphyria and in healthy men." Clin Pharmacol Ther **56**(1): 9-13.

Mustajoki, P. and Y. Nordmann (1993). "Early administration of heme arginate for acute porphyric attacks." Arch Intern Med **153**(17): 2004-8.

Mustajoki, P., R. Tenhunen, et al. (1987). "Homozygous variegate porphyria. A severe skin disease of infancy." Clin Genet **32**(5): 300-5.

Nakahashi, Y., H. Fujita, et al. (1992). "The molecular defect of ferrochelatase in a patient with erythropoietic protoporphyria." Proc Natl Acad Sci U S A **89**(1): 281-5.

Nakahashi, Y., S. Taketani, et al. (1990). "Molecular cloning and sequence analysis of cDNA encoding human ferrochelatase." Biochem Biophys Res Commun **173**(2): 748-55.

Narita, S., R. Tanaka, et al. (1996). "Molecular cloning and characterization of a cDNA that encodes protoporphyrinogen oxidase of Arabidopsis thaliana." Gene **182**(1-2): 169-75.

Netzer, W. J. and F. U. Hartl (1998). "Protein folding in the cytosol: chaperonin-dependent and -independent mechanisms." Trends Biochem Sci **23**(2): 68-73.

Nishi, T., F. Nagashima, et al. (1989). "Import and processing of precursor to mitochondrial aspartate aminotransferase. Structure-function relationships of the presequence." J Biol Chem **264**(11): 6044-51.

Nishimura, K., T. Nakayashiki, et al. (1995a). "Cloning and identification of the hemG gene encoding protoporphyrinogen oxidase (PPO) of Escherichia coli K-12." DNA Res **2**(1): 1-8.

Nishimura, K., S. Taketani, et al. (1995b). "Cloning of a human cDNA for protoporphyrinogen oxidase by complementation in vivo of a hemG mutant of Escherichia coli." J Biol Chem **270**(14): 8076-80.

Nordmann, Y., B. Grandchamp, et al. (1977). "Coproporphyrinogen-oxidase deficiency in hereditary coproporphyria." Lancet **1**(8003): 140.

Norris, P. G., G. H. Elder, et al. (1990a). "Homozygous variegate porphyria: a case report." Br J Dermatol **122**(2): 253-7.

Norris, P. G., A. V. Nunn, et al. (1990b). "Genetic heterogeneity in erythropoietic protoporphyria: a study of the enzymatic defect in nine affected families." J Invest Dermatol **95**(3): 260-3.

Nunn, A. V., P. Norris, et al. (1988). "Zinc chelatase in human lymphocytes: detection of the enzymatic defect in erythropoietic protoporphyria." Anal Biochem **174**(1): 146-50.

O'Neil, K. T. and W. F. DeGrado (1990). "A thermodynamic scale for the helix-forming tendencies of the commonly occurring amino acids." Science **250**(4981): 646-51.

Ono, H. (2002). "[Protein translocation across the inner mitochondrial membrane]." Nippon Rinsho **60 Suppl 4**: 74-8.

Ono, H. and S. Tuboi (1986). "Translocation of proteins into rat liver mitochondria. The precursor polypeptides of a large subunit of succinate dehydrogenase and ornithine aminotransferase and their imports into their own locations of mitochondria." Eur J Biochem **155**(3): 543-9.

Ono, H. and S. Tuboi (1988). "The cytosolic factor required for import of precursors of mitochondrial proteins into mitochondria." J Biol Chem **263**(7): 3188-93.

Ou, W. J., A. Ito, et al. (1989). "Purification and characterization of a processing protease from rat liver mitochondria." Embo J **8**(9): 2605-12.

Palmer, R. A., G. H. Elder, et al. (2001). "Homozygous variegate porphyria: a compound heterozygote with novel mutations in the protoporphyrinogen oxidase gene." Br J Dermatol **144**(4): 866-9.

Patti, E., F. Martinez di Montemuros, et al. (2003). Molecular analysis of the PPOX gene in Italian patients with variegate porphyria (VP) : identification of 3 novel mutations. Porphyrins and Porphyrias 2003, Prague, Czech Republic.

Pfanner, N. (2000). "Protein sorting: recognizing mitochondrial presequences." Curr Biol **10**(11): R412-5.

Pfanner, N. and A. Chacinska (2002). "The mitochondrial import machinery: preprotein-conducting channels with binding sites for presequences." Biochim Biophys Acta **1592**(1): 15.

Pfanner, N., E. A. Craig, et al. (1997). "Mitochondrial preprotein translocase." Annu Rev Cell Dev Biol **13**: 25-51.

Pfanner, N. and A. Geissler (2001). "Versatility of the mitochondrial protein import machinery." Nat Rev Mol Cell Biol **2**(5): 339-49.

Pfanner, N., P. Hoeben, et al. (1987). "The carboxyl-terminal two-thirds of the ADP/ATP carrier polypeptide contains sufficient information to direct translocation into mitochondria." J Biol Chem **262**(31): 14851-4.

Pfanner, N. and W. Neupert (1990). "The mitochondrial protein import apparatus." Annu Rev Biochem **59**: 331-53.

Pfanner, N., J. Rassow, et al. (1992). "A dynamic model of the mitochondrial protein import machinery." Cell **68**(6): 999-1002.

Phillips, J. D., F. G. Whitby, et al. (1997). "Characterization and crystallization of human uroporphyrinogen decarboxylase." Protein Sci **6**(6): 1343-6.

Picat, C., F. Bourgeois, et al. (1991). "PCR detection of a C/T polymorphism in exon 1 of the porphobilinogen deaminase gene (PBGD)." Nucleic Acids Res **19**(18): 5099.

Pilgrim, D. and E. T. Young (1987). "Primary structure requirements for correct sorting of the yeast mitochondrial protein ADH III to the yeast mitochondrial matrix space." Mol Cell Biol **7**(1): 294-304.

Ploux, O. and A. Marquet (1996). "Mechanistic studies on the 8-amino-7-oxopelargonate synthase, a pyridoxal-5'-phosphate-dependent enzyme involved in biotin biosynthesis." Eur J Biochem **236**(1): 301-8.

Poh-Fitzpatrick, M. B. (1977). "Erythropoietic porphyrias: current mechanistic, diagnostic, and therapeutic considerations." Semin Hematol **14**(2): 211-9.

Poh-Fitzpatrick, M. B. (1980). "A plasma porphyrin fluorescence marker for variegate porphyria." Arch Dermatol **116**(5): 543-7.

Prasad, A. R. and H. A. Dailey (1995). "Effect of cellular location on the function of ferrochelatase." J Biol Chem **270**(31): 18198-200.

Prasher, D. C., V. K. Eckenrode, et al. (1992). "Primary structure of the Aequorea victoria green-fluorescent protein." Gene **111**(2): 229-33.

Proulx, K. L. and H. A. Dailey (1992). "Characteristics of murine protoporphyrinogen oxidase." Protein Sci **1**(6): 801-9.

Proulx, K. L., S. I. Woodard, et al. (1993). "In situ conversion of coproporphyrinogen to heme by murine mitochondria: terminal steps of the heme biosynthetic pathway." Protein Sci **2**(7): 1092-8.

Puy, H., A. M. Robreau, et al. (1996). "Protoporphyrinogen oxidase: complete genomic sequence and polymorphisms in the human gene." Biochem Biophys Res Commun **226**(1): 226-30.

Rassow, J., F. U. Hartl, et al. (1990). "Polypeptides traverse the mitochondrial envelope in an extended state." FEBS Lett **275**(1-2): 190-4.

Rassow, J. and N. Pfanner (1991). "Mitochondrial preproteins en route from the outer membrane to the inner membrane are exposed to the intermembrane space." FEBS Lett **293**(1-2): 85-8.

Riddle, R. D., M. Yamamoto, et al. (1989). "Expression of delta-aminolevulinate synthase in avian cells: separate genes encode erythroid-specific and nonspecific isozymes." Proc Natl Acad Sci U S A **86**(3): 792-6.

Rimington, C. (1985). "A review of the enzymic errors in the various porphyrias." Scand J Clin Lab Invest **45**(4): 291-301.

Rimington, C. and R. V. Belcher (1967). "Separation of porphyrins on Sephadex dextran gels." J Chromatogr **28**(1): 112-7.

Rizzuto, R., M. Brini, et al. (1995). "Chimeric green fluorescent protein as a tool for visualizing subcellular organelles in living cells." Curr Biol **5**(6): 635-42.

Roberts, A. G. and G. H. Elder (1997). "Purification and properties of uroporphyrinogen decarboxylase from human erythrocytes." Methods Enzymol **281**: 349-55.

Roberts, A. G. and G. H. Elder (2001). "Alternative splicing and tissue-specific transcription of human and rodent ubiquitous 5-aminolevulinate synthase (ALAS1) genes." Biochim Biophys Acta **1518**(1-2): 95-105.

Roberts, A. G., G. H. Elder, et al. (1995a). "A mutation (G281E) of the human uroporphyrinogen decarboxylase gene causes both hepatoerythropoietic porphyria and overt familial porphyria cutanea tarda: biochemical and genetic studies on Spanish patients." J Invest Dermatol **104**(4): 500-2.

Roberts, A. G., G. H. Elder, et al. (1988). "Heterogeneity of familial porphyria cutanea tarda." J Med Genet **25**(10): 669-76.

Roberts, A. G., H. Puy, et al. (1998). "Molecular characterization of homozygous variegate porphyria." Hum Mol Genet **7**(12): 1921-5.

Roberts, A. G., S. D. Whatley, et al. (1996). "Identification of a mutation in the protoporphyrinogen oxidase gene in homozygous variegate porphyria" Hepatology. **23**: 309H.

Roberts, A. G., S. D. Whatley, et al. (1995b). "Partial characterization and assignment of the gene for protoporphyrinogen oxidase and variegate porphyria to human chromosome 1q23." Hum Mol Genet **4**(12): 2387-90.

Robinson, K. M. and B. D. Lemire (1996a). "Covalent attachment of FAD to the yeast succinate dehydrogenase flavoprotein requires import into mitochondria, presequence removal, and folding." J Biol Chem **271**(8): 4055-60.

Robinson, K. M. and B. D. Lemire (1996b). "A requirement for matrix processing peptidase but not for mitochondrial chaperonin in the covalent attachment of FAD to the yeast succinate dehydrogenase flavoprotein." J Biol Chem **271**(8): 4061-7.

Robreau-Fraolini, A. M., H. Puy, et al. (2000). "Porphobilinogen deaminase gene in African and Afro-Caribbean ethnic groups: mutations causing acute intermittent porphyria and specific intragenic polymorphisms [In Process Citation]." Hum Genet **107**(2): 150-9.

Roenigk, H. H., Jr. and M. E. Gottlob (1970). "Estrogen-induced porphyria cutanea tarda. Report of three cases." Arch Dermatol **102**(3): 260-6.

Roise, D. (1988). "Import of proteins into mitochondria." Prog Clin Biol Res **282**: 43-53.

Roise, D., S. J. Horvath, et al. (1986). "A chemically synthesized pre-sequence of an imported mitochondrial protein can form an amphiphilic helix and perturb natural and artificial phospholipid bilayers." Embo J **5**(6): 1327-34.

Roise, D. and M. Maduke (1994). "Import of a mitochondrial presequence into P. denitrificans. Insight into the evolution of protein transport." FEBS Lett **337**(1): 9-13.

Roise, D. and G. Schatz (1988). "Mitochondrial presequences." J Biol Chem **263**(10): 4509-11.

Roise, D., F. Theiler, et al. (1988). "Amphiphilicity is essential for mitochondrial presequence function." Embo J **7**(3): 649-53.

Romana, M., A. Dubart, et al. (1987a). "Structure of the gene for human uroporphyrinogen decarboxylase." Nucleic Acids Res **15**(18): 7343-56.

Romana, M., P. Le Boulch, et al. (1987b). "Rat uroporphyrinogen decarboxylase cDNA: nucleotide sequence and comparison to human uroporphyrinogen decarboxylase." Nucleic Acids Res **15**(17): 7211.

Romeo, G. and E. Y. Levin (1969). "Uroporphyrinogen 3 cosynthetase in human congenital erythropoietic porphyria." Proc Natl Acad Sci U S A **63**(3): 856-63.

Romeo, P. H., N. Raich, et al. (1986). "Molecular cloning and nucleotide sequence of a complete human uroporphyrinogen decarboxylase cDNA." J Biol Chem **261**(21): 9825-31.

Rosipal, R., J. Lamoril, et al. (1999). "Systematic analysis of coproporphyrinogen oxidase gene defects in hereditary coproporphyria and mutation update." Hum Mutat **13**(1): 44-53.

Rost, B. (1996). "PHD: predicting one-dimensional protein structure by profile-based neural networks." Methods Enzymol **266**: 525-39.

Rufenacht, U. B., L. Gouya, et al. (1998). "Systematic analysis of molecular defects in the ferrochelatase gene from patients with erythropoietic protoporphyria." Am J Hum Genet **62**(6): 1341-52.

Ryan, K. R., R. S. Leung, et al. (1998). "Characterization of the mitochondrial inner membrane translocase complex: the Tim23p hydrophobic domain interacts

with Tim17p but not with other Tim23p molecules." Mol Cell Biol **18**(1): 178-87.

Sadlon, T. J., T. Dell'Oso, et al. (1999). "Regulation of erythroid 5-aminolevulinate synthase expression during erythropoiesis." Int J Biochem Cell Biol **31**(10): 1153-67.

Saeki, K., H. Suzuki, et al. (2000). "Identification of mammalian TOM22 as a subunit of the preprotein translocase of the mitochondrial outer membrane." J Biol Chem **275**(41): 31996-2002.

Sancovich, H. A., A. M. Battle, et al. (1969). "Porphyrin biosynthesis. VI. Separation and purification of porphobilinogen deaminase and uroporphyrinogen isomerase from cow liver. Porphobilinogenase an allosteric enzyme." Biochim Biophys Acta **191**(1): 130-43.

Sarkany, R. P., G. J. Alexander, et al. (1994). "Recessive inheritance of erythropoietic protoporphyria with liver failure [see comments]." Lancet **343**(8910): 1394-6.

Sasarman, A., J. Letowski, et al. (1993). "Nucleotide sequence of the hemG gene involved in the protoporphyrinogen oxidase activity of Escherichia coli K12." Can J Microbiol **39**(12): 1155-61.

Sassa, S. (1998). "ALAD porphyria." Semin Liver Dis **18**(1): 95-101.

Schatz, G. (1997). "Just follow the acid chain." Nature **388**(6638): 121-2.

Scherer, P. E., U. C. Krieg, et al. (1990). "A precursor protein partly translocated into yeast mitochondria is bound to a 70 kd mitochondrial stress protein." Embo J **9**(13): 4315-22.

Schleiff, E. and H. McBride (2000). "The central matrix loop drives import of uncoupling protein 1 into mitochondria." J Cell Sci **113 (Pt 12)**: 2267-72.

Schleyer, M. and W. Neupert (1985). "Transport of proteins into mitochondria: translocational intermediates spanning contact sites between outer and inner membranes." Cell **43**(1): 339-50.

Schlossmann, J., K. Dietmeier, et al. (1994). "Specific recognition of mitochondrial preproteins by the cytosolic domain of the import receptor MOM72." J Biol Chem **269**(16): 11893-901.

Schneider, H., T. Sollner, et al. (1991). "Targeting of the master receptor MOM19 to mitochondria." Science **254**(5038): 1659-62.

Schneider-Yin, X., L. Gouya, et al. (2000). "New insights into the pathogenesis of erythropoietic protoporphyria and their impact on patient care [In Process Citation]." Eur J Pediatr **159**(10): 719-25.

Schneider-Yin, X., B. W. Schafer, et al. (1994). "Molecular defects in erythropoietic protoporphyria with terminal liver failure." Hum Genet **93**(6): 711-3.

Schneider-Yin, X., B. W. Schafer, et al. (1995). "Human ferrochelatase: a novel mutation in patients with erythropoietic protoporphyria and an isoform caused by alternative splicing." Hum Genet **95**(4): 391-6.

Scholnick, P. L., L. E. Hammaker, et al. (1972). "Soluble -aminolevulinic acid synthetase of rat liver. II. Studies related to the mechanism of enzyme action and hemin inhibition." J Biol Chem **247**(13): 4132-7.

Schubert, H. L., E. Raux, et al. (2002). "Structural diversity in metal ion chelation and the structure of uroporphyrinogen III synthase." Biochem Soc Trans **30**(4): 595-600.

Scobie, G. A., D. H. Llewellyn, et al. (1990). "Acute intermittent porphyria caused by a C----T mutation that produces a stop codon in the porphobilinogen deaminase gene." Hum Genet **85**(6): 631-4.

Scott, A. I., C. A. Townsend, et al. (1972). "Biosynthesis of corrinoids. Uroporphyrinogen 3 as a precrusor of vitamin B 12." J Am Chem Soc **94**(23): 8269-71.

Segui-Real, B., G. Kispal, et al. (1993). "Functional independence of the protein translocation machineries in mitochondrial outer and inner membranes:

passage of preproteins through the intermembrane space." Embo J **12**(5): 2211-8.

Segui-Real, B., R. A. Stuart, et al. (1992). "Transport of proteins into the various subcompartments of mitochondria." FEBS Lett **313**(1): 2-7.

Seki, Y., S. Kawanishi, et al. (1986). "Uroporphyrinogen decarboxylase purification from chicken erythrocytes." Methods Enzymol **123**: 415-21.

Senior, N. M., K. Brocklehurst, et al. (1996). "Comparative studies on the 5-aminolaevulinic acid dehydratases from Pisum sativum, Escherichia coli and Saccharomyces cerevisiae." Biochem J **320 (Pt 2)**: 401-12.

Senior, N. M., G. Siligardi, et al. (1997). "Structural studies on 5-aminolaevulinic acid dehydratase from Saccharomyces cerevisiae (yeast)." Biochem Soc Trans **25**(1): 78S.

Sheffield, W. P., G. C. Shore, et al. (1990). "Mitochondrial precursor protein. Effects of 70-kilodalton heat shock protein on polypeptide folding, aggregation, and import competence." J Biol Chem **265**(19): 11069-76.

Shimomura, O. and A. Shimomura (1982). "EDTA-binding and acylation of the Ca2+-sensitive photoprotein aequorin." FEBS Lett **138**(2): 201-4.

Shoolingin-Jordan, P. M. (1998). "Structure and mechanism of enzymes involved in the assembly of the tetrapyrrole macrocycle." Biochem Soc Trans **26**(3): 326-36.

Shoolingin-Jordan, P. M. (2003). The biosynthesis of coproporphyrinogen III. The Iron and Cobalt Pigments : Biosynthesis, Structure and degradation. K. M. Kadish, K. M. Smith and R. Guilard. California, U.S.A., Academic Press. **12:** 33-74.

Shoolingin-Jordan, P. M., S. Al-Daihan, et al. (2003a). "5-Aminolevulinic acid synthase: mechanism, mutations and medicine." Biochim Biophys Acta **1647**(1-2): 361-6.

Shoolingin-Jordan, P. M., A. Al-Dbass, et al. (2003b). "Human porphobilinogen deaminase mutations in the investigation of the mechanism of dipyrromethane cofactor assembly and tetrapyrrole formation." Biochem Soc Trans **31**(Pt 3): 731-5.

Shoolingin-Jordan, P. M., M. J. Warren, et al. (1996). "Discovery that the assembly of the dipyrromethane cofactor of porphobilinogen deaminase holoenzyme proceeds initially by the reaction of preuroporphyrinogen with the apoenzyme." Biochem J **316**(Pt 2): 373-6.

Shoolingin-Jordan, P. M., M. J. Warren, et al. (1997). "Dipyrromethane cofactor assembly of porphobilinogen deaminase: formation of apoenzyme and preparation of holoenzyme." Methods Enzymol **281**: 317-27.

Siemering, K. R., R. Golbik, et al. (1996). "Mutations that suppress the thermosensitivity of green fluorescent protein." Curr Biol **6**(12): 1653-63.

Siepker, L. J., M. Ford, et al. (1987). "Purification of bovine protoporphyrinogen oxidase: immunological cross-reactivity and structural relationship to ferrochelatase." Biochim Biophys Acta **913**(3): 349-58.

Sirrenberg, C., M. F. Bauer, et al. (1996). "Import of carrier proteins into the mitochondrial inner membrane mediated by Tim22." Nature **384**(6609): 582-5.

Smith, K. M. (1975). General features of the structure and chemistry of porphyrin compounds. Porphyrins and Metalloporphyrins. K. M. Smith. Amsterdam, Elsevier: 3-28.

Smith, S. J. and T. M. Cox (1997). "Translational control of erythroid delta-aminolevulinate synthase in immature human erythroid cells by heme." Cell Mol Biol (Noisy-le-grand) **43**(1): 103-14.

Smythe, E. and D. C. Williams (1988). "Rat liver uroporphyrinogen III synthase has similar properties to the enzyme from Euglena gracilis, including absence of a requirement for a reversibly bound cofactor for activity." Biochem J **253**(1): 275-9.

Smythe, E. and D. C. Williams (1988). "Rat liver uroporphyrinogen III synthase has similar properties to the enzyme from Euglena gracilis, including absence of a requirement for a reversibly bound cofactor for activity." Biochem J **253**(1): 275-9.

Solis, C., G. I. Aizencang, et al. (2001). "Uroporphyrinogen III synthase erythroid promoter mutations in adjacent GATA1 and CP2 elements cause congenital erythropoietic porphyria." J Clin Invest **107**(6): 753-62.

Soret, J. L. (1883). "Récherches sur l'absorption des rayons ultra-violet par diverses substances." Arch Sci Phys et Nat **10**: 430-485.

Srivastava, G., I. A. Borthwick, et al. (1983). "Evidence for a cytosolic precursor of chick embryo liver mitochondrial delta-aminolevulinate synthase." Biochem Biophys Res Commun **110**(1): 23-31.

Srivastava, G., I. A. Borthwick, et al. (1988). "Regulation of 5-aminolevulinate synthase mRNA in different rat tissues." J Biol Chem **263**(11): 5202-9.

Stamford, N. P., A. Capretta, et al. (1995). "Expression, purification and characterisation of the product from the Bacillus subtilis hemD gene, uroporphyrinogen III synthase." Eur J Biochem **231**(1): 236-41.

Stan, T., J. Brix, et al. (2003). "Mitochondrial protein import: recognition of internal import signals of BCS1 by the TOM complex." Mol Cell Biol **23**(7): 2239-50.

Straka, J. G. and J. P. Kushner (1983). "Purification and characterization of bovine hepatic uroporphyrinogen decarboxylase." Biochemistry **22**(20): 4664-72.

Surinya, K. H., T. C. Cox, et al. (1997). "Transcriptional regulation of the human erythroid 5-aminolevulinate synthase gene. Identification of promoter elements and role of regulatory proteins." J Biol Chem **272**(42): 26585-94.

Surinya, K. H., T. C. Cox, et al. (1998). "Identification and characterization of a conserved erythroid-specific enhancer located in intron 8 of the human 5-aminolevulinate synthase 2 gene." J Biol Chem **273**(27): 16798-809.

Sutherland, G. R., E. Baker, et al. (1988). "5-Aminolevulinate synthase is at 3p21 and thus not the primary defect in X-linked sideroblastic anemia." Am J Hum Genet **43**(3): 331-5.

Taketani, S., J. Inazawa, et al. (1995a). "The human protoporphyrinogen oxidase gene (PPOX): organization and location to chromosome 1." Genomics **29**(3): 698-703.

Taketani, S., J. Inazawa, et al. (1992). "Structure of the human ferrochelatase gene. Exon/intron gene organization and location of the gene to chromosome 18." Eur J Biochem **205**(1): 217-22.

Taketani, S., H. Kohno, et al. (1994). "Molecular cloning, sequencing and expression of cDNA encoding human coproporphyrinogen oxidase." Biochim Biophys Acta **1183**(3): 547-9.

Taketani, S., Y. Nakahashi, et al. (1990). "Molecular cloning, sequencing, and expression of mouse ferrochelatase." J Biol Chem **265**(32): 19377-80.

Taketani, S. and R. Tokunaga (1981). "Rat liver ferrochelatase. Purification, properties, and stimulation by fatty acids." J Biol Chem **256**(24): 12748-53.

Taketani, S. and R. Tokunaga (1982). "Purification and substrate specificity of bovine liver-ferrochelatase." Eur J Biochem **127**(3): 443-7.

Taketani, S., T. Yoshinaga, et al. (1995b). "Induction of terminal enzymes for heme biosynthesis during differentiation of mouse erythroleukemia cells." Eur J Biochem **230**(2): 760-5.

Tan, D., T. Harrison, et al. (1998). "Role of arginine 439 in substrate binding of 5-aminolevulinate synthase." Biochemistry **37**(6): 1478-84.

Tanudji, M., S. Sjoling, et al. (1999). "Signals required for the import and processing of the alternative oxidase into mitochondria." J Biol Chem **274**(3): 1286-93.

Tarasova, N. I., R. H. Stauber, et al. (1997). "Visualization of G protein-coupled receptor trafficking with the aid of the green fluorescent protein. Endocytosis

and recycling of cholecystokinin receptor type A." J Biol Chem **272**(23): 14817-24.

Thunell, S., L. Holmberg, et al. (1987). "Aminolaevulinate dehydratase porphyria in infancy. A clinical and biochemical study." J Clin Chem Clin Biochem **25**(1): 5-14.

Tian, H., L. Yu, et al. (1998). "Flexibility of the neck region of the rieske iron-sulfur protein is functionally important in the cytochrome bc1 complex." J Biol Chem **273**(43): 27953-9.

Tidman, M. J., E. M. Higgins, et al. (1989). "Variegate porphyria associated with hepatocellular carcinoma." Br J Dermatol **121**(4): 503-5.

Todd, D. J., A. E. Hughes, et al. (1993). "Identification of a single base pair deletion (40 del G) in exon 1 of the ferrochelatase gene in patients with erythropoietic protoporphyria." Hum Mol Genet **2**(9): 1495-6.

Toney, M. D., E. Hohenester, et al. (1995). "Structural and mechanistic analysis of two refined crystal structures of the pyridoxal phosphate-dependent enzyme dialkylglycine decarboxylase." J Mol Biol **245**(2): 151-79.

Troup, B., M. Jahn, et al. (1994). "Isolation of the hemF operon containing the gene for the Escherichia coli aerobic coproporphyrinogen III oxidase by in vivo complementation of a yeast HEM13 mutant." J Bacteriol **176**(3): 673-80.

Tsai, S. F., D. F. Bishop, et al. (1987). "Coupled-enzyme and direct assays for uroporphyrinogen III synthase activity in human erythrocytes and cultured lymphoblasts. Enzymatic diagnosis of heterozygotes and homozygotes with congenital erythropoietic porphyria." Anal Biochem **166**(1): 120-33.

Tsai, S. F., D. F. Bishop, et al. (1988). "Human uroporphyrinogen III synthase: molecular cloning, nucleotide sequence, and expression of a full-length cDNA." Proc Natl Acad Sci U S A **85**(19): 7049-53.

Tsukamoto, I., T. Yoshinaga, et al. (1980). "Zinc and cysteine residues in the active site of bovine liver delta-aminolevulinic acid dehydratase." Int J Biochem **12**(5-6): 751-6.

Tugores, A., S. T. Magness, et al. (1994). "A single promoter directs both housekeeping and erythroid preferential expression of the human ferrochelatase gene." J Biol Chem **269**(49): 30789-97.

Tzschoppe, K., S. D. Kohlwein, et al. (2000). "Yeast translational activator Cbs2p: mitochondrial targeting and effect of overexpression." Biol Chem **381**(12): 1175-83.

Van den Bergh, A. A. H. and W. Grotepass (1937). "Ein bemerkenswerter Fall von Porphyrie." Wien Klin Wochenschr. **50**: 830-1.

Venerando, R., G. Miotto, et al. (1996). "Mitochondrial alterations induced by aspirin in rat hepatocytes expressing mitochondrially targeted green fluorescent protein (mtGFP)." FEBS Lett **382**(3): 256-60.

Viljoen, D. J., R. Cummins, et al. (1983). "Protoporphyrinogen oxidase and ferrochelatase in porphyria variegata." Eur J Clin Invest **13**(4): 283-7.

Volland, C. and D. Urban-Grimal (1988). "The presequence of yeast 5-aminolevulinate synthase is not required for targeting to mitochondria." J Biol Chem **263**(17): 8294-9.

von Ahsen, O., W. Voos, et al. (1995). "The mitochondrial protein import machinery. Role of ATP in dissociation of the Hsp70.Mim44 complex." J Biol Chem **270**(50): 29848-53.

von Heijne, G. (1985). "Signal sequences. The limits of variation." J Mol Biol **184**(1): 99-105.

von Heijne, G. (1986). "Mitochondrial targeting sequences may form amphiphilic helices." Embo J **5**(6): 1335-42.

von Heijne, G. (1989). "The structure of signal peptides from bacterial lipoproteins." Protein Eng **2**(7): 531-4.

von und zu Fraunberg, M. and R. Kauppinen (2000). "Diagnosis of variegate porphyria--hard to get?" Scand J Clin Lab Invest **60**(7): 605-10.

Von Und Zu Fraunberg, M. and R. Kauppinen (2003). Mitochondrial targeting mechanisms of protoporphyrinogen oxidase : identification and characterization of internal targeting sequences. Porphyrins and Porphyrias 2003, Prague, Czech Republic.

Von Und Zu Fraunberg, M., T. Nyronen, et al. (2003). "Mitochondrial targeting of normal and mutant protoporphyrinogen oxidase." J Biol Chem **278**(15): 13376-81.

von und zu Fraunberg, M., R. Tenhunen, et al. (2001). "Expression and characterization of six mutations in the protoporphyrinogen oxidase gene among Finnish variegate porphyria patients." Mol Med **7**(5): 320-8.

Voos, W., B. D. Gambill, et al. (1993). "Presequence and mature part of preproteins strongly influence the dependence of mitochondrial protein import on heat shock protein 70 in the matrix." J Cell Biol **123**(1): 119-26.

Waldenstrom, J. (1957). "The porphyrias as inborn errors of metabolism." Am. J. Med. **22**: 758-773.

Walter, P., R. Gilmore, et al. (1984). "Protein translocation across the endoplasmic reticulum." Cell **38**(1): 5-8.

Wang, K.F., T.A. Dailey, et al. (2001). "Expression and characterization of the terminal heme synthetic enzymes from the hyperthermophile *Aquifex aeolicus*. FEMS Microbiol Lett. **202**(1):115-9.

Wang, X., M. Poh-Fitzpatrick, et al. (1994). "Screening for ferrochelatase mutations: molecular heterogeneity of erythropoietic protoporphyria." Biochim Biophys Acta **1225**(2): 187-90.

Warnich, L., M. J. Kotze, et al. (1996). "Identification of three mutations and associated haplotypes in the protoporphyrinogen oxidase gene in South African families with variegate porphyria." Hum Mol Genet **5**(7): 981-4.

Warren, M. J. and P. M. Jordan (1988). "Investigation into the nature of substrate binding to the dipyrromethane cofactor of Escherichia coli porphobilinogen deaminase." Biochemistry **27**(25): 9020-30.

Watanabe, N., F. S. Che, et al. (2001). "Dual targeting of spinach protoporphyrinogen oxidase II to mitochondria and chloroplasts by alternative use of two in-frame initiation codons." J Biol Chem **276**(23): 20474-81.

Watanabe, N., F. S. Che, et al. (2000). "Purification and properties of protoporphyrinogen oxidase from spinach chloroplasts." Plant Cell Physiol **41**(7): 889-92.

Watanabe, N., N. Hayashi, et al. (1983). "delta-Aminolevulinate synthase isozymes in the liver and erythroid cells of chicken." Biochem Biophys Res Commun **113**(2): 377-83.

Watanabe, N., N. Hayashi, et al. (1984). "Relation of the extra-sequence of the precursor form of chicken liver delta-aminolevulinate synthase to its quaternary structure and catalytic properties." Arch Biochem Biophys **232**(1): 118-26.

Weiss, G., T. Houston, et al. (1997). "Regulation of cellular iron metabolism by erythropoietin: activation of iron-regulatory protein and upregulation of transferrin receptor expression in erythroid cells." Blood **89**(2): 680-7.

Westermann, B., B. Gaume, et al. (1996). "Role of the mitochondrial DnaJ homolog Mdj1p as a chaperone for mitochondrially synthesized and imported proteins." Mol Cell Biol **16**(12): 7063-71.

Westermann, B. and W. Neupert (1997). "Mdj2p, a novel DnaJ homolog in the mitochondrial inner membrane of the yeast Saccharomyces cerevisiae." J Mol Biol **272**(4): 477-83.

Wetmur, J. G., D. F. Bishop, et al. (1986a). "Human delta-aminolevulinate dehydratase: nucleotide sequence of a full-length cDNA clone." Proc Natl Acad Sci U S A **83**(20): 7703-7.

Wetmur, J. G., D. F. Bishop, et al. (1986b). "Molecular cloning of a cDNA for human delta-aminolevulinate dehydratase." Gene **43**(1-2): 123-30.

Whatley, S. D., H. Puy, et al. (1999a). "Variegate Porphyria in Western Europe: Identification of PPOX Gene Mutations in 104 Families, Extent of Allelic Heterogeneity, and Absence of Correlation between Phenotype and Type of Mutation." Am J Hum Genet **65**(4): 984-994.

Whatley, S. D., H. Puy, et al. (1999b). "Variegate porphyria in Western Europe: identification of PPOX gene mutations in 104 families, extent of allelic heterogeneity, and absence of correlation between phenotype and type of mutation." Am J Hum Genet **65**(4): 984-94.

Whatley, S. D., A. G. Roberts, et al. (1995). "De-novo mutation and sporadic presentation of acute intermittent porphyria." Lancet **346**(8981): 1007-8.

Whitby, F. G., J. D. Phillips, et al. (1998). "Crystal structure of human uroporphyrinogen decarboxylase." Embo J **17**(9): 2463-71.

Williams, L. R., S. R. Ellis, et al. (2000). "Splicing before import - an intein in a mitochondrially targeted preprotein folds and is catalytically active in the cytoplasm in vivo." FEBS Lett **476**(3): 301-5.

Wiman, A., P. Harper, et al. (2003). "Nine novel mutations in the protoporphyrinogen oxidase gene in Swedish families with variegate porphyria." Clin Genet **64**(2): 122-30.

Winderbank, A. J. and H. I. Bonkovsky (1992). Porphyric neuropathy. Philadelphia, Saunders.

Wolff, C., F. Piderit, et al. (1991). "Deficiency of porphobilinogen synthase associated with acute crisis. Diagnosis of the first two cases in Chile by laboratory methods." Eur J Clin Chem Clin Biochem **29**(5): 313-5.

Wu, C., W. Xu, et al. (1996). "Mouse uroporphyrinogen decarboxylase: cDNA cloning, expression, and mapping." Mamm Genome **7**(5): 349-52.

Wu, C. K., H. A. Dailey, et al. (2001). "The 2.0 A structure of human ferrochelatase, the terminal enzyme of heme biosynthesis." Nat Struct Biol **8**(2): 156-60.

Wu, W. H., D. Shemin, et al. (1974). "The quaternary structure of delta-aminolevulinic acid dehydratase from bovine liver." Proc Natl Acad Sci U S A **71**(5): 1767-70.

Xu, K. and T. Elliott (1993). "An oxygen-dependent coproporphyrinogen oxidase encoded by the hemF gene of Salmonella typhimurium." J Bacteriol **175**(16): 4990-9.

Xu, W., K. H. Astrin, et al. (1996). "Molecular basis of congenital erythropoietic porphyria: mutations in the human uroporphyrinogen III synthase gene." Hum Mutat **7**(3): 187-92.

Xu, W., C. A. Kozak, et al. (1995). "Uroporphyrinogen-III synthase: molecular cloning, nucleotide sequence, expression of a mouse full-length cDNA, and its localization on mouse chromosome 7." Genomics **26**(3): 556-62.

Yamamoto, M., N. Hayashi, et al. (1982). "Evidence for the transcriptional inhibition by heme of the synthesis of delta-aminolevulinate synthase in rat liver." Biochem Biophys Res Commun **105**(3): 985-90.

Yamauchi, K., N. Hayashi, et al. (1980). "Translocation of delta-aminolevulinate synthase from the cytosol to the mitochondria and its regulation by hemin in the rat liver." J Biol Chem **255**(4): 1746-51.

Yang, T. T., L. Cheng, et al. (1996). "Optimized codon usage and chromophore mutations provide enhanced sensitivity with the green fluorescent protein." Nucleic Acids Res **24**(22): 4592-3.

Yeung Laiwah, A. C., M. R. Moore, et al. (1987). "Pathogenesis of acute porphyria." Q J Med **63**(241): 377-92.

Yomogida, K., M. Yamamoto, et al. (1993). "Structure and expression of the gene encoding rat nonspecific form delta-aminolevulinate synthase." J Biochem (Tokyo) **113**(3): 364-71.

Yoshinaga, T. and S. Sano (1980). "Coproporphyrinogen oxidase. II. Reaction mechanism and role of tyrosine residues on the activity." J Biol Chem **255**(10): 4727-31.

Zagorec, M., J. M. Buhler, et al. (1988). "Isolation, sequence, and regulation by oxygen of the yeast HEM13 gene coding for coproporphyrinogen oxidase." J Biol Chem **263**(20): 9718-24.

Zara, V., F. Palmieri, et al. (1992). "The cleavable presequence is not essential for import and assembly of the phosphate carrier of mammalian mitochondria but enhances the specificity and efficiency of import." J Biol Chem **267**(17): 12077-81.

Zimmermann, T., J. Rietdorf, et al. (2003). "Spectral imaging and its applications in live cell microscopy." FEBS Lett **546**(1): 87-92.

Zolotukhin, S., M. Potter, et al. (1996). "A "humanized" green fluorescent protein cDNA adapted for high-level expression in mammalian cells." J Virol **70**(7): 4646-54.

APPENDICES : EXPERIMENTAL METHODOLOGY AND MATERIALS

APPENDICES : EXPERIMENTAL METHODOLOGY AND MATERIALS

1.ENGINEERING OF VP-CAUSING MUTANT PPOXs

1.1 Optimisation of PCR annealing temperatures

Equipment

Robocycler Gradient 40 Temperature Cycler (Stratagene Cloning Systems, California, USA)
Hybaid Omnigene Thermal cycler (Hybaid Ltd., Middlesex, England)
Tabletop Centrifuge (Denver Instruments, Colorado, USA)
GeneQuant Spectrophotometer (Pharmacia Biotech (Biochrom) Ltd., Cambridge, England)
Tabletop Mistral Vortex Mixer (Laboratory & Scientific, Cape Town, South Africa)
Microcentrifuge tubes – 1.5ml (Promega Corporation, WI, USA)
Microcentrifuge tubes – 0.6ml (Promega Corporation, WI, USA)

Reagents

Magnesium-free, Thermophilic DNA Polymerase 10X Buffer (Promega Corporation, WI, USA)
Taq DNA Polymerase 10X Buffer containing 15mM $MgCl_2$ (Promega Corporation, WI, USA)
Taq DNA Polymerase (5U/µl, Promega Corporation, WI, USA)
Deoxynucleotide Triphosphates (dNTPs) (Promega Corporation, WI, USA) (see Appendix 13)
Appropriate oligonucleotide sets, (Integrated DNA Technologies Inc., Coralville, IA, USA)
Mineral Oil (Promega Corporation, WI, USA)
Sterile deionized water

Method

For all PCR-based reactions, the oligonucleotide sets (ie. forward and reverse) were optimised by gradient PCR on the Robocycler thermal cycler. The gradient block allowed simultaneous evaluation of up to 8 different annealing temperatures for cycling reactions.

Table 1. Pre-programmed temperature ranges for the gradient block on the Robocycler thermal cycler

Temperature Range (°C)	Temperature difference/row
37-44	1°C
42-56	2°C
51-65	2°C
60-74	2°C
Custom range	-

The following 1 x reaction was set up on ice :

Magnesium-free, Thermophilic DNA Polymerase 10X buffer	5µl
10X Buffer containing 25mM $MgCl_2$	5µl
dNTPs (2.5mM)	2µl
Appropriate forward oligonucleotide, 25µM	1µl
Appropriate reverse oligonucleotide, 25µM	1µl
Taq DNA Polymerase (5U/µl)	2µl
Sterile deionised water to a volume of	**45µl**

These volumes were scaled up to make sufficient mixture for the number of PCRs required. In addition, a blank (ie no DNA) was added. The PCR was performed in 0.6ml eppendorf tubes. Approximately 250ng of cDNA was added and the mixture vortexed briefly. The contents were centrifuged in a tabletop centrifuge and the mixture overlayed with 1-2 drops of mineral oil. The samples were run on a Robocycler thermal cycler using the following programme (table 2) with a specific annealing range (see table 1) :

Table 2. PCR profile for optimisation of PCR annealing temperatures

	Temperature (°C)	Time (s)	Cycle no.
Initial Denaturation	94	120	1
Denaturation	94	60	
Annealing	relevant gradient temp. range	30	32
Extension	72	60	
Final Extension	72	300	1

The PCR products were visualised on an ethidium bromide-stained, 6% non-denaturing polyacrylamide gel (see 5.0).

1.2 Denaturation of double-stranded DNA (dsDNA)

Equipment

Tabletop Centrifuge (Denver Instruments, Colorado, USA)
Refrigerated microcentrifuge (Sorvall Instruments, DuPont, USA)
GeneQuant Spectrophotometer (Pharmacia Biotech (Biochrom) Ltd., Cambridge, England)

Reagents/Materials

DNA Template
0.8% agarose gel (FMC Bioproducts, Maine, USA) (see 4.0)
2M Ammonium acetate (pH 4.6) (see Appendix 13)
2M NaOH, 2mM EDTA (see Appendix 13)
Ethanol (70% and 100%)
Sterile deionized water

Method

Approximately 2μg of dsDNA template (pTrcHis-PPOX) was added to 2μl of 2M NaOH, 2mM EDTA in a 20μl final volume and allowed to denature for 5 min at room temperature. The mixture was neutralised with 2μl of 2M ammonium acetate (pH 4.6), 75μl of 100% ethanol added and the DNA allowed to precipitate at -70°C overnight. The precipitated DNA was centrifuged for 15 min at 4°C in a refrigerated microcentrifuge. The pellet was drained and washed with 200μl of 70% ethanol and

re-centrifuged. The pellet was air-dried at room temperature for 20 min, resuspended in 50µl of sterile deionised water, and quantified using a GeneQuant spectrophotometer. Ten µl of the sample was run on a 0.8% agarose gel (see section 4) in order to check the integrity of the DNA.

1.3 Mutagenesis Reaction

Equipment

Hybaid Omnigene Thermal cycler (Hybaid Ltd., Middlesex, England)
Water bath (Memmert GmbH+Co.KG, Schwabach, Germany)
Heating block (Techne Dri-Block, Cambridge, England)
Tabletop Centrifuge (Denver Instruments, Colorado, USA)
Refrigerated microcentrifuge (Sorvall Instruments, DuPont, USA)
Orbital shake incubator (Yih der LM-510, Taiwan, Japan)
GeneQuant Spectrophotometer (Pharmacia Biotech (Biochrom) Ltd., Cambridge, England)

Reagents/Materials

GeneEditor *in vitro* Site-Directed Mutagenesis System (Promega, Madison, WI, USA)
Denatured DNA Template (see Appendix 1.2)
Mutagenic oligonucleotides, 5'-phosphorylated (Integrated DNA Technologies, Inc, Iowa, USA)
Sterile 17x100mm polypropylene tubes (Laboratory and Scientific Equipment, SA)
0.8% agarose gel (FMC Bioproducts, Maine, USA)
Sterile deionized water

Method

Table 3. Phosphorylated mutagenic oligonucleotides used in the mutagenesis reactions (the mutated base is underlined and in bold) :

Mutant	Oligonucleotide sequence	Oligo. length	Optimised Annealing Temp. (°C)
H20P	5'-CCGGCTCAGG**G**GGTAACTGGC-3'	21-mer	53
R59W	5'-CTTGGACCT**T**GGGGAATTAG-3'	20-mer	57

The following protocol was used for both mutagenesis reactions :

Template denatured DNA	10µl (0.05pmol)
Appropriate Selection Oligonucleotide (2.9ng/µl)	1µl (0.25pmol)
Phosphorylated Mutagenic Oligonucleotide (see table above)	2µl (1.25pmol)
Annealing 10X Buffer	2µl
Sterile deionized water to a final volume of	**20µl**

The reaction mixture was placed in a thermal cycler at the optimal annealing temperature (see table 2) for 5 min and then the temperature reduced at 1.5°C per min until 37°C. The sample was briefly spun in a microcentrifuge. The following kit components were added :

Sterile deionized water	5µl
Synthesis 10X Buffer	3µl
T4 DNA Polymerase	1µl (10U)
T4 DNA Ligase	1µl (3U)
Final volume	**30µl**

The reaction was incubated on a heating block at 37°C for exactly 90 min to allow mutant strand synthesis and ligation.

1.4 Transformation of BMH 71-18 *mut*S Competent Cells

Equipment

Water bath (Memmert GmbH+Co.KG, Schwabach, Germany)
Orbital shake incubator (Yih der LM-510, Taiwan, Japan)

Reagents/Materials

Supercompetent sterile BMH 71-18 mutS cells (Promega, Madison, WI, USA)
GeneEditor Mutagenesis Kit Antibiotic Selection Mix (Promega, Madison, WI, USA)
Sterile 17x100mm polypropylene tubes (Laboratory and Scientific Equipment, SA)
Luria Broth (LB) Medium (see Appendix 13)
LB plates containing 125µg/ml ampicillin

Method

Sterile 17x100mm polypropylene tubes were pre-chilled on ice. Frozen supercompetent BMH 71-18 *mut*S cells were removed from -70°C and placed on ice for 5 min to thaw. One hundred µl of the thawed competent cells were added to the pre-chilled culture tubes, followed by 1.5µl of the mutagenesis reaction, with moving the pipette tip through the cells while dispensing. The tube was flicked several times and immediately placed on ice for 10 min. The cells were heat-shocked for 50s in a water-bath at exactly 42°C without shaking. The tubes were transferred to ice for 2 min, and 900µl of room temperature LB broth without antibiotic, added. Incubation at 37°C for 1h in an orbital shaker with shaking (225rpm), followed. Thereafter the culture was added to 4ml of LB containing 50µl of the GeneEditor Antibiotic Selection Mix, and incubated with shaking overnight at 37°C.

1.5 Transformation of JM109 Competent Cells with Plasmid DNA

Equipment

Water bath (Memmert GmbH+Co.KG, Schwabach, Germany)
Orbital shake incubator (Yih der LM-510, Taiwan, Japan)

Reagents/Materials

Supercompetent sterile JM109 cells (Promega, Madison, WI, USA)
Sterile 17x100mm polypropylene tubes (Laboratory and Scientific Equipment, SA)
LB plates containing 125µg/ml ampicillin
SOC Medium (see Appendix 13)

Method

Sterile 17x100mm polypropylene tubes were pre-chilled on ice. Frozen supercompetent cells were removed from -70°C and placed on ice for 5 min to thaw. One hundred µl of thawed competent cells were added to the pre-chilled culture tubes followed by 10ng pure plasmid DNA (ex mutS cells, see 1.4) with moving of the pipette tip through the cells while dispensing. The tube was flicked several times and immediately placed on ice for 30 min. The cells were heat-shocked for 50s in a water-bath at exactly 42°C without shaking. The tubes were transferred to ice for 2 min and 900µl of room temperature SOC medium (appendix 13) without antibiotic,

added. The tubes were incubated at 37°C for 1h in an orbital shaker with shaking (225rpm). Seventy µl of the culture was spread onto an LB plate containing 125µg/ml ampicillin using a sterile glass L-shaped rod. The plates were dried upright in an incubator at 37°C for 20 min, inverted and incubated at 37°C overnight to obtain isolated colonies.

1.6 Confirmation of Mutants :

1.6.1 Rapid Screening of Bacterial Colonies

Equipment

Horizontal mini-gel system (Mgu-202T), (CBS Scientific Company Inc., Del Mar, USA)
Electrophoresis Power Supply (EPS-250 Series II), (CBS Scientific Company Inc., Del Mar, USA)
Electronic UV Transilluminator (Ultralum, Whitehead Scientific (Pty) Ltd, SA)
UV Gel-doc Photographic system (UVItec, Cambridge, UK)

Reagents

SeaKem LE Agarose (FMC Bioproducts, Rockland, Maine, U.S.A.)
Ethidium Bromide (Roche Diagnostics (Pty) Ltd, Randburg, SA)
Agarose sample-loading dye (Appendix 13)
Protoplasting buffer (Appendix 13)
1 x Tris-Borate-SDS buffer (Appendix 13)
Lysis buffer (Appendix 13)

Method

The method used was a modification of that of Sekar (1987). Ten to15 colonies from an overnight incubation, were randomly chosen and transferred to a reference master plate. The master plate was incubated at 37°C overnight. While transferring to the master plate, a small amount (~10% of the bacterial colony ie. ±1mm in diameter) of the randomly selected transformants were individually resuspended by vigorous mixing into 5µl each of the protoplasting buffer (see Appendix 13) and left at room

temperature for 30 min. A 0.8% agarose gel (Appendix 13) was prepared in Tris-Borate-SDS buffer and each of the gel slots preloaded with 2µl lysis buffer (see Appendix 13). Protoplast suspension of the individual transformant colonies were then loaded into the sample wells underneath the lysis solution. Electrophoresis was conducted in Tris-Borate-SDS buffer initially at 30V for 15 min and for an additional 2-2.5 hours at 120V. The gel was viewed and photographed under UV illumination.

1.6.2 PCR of the mutated cDNA fragment

Equipment

Hybaid Omnigene Thermal cycler (Hybaid Ltd., Middlesex, England)
Tabletop Centrifuge (Denver Instruments, Colorado, USA)
GeneQuant Spectrophotometer (Pharmacia Biotech (Biochrom) Ltd., Cambridge, England)
Tabletop Mistral Vortex Mixer (Laboratory & Scientific, Cape Town, South Africa)
Microcentrifuge tubes – 1.5ml (Promega Corporation, WI, USA)
Microcentrifuge tubes – 0.6ml (Promega Corporation, WI, USA)

Reagents

Magnesium-free, Thermophilic DNA Polymerase 10X Buffer (Promega Corporation, WI, USA)
Taq DNA Polymerase 10X Buffer containing 15mM $MgCl_2$ (Promega Corporation, WI, USA)
Taq DNA Polymerase (5U/µl, Promega Corporation, WI, USA)
Sterile deionized water
Deoxynucleotide Triphosphates (dNTPs) (Promega Corporation, WI, USA) (see Appendix 13)
Fragment-specific oligonucleotide sets, (see table 4), (Integrated DNA Technologies Inc., Coralville, IA, USA)
Mineral Oil (Promega Corporation, WI, USA)

Method

Oligonucleotide sets were designed using the Primer Designer for Windows Software package (Soft Packaging V.2, Scientific and Education Software). The following table contains the oligonucleotide sets used to PCR all 4 human PPOX cDNA fragments :

Table 4. Oligonucleotides used to PCR the complete PPOX gene and the associated fragment sizes

Fragment Number	Oligonucleotide Sequences (5'-3')	Fragment Size (bp)
1	PF1 = CATCATGGTATGGCTAGTCC PR1 = AGACTGTCCATGGCTAGAGA	533
2	PF2 = CTGCATGCCCTACCCACTG PR2 = TTCAAGGCCTGAGGCAACA	411
3	PF3 = ACTTCGTGGAGGTCTAGAGA PR3 =CCGTCCTGCTCAGGGAAAGCAAC	390
4	PF4 = GTGCCATCTTCAGAAGATCC PR4 = TCAGCTGTTAGGTTCTGTGC	432

The following 1 x reaction was set up on ice :

Magnesium-free, Thermophilic DNA Polymerase 10X buffer	5µl
10X Buffer containing 25mM $MgCl_2$	5µl
dNTPs (2.5mM)	2µl
Appropriate forward oligonucleotide (25µM)	1µl
Appropriate reverse oligonucleotide (25µM)	1µl
Taq DNA Polymerase (5U/µl)	2µl
Sterile deionised water to a volume of	**45µl**

These volumes were scaled up to allow for sufficient volume for the number of tubes required, including a blank (ie. no DNA). Approximately 250ng of cDNA was added and the mixture vortexed briefly. The contents were spun to the bottom of a 0.6ml microcentrifuge tube using a tabletop centrifuge and the mixture overlayed with 1-2 drops of mineral oil. The samples were run on the Hybaid thermal cycler using specific programmes as shown in the following table.

Table 5. Temperature profile for PCR of the fragments of the PPOX gene

Fragments 1 & 4

	Temperature (°C)	Time (s)	Cycle Number
Initial Denaturation	94	120	1
Denaturation	94	60	
Annealing	51	30	32
Extension	72	60	
Final Extension	72	300	1

Fragment 2

	Temperature (°C)	Time (s)	Cycle Number
Initial Denaturation	94	120	1
Denaturation	94	30	
Annealing	40	120	40
Extension	72	30	
Final Extension	72	300	1

Fragment 3

	Temperature (°C)	Time (s)	Cycle Number
Initial Denaturation	94	60	1
Denaturation	94	30	
Annealing	65	30	32
Extension	72	30	
Final Extension	72	300	1

1.6.3 Restriction Analysis

Equipment

Techni dry block BD-2D (Laboratory & Scientific, Cape Town, South Africa)

Force 14 microcentrifuge (Denver Instruments, Laboratory & Scientific, Cape Town, South Africa)

Further equipment as for the 6% non-denaturing gel electrophoresis (see Appendix 5.0)

Reagents/Materials

Restriction endonuclease, Ava I (10U/µl) (Promega, Madison, WI, USA)
Restriction endonuclease buffer B (Promega, Madison, WI, USA)
Restriction endonuclease, BsaJ1 (2.5U/µl) (New England Biolabs (UK), Ltd.)
Restriction endonuclease buffer NE2 (New England Biolabs (UK), Ltd.)
Sterile 17x100mm polypropylene tubes (Laboratory and Scientific Equipment, SA)
Sterile deionized water

Method

All volumes quoted below were for a single digestion reaction. These volumes were scaled up to allow for the number of digests required. A positive and negative control were always included. All the digests were analysed on a 6% polyacrylamide gel (see 5.0). A pre- and post-digested product was always run.

Ava I

This was used for identification of R59W in Fragment 1 of the PPOX cDNA and recognised the following sequence (the arrows indicate the enzyme's cutting position) :

5' C↓(T/C)CG(A/G)G 3'
3' G(A/G)GC(T/C)↑C 5'

Wild-type : 533bp with two cutting sites yielded fragments = 237, 209 and 87bp.

Mutant: one cutting site was abolished yielding two fragments of 446 and 87bp

Bsa J1

This was used for identification of R168C in Fragment 2 of the PPOX cDNA and recognised the following sequence (the arrows indicate the enzyme's cutting position) :

5' C↓CNNGG 3'
3' GGNNC↑C 5'

Wild-type : 411bp with five cutting sites yielded fragments = 155, 97, 67, 50, 26 and 16bp.

Mutant : one cutting site was abolished yielding fragments – 171, 97, 67, 50 and 26bp

The digests were prepared as follows:

Appropriate buffer 10x	2.0µl
Bovine serum albumin (BSA) 10 mg/ml	0.20µl
Sterile deionized H_2O	7.3µl
Enzyme (10U/µl)	0.5µl
Total	**10 µl**

The mixture was vortexed and briefly microcentrifuged. Ten µl of the above mixture and 1 – 1.5 µg PCR product were added to a 0.6ml microcentrifuge tube, mixed, and a drop of mineral oil added. The sample was incubated at 37°C for 4 h.

1.6.4 QIAEX II DNA Purification in preparation for Direct Sequencing

Equipment

Heating Block (Techne Dri-Block, Cambridge, England)
Tabletop Centrifuge (Denver Instrument Company, Colorado, USA)
GeneQuant Spectrophotometer (Pharmacia Biotech (Biochrom) Ltd., Cambridge, England)
Microwave oven (Defy, South Africa)
Weighing balance (M-120, Denver Instrument Company, Colorado, USA)
Weighing balance (XL-1810, Denver Instrument Company, Colorado, USA)
Electronic UV Transilluminator (Trans-Lum, California, USA)
1.5ml Microcentrifuge tubes (Promega Corporation, WI, USA)

Reagents

QIAEX II Gel Extraction Kit (Qiagen GmbH, Hilden, Germany)
Ethidium bromide stock solution (1mg/ml)
Bromophenol blue sample-loading dye (see Appendix 13)

Method

The PCR product was run on a 1% agarose gel (see Appendix 13) and stained with ethidium bromide. The DNA band of interest was visualised on a UV transilluminator, excised with a sterile scalpel blade, and weighed in a 1.5ml microcentrifuge tube. Three hundred µl Buffer QX1 was added to every 100mg of gel. QIAEX II silica beads were resuspended by vortexing for 30s and 30µl was added to the gel slice. The sample was incubated at 50°C for 20 min with mixing by vortexing every 2 min to keep the QIAEX II in suspension. The sample was centrifuged at 14,000 x g in a tabletop centrifuge for 30s at room temperature. The supernatant was removed and the pellet resuspended in 500µl Buffer QX1. Centrifugation was repeated for 30s and the supernatant discarded. The pellet was resuspended in 500µl Buffer PE and re-centrifuged using the same parameters. This step was repeated. The supernatant was carefully removed and the pellet air-dried for 30 min. The QIAEX II pellet was resuspended in 20µl sterile deionized water and the DNA eluted off the silica beads by incubation at room temperature for 5 min, followed by incubation at 4°C overnight. The sample was then centrifuged for 30s, approximately 10µl of the supernatant (which now contained the purified DNA) transferred into a clean microcentrifuge tube, and the pellet resuspended in a further 10µl of water. After incubating the sample for 5 min at room temperature, it was re-centrifuged for 30s and the supernatant added to the previous amount. Six µl of the supernatant was used on the GeneQuant for DNA quantification. Five µl of 10ng/µl DNA was sent for direct sequencing.

Direct sequencing was performed with a Big Dye terminator cycle sequencing kit on an ABI prism 377 DNA sequencer, by the Core DNA sequencing facility of the University of Stellenbosch.

1.7 Mutagenesis and confirmation of VP PPOX-GFP constructs

The R59W, R168C and H20P VP PPOXs contained a stop codon at the carboxy terminal end that had to be removed in order to produce an in-frame, PPOX-GFP fusion protein. To remove the stop codon, a HindIII site was inserted upstream of the ATG stop codon using site-directed mutagenesis on the VP PPOX cDNAs (ie. R59W, R168C and H20P). Site-directed mutagenesis was conducted identically as

described in appendices 1.3-1.5. The phosphorylated mutagenic oligonucleotide used in the reaction is detailed in the following table :

Table 6 : Oligonucleotide used to engineer the VP-causing PPOX-GFP, Hind III mutants.

Mutant	**Phosphorylated Oligonucleotide**			**Optimised annealing temp (°C)**
	Sequence (5'-3')	**Direction**	**Length (bp)**	
PPOX,HindIII	CTGGGCACAGAAGCTTACAGCTGATCC	TOP	27	48

Mutated cDNA (ie. insertion of the Hind III site) was confirmed by PCR of the mutated DNA fragment (see 1.6.2) using the following oligonucleotide pair :

PF4 = 5' – GTGCCATCTTCAGAAGATCC – 3' (forward)
pEGFP-N1/R = 5' - AACTTGTGGCCGTTTACGTC - 3' (reverse),

This was followed by restriction analysis using Hind III (2.3.2). Further confirmation included direct sequencing (see 1.6.4).

2. ENGINEERING OF EXPERIMENTAL PPOX FRAGMENTS

2.1 PCR-based Mutagenesis

Equipment

Robocycler Gradient 40 Temperature Cycler (Stratagene Cloning Systems, California, USA)
Tabletop Centrifuge (Denver Instruments, Colorado, USA)
GeneQuant Spectrophotometer (Pharmacia Biotech (Biochrom) Ltd., Cambridge, England)
Tabletop Mistral Vortex Mixer (Laboratory & Scientific, Cape Town, South Africa)

Reagents

Magnesium-free, Thermophilic DNA Polymerase 10X Buffer (Promega Corporation, WI, USA)
10X Buffer containing 25mM $MgCl_2$ (Promega Corporation, WI, USA)
Taq DNA Polymerase (5U/µl, Promega Corporation, WI, USA)
Sterile deionized water
Template DNA (PPOX cDNA, 50ng/µl)
Deoxynucleotide Triphosphates (dNTPs) (Promega Corporation, WI, USA) (see Appendix 13)
Mutant-specific Oligonucleotides, 100nmole (Integrated DNA Technologies, Inc., Coralville, IA, USA)
Mineral Oil (Promega Corporation, WI, USA)

Table 6. Experimental human PPOX constructs, the oligonucleotides used to engineer them, and their associated bp sizes. Where amino acids have been changed from wild-type, they are indicated in blue. The incorporated Bgl II restriction endonuclease site is bolded and underlined. The Hind III site is bolded and twice underlined.

Mutant Name	Oligonucleotide Sequence/s (5'-3'), 31-mer	Fragment Size (bp)
PPOX12	F : GTT TCT T**AG ATC T**AG CAT GGG CCG GAC CGT G R : AAG AAA C**AA GCT T**GA TGC CTC CGC CCA GCA C	65 bp
PPOX14	F : GTT TCT T**AG ATC T**AG CAT GGG CCG GAC CGT G R : AAG AAA C**AA GCT T**GC CGC TGA TGC CTC CGC C	71 bp
PPOX15	F : GTT TCT T**AG ATC T**AG CAT GGG CCG GAC CGT G R : AAG AAA C**AA GCT T**CA AGC CGC TGA TGC CTC C	74 bp
PPOX16	F : GTT TCT T**AG ATC T**AG CAT GGG CCG GAC CGT G R : AAG AAA C**AA GCT T**GG CCA AGC CGC TGA TGC C	77 bp
PPOX17	F : GTT TCT T**AG ATC T**AG CAT GGG CCG GAC CGT G R : AAG AAA C**AA GCT T**GG CGG CCA AGC CGC TGA T	80 bp
PPOX17/R3S	F : GTT TCT T**AG ATC T**AG CAT GGG C**AG C**AC CGT G R : AAG AAA C**AA GCT T**GG CGG CCA AGC CGC TGA T	80 bp
PPOX17/R3E	F : GTT TCT T**AG ATC T**AG CAT GGG C**GA G**AC CGT G R : AAG AAA C**AA GCT T**GG CGG CCA AGC CGC TGA T	80 bp
PPOX17/R3K	F : GTT TCT T**AG ATC T**AG CAT GGG C**AA G**AC CGT G R : AAG AAA C**AA GCT T**GG CGG CCA AGC CGC TGA T	80 bp
PPOX20	F : GTT TCT T**AG ATC T**AG CAT GGG CCG GAC CGT G R : AAG AAA C**AA GCT T**GT GGT AAC TGG CGG CCA A	89 bp
PPOX20/H20P	F : GTT TCT T**AG ATC T**AG CAT GGG CCG GAC CGT G R : AAG AAA C**AA GCT TGG G**GT AAC TGG CGG CCA A	89 bp
PPOX20/H20S	F : GTT TCT T**AG ATC T**AG CAT GGG CCG GAC CGT G R : AAG AAA C**AA GCT TGC T**GT AAC TGG CGG CCA A	89 bp
PPOX20/H20A	F : GTT TCT T**AG ATC T**AG CAT GGG CCG GAC CGT G R : AAG AAA C**AA GCT TGG C**GT AAC TGG CGG CCA A	89 bp
PPOX20/H20K	F : GTT TCT T**AG ATC T**AG CAT GGG CCG GAC CGT G R : AAG AAA C**AA GCT TCT T**GT AAC TGG CGG CCA A	89 bp
PPOX20/H20E	F : GTT TCT T**AG ATC T**AG CAT GGG CCG GAC CGT G R : AAG AAA C**AA GCT TCT C**GT AAC TGG CGG CCA A	89 bp
PPOX20/H20G	F : GTT TCT T**AG ATC T**AG CAT GGG CCG GAC CGT G R : AAG AAA C**AA GCT TGC C**GT AAC TGG CGG CCA A	89 bp
PPOX24	F : GTT TCT T**AG ATC T**AG CAT GGG CCG GAC CGT G R : AAG AAA C**AA GCT T**GG CCC GGC TCA GGT GGT A	101 bp
PPOXΔ1-17	F : GTG T**AG ATC T**AT GAG TTA CCA CCT GAG CCG G R : ACA C**AA GCT T**TG AGC TGT TAG GTT CTG TGC C	101 bp

Note : The PPOX24-GFP construct (ie. PPOX residues 1-24) was chosen first to test for mitochondrial targeting as it included the complete predicted α-helix. After it showed efficient mitochondrial targeting, the number of residues were reduced to 20 (PPOX20-GFP) and then to 12 (PPOX12-GFP). PPOX12-GFP abolished mitochondrial targeting. Residues were then progressively added (PPOX14, 15, 16 and 17-GFP) till targeting was re-established.

Mutant Oligonucleotides were designed using the Primer Designer for Windows Software package (Soft Packaging V.2, Scientific and Education Software).

The following 1 x reaction was set up on ice in a 0.6ml microcentrifuge tube :

Magnesium-free, Thermophilic DNA Polymerase 10X buffer	5µl
10X Buffer containing 25mM $MgCl_2$	5µl
dNTPs (2.5mM)	2µl
Appropriate forward oligonucleotide, 25µM (see table above)	1µl
Appropriate reverse oligonucleotide, 25µM (see table above)	1µl
Taq DNA Polymerase (5U/µl)	2µl
Sterile distilled water to a volume of	**45µl**

5µl of wild-type PPOX cDNA was added and the mixture vortexed. After microcentrifuging briefly, the mixture was overlayed with 1-2 drops of mineral oil. All PCR reactions were performed on the Robocycler thermal cycler using the programme shown below.

Table 7. PCR profile for the experimental PPOX fragments

	Temperature (°C)	Time (s)	Cycle Number
Initial Denaturation	94	120	1
Denaturation	94	60	32
Annealing	53	30	
Extension	72	60	
Final Extension	72	300	1

Five µl of the PCR product was mixed with 5µl sucrose sample solution (see Appendix 13) and the mixture run on a polyacrylamide gel (see 5.0) at 250V for 1.5h. The gel was stained for 10 min in ethidium bromide (1mg/ml) and visualised under UV transillumination.

2.2 Restriction Digests and Ligation

Equipment

Water bath (Memmert GmbH+Co.KG, Schwabach, Germany)

Orbital shake incubator (Yih der LM-510, Taiwan, Japan)

Techni dry block BD-2D (Laboratory & Scientific, Cape Town, South Africa)

Force 14 microcentrifuge (Denver Instruments, Laboratory & Scientific, Cape Town, South Africa)

Further equipment as for the 6% non-denaturing gel electrophoresis (see Appendix 5.0)

Reagents/Materials

Restriction endonuclease, Bgl II (10U/µl) (Promega, Madison, WI, USA)

Restriction endonuclease, Hind III (10U/µl) (Promega, Madison, WI, USA)

Restriction endonuclease buffer B (Promega, Madison, WI, USA)

pEGFP-N1 Vector (Clontech Laboratories, Inc., California, U.S.A.)

T4 DNA Ligase, 20U/µl (Promega, Madison, WI, USA)

T4 DNA Ligase buffer, 10X (Promega, Madison, WI, USA)

Supercompetent sterile JM109 cells (Promega, Madison, WI, USA)

Sterile 17x100mm polypropylene tubes (Laboratory and Scientific Equipment, SA)

Sterile deionized water

LB plates containing 30µg/ml kanamycin (Roche Diagnostics SA Pty.Ltd, South Africa)

SOC Medium (Appendix 13)

LB Broth (Appendix 13)

Method

The PCR products (±1µg) and pEGFP-N1 DNA (±250ng) were separately digested as described below :

DNA (PCR product/pEGFP-N1 vector)	1µg/250ng
Hind III endonuclease (10U/µl)	1µl
Bgl II endonuclease (10U/µl)	1µl
10 X Buffer B	2µl
Bovine serum albumin (BSA,100µg/ml)	0.2µl
Sterile distilled water to volume of	**20µl**

The samples were digested for 3h at 37°C. The following ligation reaction (1:7, vector:insert) was then prepared :

Vector DNA (pEGFP-N1)	50ng
Insert DNA (PCR product)	350ng
Ligase 10 X Buffer	1µl
T4 DNA Ligase (Weiss Units)	3U
Nuclease-free water to volume	**10µl**

The reaction was mixed by gently pipetting up and down and incubated at 4°C overnight. The above 10µl were transformed into competent JM109 bacterial cells as described in 1.5.

2.3 Identification of PPOX-GFP constructs :

2.3.1 Identification by PCR

Equipment

Robocycler Gradient 40 Temperature Cycler (Stratagene Cloning Systems, California, USA)
Tabletop Centrifuge (Denver Instruments, Colorado, USA)
GeneQuant Spectrophotometer (Pharmacia Biotech (Biochrom) Ltd., Cambridge, England)
Tabletop Mistral Vortex Mixer (Laboratory & Scientific, Cape Town, South Africa)
Microcentrifuge tubes – 1.5ml (Promega Corporation, WI, USA)
Microcentrifuge tubes – 0.6ml (Promega Corporation, WI, USA)

Reagents

Magnesium-free, Thermophilic DNA Polymerase 10X Buffer (Promega Corporation, WI, USA)

10X Buffer containing 25mM $MgCl_2$ (Promega Corporation, WI, USA)

Taq DNA Polymerase (5U/µl, Promega Corporation, WI, USA)

Sterile deionized water

Deoxynucleotide Triphosphates (dNTPs) (Promega Corporation, WI, USA) (see Appendix 13)

Specific oligonucleotide set (Integrated DNA Technologies Inc., Coralville, IA, USA)

Mineral Oil (Promega Corporation, WI, USA)

Method

The oligonucleotide set used to confirm all the GFP chimeras was :

PPOX17F = 5'-GTTTCTTAGATCTAGCATGGGCCGGACCGTG-3'

pEGFP-N1/R = 5' - AACTTGTGGCCGTTTACGTC - 3'

Two-hundred and fifty nanograms of DNA from the mutant clones were used in the PCR as described in 1.6.2. The size of the PCR products varied for each mutant and are shown in table 8:

Table 8. Engineered mutants and their associated base-pair sizes once identified as positive clones.

Mutant Name	Fragment Size (bp)
PPOX12	204 bp
PPOX14	210 bp
PPOX15	213 bp
PPOX16	216 bp
PPOX17	219 bp
PPOX17/R3S	219 bp
PPOX17/R3E	219 bp
PPOX17/R3K	219 bp
PPOX20	228 bp
PPOX20/H20P	228 bp
PPOX20/H20S	228 bp
PPOX20/H20A	228 bp
PPOX20/H20K	228 bp
PPOX20/H20E	228 bp
PPOX20/H20G	228 bp
PPOX24	240 bp
PPOXΔ1-17*	600 bp

(* For the PPOXΔ1-17 engineered mutant, PF4 and pEGFP-N1/R oligonucleotides (appendix 1.7) were used with the PCR programme optimised for fragment 4 (appendix 1.6.2, table 5)).

The samples were run on the Robocycler thermal cycler using a programme with an annealing temperature previously optimised for the PPOX17F/pEGFP-N1/R oligonucleotide set. The PCR programme is shown in the following table :

Table 9. PCR profile used to confirm positive PPOX-GFP colonies.

	Temperature (°C)	Time (s)	Cycle Number
Initial Denaturation	94	120	1
Denaturation	94	60	
Annealing	53	30	32
Extension	72	60	
Final Extension	72	300	1

PCR products were visualised on an ethidium bromide-stained, 6% non-denaturing polyacrylamide gel.

2.3.2 Identification by restriction analysis

Equipment

Techni dry block BD-2D (Laboratory & Scientific, Cape Town, South Africa)

Force 14 microcentrifuge (Denver Instruments, Laboratory & Scientific, Cape Town, South Africa)

Further equipment as for the 6% non-denaturing gel electrophoresis (see 5.0)

Reagents/Materials

Restriction endonuclease, Bgl II (10U/µl) (Promega, Madison, WI, USA)

Restriction endonuclease, Hind III (10U/µl) (Promega, Madison, WI, USA)

Restriction endonuclease buffer B (Promega, Madison, WI, USA)

Sterile 17x100mm polypropylene tubes (Laboratory and Scientific Equipment, SA)

Sterile deionized water

Agarose sample loading dye (see Appendix 13)

Method

All volumes quoted below were for a single digestion reaction. These volumes were scaled up to allow for the number of digests required. A positive and negative control as well as a pre- and post-digested sample were included in each run. All the digests were analysed on a 6% polyacrylamide gel (see Appendix 5.0)

Double digests : Bgl II/Hind III

This double digest was used to remove the PPOX insert from the pEGFP-N1 in order to confirm a successful ligation. Bgl II and Hind III recognised the following sequences (the arrows indicate the enzyme's cutting position) :

Bgl II :

5' A↓GATCT 3'
3' AGATC↑T 5'

Hind III

5' A↓AGCTT 3'
3' AAGCT↑T 5'

Bgl II/Hind III digest results in two fragments:

- Mutant PPOX fragment (see Table 8) + 4.4kb pEGFP-N1 Vector

The digest was prepared as follows:

PPOX-GFP cDNA	250ng
10 x Buffer B	1.0µl
Bovine serum albumin (BSA) 10 mg/ml	0.20µl
Bgl II (10U/µl)	1.0µl
Hind III (10U/µl)	1.0µl
Made up with sterile deionized H_2O	**10 µl**

The mixture was vortexed and briefly microcentrifuged. The sample was incubated at 37°C for 3h. The sample was mixed with 2µl agarose sample loading dye and run on a 1% agarose gel at 120V for 2h and visualised under UV illumination.

2.3.3 Confirmation by direct sequencing

The DNA from the positive mutant clones was extracted (Appendix 3.0) and used to PCR the fragment as seen in table 8. Purity was assessed by PAGE (Appendix 5.0), extracted using QIAEX II (see 1.6.4), and sent for direct sequencing. Direct sequencing was performed with a Big Dye terminator cycle sequencing kit on an ABI

prism 377 DNA sequencer, by the Core DNA sequencing facility of the University of Stellenbosch.

3. Plasmid DNA Extraction and Purification

Equipment

Bench top Centrifuge (Hermle Labortechnik GmbH, Wehingen, Germany)
Tabletop Centrifuge (Denver Instruments, Colorado, USA)
GeneQuant Spectrophotometer (Pharmacia Biotech, (Biochrom) Ltd., Cambridge, England)

Reagents

Wizard *Plus* SV Minipreps DNA Purification System (Promega Corporation, Madison, WI, USA)

Method

An overnight bacterial culture was pelleted in a bench top centrifuge at 2,500 x g for 10 min. The supernatant was discarded, the pellet resuspended in 1ml LB broth and transferred to a 1.5ml microcentrifuge tube which were re-centrifuged in a tabletop centrifuge for 5 min at 10,000 x g. The supernatant was discarded and the pellet completely resuspended by vortexing in 250µl of Wizard *Plus* SV Minipreps Cell Resuspension Solution. Two hundred and fifty µl of Cell Lysis Solution was added and the mixture gently inverted four times. The mixture was incubated at room temperature for 3 min to ensure complete cell lysis. Ten µl of Alkaline Protease Solution was added, the mixture inverted and incubated at room temperature for 5 min. Three hundred and fifty µl Neutralization Solution was added and the tube inverted. The bacterial lysate was centrifuged at 14,000 x g for 10 min at room temperature. The cleared lysate, approximately 850µl, was transferred to a Wizard *Plus* SV Minipreps Spin Column inserted into a 2ml Collection tube. The lysate was centrifuged at 14,000 x g for 1 min at room temperature and the flow-through discarded. Seven hundred and fifty µl Column Wash Solution, previously diluted with 95% ethanol, was added to the Spin Column and the centrifugation at 14,000 x g for 1 min repeated. After the flow-through was discarded, a further 250µl of Column

Wash Solution was added and the centrifugation repeated at 14,000 x g for 2 min, and the flow-through discarded. The Spin Column was transferred to a clean, sterile 1.5ml microcentrifuge tube. The pure DNA was eluted from the Spin Column by adding 100µl Nuclease-free water and centrifuging at 14,000 x g for 2 min. The DNA was then quantified on a GeneQuant spectrophotometer and stored at -20°C.

4. Agarose Gel Electrophoresis

Equipment

Horizontal mini-gel system (Mgu-202T), (CBS Scientific Company Inc., Del Mar, USA)
Electrophoresis Power Supply (EPS-250 Series II), (CBS Scientific Company Inc., Del Mar, USA)
Electronic UV Transilluminator (Ultralum, Whitehead Scientific (Pty) Ltd, SA)

Reagents

SeaKem LE Agarose (FMC Bioproducts, Rockland, Maine, U.S.A.)
Ethidium Bromide (Roche Diagnostics (Pty) Ltd, Randburg, SA)
Agarose sample-loading dye (Appendix 13)
1 x TBE Buffer (Appendix 13)

Method

For the detailed method, see Appendix 13. After loading the samples, the gel was run at 120V for 2 h, the DNA/PCR product visualised on a UV transilluminator, and photographed using the UV gel documentation system.

5. 6% Non-denaturing polyacrylamide gel electrophoresis

Equipment

SE600 vertical slab gel electrophoresis unit, (Hoefer Scientific Instruments Pharmacia Biotech, Cambridge, UK).

PS1200 DC power supply, (Hoefer Scientific Instruments Pharmacia Biotech, Cambridge, UK).

Uvi-doc gel documentation system, (UVItec, Cambridge, UK).

Hamilton syringe

Reagents

Ethidium Bromide, (Stock solution 1 mg/ml, see Appendix 13).

Sucrose sample solution (Appendix 13)

100 bp DNA ladder, (Promega Corporation, WI, USA).

10 x TBE (Appendix 13)

A-Bis-A solution (30% acrylamide, 0.8% bisacrylamide)

10% Ammonium persulphate (APS) (Sigma-Aldrich S.A. (Pty) Ltd.)

N,N,N',N'-Tetramethylethylenediamine (TEMED) (Sigma-Aldrich S.A. (Pty) Ltd.)

Method

To a 100 ml beaker was added:

- 5 ml 10x TBE
- 10 ml A-Bis-A solution (30% acrylamide, 0.8% bisacrylamide)
- 500µl ammonium persulphate (10%)
- 50µl TEMED

The above was made up to 50ml with sterile, deionized water. The solution was poured into the space between the 2 clamped glass gel plates (1.5mm spacers) and mounted in the gel casting stand. A 20 sample bay spacer comb was inserted into the space and the gel allowed to set at room temperature for 1h. The upper buffer chamber was positioned on top of the gel plate and filled with 500ml 1 x TBE. The lower buffer chamber was filled with 2L of 1 x TBE. The PCR product, diluted 1:1 with sucrose sample solution, was loaded into the sample bays using a Hamilton syringe.

A 100bp DNA marker diluted 1:1 with sucrose sample solution, was loaded in a bay and the gel was run at 150V for ± 2h. Water-based cooling was applied for the duration of the gel run. The gel was removed and stained gel in ethidium bromide for 10 min, rinsed in water and visualized under UV light. The gel was photographed using a gel documentation system.

6. Single stranded conformation polymorphism (SSCP) and heteroduplex (HD) analysis

Equipment

SE600 vertical slab gel electrophoresis unit, PS1500 DC power supply (Hoeffer Scientific Instruments/Pharmacia Biotech, Cambridge, UK)

Techni dri block BD-2D (Laboratory & Scientific, Cape Town, South Africa)

Hybaid Omnigene thermal cycler (Hybaid Limited, Teddington, UK)

1mm Spacer (Hoeffer Scientific Instruments/Pharmacia Biotech, Cambridge, UK)

1mm Sample comb (Hoeffer Scientific Instruments/Pharmacia Biotech, Cambridge, UK)

Reagents

MDE gel solution (FMC BioProducts, Rockland Maine, USA.)

Sample loading buffer (see Appendix 13)

Glycerol (Sigma-Aldrich S.A. (Pty) Ltd.)

Method

6.1 Casting of MDE gel

Two glass gel plates (using 1 mm spacers) were clamped and mounted in a gel-casting stand.

The gel solution was prepared as follows :

15ml 2x MDE gel solution

1.8 ml 10x TBE (final concentration=0.6x TBE)

3 ml glycerol (final concentration=10%; for gels without glycerol the 3ml glycerol was replaced with H_2O)

Deionized water was added to a final volume of 30ml.

Prior to casting, a fast setting gel was prepared to use as a plug at the bottom of the plates.

To 5ml of the above-made 30ml, the following was added :

20µl 10% Ammonium persulphate (APS)

20µl TEMED

Approximately 1cm of this fast-setting gel was poured between the plates and allowed to set for 10 min. To the remainder of the MDE solution (25ml), 175µl 10% ammonium persulphate and 17.5µl TEMED were added. This was poured on top of the set gel plug until the space between glass plates was almost filled. A 1mm, 20-sample well comb was inserted and the gel allowed to set for 1h. Once set, the comb was removed and the upper tank chamber filled with 500ml 0.6x TBE. The lower tank chamber was filled with 4.5L of 0.6 x TBE. The samples were prepared for loading as below and loaded immediately :

5µl PCR product + 5µl sample loading buffer (see Appendix 13).

Denatured for 5 min at 95°C in thermocycler.

Chilled on ice for 5 min.

The gel was run at room temperature between 150 and 400V for ±19h depending on the size of the PCR product. It is vital that good separation is achieved, otherwise aberrant mobility shifts may not be detected. The gel was run in both the presence and absence of 10% glycerol. When absent, the voltage was halved.

6.2 Silver staining of MDE gel

The MDE gel was removed from between the 2 gel plates and rinsed in deionized H_2O. The gel was transferred to a glass dish containing 0.1% $AgNO_3$ and gently agitated for 20 min. The gel was rinsed twice in deionized H_2O for 5 min and then agitated in the following solution in a fume cupboard for 20 min:

1.5% NaOH

0.01% Na Borohydride

0.15% Formaldehyde.

It was then rinsed in enhancer (0.75% $NaCO_3$), rinsed in deionized H_2O and visualized on a light box. The gel was sealed in clear plastic and stored. (These gels cannot be dried as they crack.)

7. Tissue Culture

Equipment

Laminar Flow Hood (Laminaire Ltd., SA)

37°C Water-jacket Incubator (Forma Scientific Inc., Ohio, USA)

Sterile Tissue culture dishes,10cm^2 (Laboratory and Scientific Company (Pty) Ltd., SA)

Sterile tissue culture-grade 6-well plates (Laboratory and Scientific Company (Pty) Ltd., SA)

Automatic pipette (Labopet 240, Laboratory and Scientific Company (Pty) Ltd., SA)

Automatic Medi-suction pump (Laboratory and Scientific Company (Pty) Ltd., SA)

Sterile glass pipettes (Laboratory and Scientific Company (Pty) Ltd., SA)

Bench top Centrifuge (Hermle Labortechnik GmbH, Wehingen, Germany)

Reagents

Dulbecco's Modified Eagle Medium (DMEM) with Glutamax I (Laboratory Specialist Services, SA)

Phosphate Buffered Saline (PBS), pH 7.4 (see Appendix 13)

Foetal Bovine Serum (FBS), (Laboratory Specialist Services, SA)

Filtered, sterile glycerol (Sigma-Aldrich Ltd., Cambridge, UK)

1 x Trypsin (Laboratory and Scientific Company (Pty) Ltd., SA)

Method

All tissue culture equipment was gas or heat-sterilized before use. For all tissue culture techniques, an immortal human hepatoma cell line (HepG2) was used. These cells (a gift from Dr Edward Sturrock, Dept of Medical Biochemistry, University of Cape Town) were obtained as frozen stocks and further propagated into stocks stored in liquid nitrogen at –70°C. One ml of stock was thawed and aliquoted into a 10cm^2 sterile culture dish containing 10ml DMEM. The cells were allowed to adhere overnight by incubation at 37°C in a 5% O_2 : 95% CO_2 incubator. The following day, the medium was aspirated off the cells, the cells washed twice with room temperature PBS, and fresh medium added. The cells were rinsed and fresh medium replaced every second day until confluent. At confluence (which represents approximately 1.3 x 10^6 cells/ml), the cells were rinsed with PBS and 1ml trypsin

added. Cells were incubated at 37°C for 5 min to allow the cells to lift off the plate. The trypsin was inactivated by addition of 2ml DMEM and the cells pelleted at 2 600xg for 5 min in a benchtop centrifuge. Cells were resuspended in 1ml and counted in a haemocytometer using the following formula :

Cells/ml = Average count per square **x** dilution factor **x** 10^4

Total Cells = Cells/ml **x** Total original vol. of cell suspension from which cells were taken

Cells were further passaged into 3 x 10cm^2 dishes for every 1 confluent dish.

8. Cell Transfections

Equipment

Laminar Flow Hood (Laminaire Ltd., SA)

37°C Water-jacket Incubator (Forma Scientific Inc., Ohio, USA)

Sterile Tissue culture dishes,10cm^2 (Laboratory and Scientific Company (Pty) Ltd., SA)

Sterile tissue culture-grade 6-well plates (Laboratory and Scientific Company (Pty) Ltd., SA)

Automatic pipette (Labopet 240, Laboratory and Scientific Company (Pty) Ltd., SA)

Automatic Medi-suction pump (Laboratory and Scientific Company (Pty) Ltd., SA)

Sterile glass pipettes (Laboratory and Scientific Company (Pty) Ltd., SA)

Benchtop Centrifuge (Hermle Labortechnik GmbH, Wehingen, Germany)

Frosted Glass Microscope Slides (Chance Propper Ltd, UK)

Glass microscope coverslips, 24mm^2 (Euroslip Inc., Germany)

Reagents

Dulbecco's Modified Eagle Medium (DMEM) with Glutamax I (Laboratory Specialist Services, SA) containing 10% FCS

Phosphate Buffered Saline (PBS), pH 7.4 (Appendix 13)

DOTAP Liposomal Transfection Reagent (Roche Molecular Biochemicals, Indianapolis, USA)

Permafluor Mounting Medium (Immunotech, Marseille, France)

Clear Nail Varnish (Revlon, Isando, South Africa)

20mM Hepes-buffered Saline (HBS), pH 7.4, sterile (Appendix 13)

Method

For all cell transfection experiments, ±1 x 10^5 HepG2 cells were plated onto 35mm^2 coverslips in 500µl DMEM. The coverslips were placed in sterile tissue culture-grade 6-well plates and the cells allowed to adhere overnight by incubation at 37°C in a 5% CO_2 : 95% O_2 incubator. The following day cells were rinsed in PBS and the following table used to prepare the DOTAP/nucleic acid mixture for transfections (the grey box show the amounts predominantly used for transfections on coverslips). All the mixtures were diluted using Hepes buffer.

Table 9. Amounts used to prepare the DOTAP/nucleic acid mixture for transfections in different sized culture dishes.

Culture dish	35mm	60mm	100mm
DNA	~ 2.5µg	~5µg	~7.5µg
diluted to a final volume of	25µl	50µl	75µl
DOTAP	15µl	30µl	45µl
diluted to a final volume of	50µl	100µl	140µl

The DNA and DOTAP mixtures were mixed in separate reaction tubes. The nucleic acid solution was transferred to the reaction tube already containing the DOTAP mixture and carefully mixed by gently pipetting the mixture up and down several times. Please note : it is not recommended that the mixture be vortexed or centrifuged. The transfection mixture was incubated for 10-15 min at room temperature. The volume of the transfection mixture was brought up to 450µl per sample with room temperature DMEM and mixed by gently pipetting up and down. The mixture was pipetted onto the cells and incubated for 18h at 37°C (a transfection time-course experiment was conducted over 24 hours, and 18 hours was proven to

be the optimal time-frame). Hereafter, the medium was removed, the cells washed twice with pre-warmed PBS and the coverslips mounted onto microscope slides with a drop of Permafluor mounting medium. After 1h, the slides were sealed with clear nail varnish and left to dry at room temperature for 1h prior to microscopic analysis.

9. Photomicrography

Equipment

Axioskop 2 MOT Photomicroscopic System (Carl Zeiss Microscopy, Jena, Germany)

Axiovision Software Version 2.05 (Carl Zeiss Vision GmbH, Munchen-Hallbergmoos, Germany)

Axiocam Digital Camera (Carl Zeiss Microscopy, Jena, Germany)

Recordable and Rewritable Compact Discs (Verbatim, SA)

Adobe Photoshop, v5

Reagents

MitoTracker Fluorescent Dye (Laboratory Specialist Services, SA)

Microscope Oil (Carl Zeiss Microscopy, Jena, Germany)

Method

The maximum excitation and emission wavelengths for green fluorescent protein are 488nm and 507nm, respectively. The cells were viewed at magnifications of 20x, 40x and 100x. The 100x was an oil immersion lens. The fusion proteins were visualised using a band pass filter set with an excitation range of 450-490nm and an emission wavelength of 520nm at a screen resolution of 1024 x 800 pixels. The resultant images were fluorescent green. A mitochondrial-specific dye, MitoTracker, was viewed at the same magnifications with a band pass filter set at an excitation wavelength of 546nm and emission at 590nm. The images appeared red. Orange/yellow merged images were created with Adobe Photoshop software by overlaying the fluorescent green and mitotracker red images.

10. Computer-predicted Analyses

A number of computer-based predictions were used to analyse the predicted mitochondrial targeting sequence and other aspects of human PPOX.

10.1 MitoProt

MitoProt calculates the N-terminal protein region that can support a Mitochondrial Targeting Sequence and the cleavage site. The official site is found at :
http://websvr.mips.biochem.mpg.de/proj/medgen/mitop/
A complete description of the prediction methodology is available in: *M.G. Claros, P. Vincens. Computational method to predict mitochondrially imported proteins and their targeting sequences. Eur. J. Biochem. 241, 779-786 (1996).* The Mitoprot software is available at:
ftp://ftp.rediris.es/software/incoming/science
ftp://ftp.ens.fr/pub/molbio

10.2 PredictProtein

PredictProtein is a secondary structure predictor for an input amino acid sequence. It compares the input sequence with a large database (PROSITE) and the results are output as predictions of multiple sequence alignments (PSI-BLAST and MAXHOM), secondary protein structural information ie. alpha helices and beta sheet content (PROF) and prediction of protein globularity (GLOBE). The official website for PredictProtein is :
http://cubic.bioc.columbia.edu
A complete description of the method can be found in : *Rost, B. (1996) Methods in Enzymology, 266 : 525-539.*

10.3 α-HelixWheel prediction

HelixWheel is shareware that analyzes the input sequence for its ability to form an α-helix and then plots this on a wheel diagram indicating hydrophobic, hydrophilic, positive and negative-charged residues using a colour scheme. The predictive software used can be found at :
(http://www.site.uottawa.ca/~turcotte/resources/HelixWheel).

11. Amino acid structure classification

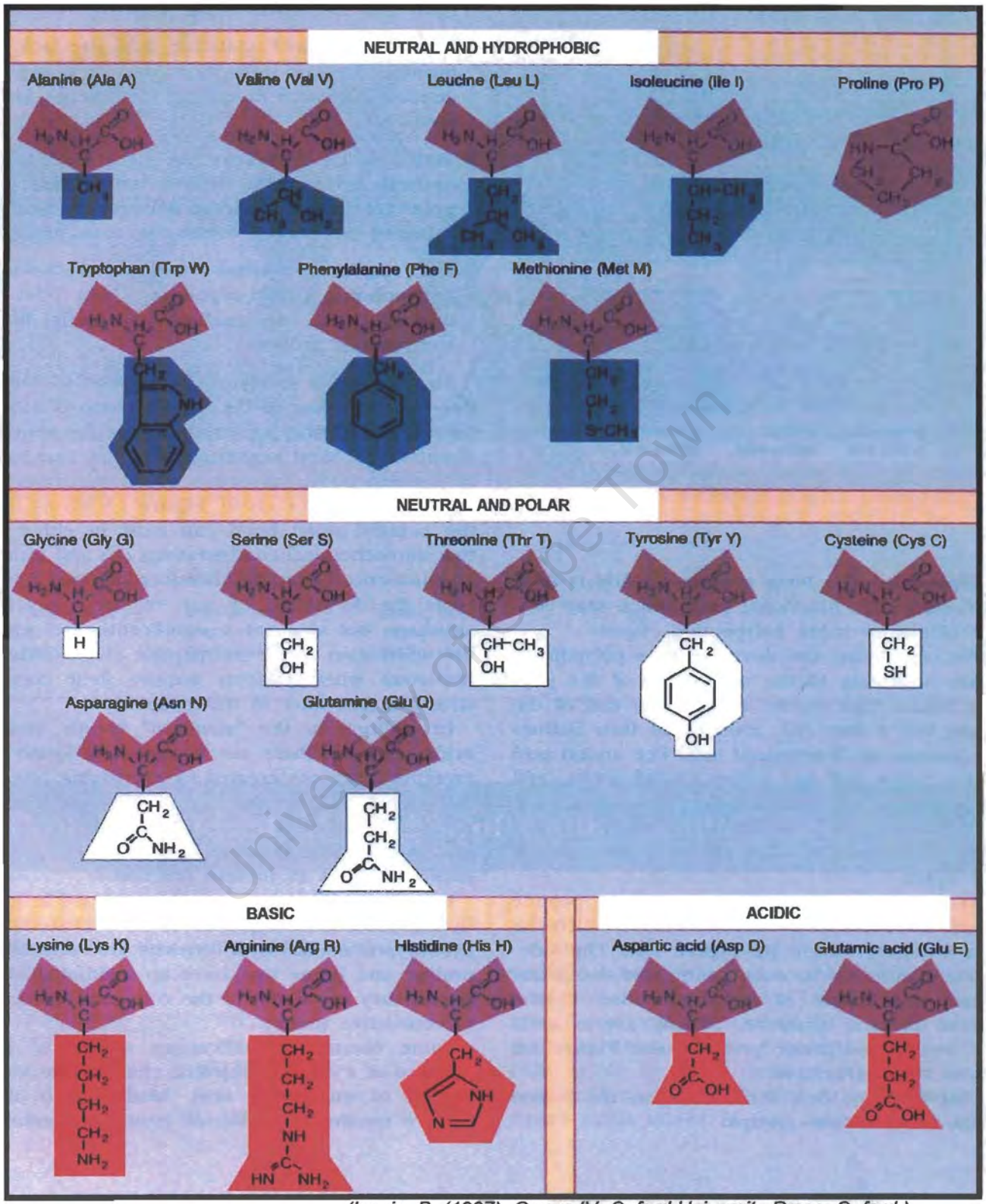

(Lewin, B. (1997). Genes IV. Oxford University Press: Oxford.)

12. PPOX cDNA Sequence

Table 10. cDNA sequence for human PPOX (Nishimura, K. et al. Cloning of a human cDNA for protoporphyrinogen oxidase by complementation *in vivo* of a hemG mutant of *E. coli*. J. Biol. Chem. 270 (14), 8076-8080 (1995), Accesion #D38537). Oligonucleotide sets were designed to PCR the entire gene in four fragments. The forward oligonucleotides are underlined, and the reverse oligonucleotides are double-underlined. The mutations of interest in this study are colour-coded in the right-hand column. The start (ATG) and termination (TGA) codons are boxed in red.

GAATTCGGGG GGAGAACAGA GTGGACGGAG AGTAGGAGAG	
ACCGAAAAGG CTGGGGGTGG GAGTAGCGGA TTTGAAGCAC	
TTGTTGGCCT ACAGAGGTGT GGCAAGCAGA GCACCTCAGA	
ACTCAGGCGT ACTGCCCGCC GCCCGAGCCC TGCGAGGGCC	
GATAGCGAGG GTGTGGCCCT TATCTGCACC CAGCAGAGCG	
CCGGCGGGGT ACGGTCTTAG GACCTCGATC TCCTTCTCCC	
TCATTTTCTC TCATCCCTAC CTATTGTGGG TTTCCGCATG	
GGCCGGACCG TGGTCGTGCT GGGCGGAGGC ATCAGCGGCT	
TGGCCGCCAG TTACCACCTG AGCCGGGCCC CCTGCCCCCC	H20P (A→C)
TAAGGTGGTC CTAGTGGAGA GCAGTGAGCG TCTGGGAGGC	
TGGATTCGCT CCGTTCGAGG CCCTAATGGT GCTATCTTTG	
AGCTTGGACC TCGGGGAATT AGGCCAGCGG GAGCCCTAGG	R59W (C→T)
GGCCCGGACC TTGCTCCTGG TTTCTGAGCT TGGCTTGGAT	
TCAGAAGTGC TGCCTGTCCG GGGAGACCAC CCAGCTGCCC	
AGAACAGGTT CCTCTACGTG GGCGGTGCCC TGCATGCCCT	
ACCCACTGGC CTCAGGGGGC TACTCCGCCC TTCACCCCCC	
TTCTCCAAAC CTCTGTTTTG GGCTGGGCTG AGGGAGCTGA	
CCAAGCCCCG GGGCAAAGAG CCTGATGAGA CTGTGCACAG	
TTTTGCCCAG CGCCGCCTTG GACCTGAGGT GGCGTCTCTA	
GCCATGGACA GTCT CTGCCG TGGAGTGTTT GCAGGCAACA	R168C (C→T)
GCCGTGAGCT CAGCATCAGG TCCTGCTTTC CCAGTCTCTT	
CCAAGCTGAG CAAACCCATC GTTCCATATT ACTGGGCCTG	
TTGCTGGGGG CAGGGCGGAC CCCACAGCCA GACTCAGCAC	
TCATTCGCCA GGCCTTGGCT GAGCGCTGGA GCCAGTGGTC	
ACTTCGTGGA GGTCTAGAGA TGTTGCCTCA GGCCCTTGAA	
ACCCACCTGA CTAGTAGGGG GGTCAGTGTT CTCAGAGGCC	
AGCCGGTCTG TGGGCTCAGC CTCCAGGCAG AAGGGCGCTG	

(TABLE 10 CONTD....)

GAAGGTATCT CTAAGGGACA GCAGTCTGGA GGCTGACCAC
GTTATTAGTG CCATTCCAGC TTCAGTGCTC AGTGAGCTGC
TCCCTGCTGA GGCTGCCCCT CTGGCTCGTG CCCTGAGTGC
CATCACTGCA GTGTCTGTAG CTGTGGTGAA TCTGCAGTAC
CAAGGAGCCC ATCTGCCTGT CCAGGGATTT GGACATTTGG
TGCCATCTTC AGAAGATCCA GGAGTCCTGG GAATCGTGTA
TGACTCAGTT GCTTTCCCTG AGCAGGACGG GAGCCCCCCT
GGCCTCAGAG TGACTGTGAT GCTGGGAGGT TCCTGGTTAC
AGACACTGGA GGCTAGTGGC TGTGTCTTAT CTCAGGAGCT
GTTTCAACAG CGGGCCCAGG AAGCAGCTGC TACACAATTA
GGACTGAAGG AGATGCCGAG CCACTGCTTG GTCCATCTAC
ACAAGAACTG CATTCCCCAG TATACACTAG GTCACTGGCA
AAAACTAGAG TCAGCTAGGC AATTCCTGAC TGCTCACAGG
TTGCCCCTGA CTCTGGCTGG AGCCTCCTAT GAGGGAGTTG
CTGTTAATGA CTGTATAGAG AGTGGGCGCC AGGCAGCAGT
CAGTGTCCTG GGCACAGAAC CTAACAGC[redacted]TCCCCAACT
CTCATTCATG AAAATAAAAA TTGCTGGAGC TCCCGAATCC
CGAATTC

Table 11 Engineered PPOX mutants with their corresponding fragment and size.

Mutant	Corresponding Fragment	Size (bp)
H20P	1	533
R59W	1	533
R168C	2	411

13. Reagents and Solutions

Agarose gel, 0.7%

Zero point three five grams (0.4g for 0.8%; 0.5g for 1% etc.) of intermediate strength agarose (Seakem LE, FMC Bioproducts), was melted in 50ml 1 x TBE buffer, pH 8.0 in an Ehrlenmeyer flask by heating in a microwave oven. The solution was heated for intervals of 30s with gentle swirling till the agrose was dissolved. The molten agarose was allowed to cool to ±40°C before adding 10µl ethidium bromide (1mg/ml stock), poured onto a prepared gel apparatus, and allowed to set at room temperature.

2M Ammonium Acetate (pH 4.6)

15.4g ammonium acetate was dissolved in 50ml deionized water, pH'd to 4.6 with glacial acetic acid and brought to a final volume of 100ml with deionized water.

Ampicillin Stock Solution (sterile)

125mg/ml in deionized water

Denaturing Agarose Gel, 0.8% (for Rapid Screening)

Zero point four grams (0.40g) intermediate strength agarose (Seakem LE, FMC Bioproducts) was melted in 50ml 1 x TBE/0.05% SDS buffer, pH 8.3 in an Ehrlenmeyer flask by heating in a microwave oven. The solution was heated for intervals of 10s with gentle swirling till the agrose was dissolved. The molten agarose was allowed to cool to ±40°C before adding 10µl ethidium bromide (1mg/ml stock). The agarose was poured onto a prepared gel apparatus, and allowed to set at room temperature.

Deoxynucleotide Triphosphates (dNTPs), 50µM (final concentration)

Each of the deoxynucleotide triphosphates ie. dATP, dCTP, dGTP and dTTP, were received as a 100mM stock solution. 25µl of each was added to 900µl sterile deionized water to give a concentration of 2.5mM. These were stored frozen in 10, 20 and 30µl aliquots till use. One µl of the dNTP mix/PCR reaction was used, resulting in a final concentration of 50µM.

HEPES-Buffered Saline (HBS)

20mM HEPES

150mM NaCl

Made up to 100ml in deionized water, pH to 7.4 and filter sterilized.

Kanamycin Sulphate

30μg/ml in deionized water

Luria Bertani (LB) Medium,1L

10g Tryptone

5g Yeast extract

5g NaCl

Adjusted pH to 7.5 with NaOH and autoclaved to sterilize.

LB plates plus Ampicillin or Kanamycin sulphate

Fifteen grams agar was added to 1L of LB medium. The pH was adjusted to 7.0 with NaOH and autoclaved to sterilize. The medium was cooled to 55°C before adding ampicillin (125mg/ml) or kanamycin sulphate (30μg/ml). Twenty five ml of medium were poured into 100mm petri dishes and the agar allowed to harden at room temperature. Plates were stored at 4°C for up to one month.

Lysis Buffer

89mM Tris

89mM Boric acid

2.5mM Na_2EDTA

2% SDS

5% Sucrose

0.04% Bromophenol blue

Made up to 10ml with deionized water and filter-sterilised using a 0.45μm filter.

2M NaOH, 2mM EDTA

(prepared fresh for each use)

2ml 10M NaOH

40µl 500mM EDTA

Made up to 10ml with deionized water.

Phosphate Buffered Saline (PBS, pH 7.4)

4g KCl

4g KH_2PO_4

16g NaCl

2.3g Na_2HPO_4

The above reagents were dissolved in a final volume of 2L and sterilized by autoclaving.

Protoplasting Buffer

30mM Tris-HCl, pH 8.0

5mM Na_2EDTA

50mM NaCl

20% Sucrose

50µg/ml RNAse A

50µg/ml Lysozyme

Made up to 10ml with deionized water. Filtered through a sterile 0.45µm filter and stored at 4°C.

5 x Sample Loading Dye (agarose gels), 10ml

5.74ml Glycerol

1ml 10 x TBE

0.1ml 0.25% (w/v) bromophenol blue

Made up to 10ml with deionized water. Filtered through a sterile 0.45µm filter and aliquoted into 1ml amounts. Stored at -20°C.

SOC Medium (100ml, pH 7.0)

2g Tryptone

0.5g Yeast Extract

1ml 1M NaCl

0.25ml 1M KCl

1ml 2M Mg^{2+} stock (1M $MgCl_2 \cdot 6H_2O$, 1M $MgSO_4 \cdot 7H_2O$), filter sterilized

1ml 2M glucose, filter sterilized

Added tryptone, yeast extract, NaCl and KCl to 97ml deionised water and stirred to dissolve. Autoclaved the solution and allowed it to cool to room temperature. Added 2M Mg^{2+} stock and 2M glucose stock, each to a final concentration of 20mM and filtered the complete medium through a 0.45µm filter unit.

Sucrose Sample Solution

30g Sucrose

10mg Bromophenol blue

5ml 0.5M Na_2EDTA

Made up to 50ml with deionised water, aliquoted 1ml amounts into sterile 1.5ml microcentrifuge tubes and frozen till used. This was used at a ratio of 1:1 with PCR products.

10 X Tris/Borate/EDTA (TBE) Buffer

890mM Tris Base

890mM Boric Acid

20mM EDTA, pH 8.0

Autoclaved to sterilize.

1 x Tris-Borate-SDS (TBS) Buffer

89mM Tris

89mM Boric acid

2.5mM Na_2EDTA

0.05% SDS